

Aus der Fachrichtung 2.4, Experimentelle und Klinische Pharmakologie und Toxikologie
der Medizinische Fakultät
der Universität des Saarlandes, Homburg/Saar

**Role of TRPC-channels in cardiac hypertrophy and
platelet aggregation:
*Analysis of TRPC-deficient mice***

Dissertation zur Erlangung des Grades eines Doktors der Naturwissenschaften
der Medizinischen Fakultät
der UNIVERSITÄT DES SAARLANDES
2011

vorgelegt von: **Juan Eduardo Camacho Londoño**

geboren am: 11.06.1979 in Bogotá

Curiosidad, sed insaciable de explorar el mundo; motivo de desasosiego espiritual de algunos y vitalidad de otros...

...dedicated to my family and to
my beloved Raca

Eidesstattliche Erklärung

Erklärung gemäß § 7 Abs. 1 Nr. 4

Ich erkläre hiermit an Eides statt, dass ich die vorliegende Arbeit ohne unzulässige Hilfe Dritter und ohne Benutzung anderer als der angegebenen Hilfsmittel angefertigt habe. Die aus anderen Quellen direkt oder indirekt übernommenen Daten und Konzepte sind unter Angabe der Quelle gekennzeichnet.

Weitere Personen waren an der inhaltlich-materiellen Erstellung der vorliegenden Arbeit nicht beteiligt. Insbesondere habe ich nicht die entgeltliche Hilfe von Vermittlungs- bzw. Beratungsdiensten (Promotionsberater/innen oder anderer Personen) in Anspruch genommen. Außer den Angegebenen hat niemand von mir unmittelbar oder mittelbar geldwerte Leistungen für Arbeiten erhalten, die im Zusammenhang mit dem Inhalt der vorgelegten Dissertation stehen.

Die Arbeit wurde bisher weder im Inland noch im Ausland in gleicher oder ähnlicher Form in einem anderen Verfahren zur Erlangung des Doktorgrades einer anderen Prüfungsbehörde vorgelegt.

Ich versichere an Eides statt, dass ich nach bestem Wissen die Wahrheit gesagt und nichts verschwiegen habe.

Vor Aufnahme der vorstehenden Versicherung an Eides Statt wurde ich über die Bedeutung einer eidesstattlichen Versicherung und die strafrechtlichen Folgen einer unrichtigen oder unvollständigen eidesstattlichen Versicherung belehrt.

Homburg, im März 2011

Juan Eduardo Camacho Londoño

Table of contents

Zusammenfassung	VIII
Abstract	IX
List of abbreviations	X
List of tables	XIV
List of figures	XV
List of appendices	XVIII
1. Introduction	1
2. Objectives	5
2.1 Objectives for cardiac hypertrophy project	5
2.2 Objectives for platelet's function project	5
3. Theoretical framework and state of the art	6
3.1 The TRP ion channel's family and the TRPC ion channel's subfamily	6
3.2 Development of cardiac hypertrophy	10
3.2.1 TRP channels in cardiac hypertrophy development	14
3.2.2 Neurohumoral induced cardiac hypertrophy	20
3.3 Platelet's function	26
3.3.1 Platelet's signaling and thrombosis	26
3.3.2 TRPC channels and platelet's function	31
4. Materials and methods	35
4.1 Mice	35
4.2 Neurohumoral cardiac hypertrophy induction and analysis	36
4.2.1 Micro-osmotic pump implantation and cardiac hypertrophy evaluation	36
4.2.2 Heart histology: Quantification of cardiomyocyte cross sectional area and heart fibrosis	41
4.2.3 Telemetric blood pressure recording during isoproterenol or angiotensin II treatment	44

4.2.4 Intraventricular pressure measurements (Millar Mikro-Tip catheter)	44
4.2.5 Plasma angiotensinogen determination	46
4.2.6 Isolation of adult mouse cardiomyocytes and mouse cardiac fibroblast culture	48
4.2.7 RNA isolation from cardiomyocytes and cardiac fibroblasts and RT-PCR...	53
4.2.8 Laser Capture Microdissection of mouse cardiomyocytes	55
4.2.9 Characterization of cardiac fibroblast culture by immunocytochemistry	58
4.2.10 Calcium imaging from mouse cultured cardiac fibroblasts	60
4.2.11 Surface ECG recording	62
4.2.12 Organ bath: spontaneously beating isolated right atria	63
4.3 <i>In vitro</i> analysis of platelets	65
4.3.1 Platelet counting	65
4.3.2 Hematocrit quantification from mouse samples	65
4.3.3 Isolation of mouse platelets and preparation of platelet rich plasma (PRP) and washed platelet (WP) suspensions	66
4.3.4 Platelet aggregation: turbidimetric measurements	67
4.3.5 Platelet aggregation in platelets from mice pre-treated with Clopidogrel	70
4.3.6 RNA isolation from mouse platelets and RT-PCR	70
4.3.7 Fluorescence-activated cell sorting (FACS) of mouse platelets	71
4.3.8 Western blot from mouse isolated platelets	72
4.4 Data analysis	72
5. Results	75
5.1 Cardiac hypertrophy in TRPC deficient mice	75
5.1.1 Characterization of protocols for Isoproterenol- and Angiotensin II- induced cardiac hypertrophy in wild type mice	75
5.1.2 Neurohumoral-induced cardiac hypertrophy in TRPC3/TRPC6 (-/-) ² mice..	80
5.1.3 Reduced neurohumoral-induced cardiac hypertrophy in TRPC1/TRPC4 (-/-) ² mice	83
5.1.3.1 Isoproterenol-induced cardiac hypertrophy in TRPC1 ^{-/-} and TRPC4 ^{-/-} mice	93
5.1.3.2 Angiotensin II-induced cardiac hypertrophy in TRPC1 ^{-/-} and TRPC4 ^{-/-} mice	95
5.1.4 TRP expression analysis in isolated adult mouse cardiomyocytes	98
5.1.5 Isolation, culture and characterization of adult mouse cardiac fibroblasts..	102

5.1.5.1 Characterization of cardiac fibroblast culture by immunocytochemistry	102
5.1.5.2 TRP expression analysis in adult mouse cardiac fibroblasts	104
5.1.5.3 Calcium microfluorometry from mouse cardiac fibroblasts	105
5.2 Platelet aggregation in TRPC deficient mice	108
5.2.1 TRP expression analysis in isolated mouse platelets	109
5.2.2 Turbidimetric aggregometry and characterization of the platelet preparation	111
5.2.3 ADP-, Thromboxane A ₂ analogue U46619-, Thrombin- and Collagen-induced aggregation in platelets from wild type mice	114
5.2.4 Screening of TRPC deficient platelets by turbidimetric aggregometry	117
5.2.4.1 Agonist-induced <i>in vitro</i> platelet aggregation in TRPC6 ^{-/-} platelets	122
5.2.4.2 Agonist-induced <i>in vitro</i> platelet aggregation in TRPC1/TRPC6 (-/-) ² platelets	125
5.2.4.3 Agonist-induced <i>in vitro</i> platelet aggregation in TRPC3/TRPC6 (-/-) ² platelets	131
5.2.4.4 Comparison of ADP-induced <i>in vitro</i> platelet aggregation in TRPC1/TRPC6 and TRPC3/TRPC6 deficient platelets	137
5.2.5 <i>In vitro</i> aggregation in platelets from Clopidogrel pre-treated mice	141
5.2.5.1 Effect of Clopidogrel in aggregation of platelets from wild type mice	141
5.2.5.2 Aggregation in TRPC1/TRPC6 (-/-) ² and TRPC3/TRPC6 (-/-) ² platelets from Clopidogrel pre-treated mice	142
6. Discussion	146
6.1 Role of TRPC-channels in cardiac hypertrophy: Analysis of TRPC-deficient mice...	146
6.2 Role of TRPC channels in platelet aggregation: Analysis of TRPC-deficient mice...	158
7. Conclusions	164
8. References	167
9. Acknowledgments	189

Appendices	190
Appendix A. Materials and reagents	190
Appendix B. Solutions	192
Appendix C. ECG analysis from TRPC1/TRPC4 (-/-) ² mice	196
Curriculum Vitae and publications	198

Zusammenfassung

Bereits seit ihrer Erstbeschreibung wird angenommen, dass Mitglieder der TRP-Kanal-Familie, die in Thrombozyten, im Endothel oder in kardialen Zellen exprimiert werden, bei zahlreichen kardiovaskulären Prozessen von Bedeutung sind. In dieser Arbeit habe ich die Rolle der TRP-Kanäle für die Thrombozyten-Aggregation sowie für die Entwicklung einer Herzhypertrophie untersucht. Die pathologisch gesteigerte Zunahme der Herzgröße stellt eine adaptive Antwort des Herzens auf eine mechanische Überlastung dar und kann auch durch direkte Stimulation von G-Protein gekoppelten Rezeptoren hervorgerufen werden. Charakterisiert ist sie durch erhöhte intrazelluläre diastolische Ca^{2+} Konzentrationen in Kardiomyozyten, welche Ca^{2+} -abhängige Signalkaskaden in Gang setzen, die zum kardialen Remodelling führen. Die Mechanismen, die zu einer veränderten intrazellulären Ca^{2+} -Homöostase führen sind nur ansatzweise verstanden, jedoch könnten Rezeptor-vermittelte Ca^{2+} -Kanäle beteiligt sein, die durch neurohumorale Hypertrophie-induzierende Stimuli aktiviert werden. Der Ca^{2+} -Einstrom aus dem Extrazellulärraum ins Zytosol ist auch für die Aktivierung und Aggregation von Thrombozyten und damit für die primäre Hämostase von großer Bedeutung. Hier erfolgt der Ca^{2+} -Einstrom u.a. nach Aktivierung von ADP-Rezeptoren in der Plasmamembran. Es gibt zahlreiche Hinweise, dass TRPC-Proteine solche Rezeptor-aktivierte Ca^{2+} -Kanäle bilden.

In dieser Arbeit wurden TRPC6-Proteine in Herz und Thrombozyten von Wildtyp-Mäusen, jedoch nicht von TRPC6-defizienten Mäusen nachgewiesen. Mittels RT-PCR-Experimenten wurden Transkripte von TRPC1, TRPC3, TRPC4 und TRPC6 in kardialen Fibroblasten und lediglich von TRPC1 in isolierten Kardiomyozyten detektiert. In Thrombozyten konnten TRPC1- und TRPC6-Transkripte amplifiziert werden. Die neurohumoral-induzierte kardiale Hypertrophie durch Isoproterenol und Angiotensin II (AT II) war in TRPC1/TRPC4 (-/-)² Mäusen signifikant reduziert, in TRPC3/TRPC6 (-/-)² Mäusen jedoch unverändert. Ich konnte Unterschiede in der renalen Reninsekretion, in der Plasmaangiotensinogenkonzentration und in der Blutdruckregulation als Ursache ausschließen; darüber hinaus kann die reduzierte Hypertrophieantwort in TRPC1/TRPC4-defizienten Mäusen nicht auf das Fehlen von TRPC1 oder TRPC4 alleine zurückgeführt werden. Der AT II-induzierte Anstieg der Herzfrequenz und der Ca^{2+} -Einstrom in kardiale Fibroblasten ist in TRPC1/TRPC4 (-/-)² Mäusen vermindert. Obwohl der zugrunde liegende Mechanismus noch nicht vollständig verstanden ist, konnte ich zeigen, dass TRPC1 und TRPC4 kausal an der Entstehung einer neurohumoral induzierten Herzhypertrophie beteiligt sind.

In Mäusen mit Deletion von TRPC1, TRPC5 oder TRPC6 und TRPC4/TRPC6-doppelt defizienten Mäusen ist die Thrombozytenaggregation unverändert. Dagegen ist die durch ADP-, Thromboxan A_2 - und Thrombin-induzierte Aggregation in TRPC1/TRPC6 (-/-)² und TRPC3/TRPC6 (-/-)² Mäusen deutlich abgeschwächt; diese Reduktion ist nach Inaktivierung von P2Y_{12} Rezeptoren durch Clopidogrel-Behandlung noch verstärkt, während die Kollagen-induzierte Aggregation unverändert ist. Ich schließe daher, dass TRPC1, TRPC3 und TRPC6 Proteine die ADP-induzierte und durch P2Y_1 Rezeptoren vermittelte Thrombozytenaggregation entscheidend regulieren und dadurch den Kollagen-induzierten Signalweg über Orai/STIM Proteine komplementieren.

Schlagwörter: TRPC-Proteine, Ca^{2+} , Knockout-Mäuse, kardiale Hypertrophie, Thrombozyten-Aggregation.

Abstract

Since its first description it was proposed that members of the TRP ion channel family expressed in platelets, endothelial and cardiac cells are involved in various cardiovascular processes. In this thesis I analyzed the role of TRPC channels in platelet aggregation and in the development of cardiac hypertrophy. Pathological cardiac hypertrophy is an adaptive response of the heart to mechanical load abnormalities, but can also be induced by direct stimulation of G protein coupled receptors. It is characterized by elevated intracellular diastolic Ca^{2+} levels which initiate Ca^{2+} -dependent signaling cascades. The mechanisms causing impaired intracellular Ca^{2+} homeostasis are still incompletely understood, but receptor-operated Ca^{2+} channels of the TRPC family might be activated by neurohumoral hypertrophic stimuli and could play a role here. Ca^{2+} entry from the extracellular space is also critical for platelet activation and aggregation which plays an important role in primary hemostasis. Here, Ca^{2+} entry follows activation of plasma membrane receptors including ADP receptors and TRPC proteins might contribute to this mode of platelet activation.

In this study TRPC6 proteins were identified in heart and platelets from wild type but not from TRPC6^{-/-} mice. In RT-PCR experiments transcripts from TRPC1, TRPC3, TRPC4 and TRPC6 were amplified from cardiac fibroblasts; however, only TRPC1 transcripts were amplified from isolated cardiomyocytes. TRPC1 and TRPC6 transcripts were amplified from platelets. Unexpectedly, neurohumoral cardiac hypertrophy induced by isoproterenol and angiotensin II (ATII) was not reduced in TRPC3/TRPC6^(-/-) mice. In contrast, the hypertrophic response was significantly reduced in TRPC1/TRPC4^(-/-) after isoproterenol and ATII treatment, respectively. I could rule out differences in renal renin secretion, basal plasma angiotensinogen levels or in blood pressure regulation during isoproterenol infusion; in addition, the reduced hypertrophy response in TRPC1/TRPC4^(-/-) mice is not due to deletion of either TRPC1 or TRPC4 proteins alone. An impaired ATII-induced signaling in TRPC1/TRPC4^(-/-) mice was observed and this could play a role possible through regulation of heart rate or Ca^{2+} signaling in cardiac fibroblast. Although the underlying mechanisms are not completely understood, TRPC1 and TRPC4 proteins were identified in this study as positive regulators of the neurohumoral-induced cardiac hypertrophy development.

In mice lacking either TRPC1, TRPC5 or TRPC6 and mice lacking both TRPC4 and TRPC6 platelet aggregation was found to be unaltered. In contrast, ADP-, Thromboxane A_2 -, and thrombin- induced aggregation was significantly impaired in TRPC3/TRPC6 and TRPC1/TRPC6 deficient mice, and the reduction in the aggregation response was amplified by inactivating P2Y₁₂ receptors with clopidogrel treatment. In contrast, collagen-induced aggregation was unaffected. Therefore, I propose TRPC1, TRPC3 and TRPC6 proteins as crucial regulators of ADP-induced platelet aggregation through P2Y₁ receptor signaling which could complement the collagen-triggered pathway that depends on Orai/STIM proteins.

Keywords: TRPC proteins, Ca^{2+} , knockout mice, cardiac hypertrophy, platelet aggregation.

List of abbreviations

AC: Adenylate Cyclase
ACD: Acid-Citrate-Dextrose
ACE: Angiotensin converting enzyme
Ach: Acetylcholine
ADP: Adenosine-diphosphate
AMP: Adenosine-monophosphate
2-APB: 2-aminoethoxydiphenyl borate (InsP₃R blocker)
ANOVA: Analysis of variance
ATII: Angiotensin II
ATP: Adenosine-triphosphate
BDM: 2,3-Butanedione monoxime
bp: Base pair
BPM: Beats per minute
Br: Brain
BSA: Bovine Serum Albumin
BW: Body weight
cAMP: Cyclic adenosine monophosphate
CD: Cluster of differentiation
cFB: Cardiac Fibroblast
CM: Cardiomyocyte
CRP: Collagen related peptide
CVD: Cardiovascular Diseases
DAG: Diacylglycerol
DAPI: 4',6-diamidino-2-phenylindole
d-diH₂O: distilled-deionised water
DMSO: Dimethyl sulfoxide
dn: Dominant negative
DPBS: Dulbecco's-Phosphate Buffered Saline
DTT: DL-Dithiothreitol
ECG: Electrocardiogram
EDTA: Ethylene-diamine-tetra-acetic acid
EGTA: Ethylene-glycol-tetra-acetic acid
ELISA: Enzyme-linked immunosorbent assay
ET-1: Endothelin 1
EtOH: Ethanol

FACS: Fluorescence Activated Cell Sorting
FCS: Fetal Calf Serum
FITC: Fluorescein Isothiocyanate
g: Gram
G: Gravitational (related to centrifugation)
GAPDH: Glyceraldehyde 3-phosphate dehydrogenase
GP: Glycoprotein
GPCR: G protein coupled receptor
h: Hour
H-E: Hematoxylin-Eosin
HEK: Human embryonic kidney
HF: Heart frequency
HPRT-1: Hypoxanthine Phosphoribosyltransferase 1
HW: Heart weight
ICC: Immunocytochemistry
InsP₃R: Inositol 1,4,5,-trisphosphate receptor
Iso: Isoproterenol
i.e.: In example
IL: Interleukin
i.p: Intraperitoneal administration
IP3: Inositol 1,4,5-trisphosphate
iSMC: Ileum smooth muscle cells
ITAM: Immunoreceptor tyrosine activation motif
JNK: c-JunN-terminal Kinase
kDa: KiloDalton
KO: Knockout
LCM: Laser Capture Microdissection
LW: Lung weight
LivW: Liver weight
M: Molar
MAEC: Mouse aortic endothelial cells
MF: Macrophage
MAP: Mean arterial pressure
M: Molar
mg: Milligram
min: Minutes
mm: Millimeter

mM: Millimolar
N: Normal
neg: Negative
NFAT: Nuclear factor of activated T cells
nm: Nanometer
nM: Nanomolar
NRVM: Neonatal Rat Ventricular Myocytes
ns: Not significant (probability >0.05)
nt.: Not tested
OAG: 1-Oleoyl-2-acetyl-sn-glycerol
OD: Optical density
o/n: Over night
P: Passage (referred to cell culture)
p or p-value: Probability value
PAR: Protease activated receptor
PBS: Phosphate Buffered Saline
PBST: PBS-Tween 20
PCR: Polymerase chain reaction
PE: Phenylephrine
PFA: Paraformaldehyde
PGI₂: Prostaglandin I₂ or Prostacyclin
P4HB: Prolyl-4-hydroxylase beta
PIP2: Phosphatidylinositol 4,5-bisphosphate (PIP2)
pM: Picomolar
p.o.: Oral administration
PPP: Platelet poor plasma
PRP: Platelet rich plasma
PSC: Platelet shape change
RAAS: Renin-Angiotensin-Aldosterone System
RNA: Ribonucleic Acid
ROCE: Receptor-operated calcium entry
ROI: Region of interest
ROS: Reactive oxygen species
rpm: Revolutions per minute
RT: Room temperature
RT-PCR: Reverse transcription polymerase chain reaction
s: Second

SBP: Systolic Blood Pressure
SCID: Severe combined immunodeficiency
SD: Standard deviation
SEM: Standard error of the mean
SERCA: Sarco-endoplasmic reticulum Ca²⁺-ATpase
SKF96365: 1-(β-[3-(4-methoxyphenyl)propoxyl]-4methoxyphenethyl)-1H-imidazole
SOCE: Store operated calcium entry
SPF: Specific pathogen free
SplW: Spleen weight
STIM1: Stromal interaction molecule 1
TAC: Transverse aortic constriction
TG: Thapsigargin
TK: Thymidine Kinase
TL: Tibia length
TMEM-2: Transmembrane protein 2
TNF α : Tumor necrosis factor α
TRP: Transient Receptor Potential
TRPC: Transient Receptor Potential Canonical (Classical)
TRPM: Transient Receptor Potential Melastatin
TRPV: Transient Receptor Potential Vanilloid
TxA₂: Thromboxane
U: Units referring to I.U. (International Units)
 μ g: Microgram
 μ l: Microliter
 μ M: Micromolar
UV: Ultra violet
vs.: Versus
WP: Washed platelets
WT: Wild type
%: Percentage
°C: Celsius grad

List of tables

Theoretical framework and state of the art	6
Table i1. Reported expression of TRPC channels in mammalian heart	15
Table i2. Reported expression of TRPC channels in mammalian cardiomyocytes	16
Table i3. Reported expression of TRPC channels in mammalian cardiac fibroblasts	19
Table i4. TRPC expression in mammalian platelets	33
Table i5. TRPC expression in mammalian megakaryocytes	33
Materials and methods	35
Table m1. Primer sequences and PCR conditions used for genotyping TRPC deficient mice	37
Table m2. Primers and conditions used for RT-PCR expression analysis of TRPs	56
Table m3. Immunocytochemistry conditions used for characterization of cardiac fibroblast	60
Results	75
Table 1. No differences in left ventricular pressure in TRPC3/TRPC6 (-/-) ² mice at the end of treatment with a low dose of angiotensin II	82
Table 2. Left ventricle pressure in TRPC1/TRPC4 (-/-) ² mice at the end of isoproterenol treatment	88
Table 3. Summary of TRP expression analysis in mouse cardiomyocytes and cultured cardiac fibroblasts by RT-PCR	100
Table 4. Overview of platelet aggregometry screening with TRPC deficient mouse lines	108
Table 5. Summary of TRP expression analysis in mouse platelets by RT-PCR	111
Table 6A. Summary of platelet aggregometry results from different single TRPC deficient mouse lines analyzed in platelets from female mice	119
Table 6B. Summary of platelet aggregometry results from different compound TRPC deficient mouse lines analyzed in platelets from female mice	120
Table 7A. Summary of platelet aggregometry results from different single TRPC deficient mouse lines analyzed in platelets from male mice	121
Table 7B. Summary of platelet aggregometry results from different compound TRPC deficient mouse lines analyzed in platelets from male mice	122
Table 8. Platelet aggregation in washed platelets from Clopidogrel pre-treated TRPC1/C6 and TRPC3/C6 deficient mice	145

List of figures

Theoretical framework and state of the art	6
Figure i1. Pathways contributing to the isoproterenol-induced cardiac hypertrophy	23
Materials and methods	35
Figure m1. Measurement of left intraventricular pressure from the mouse heart	46
Figure m2. Summary of the isolation procedure used to obtain mouse cardiac fibroblasts and cardiomyocytes	49
Figure m3. Perfusion system used for cardiac cell isolation and silicone isolators for fibroblast culture	51
Figure m4. Surface ECG trace from mouse	62
Figure m5. Mouse right atrial preparation for organ bath experiments	64
Figure m6. Effect of apyrase, fibrinogen or Clopidogrel in washed platelets preparations from wild type mice used for <i>in vitro</i> aggregation	68
Figure m7. Turbidimetric aggregometry	69
Results	75
Figure 1. Neurohumoral-induced cardiac hypertrophy in wild type mice	77
Figure 2. Effects of isoproterenol or ATII on blood pressure during cardiac hypertrophy induction	79
Figure 3. No reduction in cardiac hypertrophy response in TRPC3/TRPC6 (-/-) ² mice after isoproterenol or angiotensin II treatment	81
Figure 4. No reduction in cardiac hypertrophy response in TRPC3/TRPC6 (-/-) ² mice after treatment with a low dose of angiotensin II	83
Figure 5. Pilot experiment showed a reduced cardiac hypertrophy development in TRPC1/TRPC4 (-/-) ² after isoproterenol treatment	84
Figure 6. TRPC1/TRPC4 (-/-) ² mice have reduced isoproterenol-induced cardiac hypertrophy	86
Figure 7. Isoproterenol-induced increase in cardiomyocyte size and in myocardial fibrosis are reduced in TRPC1/TRPC4 (-/-) ² mice	87
Figure 8. Angiotensinogen plasma levels are not different in TRPC1/TRPC4 (-/-) ² mice despite the smaller liver size	89
Figure 9. TRPC1/TRPC4 (-/-) ² mice presented reduced angiotensin II-induced cardiac hypertrophy	90
Figure 10. Heart rate and mean arterial pressure during isoproterenol infusion in TRPC1/TRPC4 (-/-) ² mice	92

Figure 11. Reduced chronotropic response in isolated right atria from TRPC1/TRPC4 (-/-) ² mice after ATII stimulation but not after Isoproterenol stimulation	94
Figure 12. Isoproterenol-induced cardiac hypertrophy is not reduced in TRPC1-/- mice	95
Figure 13. Isoproterenol-induced cardiac hypertrophy is not reduced in TRPC4-/- mice	96
Figure 14. Angiotensin II-induced cardiac hypertrophy is not reduced in TRPC1-/- mice	97
Figure 15. Angiotensin II-induced cardiac hypertrophy is not reduced in TRPC4-/- mice	97
Figure 16. Absolute levels of cardiac fibrosis are higher in TRPC1/TRPC4 (-/-) ² mice....	98
Figure 17. Expression of TRPs in isolated mouse cardiomyocytes analyzed by RT-PCR	99
Figure 18. Systematic RT-PCR expression analysis of TRPs in LCM-isolated mouse cardiomyocytes	101
Figure 19. Characterization of cultured mouse cardiac fibroblasts	103
Figure 20. TRPC expression in cultured adult mouse cardiac fibroblasts	104
Figure 21. First Ca ²⁺ imaging experiments with cultured adult mouse cardiac Fibroblasts	106
Figure 22. Whole blood platelet counts are not altered in different TRPC deficient mouse lines	109
Figure 23. Expression analysis of TRPs in mouse platelets	110
Figure 24. Washed platelet preparation is 99.9% pure and Ca ²⁺ is required for platelet aggregation	113
Figure 25. <i>In vitro</i> platelet aggregation in male and female wild type platelets induced by ADP or by U46619	115
Figure 26. <i>In vitro</i> platelet aggregation in male and female wild type platelets induced by thrombin or by collagen	116
Figure 27. ADP- and U46619-induced platelet aggregation in washed platelets from wild type and TRPC6 -/- mice	123
Figure 28. Thrombin- and collagen-induced platelet aggregation in washed platelets from wild type and TRPC6 -/- mice	124-125
Figure 29. ADP-induced platelet aggregation in washed platelets from wild type and TRPC1/C6 (-/-) ² mice	125-126
Figure 30. U46619-induced platelet aggregation in washed platelets from wild type and TRPC1/C6 (-/-) ² mice	127-128

Figure 31. Thrombin-induced platelet aggregation in washed platelets from wild type and TRPC1/C6 (-/-) ² mice	129-130
Figure 32. Collagen-induced platelet aggregation in washed platelets from wild type and TRPC1/C6 (-/-) ² mice	130-131
Figure 33. ADP-induced platelet aggregation in washed platelets from wild type and TRPC3/C6 (-/-) ² mice	132-133
Figure 34. U46619-induced platelet aggregation in washed platelets from wild type and TRPC3/C6 (-/-) ² mice	133-134
Figure 35. Thrombin-induced platelet aggregation in washed platelets from wild type and TRPC3/C6 (-/-) ² mice	135-136
Figure 36. Collagen-induced platelet aggregation in washed platelets from wild type and TRPC3/C6 (-/-) ² mice	136-137
Figure 37. Comparison of ADP-induced platelet aggregation in TRPC1/C6 (-/-) ² and TRPC3/C6 (-/-) ² platelets from female mice	139
Figure 38. Comparison of ADP-induced platelet aggregation in TRPC1/C6 (-/-) ² and TRPC3/C6 (-/-) ² platelets from male mice	140
Figure 39. ADP-induced aggregation in platelets from Clopidogrel pre-treated wild type female mice	141
Figure 40. Platelet aggregation in washed platelets from Clopidogrel pre-treated TRPC1/C6 and TRPC3/C6 deficient female mice	143
Figure 41. Platelet aggregation in washed platelets from Clopidogrel pre-treated TRPC3/C6 deficient male mice	144
Conclusions	164
Figure 42. The isoproterenol-induced cardiac hypertrophy requires TRPC1 and TRPC4 proteins	165
Figure 43. Model of ADP mediated platelet aggregation and the possible role of TRPC channels	166
Appendices	190
Figure 1Ap. ECG analysis from TRPC1/TRPC4 (-/-) ² mice during cardiac hypertrophy induction by isoproterenol	197

List of appendices

Appendix A. Materials and reagents	190
Appendix B. Solutions	192
Appendix C. ECG analysis from TRPC1/TRPC4 (-/-) ² mice	196

1. Introduction

It is a challenge to decipher the physiological and pathophysiological mechanisms underlying cardiovascular diseases (CVD) in order to develop new strategies of prevention and treatment regarding the increasing rates in CVD as well as the high morbidity and mortality associated to them. Cardiovascular diseases cause about 48% and 42% of all deaths in Europe and in the European Union, respectively (European cardiovascular disease statistics, 2008), and about 34% in the United States (CVD statistics from 2006, American Heart Association), making it an issue with a high socio-economic impact.

Members of the TRP ion channel family, including TRPC cation channels, have been proposed to be mediators of different physiological and pathophysiological cardiovascular processes (Inoue et al., 2006; Dietrich et al., 2007a; Abramowitz and Birnbaumer, 2009; Watanabe et al., 2009; Dietrich et al., 2010). It has been postulated that TRP channels play a role in cardiac hypertrophy development (Guinamard and Bois, 2007; Nishida and Kurose, 2008) and in platelet aggregation (Authi, 2007); however, no causal evidence about their role in cardiac hypertrophy development or platelet aggregation has been presented so far; therefore the role of TRPC channels in both processes was analyzed in this thesis.

Cardiac hypertrophy is an adaptive response of the heart to mechanical load abnormalities. The hypertrophic response can be induced by stimulation of G protein coupled receptors (GPCR) such as angiotensin II receptor 1 (AT₁) or β -adrenergic receptors. It is characterized by enhanced size of cardiomyocytes (CM) and elevated intracellular diastolic Ca²⁺ levels which initiates Ca²⁺-dependent signaling cascades and reactivation of fetal genes through the calcineurin-NFAT pathway (Heineke and Molkentin, 2006). The mechanisms leading to impaired intracellular Ca²⁺ homeostasis are still incompletely understood, but receptor-operated cation channels of the TRPC family might be activated by neurohumoral hypertrophic stimuli. Additionally, cardiac hypertrophy and remodeling are regulated by other cells types. Cardiac fibroblasts are important mediators regulating the secretion of growing factors with direct impact on cardiomyocytes function, hypertrophy development and extracellular matrix formation (Brown et al, 2005). Recent reports proposed that Ca²⁺ entry mediated by TRPC proteins is involved in cardiac hypertrophy development. For example, specific cardiomyocyte over-expression of either TRPC3 or TRPC6 in mice leads to increased cardiomyocyte size, cardiac mass and heart failure (Kuwahara et al., 2006; Nakayama et al., 2006).

Platelets play an important role in primary cellular hemostasis and also in intravascular thrombus formation after atherosclerotic remodeling. Changes in intracellular Ca^{2+} concentration either due to Ca^{2+} entry from the extracellular space or due to Ca^{2+} release from internal stores are steps in activation and aggregation (Rink and Sage, 1990; Sage, 1997). Ca^{2+} entry follows activation of plasma membrane receptors including G_q -coupled such as the P2Y_1 receptor, the prostanoid receptor TP and Protease activated receptor 4 (PAR4), which are activated by ADP, Thromboxane A_2 (TxA_2) and thrombin, respectively (Woulfe et al., 2004; Offermanns, 2006). In addition, collagen activates Glycoprotein (GP) VI and induces an intracellular signaling pathway that induces elevation of intracellular calcium concentration (Hagedorn et al., 2010). These cellular signaling pathways involve Phospholipase C (PLC) activation and subsequent Diacylglycerol (DAG) and inositol 1,4,5-trisphosphate (IP_3) formation, second messengers that are known to mediate activation of TRPC channels (Clapham, 2007). It has been proposed that most proteins from the TRPC subfamily are expressed in platelets and might contribute to platelet activation as constituents of agonist-activated Ca^{2+} entry channels (Den Dekker et al., 2001; Hassock et al., 2002; Tolhurst et al., 2005; Jardin et al., 2009).

The main hypotheses that I addressed in my thesis were that the inactivation of one or more TRPC proteins lead to reduction in the development of cardiac hypertrophy and/or to impaired platelet aggregation, providing in that way causative evidence about the role of TRPC channels either for cardiac hypertrophy development or for platelet aggregation. The analysis of TRPC channels is hampered by the lack of appropriate channel blockers and agonists, and suitable antibodies to identify TRPC proteins in primary cells are not available in most cases (Freichel and Flockerzi, 2007). The use of TRPC-deficient mouse models provides a very useful tool to analyze antibody specificity and to determine the causal role of these proteins. I have been investigating the role of TRPC proteins for cardiac hypertrophy development and for platelet aggregation in mouse lines lacking either TRPC1, TRPC3, TRPC4, TRPC5 or TRPC6, as well as from TRPC compound knockout mice derived thereof. We used compound TRPC deficient mice because it has been proposed that different TRPC proteins can form heteromeric channels (Abramowitz and Birnbaumer, 2009) and the knockout of one TRPC protein can be compensated by other TRPC protein (Dietrich et al., 2005). Already, the use of TRP deficient mouse models had proven to be useful to unravel the physiological function of various TRP proteins (Wu et al., 2010a).

The expression of different TRP proteins in murine heart and platelets was analyzed using heart and platelets from TRP-deficient mice as negative controls. Using an antibody

directed against mouse TRPC6 we identified TRPC6 proteins in heart and platelets from wild type (WT) but not from TRPC6 deficient mice. I amplified TRPC1 and TRPC6 transcripts from isolated mouse platelets, and TRPC1, TRPC3, TRPC4 and TRPC6 transcripts from cardiac cells obtained by Langendorff perfusion. In addition, I amplified TRPC1, TRPC3, TRPC4, TRPC5 and TRPC6 transcripts from cultured mouse cardiac fibroblasts. In cardiomyocytes isolated by Laser Capture Microdissection only TRPC1 transcripts were detected.

After establishing methods for the *in vivo* analysis of the neurohumoral-induced cardiac hypertrophy development in TRPC deficient mice I found that TRPC1/TRPC4 (-/-)² mice, which lack both TRPC1 and TRPC4 proteins, had a reduced hypertrophy response after isoproterenol (Iso) or angiotensin II (ATII) treatment. This reduced response was not observed in TRPC1 or TRPC4 single knockout mice. In contrast, the Iso-induced and the ATII-induced hypertrophic responses were not diminished in TRPC3/TRPC6 (-/-)² mice. In addition, the effects of constant Iso or ATII infusion on blood pressure and on heart rate were characterized. Isoproterenol increased heart rate by about 30% with a minor increase of ~3mmHg in mean arterial pressure (MAP). ATII significantly increased MAP by 45mmHg and heart rate by ~7%. Isoproterenol produced a bigger increase in cardiac mass compared to ATII. In contrast, ATII generated a more pronounced fibrosis in comparison to Iso. Isoproterenol treatment produced comparable changes in MAP between WT and TRPC1/TRPC4 (-/-)² mice, and the Iso-induced increase in heart rate was reduced in TRPC1/TRPC4 deficient mice. The cellular mechanisms that are responsible for the reduced hypertrophic response in TRPC1/TRPC4 (-/-)² mice are currently investigated.

Regarding the role of TRPC channels in platelet function, I performed *in vitro* aggregation analysis by a systematic screening of platelets from different TRPC deficient mouse lines. Platelet aggregation triggered by ADP, Thromboxane A₂ analogue U46619, thrombin and collagen was first characterized with platelets from wild type mice. The deletion of TRPC1, TRPC3, TRPC4 or TRPC6 did not affect platelet counts in mice. Unexpectedly, the deletion of either TRPC1 or TRPC6 proteins did not affect platelet aggregation. From experiments with mouse lines lacking TRPC4/TRPC6 or TRPC5 proteins a relevance of TRPC4 and TRPC5 proteins for ADP-, TxA₂-, thrombin- or collagen-induced aggregation of murine platelet seems dubious at this point. On the other hand, ADP-induced aggregation was impaired in platelets from TRPC1/C6 and TRPC3/TRPC6 deficient mice. Collagen-induced platelet aggregation was not different in both genotypes. This reduction was associated with impaired response through the ADP P2Y₁ receptor, because

differences in the aggregation response between WT and TRPC1/C6 and TRPC3/TRPC6 deficient platelets were more pronounced when the P2Y₁₂ receptor was blocked by pre-treatment of the mice with Clopidogrel. Possibly, as secondary effect of a reduced ADP response, impaired aggregation responses to Thromboxane A₂ analogue U46619 and thrombin were observed in both TRPC1/C6 and TRPC3/TRPC6 deficient platelets. In the future, we will study the impact of these findings to the *in vivo* aggregation as well as the mechanisms behind the defective ADP-induced platelet aggregation in TRPC1/C6 and TRPC3/TRPC6 mice.

From these results it can be concluded that TRPC channels play a causative role in development of cardiac hypertrophy and in platelet aggregation. TRPC1 and TRPC4 proteins together positively regulate the neurohumoral cardiac hypertrophy development *in vivo* induced by isoproterenol and angiotensin II. In contrast, and unexpected due to the evidence from knock-down studies in neonatal cardiomyocytes and transgenic overexpression of TRPC3 or TRPC6 proteins in mouse heart, proposing TRPC3 and TRPC6 channels as positive regulators of cardiac hypertrophy, no evidence of reduced cardiac hypertrophy in mice deficient for TRPC3 and TRPC6 channels was observed with our neurohumoral-induced cardiac hypertrophy. Concerning platelet aggregation, our results point out that TRPC1, TRPC3 and TRPC6 are required for ADP-induced platelet aggregation through P2Y₁ receptor signaling.

2. Objectives

2.1 Objectives for cardiac hypertrophy project

The main objective of this part of my thesis was to analyze if TRPC proteins are causally involved in the development of the *in vivo* cardiac hypertrophy induced by neurohumoral mechanisms. To achieve this, it was first required that I establish in our group methodological tools for cardiac hypertrophy induction by isoproterenol or angiotensin II infusion, as well as the corresponding methods to quantify and analyze the extent of cardiac hypertrophy produced by both agents in mice. The methods included assessment of cardiac hypertrophy indexes, histomorphological analysis of cardiomyocyte cross sectional area and cardiac fibrosis, and measurements of *in vivo* ventricular function by a pressure transducer catheter. With a reliable set of established methods it was possible to test if mice deficient for one or more TRPC proteins develop cardiac hypertrophy to the same extent as the corresponding control mice after isoproterenol or angiotensin II infusion. Additional cardiac functions were analyzed using surface ECG and contraction of spontaneously beating right atria in organ bath apparatus.

Another aim of this thesis was to study the expression of different TRPs in the mouse heart, and especially in cardiomyocytes and cardiac fibroblasts. For this it was also necessary that I set up methods to isolate both cardiac cell types. To this end I developed protocols for the isolation of mouse cardiomyocytes by Laser Capture Microdissection, the isolation and culture of mouse adult cardiac fibroblasts and the corresponding characterization of the culture by RT-PCR and immunocytochemistry.

2.2 Objectives for platelet's function project

In the part of this thesis regarding the study of platelet function the first goal was to determine the role of TRPC proteins in platelet aggregation through stimulation with the four main platelet activating agonists ADP, Thromboxane A₂, thrombin and collagen using platelets from wild type and TRPC deficient mice. The second goal was to analyze the expression of different TRPs in murine platelets by RT-PCR and by western blot analysis using platelets isolated from different TRPC deficient mice as controls. To accomplish both goals it was essential that I establish methods for the isolation of mouse platelets and for the *in vitro* analysis of platelet function by turbidimetric aggregometry.

3. Theoretical framework and state of the art

3.1 The TRP ion channel's family and the TRPC ion channel's subfamily

Since 40 years ago, when a spontaneous mutation in the *Drosophila* eye was described (Cosens and Manning, 1969) and the mutated gene called *trp* was cloned (Montell and Rubin, 1989), 28 *trp* homologues have been described in mammals. From those, 27 are expressed in humans because one (TRPC2) corresponds to a pseudogene (Clapham, 2007). The TRP ion channel family has been divided, based on amino acid sequence homology, in 7 subfamilies as follows: TRPC (Canonical) subfamily with 7 members in mammals (TRPC1 to 7), TRPM (Melastatin) subfamily with 8 members (TRPM1 to 8), TRPV (Vanilloid) subfamily with 6 members (TRPV1 to 6), TRPA (Ankyrin) subfamily with one member (TRPA1), TRPN subfamily with no mammalian homologue (one member in invertebrates and zebrafish), TRPP (polycystin) with 3 mammalian members (TRPP2, 3 and 5) and TRPML (mucolipin) also composed of 3 members (TRPML1 to 3). These 28 channels share a main proposed organization of six putative transmembrane domains with both, C and N termini, being intracellularly located and is believed that TRP channels are assembled as homo- or hetero-tetramers to form cation selective channels (Montell, 2005; Pedersen et al., 2005). Beyond a general topological organization, these channels have a great diversity in activation mechanisms and selectivities and they have been proposed to be key players in sensory physiology and homeostasis regulation. But, still it is not known for most of them how they are activated and which are the physiological functions *in vivo* (Clapham, 2003; Venkatachalam and Montell, 2007; Wu et al., 2010a); despite the fact that numerous TRP channels have been related to several diseases the knowledge about their causative role of pathophysiological conditions is still sparse (Nilius and Owsianik, 2010).

General characteristics and regulation of TRPC channels. The members of the TRPC cation channel subfamily are the closest homologues of the *Drosophila* TRP and TRPL channels, and like those they are activated by signaling pathways that depends on Phospholipase C (PLC) activity. The subfamily is composed by TRPC1, TRPC2, TRPC3, TRPC4, TRPC5, TRPC6 and TRPC7 proteins and these members have been additionally subdivided into three groups, TRPC1/C4/C5, TRPC3/C6/C7 and TRPC2 (Minke, 2006). It has been proposed that TRPCs are part of the Store-Operated Ca^{2+} Entry (SOCE) being activated by store depletion, and also it has been shown that they have a role in the Receptor-Operated Calcium Entry or ROCE (Ambudkar and Ong, 2007). GPCR-mediated activation of the PLC β and receptor tyrosine kinase-mediated activation of the PLC γ

signaling systems results in hydrolysis of phosphatidylinositol-4,5-bisphosphate (PIP₂) with formation of the second messengers diacylglycerol (DAG) and inositol 1,4,5-trisphosphate (IP₃). The fall of the Ca²⁺ concentration within the lumen of the endoplasmatic reticulum by the action of inositol 1,4,5-trisphosphate (IP₃) on the IP₃ receptor (InsP₃R) or through the use of Thapsigargin (TG), a specific inhibitor of the Sarcoplasmic Reticulum Ca²⁺-ATpase (SERCA), activates a entry of Ca²⁺ across the plasma membrane which is known as Capacitative Ca²⁺ Entry (CCE) or SOCE; on the other hand, Ca²⁺ entering through the PLC-activated channels is referred to as ROCE (Parekh and Putney, 2005; Trebak et al., 2007; Abramowitz and Birnbaumer, 2009).

For each member of the TRPC channel subfamily some regulatory postulated mechanisms and characteristics reviewed by several authors (Clapham, 2003; Montell, 2005; Pedersen et al., 2005; Alexander et al., 2007; Trebak et al., 2007; Venkatachalam and Montell, 2007) are presented.

TRPC1. TRPC1 channels conduct non-selectively mono and divalent cations; they are activated by store depletion of intracellular Ca²⁺ stores with IP₃ or by inhibition of the SERCA with TG, Diacylglycerol (DAG) analogue OAG in the absence of extracellular Ca²⁺, PLC, mechanical stretch, metabotropic receptors, glutamate receptors, and can be inhibited by Lanthanides, extracellular Ca²⁺, Gadolinium (Gd³⁺), SKF96365 that it is a cation channel blocker and 2-aminoethoxydiphenyl borate (2-APB) which is a blocker of IP₃R (InsP₃R).

TRPC2. TRPC2 channels are more selective to conduct calcium compared to sodium with a $P_{Ca}/P_{Na}=2.7$, calculated from measurements in vomeronasal sensory neurons (Lucas et al., 2003); they are activated by DAG, store depletion of Ca²⁺ stores by TG treatment and GPCR (G_q-PLC β), and are inhibited by 2-APB.

TRPC3. TRPC3 channels are slightly more selective for calcium than sodium with a ratio of $P_{Ca}/P_{Na}=1.6$ measured in cultured bovine pulmonary artery endothelial cells expressing hTRPC3 (Kamouchi, 1999). TRPC3 are positively modulated by store depletion, DAG, GPCR (G_{q/11}-PLC β), exocytosis, PLC γ , src Thymidine Kinase (TK), IP₃, and can be inhibited by Lanthanides, Gd³⁺, Ni²⁺, SKF96365, 2-APB, flufenamic acid, phorbol ester and recently the pyrazole compound Pyr3 was proposed to be an specific TRPC3 antagonist (Kiyonaka et al., 2009).

TRPC4. TRPC4 channels have a selectivity for calcium compared to sodium (P_{Ca}/P_{Na}) between 1.05 measured in embryonic kidney (HEK293) cells transfected with a TRPC4 murine variant (Schaefer et al., 2000) and 7.7 observed also in HEK293 cells, but transfected with a TRPC4 bovine variant (Philipp et al., 1996). TRPC4 channels are activated by GPCR ($G_{q/11}$ -PLC β), $GTP\gamma S$, La^{3+} , calmidazolium and, possibly, by store depletion, and TRPC4 channels are inhibited by Gd^{3+} and 2-APB.

TRPC5. TRPC5 channels are more selective for conducting calcium compared to sodium with a P_{Ca}/P_{Na} values between 1.79 obtained from HEK293 cells transiently expressing a TRPC5 murine variant (Schaefer et al., 2000), 9.5 (Montell, 2005) and 14.3 in recordings from HEK293 cells expressing also a TRPC5 from mouse (Okada et al., 1998). TRPC5 channels are activated by store depletion, exocytosis, GPCR ($G_{q/11}$ -PLC β), $GTP\gamma S$, La^{3+} , sphingosine-1-phosphate, IP3, Gd^{3+} , extracellular Ca^{2+} , Rac, and modest elevation of intracellular [Ca^{2+}], and TRPC5 channels are blocked by 2-APB, SKF96365, and DAG (OAG).

TRPC6. TRPC6 channels conduct cations but with preference of divalent ones with a $P_{Ca}/P_{Na}=5$ quantified in Chinese hamster ovary (CHO)-K1 cells over-expressing the hTRPC6 (Hofmann et al., 1999). TRPC6 channels are activated by DAG (OAG), src Tyrosine Kinase, 20-Hydroxyarachidonic acid (20-HETE), AlF_4 , flufenamate, GPCR ($G_{q/11}$ -PLC β), $GTP\gamma S$, intracellular Ca^{2+} and PIP_3 , and TRPC6 channels are inhibited by SKF96365, 2-APB, Lanthanides and phorbol esters.

TRPC7. TRPC7 channels conduct preferentially divalent over monovalent cations with $P_{Ca}/P_{Na}=1.9$ for spontaneous currents and $P_{Ca}/P_{Na}=5.9$ for ATP-enhanced currents measured in HEK293 cells transfected with a TRPC7 mouse variant (Okada et al., 1999). These channels are activated by DAG, 20-HETE, store depletion, GPCR ($G_{q/11}$ -PLC β), changes in intracellular Ca^{2+} concentration, and TRPC7 channels are inhibited by La^{3+} , SKF96365, amiloride, 2-APB, flufenamic acid and phorbol esters.

Reported phenotypes from TRPC deficient mice. On the systemic level and up to the date only a few physiological roles for some TRPC channels based on the analysis of TRPC deficient mice have been proposed (see for review Freichel et al., 2005; Wu et al., 2010a).

TRPC1^{-/-} mice. From the analysis of TRPC1 deficient mice no differences in the pressure-induced constriction of cerebral arteries and no differences in SOCE from

smooth muscle cells were observed, but increased body weight in TRPC1^{-/-} mice was reported (Dietrich et al., 2007b). In contrast, it was reported that TRPC1^{-/-} mice have a reduced SOCE in salivary glands associated with reduced saliva secretion (Liu et al., 2007). In recent report it was claimed that TRPC1 deficiency led to an enhanced endothelium-derived hyperpolarizing factor (EDHF) type vasodilatation in resistance arterioles *in vivo* and also TRPC1 deficiency led to increased systolic blood pressure, observation from tail-cuff measurements under anesthesia from only four mice (Schmidt et al., 2010).

TRPC2^{-/-} mice. TRPC2 channels are important in pheromone signaling since an abnormal sexual and mating behavior was observed in TRPC2^{-/-} mice (Stowers et al., 2002; Kimchi et al., 2007).

TRPC3^{-/-} mice. TRPC3^{-/-} mice seem to develop normal but they have impaired walking behavior, and cerebellar Purkinje cells from these mice lack slow synaptic potentials and mGluR-mediated inward currents, a phenotype that was not observed in TRPC1/TRPC4 deficient mice (Hartmann et al., 2008). Another study of TRPC3 deficient mice showed the severity in acute pancreatitis induced by cerulein treatment was alleviated and pancreatic acini from these mice had diminished ROCE and SOCE related with altered exocytosis and intracellular trypsin activation (Kim et al., 2009).

TRPC4^{-/-} mice. TRPC4^{-/-} mice are fertile and have no signs of disease, but vascular endothelial cells from these mice have an impaired store-operated calcium function that leads to impaired agonist-induced vasorelaxation (Freichel et al., 2001). Similarly, calcium entry induced by thrombin stimulation is reduced in endothelial cells from lung of TRPC4 knockout mice, and it is associated with reduced vascular permeability in these mice (Tiruppathi et al., 2002), plus a reduced thrombin-induced activation of the nuclear factor- κ B (NF- κ B), factor that is important for the pathogenesis of inflammation and tissue injury (Bair et al., 2009). In other study using TRPC4 deficient mice was shown that serotonin-mediated *gamma*-Aminobutyric acid (GABA) release is altered in thalamic interneurons (Munsch et al., 2003).

TRPC5^{-/-} mice. TRPC5 deficient mice were recently reported by Riccio and coworkers (2009). TRPC5 mice breed and grow normally, and have no basic motor functions impairment; but, TRPC5^{-/-} mice have a diminished innate fear level linked to reduced responses mediated by synaptic activation of group I metabotropic glutamate and cholecystokinin 2 receptors in neurons from the amygdala.

TRPC6^{-/-} mice. Analysis of TRPC6 knockout mice showed that they are viable, fertile and have no obvious phenotype. These mice have an elevated blood pressure measured by telemetric devices that was correlated with enhanced agonist-induced contractility from isolated aortic rings and cerebral arteries, increased basal calcium entry in smooth muscle cells (SMC) and up-regulation of TRPC3 and TRPC7 expression (Dietrich et al., 2005). In another report it was shown that TRPC6^{-/-} mice do not present the acute hypoxic pulmonary vasoconstriction response, leading to partial occlusion of alveolar ventilation and provoking severe hypoxemia in these mice (Weissmann et al., 2006). In addition, TRPC6 knockout mice have increased airway hyperresponsiveness by metacholine, increased agonist-induced contractility of tracheal rings and TRPC3 upregulation in tracheal SMC, however, the allergic response in TRPC6 deficient mice was reduced (Sel et al., 2008). Our group analyzed TRPC6, TRPC4 and TRPC4/TRPC6 knockout mice and showed that both channels determine the muscarinic receptor-induced cation current in intestinal SMC, a finding that was associated with a slower intestinal transit in double knockout mice (Tsvilovskyy et al., 2009). It was recently reported that TRPC6 deficient mice have reduced exploration in open field and star maze experiments, postulating a role of TRPC6 in behavior (Beis et al., 2011).

TRPC7^{-/-} mice. TRPC7^{-/-} mice have not been reported so far.

3.2 Development of cardiac hypertrophy

Cardiac hypertrophy represents an increase of myocardial mass that is caused by a variety of stimuli. In many cases it is an adaptative response to an overload of the cardiovascular system. When the working load increases, the cardiomyocytes enlarge to preserve the cardiac function and the related remodeling process can be classified in three forms: 1) physiological hypertrophy, for example, associated with exercise or pregnancy; 2) developmental hypertrophy, which implies the normal cardiac growth during aging; and 3) pathological hypertrophy that is linked to disease-inducing stimuli and detrimental cardiac function states. Both the physiological and the developmental hypertrophy are characterized by homogeneous growth of ventricular wall and interventricular septum in proportion to the increase of heart chamber dimensions which is named eccentric hypertrophy. On the other hand, pathological hypertrophy or concentric hypertrophy is characterized by the increase in ventricular wall and septum thickness associated with a net decrease in ventricular chamber size and collagen accumulation (Gupta et al., 2007). In pathological conditions myocardial hypertrophy predisposes to

heart failure, arrhythmia and sudden death, and irrespective of mechanisms and loading conditions, the evolution of cardiac hypertrophy to ventricular dysfunction is an irreversible on-going process dependent upon several factors (Olivetti et al., 2000).

Models to study cardiac hypertrophy development and remodeling. Different experimental animal models have been described to study cardiac hypertrophy development and remodeling. Three of them have been reviewed by Gupta and collaborators (2007) and briefly described as: 1) pressure overload by banding of the ascending or abdominal aorta which creates a mechanically induced cardiac pressure overload. 2) Volume overload used to reproduce conditions observed in aortic and/or mitral valve regurgitant disease; in general the model is induced by an aorto-caval shunt and cardiac hypertrophy develops within 4–5 weeks with compromised left-ventricular contractility and increased end-diastolic pressure. 3) Transgenic mouse models in which altered expression of individual proteins leads to cardiac hypertrophy and remodeling. 4) In addition, the neurohumoral induced-hypertrophy models are used to mimic altered levels of substances like ATII or catecholamines which are involved in cardiac hypertrophy development (Grieve et al., 2006). A more detailed description about neurohumoral-induced hypertrophy is presented under section 3.2.2.

Signals that trigger the cardiac hypertrophy response. Between the initial triggering factors that lead to cardiac hypertrophy, there are two main groups: 1) biomechanical and stretch-sensitive mechanisms; and 2) neurohumoral mechanisms that are associated with release of hormones, cytokines and peptide growth factors. Cardiac hypertrophy is coupled with molecular and biochemical responses of different cardiac cell types such as cardiomyocytes and fibroblasts; it is related with changes in the expression profile and the reactivation of genes usually expressed only in the fetal heart such as atrial natriuretic peptide (ANP), B-type natriuretic peptide (BNP), and the cytoskeletal proteins α -actin and β -myosin heavy chain (Hannan et al., 2003). The metabolic remodeling and the altered energy demand produced during hypertrophy drives to an increase in the oxidative stress and disturbed calcium handling in cardiac myocytes (Zhang, 2002; Ritchie and Delbridge, 2006).

Different signaling pathways have been characterized from *in vitro* and *in vivo* models as mediators of the hypertrophic response, including signaling through GPCR (ATII receptors, ET-1 receptors, and adrenergic receptors), small GTPases (Ras, RhoA, and Rac), mitogen-activated protein kinase (MAPK) cascades, protein kinase C (PKC), Calmodulin kinase II (CaMKII), gp130-signal transducer and activator of transcription,

insulin-like growth factor I (IGF-I) receptor pathway, fibroblast growth factor and transforming growth factor β (TGF- β) receptor pathways, Ca^{2+} /calcineurin/NFAT signaling, among others (Sugden and Clerck, 1998; Molkenin and Dorn, 2001; Heineke and Molkenin, 2006).

The Ca^{2+} -Calcineurin-NFAT pathway in cardiac hypertrophy development. Calcium is an important second messenger in cardiac function. It is critical for the excitation-contraction coupling process that regulates the contraction and relaxation of the heart (Bers, 2002); but, calcium is also important in the activation of signal transduction pathways responsible for hypertrophic cardiac growth and heart failure, for example, controlling gene transcription by calcium/calmodulin dependent signaling (Frey et al., 2000; Frey et al., 2004; Roderick et al., 2007). One key integrator of the hypertrophy signaling regulated by calcium is the Ca^{2+} -calmodulin-activated phosphatase calcineurin (Wilkins and Molkenin, 2002). Molkenin and collaborators (1998) showed that the overexpression of an active form of calcineurin or of the Nuclear factor of activated T-cells 3 (NFAT3) in mouse heart produced cardiac hypertrophy and heart failure. This calcineurin-dependent hypertrophy was prevented by pharmacological blocking of calcineurin with Cyclosporine A (CsA). CsA also prevented cardiac hypertrophy in rats subjected to abdominal aortic banding (Sussman et al., 1998). Transgenic mice expressing a calcineurin inhibitory domain in the heart develop reduced hypertrophy induced by abdominal aortic banding or by isoproterenol infusion (De Windt et al., 2001), and mice deficient for the catalytic subunit β of calcineurin (CnA β) have reduced hypertrophy responses either induced by abdominal aortic banding, isoproterenol infusion or ATII infusion (Bueno et al., 2002). However, pharmacological blockage of calcineurin has failed to inhibit cardiac hypertrophy in some cases (Müller et al., 1998; review by Wilkins and Molkenin, 2004) and, additionally, in physiological hypertrophy models the NFAT-Calcineurin pathway is not a key component (Wilkins et al., 2004). It is postulated that NFAT is a mediator of calcineurin signaling as transcriptional effector; it has been shown that deletion of NFATc3 in mice produces a significant reduction in three hypertrophy models: Calcineurin transgene-induced hypertrophy, abdominal aortic banding or ATII treatment (Wilkins et al., 2002), and indeed, different NFAT isoforms are expressed in cardiomyocytes and regulate cellular hypertrophy (van Rooij et al., 2002).

Calcium sources that contribute to cardiac hypertrophy development. The mechanisms whereby calcium leads to calcineurin activation under repetitive calcium concentration changes during contraction cycle are still not completely understood, and the sources the calcium elevation are controversial (Houser, 2009). Houser and Molkenin

(2008) proposed that calcineurin-NFAT signaling and resultant pathological hypertrophy occurs in specific localized subcellular microdomains.

Beyond the calcium derived from Ca^{2+} -induced- Ca^{2+} release and from the sarcoplasmic reticulum during each contractility event, also plasmalemmal channel complexes that mediate Ca^{2+} -entry from the extracellular space into the cytosol have been postulated as mediators of the hypertrophic response (Wilkins and Molkentin, 2004; Molkentin 2006). Up to now there is evidence supporting all these different calcium entry pathways which probably regulate the calcineurin/NFAT-mediated cardiac hypertrophy.

1) L-type Ca^{2+} channels in special membrane domains. From experiments with neonatal rat ventricular myocytes (NRVM) it was shown that stretch induced calcineurin activity and cellular hypertrophy were suppressed by blocking L-type channels with nifedipine (Zobel et al., 2007). Besides this, calcineurin can bind to the C and N termini of L-type channels ($\alpha_11.2$) and its function is increased in NRVM expressing an active form of calcineurin (Tandan et al., 2009). In addition, in rat atrial preparations changes in pacing frequency increases basal Ca^{2+} levels without altering the amplitude of the Ca^{2+} transients, an observation linked to calcineurin-NFAT dependent activation and expression of the hypertrophy marker BNP (Tavi et al., 2004), following these observations, Colella and co-workers (2008) showed that in NRVM calcineurin/NFAT mechanisms are activated by changes in frequency of Ca^{2+} oscillations and NFAT activity was prevented by using Verapamil, a blocker of voltage-gated Ca^{2+} channels.

2) T-type calcium channels. Regarding T-Type channels Chiang and co-workers (2009) showed that $\text{Ca}_v3.2$ -/- mice or mice treated with ethosuximide as T-Type channel blocker did not increase cardiac mass after transverse aortic banding or ATII treatment. Furthermore, calcineurin activation induced by aortic banding was abolished in $\text{Ca}_v3.2$ -/- mice, but other hypertrophy associated effects like fibrosis development were similar to wild type mice. Curiously, the hypertrophic markers α -MHC, β -MHC, ANF, BNP were significantly enhanced in $\text{Ca}_v3.2$ deficient mice under these conditions.

3) Ca^{2+} release from the nucleus. Evidence supporting a role of Ca^{2+} pools independent from those linked to contraction events was presented by Wu and collaborators (2006) using adult rabbit cardiomyocytes, they proposed that ET-1 can produce a local Ca^{2+} release from the nucleus via InsP3-receptors which produces CaMKII activation and subsequent exporting of the transcription suppressor histone deacetylase (HDAC5) due to

phosphorylation, and finally the myocyte enhancer factor-2 (MEF2), which is associated with the hypertrophy development, is derepressed.

4) SOC entry alone or in conjunction with IP3R-mediated release from the endoplasmic reticulum. Among the Ca^{2+} pools independent from those linked to contraction it has been proposed that other hypertrophic Ca^{2+} source is SOCE through TRPC channels (Toko et al., 2007). This mechanism in cardiac myocytes is plausible since it was shown that SOCE contributes to the translocation of NFAT from the cytosol to the nucleus and to the development of cellular hypertrophy after ATII or PE stimulation in cultured NRVM (Hunton et al., 2002) and, furthermore, SOCE has been described in cardiomyocytes from adult rats (Hunton et al, 2004) and from mice (Nakayama et al., 2006), and in the mouse sinoatrial node (Ju et al., 2007). Also, several cation channels that exhibit features of TRPC channels were reported in cardiomyocytes.

However, reported evidence from different Ca^{2+} -pools contributing to the development of cardiac hypertrophy requires careful interpretation because as stated by House and Molkenin (2008): “microdomains in which Ca^{2+} -mediated signaling might take place could be very different in adult myocytes *in vivo* compared with cultured neonatal myocytes”. This also can be applied to transgenic models where the native protein levels are altered by over-expression of a determined protein; this can alter the normal interaction between protein partners, as well as the normal Ca^{2+} handling within the cells.

3.2.1 TRP channels in cardiac hypertrophy development

Expression of TRPC channels in the heart. TRPC proteins are proposed to mediate store-operated Ca^{2+} entry in cells of the cardiovascular system (Freichel et al., 1999). Indeed, the expression of several TRPs including all TRPC channels has been reported in the heart (Table i1) and in cardiomyocytes (Table i2). Although, the protein expression analysis of TRPCs reported so far did not include tests of antibody specificity with cells or tissue from TRPC-deficient mice, except in a work of Seth and coworkers (2009) that used heart lysates from wild type and TRPC1^{-/-} mice. More over, the purity of cardiomyocyte preparation used so far has not been clearly proven.

Table i1. Reported expression of TRPC channels in mammalian heart.

TRPC	Western blot	RT-PCR	References
TRPC1	X	X	Garcia and Schilling, 1997 (Rat) Kuwahara et al., 2006 (Mouse) Bush et al., 2006 (Human, only mentioned) Kunert-Keil et al., 2006 (Mouse) Ohba et al., 2006 (Mouse) Ohba et al., 2007 (Rat) Ju et al., 2007 (Mouse, atria and SAN) Shan et al., 2008 (Mouse) Seth et al., 2009 (Mouse, WT vs. TRPC1 ^{-/-} mice)
TRPC2	not defined	X	Kunert-Keil <i>et al.</i> , 2006 (Mouse) Ohba et al., 2006 (Mouse) Ju et al., 2007 (Mouse, SAN).
TRPC3	X	X	Garcia and Schilling, 1997 (Rat) Kuwahara et al., 2006 (Mouse) Bush et al. 2006 (Mouse and rat) Nakayama et al., 2006 (Mouse) Kunert-Keil et al., 2006 (Mouse) Ohba et al., 2006 (Mouse) Ohba et al., 2007 (Rat) Ju et al., 2007 (Mouse, atria and SAN) Shan et al., 2008 (Mouse) Seth et al., 2009 (Mouse, WT vs. TRPC1 ^{-/-} mice) Wu et al., 2010 (Mouse)
TRPC4	X	X	Garcia and Schilling, 1997 (Rat) Kuwahara et al., 2006 (Mouse) Bush et al., 2006 (Human, only mentioned) Ju et al., 2007 (Mouse, atria and SAN) Liu et al., 2009 (Rat) Seth et al., 2009 (Mouse, WT vs. TRPC1 ^{-/-} mice) Wu et al. 2010 (Mouse)
TRPC5	X	X	Bush et al., 2006 (Human) Ohba et al., 2007 (Rat) Liu et al., 2009 (Rat)
TRPC6	X	X	Garcia and Schilling, 1997 (Rat) Kuwahara et al., 2006 (Human and Mouse) Bush et al., 2006 (Human, mentioned only) Kunert-Keil et al., 2006 (Mouse) Ohba et al., 2006 (Mouse) Ohba et al., 2007 (Rat) Ju et al., 2007 (Mouse, atria and SAN) Seth et al., 2009 (Mouse, WT vs. TRPC1 ^{-/-} mice) Wu et al. 2010 (Mouse)
TRPC7	not defined	X	Kunert-Keil et al., 2006 (Mouse) Satoh et al., 2007 (Rat, northern blot) Ju et al., 2007 (Mouse, atria and SAN)

Expression analysis of TRPC proteins by Western blot analysis and/or transcripts by RT-PCR was described in this selection of reports in the heart. In any of these reports where the protein expression was analyzed by western blot were included protein preparations of TRPC deficient mice as control for antibody specificity, except for Seth et al., (2009). WT: wild type; SAN: Sino-Atrial Node.

Table i2. Reported expression of TRPC channels in mammalian cardiomyocytes.

TRPC	Western blot	RT-PCR	References
TRPC1	X	X	Nakayama et al., 2006 (Mouse, adult CM) Onohara et al., 2006 (NRVM, only mentioned) Ohba et al., 2007 (NRVM) Brenner and Dolmetsch, 2007 (NRVM) Ju et al., 2007 (Mouse, ICC of pacemaker cells) Seth et al., 2009 (Mouse, ICC of CM from WT and TRPC1-/- mice) Alvarez et al., 2008 (Rat, CM)
TRPC2	not defined	X	Brenner and Dolmetsch, 2007 (NRVM)
TRPC3	X	X	Onohara et al., 2006 (NRVM) Bush et al., 2006 (NRVM) Nakayama et al., 2006 (Mouse, adult CM) Kunert-Keil et al., 2006 (Mouse, in situ hybridization of CM) Brenner and Dolmetsch, 2007 (NRVM) Ju et al., 2007 (Mouse, ICC of pacemaker cells) Alvarez et al., 2008 (Rat, CM)
TRPC4	X	X	Onohara et al., 2006 (NRVM, only mentioned) Nakayama et al., 2006 (M, adult CM) Brenner and Dolmetsch, 2007 (NRVM) Ju et al., 2007 (Mouse, ICC of pacemaker cells) Alvarez et al., 2008 (Rat, CM)
TRPC5	X	X	Onohara et al., 2006 (NRVM, only mentioned) Nakayama et al., 2006 (Mouse, adult CM) Brenner and Dolmetsch, 2007 (NRVM)
TRPC6	X	X	Onohara et al., 2006 (NRVM, only mentioned) Kuwahara et al., 2006 (NRVM) Kunert-Keil et al., 2006 (Mouse, in situ hybridization of CM) Brenner and Dolmetsch, 2007 (NRVM) Ju et al., 2007 (Mouse, ICC of pacemaker cells)
TRPC7	X	X	Onohara et al., 2006 (NRVM) Brenner and Dolmetsch, 2007 (NRVM) Alvarez et al., 2008 (Rat, CM)

Expression analysis of TRPC proteins by Western blot analysis and/or transcripts by RT-PCR was described in this selection of reports in cardiomyocytes. Only Seth et al., (2009) used TRPC deficient mice as control for antibody specificity. CM: cardiomyocytes, NRVM: Neonatal Rat Ventricular Myocytes, ICC: Immunocytochemistry.

Proposed roles for TRPC channels in cardiomyocytes. A nonselective cation current (I_{ATP}) which exhibits several features of over-expressed TRPC3/C7 channels has been described in adult rat cardiomyocytes (Alvarez et al., 2008). An ATII-induced TRPC like current was measured in NRVM (Onohara et al., 2006). SOCE described in adult mouse cardiomyocytes was enhanced in cardiomyocytes with overexpression of TRPC3 channels (Nakayama et al., 2006). A nonselective current in adult mouse cardiomyocytes from hypertrophied hearts was attributed to TRPC1 channels (Seth et al., 2010). Increased expression of TRPC4/C5 and SOCE activity was observed when the type 2 Sarco-Endoplasmatic Reticulum Ca^{2+} -ATpase (SERCA2) was knockdown in neonatal cardiac myocytes (Seth et al., 2004). NFAT consensus sites in the promoter of the TRPC6 gene have been reported (Kuwahara et al., 2006), and currents with characteristics of TRPC channels have been reported in cardiac fibroblasts (Rose et al., 2007).

Concomitant with the expression analysis of different TRPC proteins in the heart there is evidence from *in vivo* and *in vitro* models proposing a role of these channels in cardiac hypertrophy and remodeling; for instance, the main models used so far are NRVM and transgenic mice overexpressing TRPC proteins in the heart. Several reports propose a contribution of TRPC-mediated Ca^{2+} entry and/or depolarization of the cell membrane to cellular hypertrophy of NRVM (Bush et al., 2006; Kuwahara et al., 2006; Onohara et al., 2006; Brenner and Dolmetsch, 2007; Nishida et al., 2007; Ohba et al., 2007). However, it is still lacking a causal link between TRPC protein function and cardiac hypertrophy development. In addition, specific agonists or antagonists that regulate cation entry mediated by individual TRPC proteins are not available.

In different rodent models of cardiac hypertrophy it has been reported increased expression of TRPC1 (Ohba et al., 2006; Ohba et al., 2007; Seth et al., 2009), TRPC2 (Ohba et al., 2006), TRPC3 (Bush et al., 2006; Ohba et al., 2006^{*}; Brenner and Dolmetsch, 2007; Seth et al., 2009; Koitabashi et al., 2010) and TRPC6 (Kuwahara et al., 2006; Ohba et al., 2006; Nishida et al., 2007; Seth et al., 2009; Koitabashi et al., 2010). Additionally, increased expression of TRPC1 and TRPC5 in human failing hearts (Sucharov and Bristow, 2005; Bush et al., 2006; Kuwahara et al., 2006), increased TRPC6 mRNA in human hearts with dilated cardiomyopathy (Kuwahara et al., 2006) and down regulation of TRPC4 in ventricular myocytes in biopsies from patients with ischemic cardiomyopathy based on a microarray screening (Gronich et al., 2010) were reported. Major observations related with these expression changes are presented below.

Knock-down of TRPCs in cardiomyocytes as cellular model. *In vitro* models using cardiac cells pointed that TRPC3 expression induces cellular hypertrophy in NRVM and it activates the calcineurin-NFAT signaling (Bush et al., 2006). It was shown using siRNA in NRVM that TRPC3 mediates the expression of ANP and BNP, but it does not mediate changes in cell size or beating frequency (Brenner and Dolmetsch, 2007). Similarly, in NRVM the ET-1 induced NFAT activation and protein synthesis were significantly reduced after treatment with siRNAs directed against TRPC6 (Nishida et al., 2007). From the mechanistic point of view it was proposed that stimulation of NRVM with ATII leads to the activation of TRPC3/TRPC6 channels through DAG, its activation causes slow increases in the membrane potential with the subsequent increase in L-type channel activity and, finally, dephosphorylation of NFAT by calcineurin (Onohara et al., 2006). In adult cardiomyocytes from TRPC3/TRPC6 (-/-)² mice it was shown that the peak of ATII-

^{*} In this report from Ohba et al. (2006) the expression of different TRPC channels was analyzed in transgenic mice overexpressing a dominant negative form of the Neuron-restrictive silencer factor (dnNRSF under α -MHC promotor) that exhibited dilated cardiomyopathy; they reported that TRPC3 protein levels were increased in these mice, but TRPC3 transcripts were decreased.

induced Ca^{2+} transients and ATII L-type currents observed in cells from wild type mice were abolished in cells from TRPC3/TRPC6 deficient mice (Klaiber et al., 2010). However, the mechanisms behind this reduction remain elusive and the contribution of individual TRPC proteins to agonist-induced Ca^{2+} entry or to membrane depolarization has not been demonstrated in primary adult cardiomyocytes.

Initial evidence pointing a role of TRPC1 channels in cardiac hypertrophy came from the fact that the TRPC1 murine gene has a NRSE (Neuron-Restrictive Silencer Elements)-like sequence; this kind of sequences are target of Neuron-Restrictive Silencer Factors (NRSF) that are involved in regulation of cardiac genes and cardiac remodeling. TRPC1 upregulation in transgenic α -MHC-dnNRSF mice was correlated with increased NFAT activity in NRVM overexpressing TRPC1 (Ohba et al., 2006). In NRVM it was shown that increases in cell size and in expression of ANP and BNP triggered by ET-1, ATII or PE, as well as the ET-1 induced SOCE were attenuated by TRPC1 knockdown (Ohba et al., 2007). Others reported that the hypertrophic response mediated by the serotonin receptor 5HT_{2A} was suppressed by TRPC1 knockdown (Vindis et al., 2010). Using NRVM it was proposed that TRPC7 channels could mediate the myocardial apoptosis response triggered by ATII (Satoh et al., 2007).

Role or TRPs in cardiac fibroblasts. Within the past years an increasing attention has been given to the role of cardiac fibroblasts which are involved in myocardial development and in pathologies characterized by changes in the extracellular matrix such as fibrosis. Fibroblasts regulate the environment in which cardiac myocytes are embedded through paracrine signaling by cytokines like IL-1, IL-6, $\text{TGF}\beta$, and also by direct communication from cell-to-cell interaction, and they have a critical role in cardiac hypertrophy, cardiac remodeling, and atrial fibrillation (Baudino et al., 2006; Souders et al., 2009; Kakkar and Lee, 2010). Expression of TRPC channels in cardiac fibroblasts has been reported (Table i3) but the functional role of TRPCs in cardiac fibroblasts is still unknown (Yue et al., 2011). In rat ventricular fibroblasts a non selective cation current triggered by stimulation of the C-type natriuretic peptide (CNP) receptors was characterized as sensitive to TRPC blockers and was linked to PLC and DAG signaling, and to TRPC expression in these cells (Rose et al., 2007). Spontaneous Ca^{2+} oscillations in human fibroblasts can be abolished by SOC blocking by La^{3+} or PLC inhibition (Chen et al., 2010) and it was reported that in atrial human fibroblasts a TRP protein (TRPM7) conducts the calcium responsible for fibroblast differentiation and proliferation by $\text{TGF-}\beta 1$ stimulation (Du et al., 2010). From experiments with rat fibroblasts TRPC6 has been postulated as regulator of ET-1 induced myofibroblast differentiation in neonatal cardiac fibroblasts; fibroblasts

expressing active $G\alpha_{12}$ or $G\alpha_{13}$ proteins or stimulated by ET-1 presented increased TRPC6 expression, enhanced Ca^{2+} influx and increased NFAT activation; these responses were reduced by knockdown of TRPC6, but interestingly, the myofibroblast formation was enhanced by TRPC6 inhibition (Nishida et al., 2007).

Table i3. Reported expression of TRPC channels in mammalian cardiac fibroblasts.

TRPC	Western blot	RT-PCR	References
TRPC1	not defined	X	Rose et al., 2007 (Rat, acute isolated) Nishida et al., 2007 (Rat, neonatal fibroblasts) Chen et al., 2010 (Human) Du et al., 2010 (Human atrial cells, Mouse)
TRPC2	not defined	X	Rose et al., 2007 (Rat, acute isolated)
TRPC3	X	X	Rose et al., 2007 (Rat, acute isolated) Nishida et al., 2007 (Rat, neonatal fibroblasts) Chen et al., 2010 (Human) Du et al., 2010 (Human atrial cells, Mouse)
TRPC4	not defined	X	Rose et al., 2007 (Rat, acute isolated) Chen et al., 2010 (Human) Du et al., 2010 (Human atrial cells, Mouse)
TRPC5	not defined	X	Rose et al., 2007 (Rat, acute isolated)
TRPC6	X	X	Rose et al., 2007 (Rat, acute isolated) Nishida et al., 2007 (Rat, neonatal fibroblasts) Chen et al., 2010 (Human) Du et al., 2010 (Human atrial cells, Mouse)
TRPC7	X	X	Rose et al., 2007 (Rat, acute isolated) Nishida et al., 2007 (Rat, neonatal fibroblasts)

Expression analysis of TRPC proteins by Western blot analysis and/or transcripts by RT-PCR was described in this selection of reports in cardiac fibroblasts. In any of these reports where the protein expression was analyzed by western blot were included protein preparations of TRPC deficient mice as control for antibody specificity.

Mouse models with cardiomyocyte-specific overexpression of TRPCs. In 2006 two independent groups showed that overexpression either of TRPC3 or TRPC6 proteins under control of the cardiomyocyte specific α -MHC promoter in mice leads to cardiac hypertrophy. Transgenic α -MHC-TRPC3 mice develop cardiac hypertrophy with aging. They present increased ATII/PE- and transverse aortic banding (TAC)-induced hypertrophy, associated with increased NFAT activation and increased SOCE; in addition, after 14 days of aortic banding TRPC3-transgenic develop cardiac failure (Nakayama et al., 2006). This hypertrophic phenotype was attenuated by the specific overexpression in cardiomyocytes of the Plasma Membrane Ca^{2+} ATPase 4b (PMCA4b); the authors interpreted this finding as a result of the removal of Ca^{2+} excess provoked by TRPC3 overexpression (Wu et al., 2009). Additionally, it was reported that a pyrazole compound (Pyr3) which blocks overexpressed TRPC3 channels can attenuate TAC-induced hypertrophy in mice (Kiyonaka et al., 2009). Since TRPC6 regulates and it is regulated by the calcineurin-NFAT pathway, Kuwahara and coworkers (2006) analyzed the effect of

TRPC6 overexpression in mouse cardiomyocytes. Transgenic α -MHC-TRPC6 mice with the higher expression levels die between 5-12 days after birth, possibly due to severe cardiomyopathy; transgenic mice with intermediate expression levels develop cardiomegaly and congestive heart failure around 30 weeks of age; and those mice with lower expression levels have no obvious defect, but they have a significant higher response to aortic banding measured by HW/BW.

From other two *in vivo* approaches it was postulated that cardiomyocytes from hypertrophied hearts after aortic banding have an increased Ca^{2+} influx or a non-selective current associated with TRPC channels and not L-type or the $\text{Na}^+/\text{Ca}^{2+}$ exchanger (Seth et al., 2009; Wu et al., 2010). The first approach attributed the non-selective current to TRPC1 channels because this current was not detected in cardiomyocytes from TRPC1^{-/-} mice; furthermore, TRPC1^{-/-} mice had reduced TAC- and ATII-induced hypertrophy responses (Seth et al., 2009). The second approach presented evidence showing that transgenic mice with specific cardiomyocyte expression of dominant-negative constructs either of TRPC3, TRPC4 or TRPC6 had reduced pathological hypertrophy induced by TAC or ATII/PE infusion, and also cardiomyocytes from some of these transgenic mice had reduced hypertrophy-induced Ca^{2+} entry (Wu et al., 2010b).

Not only TRPC channels from the TRP family, but also other members have been proposed to play role in pathological hypertrophy and cardiac remodeling. It was recently reported from our group that mice deficient for the TRPM4 channel are hypertensive, observation associated with higher circulating catecholamine levels and mild cardiac hypertrophy development at six months of age in TRPM4^{-/-} mice that could be secondary to hypertension (Mathar et al., 2010). A second example came from mice overexpressing TRPV2 under a cardiac promoter; these mice exhibit enlarged hearts, increased fibrosis and myocardial structural defects, depending on expression levels (Iwata et al., 2003).

3.2.2 Neurohumoral induced cardiac hypertrophy

In hypertrophy experiments with rodents neurohumoral agonists such as ATII or isoproterenol (Iso) have effects on: 1) heart weight, 2) cardiomyocyte size, 3) cardiac fibrosis, 4) blood pressure, 5) heart rate, 6) circulating or local components of the Renin-Angiotensin-Aldosterone System (RAAS) and cytokines, 7) cardiac contractility and 8) body weight. A summary of these effects produced by different doses of isoproterenol and ATII is presented below.

Cardiac hypertrophy induced by chronic isoproterenol infusion. A wide range of isoproterenol doses has been described to study the effect of β -adrenergic stimulation on the cardiovascular system. From a selection of reports the isoproterenol effects can be summarized as follows:

1) Effects of isoproterenol infusion on heart weight. Changes in heart weight are analyzed by hypertrophy indexes such heart weight/body weight (HW/BW) and heart weight/tibia length (HW/TL). In mice treated with Iso in a range of doses among 0.027 and 120mg/kg/day used from 7 up to 14 days the HW/BW and the HW/TL index were increased between 24% and 61% (Friddle et al. 2000; Rothermel et al., 2000; De Windt et al., 2001; Bueno et al., 2002; Braz et al., 2003; Kedzierski et al., 2003; Vega et al., 2003; Patterson et al., 2004; Song et al., 2006; Zhang et al., 2007; Shen et al., 2008). A dose of 30mg/kg/day Iso produced increases between 31% and 59% in HW/BW after 5 days (Jaffré et al., 2004; Monassier et al., 2008). The same dose produced increments in HW/BW between 20% and 25% after 7 days (Keys et al., 2002; Maass et al., 2004) or increments of 17% after 14 days (Iaccarino et al., 1999). Isoproterenol-induced cardiac hypertrophy in rats has been also reported (Hayes et al., 1984; Allard et al., 1990; Kitagawa et al., 2004; Shizukuda et al., 1998).

2) Effects of isoproterenol infusion on cardiomyocyte size. Isoproterenol in mice applied between 0.672 and 30mg/kg/day during 7 to 14 days produced increments of 30% to 70% in cardiomyocyte size (Iaccarino et al., 1999; Friddle et al. 2000; Zhang et al., 2007; Shen et al., 2008). Similar increments were reported in rats (Kitagawa et al., 2004).

3) Effects of isoproterenol infusion on cardiac fibrosis. Cardiac fibrosis is measured by changes in the mRNA expression of collagen or by staining of collagen fibers by Sirius red or Masson's Trichrome. In mice a dose of 15mg/kg/day (7 days) produced no fibrosis evidence (Friddle et al. 2000) but the same dose after 11 days generated a 2 times higher expression of collagen in the heart (Zhang et al., 2007). Doses of 30 or 60mg/kg/day (7 to 26 days) also produced fibrosis in mice (Kudej et al., 1997; Bueno et al., 2002; Wang et al., 2005; Wittköpper et al., 2010). Isoproterenol treatment can also increase cardiac fibrosis in rats (Allard et al., 1990; Shizukuda et al., 1998; Kitagawa et al., 2004).

4) Effects of isoproterenol infusion on blood pressure. Systolic blood pressure (SBP) measured by tail-cuff in mice treated with 15mg/kg/day (11 days) or 30mg/kg/day Iso (5 days) was not significantly different (Zhang et al., 2007; Monassier et al., 2008). From

blood pressure measurements via carotid catheterization it was observed that 30mg/kg/day (7 days) produced an increment of 40mmHg in mean arterial pressure (MAP) (Keys et al., 2002). In rats it was reported that isoproterenol increased (Allard et al., 1990), decreased (Leenen et al., 2001) or had no effect on blood pressure (Kitagawa et al., 2004; Shizukuda et al., 1998; Nagano et al., 1992).

5) Effects of isoproterenol infusion on heart rate. Doses between 15 and 30mg/kg/day used in a period of 5 to 14 days raised heart rate in mice between 23% and 56% (Jaffré et al., 2004; Zhang et al., 2007; Monassier et al., 2008; Wittköpper et al., 2010). Comparable results were reported in rats (Allard et al., 1990; Nagano et al., 1992; Leenen et al., 2001).

6) Effects of isoproterenol on circulating or local RAAS components and cytokines.

In mice, 30mg/kg/day (5 or 7 days) produced increments in plasma levels of Interleukin-1 β (IL-1 β), IL-6, tumor necrosis factor- α (TNF α) and TGF- β 1 (Jaffré et al., 2004; Jaffré et al., 2009). In rats it was observed that isoproterenol increased Aldosterone serum levels (Allard et al., 1990) and produced augmentation of plasma and cardiac ATI and ATII concentrations, and plasma and ventricular renin activity (Leenen et al., 2001; Nagano et al., 1992).

7) Effects of isoproterenol on cardiac contractility. It was reported that in mice 15mg/kg/day (10 days) produced an increase of peak velocity of left outflow tract and a decrease of the ejection time in echocardiography measurements (Kedzierski et al., 2003). A dose of 30mg/kg/day (7 days) reduced significantly both fractional shortening and systolic ejection volume in mice (Jaffré et al., 2009).

8) Effects of isoproterenol on body weight. It was reported that in mice a dose of 15mg/kg/day (7 days) of isoproterenol produced no changes in body weight (Friddle et al. 2000). However, with 30mg/kg/day (13 days) a significant increase of 22% in body weight from treated mice was observed, and it was associated with gain of brown fat and muscle, and higher food intake (Kudej et al., 1997).

Mechanisms contributing to the isoproterenol induced cardiac hypertrophy.

Isoproterenol has a direct effect on the heart increasing the heart frequency (positive chronotropic) and also the contraction force (positive inotropic). Beyond this, isoproterenol can stimulate cardiac fibroblast leading to the secretion of growth factors involved in cardiac hypertrophy development. Isoproterenol stimulates renin secretion from kidneys resulting in an increase on circulating levels of angiotensin II that can act on the heart

stimulating cardiomyocytes and fibroblasts. It also may affect blood pressure by direct effects on blood vessels and by increasing circulating angiotensin II. Changes in blood pressure might also be involved in cardiac hypertrophy development. In addition, mast cells within the heart can produce Renin and mediate the conversion of AT I to AT II by action of the enzyme chymase (Reid et al., 2007). Then, mast cells also contribute to the production of AT II that stimulates cardiac myocytes and fibroblasts leading to the hypertrophy development.

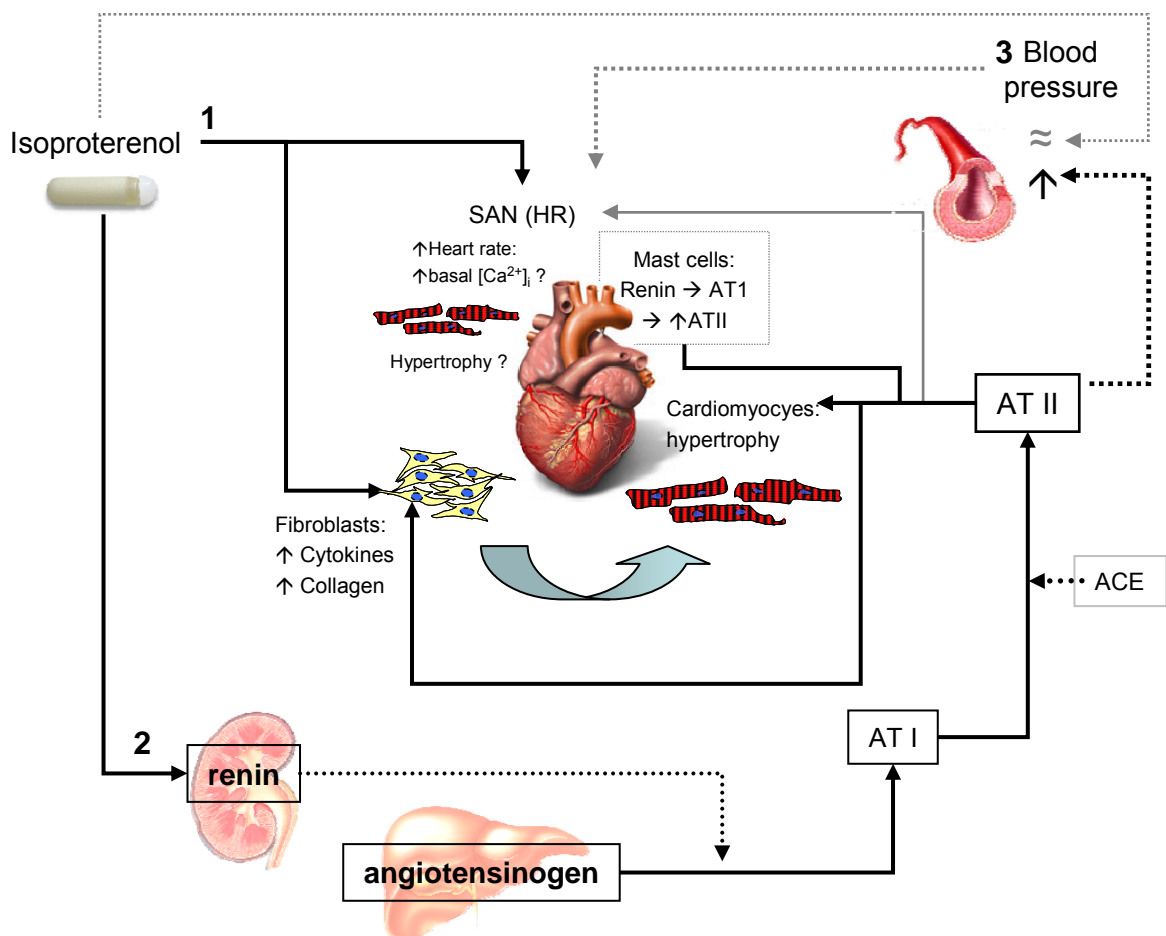


Figure i1. Pathways contributing to the isoproterenol-induced cardiac hypertrophy. 1. Isoproterenol has a direct effect on the heart 2. Isoproterenol stimulates renin secretion from kidneys resulting in an increase on circulating levels of angiotensin 3. Isoproterenol may affect blood pressure directly and by increasing circulating angiotensin II. AT I: Angiotensin I; AT II: Angiotensin II; ACE: Angiotensin Converting Enzyme.

Other effects during the isoproterenol-induced hypertrophy are the increment of cardiac reactive oxygen species (ROS) (Monassier et al., 2008), the decrease in β -adrenoreceptor density and in Adenylyl cyclase activity in the heart (Kudej et al., 1997) and reduced cardiac NFAT activity (Nakayama et al., 2006). Finally, an important contribution to

understand the mechanisms behind isoproterenol-induced hypertrophy was made by the group of L. Maroteaux. They showed that the direct isoproterenol stimulation to the cardiomyocytes is not responsible for the hypertrophic growth. They proposed that the isoproterenol stimulates the non cardiomyocyte cells, possibly cardiac fibroblast, and that these cells mediate the hypertrophy development through the secretion of different cytokines (IL-1 β , IL-6, TNF- α and TGF- β 1) and ATII signaling controlled by the serotonin receptor 5-HT_{2B} on these cells (Jaffré et al., 2009). A schematic summary about the pathways contributing to the isoproterenol-induced cardiac hypertrophy is presented in Figure i1.

Cardiac hypertrophy induced by chronic Angiotensin II infusion. Different ATII doses to induce cardiac hypertrophy have been reported; in general, ATII produces smaller increments in cardiac mass, but it produces higher fibrosis and blood pressure elevation. Some effects mediated by ATII that contribute to hypertrophy are also mentioned in Figure i1. From several reports the effects of different ATII regimes are summarized:

1) Effects of ATII infusion on heart weight. ATII applied between 0.2 and 4.6mg/kg/day in a period around one to four weeks generate increments in HW/BW between 5% and 31% when applied to mice (Friddle et al., 2000; Bendall et al., 2002; Braz et al., 2003; Kedziński et al., 2003; Francois et al., 2004; Crowley et al., 2006 ; Frank et al., 2007; Kilié et al., 2007; Tozakidou et al., 2010). A dose of 3 mg/kg/day (14 days) produced in mice a 19% increase in HW/BW (Song et al., 2006). In mice, reported increments in HW/TL treated with 0.3 or 0.432mg/kg/day ATII during 14 days were 20% (Pillai et al., 2006) and 14% to 19% (Bueno et al., 2002; Wilkins et al., 2002), respectively. Also it has been reported that ATII applied to produced similar increases in hypertrophy indexes (Harada et al., 1998; Phillips, 1999; Moser et al., 2002; De Smet et al., 2003; Huentelman et al., 2005).

2) Effects of ATII infusion on cardiomyocyte size. ATII increases cardiomyocyte size in mice from 10% to 30% when applied between 0.3 and 1.44mg/kg/day over 14 days (Bendall et al., 2002; Stagg et al., 2004; Pillai et al., 2006; Frank et al., 2007; Kilié et al., 2007).

3) Effects of ATII infusion on cardiac fibrosis. ATII produces increments in cardiac fibrosis when applied in mice. ATII doses between 0.006 and 1.44mg/kg/day applied from 7 up to 21 days produced significant increments between 60% and 600% in cardiac

fibrosis (Ichihara et al., 2001; Kuriso et al., 2003; Crowley et al., 2006). ATII also induced a significant increase of myocardial fibrosis in rats (Huentelman et al., 2005).

4) Effects of ATII infusion on blood pressure. From measurements of blood pressure by tail cuff in mice receiving a wide ATII dose range between 0.006 and 3mg/kg/day it has been reported either no effects or increasing effects (Ichihara et al., 2001; Bendall et al., 2002; Bueno et al., 2002; Gavazzi et al., Francois et al., 2004; 2006; Pillai et al., 2006; Kilié et al., 2007; Chiang et al., 2009). Only a few groups reported telemetric measurements of blood pressure in conscious mice during ATII infusion. It was reported that 0.15mg/kg/day (21 days) is as a sub-pressor dose (Brancaccio et al., 2003). In contrast, 1.44mg/kg/day ATII (21 days) showed the maximum increment after 3 days of about 46mmHg in MAP that was maintained over the treatment (Crowley et al., 2006). Similarly, 4.61mg/kg/day ATII (14 days) changed MAP by 21mmHg after 24h and maintained an increase of about 37 mmHg (Tozakidou et al., 2010). Also telemetric recordings of MAP in rats have been reported (Phillips, 1999; De Smet et al., 2003).

5) Effects of ATII infusion on heart rate. In mice 0.2mg/kg/day (Monassier et al., 2008) or 1.44mg/kg/day ATII applied for 14 days (Kuriso et al., 2003) did not alter heart rate. But in other report 1.3mg/kg/day ATII (28 days) decreased heart rate (Francois et al., 2004). In rats ATII either has no effect or increases heart rate (De Smet et al., 2003).

6) Effects of ATII on circulating or local RAAS components or cytokines. In mice it was observed that ATII reduced the kidney renin mRNA (Tozakidou et al., 2010). In rats ATII changes in plasma renin activity, plasma aldosterone and plasma ET-1 have been reported (De Smet et al., 2003).

7) Effects of ATII infusion on cardiac contractility. A dose of 1.3mg/kg/day ATII (28 days) produced in mice evidence of heart failure and 40% mortality (Francois et al., 2004); however, it was reported that 1.44mg/kg/day ATII (14 days) produced no evidence of edema in mice (Stagg et al., 2004).

8) Effects of ATII infusion on body weight. ATII can alter differently the body weight in mice. A dose of 0.288mg/kg/day (14 days) produced in mice no changes in body weight (Fridde et al., 2000); however, 1.44mg/kg/day ATII after 5 days produced a significant increase in body weight (Crowley et al., 2006). On the other hand, higher doses between 3 and to 4.6 mg/kg/day (7 to 14 days) produced weight loss (Gavazzi et al., 2006;

Tozakidou et al., 2010). In rats a reduction of body weight was reported and in some cases attributed to a reduced food intake (Brink et al., 1996; Ju et al., 1996).

Other neurohumoral-induced cardiac hypertrophy models. Neurohumoral-induced cardiac hypertrophy models using other agonists have been reported with increasing effects on HW/BW between 7% to 38%; some groups reported the use of Phenylephrine (PE) (Iaccarino et al., 1999; Braz et al., 2003; Maass et al., 2004; Niizeki et al., 2008), Nor-epinephrine (Maly et al., 2001; Moser et al., 2002; Keys et al., 2002) or in multiple combinations as PE plus ATII (Nakayama et al., 2006; Van Berlo et al., 2010; Wu et al., 2010b) or isoproterenol combined with PE (Saadane et al., 2000; Maass et al. 2004).

3.3 Platelet's function

3.3.1 Platelet's signaling and thrombosis

The hemostatic system has evolved to keep blood flowing under physiological conditions, but also to react rapidly to vessel injury by clotting. Platelets, also named thrombocytes, derive from Megakaryocytes, circulate in blood and are critical for primary hemostasis. Platelets are important for the formation of blood clots or primary hemostasis, as platelet aggregates are an essential constituent of the arterial thrombus, and as a platform for activation of coagulation proteins like thrombin and fibrin via the intrinsic pathway (Colman, 2006). In blood vessels that are damaged by atherosclerotic lesions platelets are activated leading to formation of a thrombus which can detach and finally occlude vessels in heart and brain causing myocardial infarction and stroke; this is thought to occur when the equilibrium of normal hemostasis is broken due to impaired anti-coagulant mechanisms or these mechanisms are overwhelmed by the severity of the initial injury (Mackman, 2008).

Signaling that initiates and modulates thrombus formation. The formation of the platelet plug can be explained in three phases: initiation, extension and perpetuation.

Initiation phase. After blood vessel injury, platelets are rapidly recruited to the injury site to form a monolayer through the interaction of specific platelet cell-surface receptors integrin $\alpha_1\beta_1$ and GPVI with collagen and GPb/IX/V complex and integrin $\alpha_{IIb}\beta_3$ (also known as GPIIb-IIIa) with the von Willebrand factor.

Extension phase. After the formation of the platelet's monolayer on the vessel wall the receptor-mediated binding of additional platelets leads to platelet aggregation which results in rapid growth of the thrombus. At this stage platelets become activated; important in this phase are the rapid responses of surface receptors to soluble agonists such as Thrombin, ADP and TxA₂. A major pathway of activation involves the cleavage and, consequently, the activation of protease-activated receptors (PAR) by thrombin, which is activated by the blood coagulation cascade. Activated platelets then release the content of their granules including ADP, Serotonin, ATP and Calcium, which further promotes the amplification of the coagulation response by platelet recruitment, adhesion and aggregation.

Perpetuation phase. This phase includes the late events of clot formation that stabilize the platelet plug, prevent premature disaggregation and regulate clot retraction. In addition, during the coagulation cascade fibrin is produced and this step is important for the stabilization of the thrombus (Abrams, 2005; Woulfe et al., 2006; Jackson, 2007).

Agonists involved in platelet activation. Platelet activation and aggregation signaling are mediated by different agonists, including collagen, ADP, TxA₂ and Thrombin; the agonist-induced inside-out activation of integrin complex $\alpha_{IIb}\beta_3$ is considered the final common pathway of platelet activation, mandatory for primary hemostasis and occlusive thrombus formation (Hagedorn et al., 2010). Collagen can act through GPVI-Fc γ -chain signaling and PLC γ (Watson et al., 2001; Samaha and Kahn, 2006). ADP, TxA₂ and Thrombin, in turn, stimulate GPCRs on the platelet surface that are critical to initiation of various intracellular signaling pathways, including activation of PLC β by heteromeric G_q-proteins (Offermanns et al., 1997). In both cases, there are various common intracellular signaling pathways, including activation of PLC, PKC, and phosphoinositide (PI)-3 kinase, and DAG formation. Both, calcium and PKC contribute to activation of small G proteins which are important for fibrinogen binding (Crittenden et al., 2004; Smyth et al., 2009). Beyond G_q proteins, other heteromeric G-proteins are involved in platelet signaling, for example, ADP also stimulates P2Y₁₂ receptors which are coupled to G_i proteins (Wettschureck and Offermanns, 2005).

ADP receptors in platelets. P2Y₁ ADP receptors are receptors coupled to G_q proteins and its activation leads to elevation of the intracellular Ca²⁺ concentration; ADP P2Y₁₂ receptors are G_i coupled receptors and its activation decreases cyclic adenosine monophosphate (cAMP) formation, but it does not produce elevation of the intracellular Ca²⁺ concentration (Offermanns, 2006). In platelets from mice deficient for the G_q coupled

ADP receptor P2Y₁ the ADP-induced increase in intracellular Ca²⁺ concentration as well as the platelet shape change are absent, but the ADP inhibition of cAMP formation is preserved. Platelets from P2Y₁^{-/-} mice do not aggregate *in vitro* after stimulation with different concentrations of ADP and also they have impaired responses after stimulation with some concentrations of collagen, thrombin or the thromboxane analogue U46619, possibly due to impaired amplification of the aggregation response mediated by the secreted ADP after stimulation with these three agonists. P2Y₁^{-/-} mice have prolonged tail bleeding times and are protected from thromboembolism induced by collagen and ADP injection. This observation was related to reduced thrombin generation in the knockout mice (Fabre et al., 1999; Léon et al., 1999; Léon et al., 2001). In contrast, platelets deficient for the G_i coupled ADP receptor P2Y₁₂ have normal elevation of the intracellular Ca²⁺ concentration and shape change after ADP stimulation, however this stimulus does not inhibit the cAMP formation. In addition, P2Y₁₂ deficient platelets have impaired collagen and thrombin induced *in vitro* aggregation, and P2Y₁₂ deficient mice have prolonged bleeding times and thrombi formation and stability are impaired (Foster et al., 2001; André et al., 2003).

Thromboxane A₂ receptor in platelets. Platelets deficient for the TxA₂ prostanoid receptor TP, which is coupled to G_q or G₁₂/G₁₃ proteins, do not aggregate after stimulation with the TxA₂ receptor agonist U46619. Mice lacking the TP receptor have prolonged tail bleeding times and different to WT mice they do not have the cardiovascular collapse and sudden death associated with systemic platelet aggregation, pulmonary thrombosis and coronary spasm induced by intravenous injection of U46619 or arachidonic acid (Thomas et al., 1998; Cheng et al., 2002).

Thrombin receptors in platelets. Thrombin acts on platelets through PAR receptors which are coupled to different G proteins. In human platelets are expressed PAR1 and PAR4 receptors that are coupled in most cases to G_q, G₁₂/G₁₃ proteins. In mice PAR4 receptors are also expressed and are coupled to G_q, G₁₂/G₁₃ proteins; in addition, in murine platelets the PAR3 receptor is expressed and its believed to function as a cofactor for cleavage and activation of PAR4 and it does not mediate transmembrane signaling by itself (Kahn et al., 1999; Nakanishi-Matsui et al., 2000; Offermanns, 2006). Platelets from PAR4 deficient mice show increase in the intracellular Ca²⁺ concentration, no shape change, ATP secretion or aggregation in response to thrombin. PAR4 KO mice have extended bleeding times and are protected from thrombosis in a model of arteriolar thrombosis using mesenteric arteries (Sambrano et al., 2001). Platelets deficient for the thrombin receptor PAR3 have impaired aggregation and ATP secretion induced by

thrombin, but bleeding times in the mice were reported normal (Kahn et al., 1998). Others reported that PAR3 deficient mice have prolonged bleeding times, defects in thrombus formation and are protected against thromboembolism (Weiss et al., 2002).

Collagen receptors in platelets. Collagen acts on the GPVI which triggers the activation of PLC γ . Collagen and the Collagen Related Peptide (CRP) stimulation can produce changes in the intracellular Ca²⁺ concentration of platelets (Roberts et al., 2004; Varga-Szebao et al., 2008a). From the analysis of platelets deficient for GPVI is known that they have abolished *in vitro* aggregation triggered by collagen, and impaired aggregation induced by convulxin and by ADP; GPVI deficient platelets do not adhere *in vitro* to collagen; however, GPVI^{-/-} mice have no defective tail bleeding times and are only partially protected to pulmonary thromboembolism trigger by collagen/epinephrine injection (Kato et al., 2003; Lockyer et al., 2006)

The understanding of the signaling involved in thrombus formation and coagulation permitted the development of pharmacological strategies to inhibit different steps of platelet aggregation. Current pharmacological strategies to prevent thrombus formation have been focused on the use of anticoagulants such as heparin and the following three classes of inhibitors of platelet aggregation: 1) Acetyl Salicylic Acid (ASA) or aspirin, which inhibits irreversibly the thromboxane production by blocking the Cox-1 enzyme; 2) Thienopyridines, such as Clopidogrel or Ticlopidine, that irreversible inhibit the ADP receptor P2Y₁₂ then reducing the amplification of the aggregation response by released ADP; and 3) GPIIb-IIIa or integrin $\alpha_{IIb}\beta_3$ antagonists (integrilin, abciximab and tirofiban) that bind to the integrin on unstimulated platelets and on platelets after stimulation, but are administrated only in acute coronary syndromes or after coronary artery interventions (Phillips et al., 2005; Mackman, 2008). Despite the positive outcome reached with the actual pharmacological strategies to regulate platelet function and in the prevention of arterial thrombosis, there are restrictions like limited efficacy and safety. Therefore, it is necessary to consider additional strategies to find new drug targets which can be identified by the analysis of mice with targeted disruption of proteins expressed in platelets (Jackson and Schoenwaelder, 2003; Nieswandt et al., 2005).

Calcium signaling involved in platelet activation. One important aspect of platelet activation is the calcium entry that is triggered by the above mentioned agonists ADP, TxA₂, thrombin and also collagen. Elevation of the intracellular Ca²⁺ concentration is required for platelet activation and it is increased by depletion of intracellular Ca²⁺ stores and Ca²⁺ influx from the extracellular medium; furthermore, calcium signals between adherent platelets through platelet-platelet contacts serve to propagate the signaling

through the developing thrombus (Nesbitt et al., 2003). Most platelet agonists are able to release stored Ca^{2+} from the dense tubular system, and as in other cells the activation of PLC isoforms and generation of IP3 which activates IP3 receptors leads to the subsequent release of Ca^{2+} from intracellular stores. This mechanism is reasonably well understood, but much less is known about the generation of Ca^{2+} influx in platelets (Rink and Sage, 1990; Sage 1997). Calcium influx in non-excitabile cells mainly is regulated by depletion of intracellular Ca^{2+} stores and subsequent Ca^{2+} entry (SOCE); this mechanism has been also described in platelets (Rosado and Sage, 2002; Rosado et al., 2004), but beyond SOCE other calcium entry mechanisms independent of Ca^{2+} -store depletion, like Receptor Operated Calcium Entry or ROCE, are present in platelets (Rosado and Sage, 2000a) and are regulated differently by distinct PKC isoforms (Gilio et al., 2010a; Harper and Poole, 2010).

STIM1 and Orai1. Recently, it has been postulated that two new proteins, the Stromal Interaction Molecule 1 (STIM1) and Orai1 (CRACM1), are essential components of the SOCE in non-excitabile cells, especially in cells from the immune system like lymphocytes. STIM1 senses the Ca^{2+} content of intracellular stores through the presence of an EF-hand domain that binds Ca^{2+} and it is projected into the lumen of the store. After store depletion, Ca^{2+} is released from the EF-hand domain, and STIM1 moves to the plasma membrane to activate the plasma membrane SOCE channel, Orai1. Orai1 belongs to a family of channel proteins that have four putative transmembrane domains and contain the pore forming subunits of SOCE channels in some cell types (see for review Cahalan et al., 2007; Parekh, 2010). In platelets both STIM1 and Orai1 are expressed.

Role of STIM1 in platelets. Platelets from mice expressing an activating EF hand motif of STIM1 have increased intracellular Ca^{2+} levels that end up in a pre-active state of platelets resulting in defective collagen responses; in addition, STIM1 mutant heterozygous mice ($\text{Stim1}^{\text{Sax/+}}$) have reduced platelet counts, prolonged bleeding times and defective thrombus formation (Grosse et al., 2007). STIM1 deficient platelets have defective SOCE triggered by Thapsigargin (TG), reduced agonist-induced Ca^{2+} entry and diminished *in vitro* aggregation induced by collagen, but not by ADP or thrombin. Wild type mice transplanted with bone marrow cells from STIM1^{-/-} mice were protected from arterial thrombosis without presenting higher bleeding times (Varga-Szabo et al., 2008a).

Role of Orai1 in platelets. Mouse platelets deficient in Orai1 have reduced SOCE induced by TG treatment. These platelets have also defects in agonist-induced Ca^{2+} entry. In Orai^{-/-} platelet activation, granule release and *in vitro* aggregation induced by

stimulation of the GPVI pathway with collagen or a CRP were impaired; however, after ADP or thrombin stimulation these parameters were normal in Orai^{-/-} platelets. Mice transplanted with bone marrow cells from Orai^{-/-} mice presented reduced cerebral ischemia and no differences in tail bleeding times (Braun et al., 2009). In humans a mutation of Orai1 (Orai1^{R91W}) proteins is present in patients with severe combined immunodeficiency (SCDI) and it abrogates SOCE and CRAC channel currents in T cells. Using mice transplanted with fetal liver cells from a mouse model expressing a mutated inactive form of Orai1 (Orai1^{R93W}) equivalent to the one presented in humans, it was shown that Orai1^{R93W/R93W} platelets have reduced SOCE after TG stimulation and reduced calcium entry after stimulation of PAR4 or GPVI receptors, but the aggregation responses *in vitro* induced by collagen, ADP or PAR4 activating peptide were similar to control platelets (Bergmeier et al., 2009).

Stim1 and Orai1 are not the only components SOCE in platelets. Further analysis of platelets deficient for STIM1 or Orai1 supported the evidence of impaired GPVI-dependent Ca²⁺ signaling and phosphatidylserine exposure, but only in the absence of thrombin as co-stimulatory factor. In addition, SKF96365 which blocks cation channels and TRPC-mediated cation entry among other channels (Singh et al., 2010) was able to inhibit Ca²⁺ and procoagulant responses in STIM1 or Orai1 deficient platelets, pointing for a second Ca²⁺ entry involved in these pathways, and not related with STIM2 because platelets deficient for this protein have unaffected GPVI-dependent Ca²⁺ signaling and thrombus formation (Gilio et al., 2010b). Therefore, Orai1-mediated Ca²⁺ entry is particularly important for GPVI-ITAM-mediated platelet activation by collagen, but not for agonists acting on G-protein coupled receptors, such as thrombin or ADP. Platelet activation through GPCRs would require an additional Ca²⁺ entry than Orai1 which could be formed by TRPC proteins (Authi, 2009). Indeed, it has been shown in HEK-293 cells that STIM1 can gate TRPC1 or TRPC3 channels (Huang et al., 2006; Zeng et al., 2008); and, in human platelets has been proposed that STIM1 and Orai1 interacts with different TRPC channels (C1, C3 or C6) to modulate SOCE and non-SOCE triggered by thrombin or ADP stimulation (López et al., 2006; Jardín et al., 2008a; Jardín et al., 2009; Galán et al., 2009).

3.3.2 TRPC channels and platelet's function

Expression of TRPC channels in platelets. Almost all TRPC channels have been found to be expressed in human and mouse platelets (Table i4), and also in their precursor cells,

megakaryocytes (Table i5). It has been proposed that in human platelets different TRPC1 proteins can interact (Brownlow and Sage, 2005). But the expression and function of TRPCs in platelets is still a controversial topic, especially due to the specificity of the antibodies used and lack of proper controls (Sage et al., 2002; Authi et al., 2002; Varga-Szabo et al., 2008b). Expression of TRPC in megakaryocytes is mentioned in addition because primary megakaryocytes are regarded as a *bona fide* surrogate for studies of platelet signalling, including patch clamp recordings of ionic conductances (Carter et al., 2006).

Proposed roles for TRPC channels in human platelets. Until now, the function of TRPC channels in platelets has been principally investigated in human platelets and only little is known about their role in murine platelets (Authi, 2007; Dietrich et al., 2010). Much less is known about the individual contribution of TRPC proteins for Ca^{2+} entry in platelets due to the lack of specific agonists or antagonists for these proteins. One of the firsts reports only linked the expression of TRPC channels (C1, C4 and C6) in human platelets with the SOCE evoked by thapsigargin or by thrombin in these cells (den Dekker et al., 2001).

TRPC1. Studies carried out on human platelets and TRPC1 proteins proposed it as an important part of the Ca^{2+} entry by SOCE, since it was shown, first, that both the SOCE in human platelets and the coupling between IP3R type II with TRPC1 proteins were inhibited by blockage of IP3Rs (Rosado and Sage, 2000b; Rosado and Sage, 2001). Second, the calcium entry in human platelets to refill the stores after thapsigargin or thrombin treatment was blocked by pre-incubation of platelets with an antibody against an extracellular epitope of the hTRPC1 channel (Rosado et al., 2002; Harper and Sage, 2007). It remains to be shown whether this antibody selectively blocks hTRPC1 channels.

TRPC4. TRPC4 expression in human platelets has been reported and it was postulated to be the part of the pH-dependent SOC entry of human platelets and megakaryocytes, because the SOCE observed in platelets after raising the cytoplasmic pH was blocked by the unspecific channel blocker SKF96635 (Wakabayashi et al., 2006).

TRPC6. TRPC6 channels are also expressed in human platelets and it was proposed that TRPC6 is a SOCE-independent and nonselective cation entry channel stimulated by thrombin and OAG. (Hassock et al., 2002). Another group suggested that TRPC6 channels are important for both SOCE and store independent calcium entry in human platelets, based on the observation that an antibody against hTRPC6 reduced Ca^{2+} and Mn^{2+} entry (Jardín et al., 2008b). However, the specificity of these antibodies has not been

demonstrated so far. TRPC6 proteins were also linked to the increased OAG-induced Ca^{2+} entry in platelets triggered by very high glucose concentrations (Liu et al., 2008).

Table i4. TRPC expression in mammalian platelets

TRPC	Western blot	RT-PCR	References
TRPC1	X	X	Rosado and Sage. 2000 (Human) Den Dekker et al. 2001 (Human) Hassock et al. 2002 (Human) Brownlow and Sage. 2005 (Human) Wakabayashi et al. 2006 (Human) Varga-Szabo et al. 2008 (Mouse WT vs. TRPC1 ^{-/-} mice) Liu et al. 2008 (Human, immunofluorescence assays) Tolhurst et al. 2008 (Human)
TRPC2	not defined	not defined	
TRPC3	X	X	Brownlow and Sage. 2005 (Human) Wakabayashi et al. 2006 (Human) Liu et al. 2008 (Human, immunofluorescence assays)
TRPC4	X	X	Den Dekker et al. 2001 (Human) Brownlow and Sage. 2005 (Human) Wakabayashi et al. 2006 (Human) Liu et al. 2008 (Human, immunofluorescence assays)
TRPC5	X	X	Brownlow and Sage. 2005 (Human) Liu et al. 2008 (Human, immunofluorescence assays)
TRPC6	X	X	Den Dekker et al. 2001 (Human) Hassock et al. 2002 (Human) Brownlow and Sage. 2005 (Human) Wakabayashi et al. 2006 (Human) Varga-Szabo et al. 2008 (Mouse WT vs. TRPC1 ^{-/-} mice) Liu et al. 2008 (Human, immunofluorescence assays)
TRPC7	not defined	not defined	

Expression of TRPC transcripts (RT-PCR) and/or proteins (Western blot analysis) was described in this selection of reports in platelets. Only Varga-Szabo et al. (2008) compared expression between protein fractions of platelets preparations from wild type and TRPC-deficient mice (WT vs. KO).

Table i5. TRPC expression in mammalian megakaryocytes

TRPC	Western blot	RT-PCR	References
TRPC1	X	X	Berg et al. 1997 (Human) Den Dekker et al. 2001 (Human) Carter et al. 2006 (Mouse) Wakabayashi et al. 2006 (Human) Tolhurst et al. 2008 (Mouse)
TRPC2	not defined	X	Berg et al. 1997 (Human)
TRPC3	X	X	Berg et al. 1997 (Human) Den Dekker et al. 2001 (Human) Wakabayashi et al. 2006 (Human)
TRPC4	X	X	Den Dekker et al. 2001 (Human) Wakabayashi et al. 2006 (Human)
TRPC5	not defined	not defined	
TRPC6	not defined	X	Den Dekker et al. 2001 (Human) Carter et al. 2006 (Mouse) Tolhurst et al. 2008 (Mouse)
TRPC7	not defined	not defined	

Expression of TRPC transcripts (RT-PCR) and/or proteins (Western blot analysis) was described in this selection of reports in megakaryocytes. In any of these reports the use of TRPC-deficient mice was reported as control of antibody specificity.

Additionally, some of these observations about TRPC1 function in human platelets could not be repeated by others (Authi, 2007; Varga-Szabo et al., 2008b).

TRPs in murine platelets. In murine cells, a first link between TRP channels and platelet function came from experiments that showed an ADP-induced cation channel in mouse megakaryocytes permeable for Na^+ and Ca^{2+} . In these cells the Ca^{2+} conductance was increased by treatment with Phenylarsine oxide, a compound that is supposed to potentiate TRPC channels (Tolhurst et al., 2005). Using murine megakaryocyte the same group detected the expression of TRPC1 and TRPC6 as well as other TRP channels (TRPM1, TRPM2 and TRPM7) and described that these ADP-evoked currents displayed a current-voltage relationship similar to currents displayed by cells overexpressing TRPC6 proteins. In the same report roles for TRPM2 and TRPM7 in ADP-ribose-activated currents and Mg^{2+} -dependent currents were postulated, respectively (Carter et al., 2006).

TRPC1^{-/-} mice and platelet function. Varga-Szabo and collaborators used platelets from wild type, TRPC1^{-/-} or TRPC6^{-/-} mice to demonstrate the expression of TRPC1 and TRPC6 proteins in these cells. However, Ca^{2+} entry after store depletion by thapsigargin and agonist-evoked Ca^{2+} entry by thrombin and CRP stimulation were not impaired in platelets from TRPC1^{-/-} mice. Platelet aggregation and $\alpha_{\text{IIb}}\beta_3$ activation and degranulation induced by different agonists like ADP, CRP, thrombin, and U46619 were comparable between TRPC1^{-/-} platelets and WT platelets. Also TRPC1 deficient platelets formed stable thrombi on collagen surfaces and TRPC1^{-/-} mice presented no differences in bleeding time or thrombosis after injury of mesenteric arterioles. In addition, TRPC1 deficiency did not rescue the platelet phenotype presented by the STIM1 mutant (Stim1^{Sax/+}) when both mice were crossed since it was expected that the basal increased intracellular Ca^{2+} concentrations in STIM1 mutant platelets would be compensated by the absence of TRPC1 channels (Varga-Szabo et al., 2008b). Moreover, it has been shown in TRPC-deficient mice that the deletion of one TRPC protein can be compensated by upregulation of other TRPC (Dietrich et al., 2005) or by redundant protein functions, fact that can obscure the analysis of single TRPC deficient mice and the interpretation of the related observations.

4. Materials and methods

More detailed informations about materials, reagents (catalog number and company) and solutions are listed in Appendices A and B.

4.1 Mice

All animal experiments mentioned here were reviewed and approved in accordance with the Saarland University Ethic Regulations and the animal welfare committees of Saarland's State. The experiments in this work were made using mouse lines lacking TRPC1, TRPC3, TRPC4, TRPC5, TRPC6 proteins and corresponding wild type (WT) control mice. In addition to the single knockout mice, TRPC compound knockout mice derived thereof, such as TRPC1/TRPC4 (-/-)², TRPC1/TRPC6 (-/-)², TRPC4/TRPC6 (-/-)², TRPC3/TRPC6 (-/-)², TRPC1/TRPC4/TRPC6 (-/-)³ and TRPC1/TRPC3/TRPC6 (-/-)³ were used. The generation of TRPC1^{-/-}, TRPC3^{-/-}, TRPC4^{-/-} and TRPC6^{-/-} mice were previously described (Dietrich et al., 2007b; Hartmann et al., 2008; Freichel et al., 2001; Dietrich et al., 2005). TRPC5 deficient mice were generated in our Institute (Freichel, Stolz, Weißgerber, unpublished). Mice were bred and kept in a specific pathogen free (SPF) facility. They were maintained in a 12 hour light-dark cycle, and water and standard food (V1534-3, ssniff Spezialdiäten GmbH, Germany) were available to consume *ad libitum*.

All cardiac hypertrophy experiments were carried out with male mice within an age of 2.5 to 6 months. For platelet experiments mice from both genders were used (2 to 6 months old). Most TRPC-deficient mouse lines had a mixed 129SvJ/C57Bl6/N genetic background, for these mice the wild control mice of the F1 generation from 129SvJ and C57Bl6/N intercrosses were used. C57Bl6/N mice were used as controls when the experiments were done with TRPC6 deficient mice that were back crossed for at least 6 generations to the C57Bl6/N background. In some experiments I used litter-matched controls where platelets from TRPC5^{+Y} and TRPC5^{-Y} were compared. The study groups were carefully matched in terms of age, gender and specially, in terms of weight in case of cardiac hypertrophy experiments (see 4.2.1) because of the effect of some treatments on mouse weight. The breeding strategy for TRPC1/TRPC4 (-/-)² mice was directed to obtain the F1 offspring of the intercrossing between female mice from lines with a 129SvJ background (backcrossed at least for six generations) with male mice from lines with a C57Bl6/N background (backcrossed at least for six generations). Only the F1 generation

of mice from these breedings were used for the experiments and compared with wild type controls from the F1 generation from 129SvJ and C57Bl6/N intercrosses.

To identify the genotype from each mouse, a biopsy from the tip of the tail at the end of each experiment was taken. Briefly, each tail was digested with 100µl from the tail-Lysis buffer over night at 56°C, afterwards the Proteinase K inactivation was done by 95°C incubation for 20 minutes and finally 2µl from the sample was used in a 50µl PCR reaction. The PCR reactions were performed in two different thermocyclers, GeneAmp® PCR System 9700 (Applied Biosystems) and MyCycler™ (Bio-Rad). The products were run in 2% agarose gels stained with Ethidium Bromide (13µl from a 1% stock solution in a 300ml gel). To visualize the products and digitalize pictures from the PCR results a gel imaging system (GelDoc™, BioRad) was used. The utilized primers and PCR conditions for genotyping are summarized in Table m1.

4.2 Neurohumoral cardiac hypertrophy induction and analysis

4.2.1 Micro-osmotic pump implantation and cardiac hypertrophy evaluation

As model to induce cardiac hypertrophy the chronic treatment either with isoproterenol or angiotensin II was chosen. To avoid the stress and possible errors from repetitive injection of such agents, and to ensure a constant delivery of the hypertrophy inducing agents, the substances were infused via Alzet micro-osmotic pumps (DURECT Corporation, USA). The osmotic pumps models 1003D, 1007D and 1002 were used for 3, 7 and 14 days of infusion, respectively.

The main isoproterenol-induced hypertrophy model consisted on a treatment during 7 days with a dose of 30mg/kg/day referred here as Iso-30 (Keys et al., 2002; Maass et al., 2004; Jaffré et al., 2009). Also doses of 60mg/kg/day (Iso-60) or 8.7mg/kg/day over 7 days (Song et al., 2006) in two initial series of experiments were applied. In case of angiotensin II treatment the main protocol was the infusion of a dose of 3mg/kg/day over 14 days (ATII-3) (Song et al., 2006), which showed increased blood pressure after seven days of treatment according to Gavazzi and coworkers (2006). In some experiments I used a subpressor dose of angiotensin II (0.3mg/kg/day during 14 days) referred here as ATII-0.3. This dose is considered to induce hypertrophy without significant elevation of blood pressure (Grieve et al., 2006).

Table m1 (A). Primer sequences and PCR conditions used for genotyping TRPC deficient mice.

Gene/TRP		Primers (5'-3')	PCR condition	Expected product size (bp)
TRPC1-WT	C1_01	GAG ACT GTT GTC ACA AGA TGC	1	549
	C1_03	TCA GTT AAT GTC CCA TTC CGG C		
TRPC1-KO	C1_02	ACT TTG AGG GCA AAG GTT GCC	1	617
	C1_04	AGA GGC CAC TTG TGT AGC GC		
TRPC3-WT	C3LoxF	GCT ATG ATT AAT AGC TCA TAC CAA GAG ATC	2	300
	C3LoxR	GGT GGA GGT AAC ACA CAG CTA AGC C		
TRPC3-KO	C3LoxF2	GAA TCC ACC TGC TTA CAA CCA TGT G	2	329
	C3LoxR	GGT GGA GGT AAC ACA CAG CTA AGC C		
TRPC4-WT	KO-15	ACA GTG CTC TGA ACC CAC GG	1	293
TRPC4-KO	KO-40	CTC GCA CCG GAT GCC TTT GC	1	375
	KO-15	ACA GTG CTC TGA ACC CAC GG		
	NeoPa	GCC TGC TCT TTA CTG AAG GCT CT		
TRPC5-WT	C5_08	CTA GCC TAG ACA TAC AAC ACA G	1	203
	C5_09	GAC AGC TGA GCT CCC TAT TG		
TRPC5-KO	C5_09	GAC AGC TGA GCT CCC TAT TG	1	244
	C5_10	CAA GGC CAT CAA TTA CCA GAC		
TRPC6-WT	TRP6_03	CAG ATC ATC TCT GAA GGT CTT TAT GC	1	245
	TRP6_04	TGT GAA TGC TTC ATT CTG TTT TGC GCC		
TRPC6-KO	TRP6_01	ACG AGA CTA GTG AGA CGT GCT ACT TCC	1	300
	TRP6_02	GGG TTT AAT GTC TGT ATC ACT AAA GCC TCC		

Table m1 (B). Primer sequences and PCR conditions used for genotyping TRPC deficient mice.

Genotyping PCR condition 1			Genotyping PCR condition 2		
Temperature	Time	Cycles	Temperature	Time	Cycles
94°C	1.5min	1X	94°C	1.5min	1X
94°C	30s	10X	94°C	30s	10X
65°C (-0.5°C per cycle)	30s		67°C (-0.5°C per cycle)	30s	
72°C	30s	26X	72°C	30s	22X
94°C	30s		94°C	30s	
60°C	30s		62°C	30s	
72°C	30s	1X	72°C	30s	1X
72°C	5min		72°C	5min	
4°C	hold		4°C	hold	

(A) Primers utilized to determine the mouse genotype (Wildtype: WT or Knockout: KO) with the corresponding sequences and expected size for each pair. **(B)** Conditions of the PCR reactions used for TRPC mouse genotyping.

Before each series of pump implantation the weight of the mice was monitored around the week 8 of age to have a closely matched group. It was defined to have mice with a minimum weight of 26g and maximum of 30g because I found that this reduces the variation in the HW/BW index. When the mice reached the right weight range they were placed in single clean cages and they were weighed the day before the micro-osmotic pump insertion. Each series of experiments consisted of about 14 to 20 mice, half of the group were WT mice and half KO mice. In each experimental round 2-4 mice were used as control mice treated with saline solution (NaCl 0.9%) to assess whether a significant hypertrophic response was achieved by the neurohumoral stimulus. In some cases, when it was possible, three groups of mice were used per series (one WT and two KO groups) to reduce the number of mice used in the experiments.

The day before implantation the osmotic pumps were loaded, either with treatment solutions using saline solution as vehicle or only with saline. The filling of the pumps was done following the manufacturer instructions under aseptic conditions. Prior to filling the pumps the next steps were done: first, calculation of the amount of angiotensin II or Isoproterenol depending on the dose and the weight from each mouse (see formula 1).

$$[C_f] = (BW \times D)/Q \quad (1)$$

C_f refers to final concentration in the pump, BW is the body weight of the mouse in grams, D represents the dose ($\mu\text{g/g/h}$), and Q refers to the volume delivery rate of the pump ($\mu\text{l/h}$) given by the manufacturer for each pump lot.

The Isoproterenol stock solution (100mg/ml) was kept in 2ml aliquots below -20°C and only freshly thawed aliquots were used once; angiotensin II was always ordered some days before the experiments, kept under -20°C and solved just before preparing the pumps. Second, each pump with its corresponding flow moderator was individually transferred into a sterile 2ml reaction tube; afterwards the weight from each pump plus moderator was obtained. Third, the pumps were filled carefully starting with those containing only saline solution. Afterwards each pump was weighed again and the difference between empty and full pump served to verify the complete filling of the pumps. Finally, sterile saline was added ($\sim 1.5\text{ml}$) to each reaction tube and the pumps were incubated over night at 37°C in saline solution in order to assure the immediate delivery of the solution after implantation.

The implantation of the micro-osmotic pumps was done under Isoflurane* anesthesia. The isofluran was vaporized with a mixture of O₂/N₂O (1:2) using a vaporizer (Vapor 19.3, Abbot) at a concentration between 1.5 to 2%. The induction of the anesthesia was done in an Isoflurane 2.5% pre-saturated Plexiglas chamber. After the induction phase the mice were transferred on a temperature controlled plate to keep them warm at 37°C during the operation. The warming plate was adapted to connect a mask delivering the Isoflurane during the procedure where the nose and mouth from the mouse was placed. Before starting the experiment it was verified that there were not detectable reflex from the paw sole and the tip of the tail. One drop of Bepanthen cream (Bayer) was applied gently on each eye to protect them during surgery.

For the pump insertion the hair from an area of about 1.5x1cm from the lower part of the nape was removed, first using a hair clipper (ER240, Panasonic) and then with a peeling cream (elca@med, ASID-BONZ, Germany). This area was cleaned afterwards with EtOH 70% and sterile saline solution. Next, a ~8mm transversal incision on the peeled nape was made and from this a subcutaneous pocket (~2.5-3cm) on the right flank of the mouse was made using blunted scissors (14018-14, F.S.T.). Subsequently, 0.5ml of pre-warmed sterile saline solution (~37°C) was injected inside the pocket using a 1ml syringe and the pump was inserted with the cap facing the inside of the pocket. Before suturing, it was verified that the pump had enough space to accommodate once the mouse would be awake and also it was checked that the skin was not tied around the implantation area. Finally, the incision was stitched up with 3 to 4 independent stitches using a polyester 5-0 RB-1-plus suture (Mersilene, Johnson & Johnson), each suture was secured with one drop of tissue adhesive (Vetbond, 3M) and the wound was cleaned with antiseptic iodine solution (Braunol®, Braun).

The mice were weighed after pump implantation and placed back into the cage. In addition, two tissue papers were placed inside the cage. The mice were monitored during the recovery from the anesthesia and two hours thereafter to check that they removed the eye cream, if not, the cream was carefully removed with a cotton swab rinsed with sterile saline. Every day the mice were checked, twice a day for the first 2 days. The recovery was monitored qualitatively by inspection and assessment of typical mouse behavior, including nest building and brightness of the hair; this first aspect seems to be a good

* Isoflurane was selected as anesthetic because it has reduced cardiovascular effects in comparison with other anesthetics (Janssen et al. 2004). For example, from personal observations the heart rate under Isoflurane from 19 WT mice was 477±51 BPM compared with 292 ±117 BPM from 8 mice under Ketamine/xylazine anesthesia. Also, Isoflurane narcosis can be regulated faster and there is a rapid recovery after removal of the mice from the isofluran delivering mask in comparison with injected anesthetics.

indicator because all saline treated mice start to build a nest at the same day of implantation; for the Isoproterenol or angiotensin II treated mice the process took between 24 to 48h.

In some cases, one day before the end of the hypertrophy induction ECG recordings under Isoflurane anesthesia were done (see below for details). In addition, that day all the sampling tubes, materials, solutions and data collection tables were prepared. At the end of the treatment, depending if the pump model was for 3, 7 or 14 days, the procedure was the following: the mice were weighed and the weight from the pump obtained before implantation was subtracted. The mouse organs were removed, as described by others (Patterson et al. 2004) under terminal Avertin (2,2,2-tribromoethanol, Fluka) anesthesia that was given intraperitoneally (i.p. 25 μ l/g) using a 26G^{1/2}" needle (MicrolanceTM, BD). After checking the absence of reflexes, a midline abdominal incision was performed followed by a clam-shell bilateral thoracotomy, then both abdominal and thoracic cavities were exposed and the renal artery was punctured in order to reduce the blood flow going into the heart. To arrest the heart ~1ml ice cold saline solution was injected slowly into the left ventricle using a 27G^{3/4}" needle (MicrolanceTM, BD) inserted into the apex of the ventricle. The heart was quickly excised and placed into ice cold saline solution, where the excess of fat tissue and surrounding vessels was removed. Immediately, lungs, liver and spleen were dissected from the mouse and placed into a Petri dish. Before weighing the organs the excess of blood was gently removed by placing the organs into a paper tissue and then each organ was weighed (wet weight). After getting the wet weight, each heart was divided as following: the atria were put into one 1.8ml vial (CryoTubeTM vial, nunc) and transferred into liquid nitrogen. The ventricles were cut transversally into two halves, the distal half was also placed into one 1.8ml vial and was snap frozen in liquid nitrogen, the other ventricular half was transferred into a 2ml reaction tube containing Paraformaldehyde (PFA) 4% (pH 7.4) to fix the tissue over 2 days at 4°C. The frozen samples have been kept at -80°C until their analysis. The heart was processed in this way with the purpose of performing further analysis like western blot and histological analysis of cardiac hypertrophy parameters, such as cardiomyocyte cross sectional area and percentage in interstitial fibrosis.

Lungs, liver and spleen were dried at 70°C over 48h to obtain at the end the dry weight. The water content from lungs, liver and spleen was obtained from the difference between wet and dry weights from each organ. The tibia was removed and carefully cleaned from skin and muscle to get the tibia length. From each mouse the tip of the tail (~3mm) was collected in order to verify the genotype. The wet weight from each organ was normalized

to both body weight and tibia length to perform the analysis of the following ratios: heart weight (mg)/ body weight (g) (HW/BW), heart weight/ tibia length (mm) (HW/TL), lung weight (mg)/ body weight (LW/BW), lung weight/ tibia length (LW/TL), liver weight (mg)/ body weight (LivW/BW), liver weight/ tibia length (LivW/TL), spleen weight (mg)/ body weight (SplW/BW), spleen weight/ tibia length (SplW/TL).

4.2.2 Heart histology: Quantification of cardiomyocyte cross sectional area and heart fibrosis.

The heart samples were fixed in PFA 4% as mentioned. After two days (48h) of fixation at 4°C the samples were transferred into universal embedding cassettes (07-8100 BioCassettes, BioOptica). The samples were rinsed with freshly prepared PFA, dehydrated through increasing Ethanol-Xylene steps in an automatic embedding system (Tissue-TEK® VIP, Miles Scientific) and finally placed into steel tiles for inclusion of paraffin samples (07-BM24245, BioOptica) using as tissue embedding medium Paraplast regular kept at 60°C. The program used for dehydration and embedding was:

1. Ethanol 70%	1h/40°C	
2. Ethanol 80%	1h/40°C	
3. Ethanol 90%	1h/40°C	
4. Ethanol 96%	1h/40°C	
5. Ethanol 96%	1h/40°C	
6. Ethanol 100%	1h/40°C	2X
7. Xylene 96%	1h/40°C	2X
8. Paraplast	1h/60°C	4X

The paraffin tissue blocks were prepared manually to ensure the correct placing of the heart to get transversal sections from the middle region of the ventricles. This procedure was made by placing the cut edge of the heart facing down in stainless steel embedding molds (15x15x5mm, 07BM15155, BioOptica) and adding liquefied Paraplast from a Paraffin dispenser (EG1120, Leica). During this procedure the molds were kept on a warm plate (60°) and to assure that the Paraplast was liquefied the tank temperature was preset at 60°C 24h in advance. The bases of the embedding cassette, facing up, were placed on top of the molds and, finally, after some minutes when the paraffin was not completely liquid, the molds were transferred into a cuvette with ice to complete the Paraplast polymerization.

When the blocks were polymerized 5µm sections were cut with a 2040 AutoCut microtome (Reichert-Jung). Consecutive tissue sections were mounted on glass slides (regular pre-cleaned microscope slides, R. Langenbrinck) and fixed to the slide by incubation at 90°C during 30 minutes. From each heart at least 10 sections were obtained to get enough material for staining either with Hematoxylin-Eosin (H-E) or picosirius red.

The Hematoxylin-Eosin protocol for the deparaffinization, rehydration, staining, and dehydration was:

1. Xylene 3min 2X
2. Ethanol 99% 3min 2X
3. Ethanol 96% 3min 2X
4. Ethanol 70% 3min 2X
5. Rinse in distilled water
6. Staining in Mayer Hemalaum solution for ~5 minutes
7. Clear with run tap water for 10 minutes
8. Stain in Eosin Y-solution between 5-10 minutes
9. Rinse in distilled water
10. Rinse 2X in 70% EtOH, 2X 96% EtOH and 1X 99%EtOH.
11. Ethanol 99% 3min 2X
12. Xylene 3min 2X
13. Mount and cover the samples with cover slips using either DePex or Eukitt resins. Let the samples dry over night.

For the picosirius red staining the following deparaffinization, rehydration, staining and dehydration steps were done:

1. Xylene 3min 2X
2. Ethanol 99% 2min 2X
3. Ethanol 96% 2min 2X
4. Ethanol 70% 2min 2X
5. Distilled water 5min
6. Distilled water 10min
7. Staining in Picosirius red solution for 60 minutes
8. Rinse briefly two times in 0.5% acetic acid
9. Ethanol 96% 2min 1X
10. Ethanol 99% 2min 1X

11. Xylene 3min 2X

12. Mount and cover the samples with cover slips using either DePex or Eukitt resins. Let the samples dry over night.

Quantification of cardiomyocyte cross sectional area. After staining the heart samples, three to five H-E stained sections per mouse were analyzed through the left ventricle free wall. The mean cross-sectional area per mouse was obtained by measuring ~100 transversally cut cardiomyocytes with a centrally located nucleus; these criteria of morphometrical analysis have been already used by others (Kilié et al., 2007). The images were obtained using an inverted microscope (Axiovert 40 CFL, Zeiss) coupled to a digital color camera (MRc5, Zeiss) and with a 40X immersion oil objective (Fluar40X, Zeiss). The images were digitalized and analyzed with the AxioVision software (versions 4.5 to 4.8, Zeiss) using the measuring tools to obtain the cardiomyocyte cross sectional area. The absolute mean values and the relative increase in comparison with the corresponding control were compared and analyzed.

Quantification of cardiac fibrosis. To determine the interstitial collagen fraction, picrosirius red stained transversal sections from the left ventricle were analyzed. Ten pictures per heart were made through the entire left ventricular region in order to have a representative mean value from the complete ventricle. To take the photos from each series, light intensity, contrast and acquisition parameters were not changed once they were standardized. The pictures were obtained using an inverted microscope (Axio Observer A.1, Zeiss) with an Axio Imager condenser (0.8/1.4, Zeiss) and coupled to a digital color camera (MRc5, Zeiss). A 10X objective (ACHROPLAN, Zeiss) was used to cover the left ventricle in 10 images. The pictures were digitalized and analyzed with the segmentation tool from the AutoMeasure module (AxioVision software 4.8.1, Zeiss). The principle of the segmentation allowed separating each picture into three different layers, the first including all the pixels from the picture, the second containing only the pixels that corresponded to the background or region without tissue and the third one with the red pixels that matched to the Sirius red stained collagen fibers. At this point the program permitted to exclude manually the perivascular areas from the analysis. The total number of background pixels was subtracted from the total number of pixels in the picture and this value represented the complete analyzed ventricular area. Then, the collagen fraction per specimen was obtained by calculating the ratio, in percentage, corresponding to picrosirius red stained tissue in relation to the total cardiac tissue from the corresponding section. At the end from each heart the area of fibrosis in percentage was obtained. The mean values of Sirius red stained tissue and the relative increase compared with the

corresponding saline controls were compared and analyzed. During the complete sampling and analysis procedure the operator was blind to the genotype and treatment of each specimen.

4.2.3 Telemetric blood pressure recording during isoproterenol or angiotensin II treatment

To evaluate the effect of chronic treatment of Isoproterenol or angiotensin II on blood pressure we implanted telemetric blood pressure transmitters in mice. After one week of recovery from the transmitter implantation surgery blood pressure was recorded continuously during one week to obtain base line levels. Afterwards, osmotic pumps were implanted and blood pressure recorded during the treatment. The blood pressure transmitter implantation and blood pressure measurements were made by Ilka Mathar from our laboratory as described (Mathar et al., 2010). Shortly, a radio telemetry system (PA-C10, Data Science International) was used to monitor blood pressure in conscious, unrestrained mice. The pressure sensing catheter was inserted under Isoflurane anesthesia into the left carotid artery and the transducer unit was implanted into a subcutaneous pouch along the right flank. After the recovery period we collected, stored and analyzed arterial pressure recordings with the Dataquest A.R.T. software 3.0. We acquired data of basal blood pressure with a 10s scheduled sampling every 3 minutes, 24h mean values for mean arterial blood pressure (MAP) and heart rate (HR) were calculated.

4.2.4 Intraventricular pressure measurements (Millar Mikro-Tip catheter)

Intraventricular pressure measurements were made under anesthesia either by Avertin i.p. 25µl/g or by Isofluran 1.8-2.5%. For these measurements the mice were intubated and air ventilated using a mechanic ventilation system (MiniVent type 845, Hugo Sachs Elektronik-Harvard Apparatus). The ventilation was set at 125 strokes per minute and a volume of 180µl. The mice were placed on their back on a warm plate at 37°C. After checking the absence of reflexes the skin from the left chest was removed to visualize the thoracic musculature. The left *pectoralis major* muscle was partially blunt dissected, pulled and fixed to the right side together with the *sternalis* muscle using a suture thread. Afterwards, the *pectoralis minor* was also blunt dissected until the *intercostalis* muscles were visualized. Finally a small incision through the 2nd and 3rd intercostal space was done

and from this incision a small window (~4x4mm) was opened by removing part of the third rib and *intercostalis* permitting the exposure of the left ventricle. During the procedure it was very important to reduce the vessel damage to avoid the bleeding and related changes in pressure that could alter the measurements. The chest cavity was entered at the middle of the third intercostal space to visualize the heart. The pericardium was gently removed from the left ventricle by pulling it to one side. The introduction of the catheter directly in the left ventricle was performed through a hole made on the left ventricle tip using a 23G 1" needle (Microlance™, BD).

The Intraventricular pressure was measured with a 1.4F Mikro-Tip Catheter pressure transducer (SPR 671, Millar Instruments). The catheter was connected to the corresponding control unit (TC-510, Millar Instruments) that works as a passive interface between the pressure sensor and the recording systems to have balance and calibration controls of the transducer. The control unit was then connected to an Amplifier (MIO-0501 DC, FMI-Föhr Medical Instruments, Germany) which was calibrated in such way that 1V was equivalent to 100 mmHg. Finally, the amplifier was coupled to a PowerLab 8/S (ADInstruments). The ventricular pressure was recorded for 3 minutes using the LabChart software v5.5.5 (ADInstruments). For the analysis the Blood Pressure Module (ChartPro v5.5.5 or LabChart v6.0) set for ventricular pressure was used. The analysis was performed from a selection of the recording where the signal was stable (usually some seconds after the insertion of the catheter until the end of the recording). In the Blood Pressure Module settings it was determined to include only pressure cycles higher than 20mmHg. A mean pressure cycle (Figure m1) made from 10 cycles was obtained to calculate the following parameters: Maximum Pressure (mmHg), Minimum Pressure (mmHg), End Diastolic Pressure (mmHg), Mean Pressure (mmHg), difference between Maximum and Minimum Pressure (mmHg), Systolic Duration (s), Diastolic Duration (s), Cycle Duration (s), Heart Rate (BPM), Maximum dP/dt (mmHg/s), Minimum dP/dt (mmHg/s), Tau (τ) or exponential time constant of relaxation (s), Contractility Index (1/s) and Pressure Time Index (mmHg.s). The Contractility index is defined as the Maximum dP/dt divided by the pressure on the time of Maximum dP/dt. The Pressure-time index (Tension-time index) is the average ventricular pressure during systole multiplied by the systolic duration. At the end the mean value for each of the parameters mentioned before was obtained for every recording.

Before starting, the calibration from the setup was checked connecting the pressure transducer to a pressure manometer and different pressures were given and compared with the obtained measurements. After each measurement session the catheter was

cleaned by incubation for 15min in a 1% enzymatic solution (Terg-A-Zyme® Alconox Inc, USA) and finally rinsed with abundant d-diH₂O.

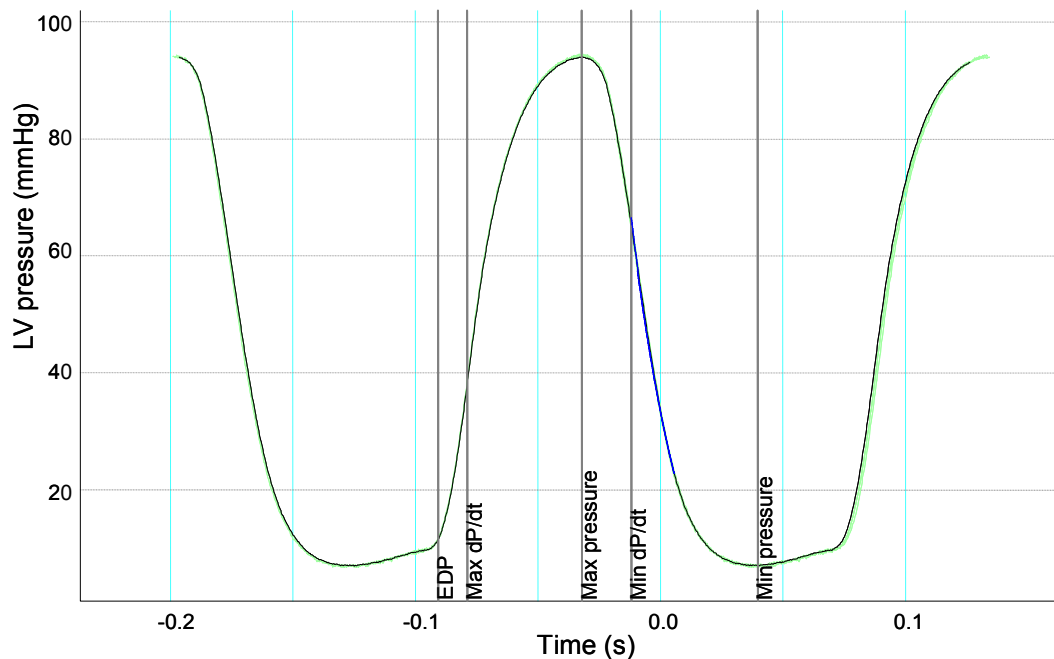


Figure m1. Measurement of left intraventricular pressure from the mouse heart. Original trace from a measurement of the pressure inside a mouse left ventricle using a Pressure Millar Catheter. The mean parameters used to analyze each pressure cycle are shown. EDP: End diastolic pressure.

4.2.5 Plasma angiotensinogen determination

Ten wild type and nine TRPC1/TRPC4 $(-/-)^2$ mice were used to determine the plasma levels of angiotensinogen. 60 to 80 μ l of blood were obtained via submandibular bleeding from conscious mice as described by Golde and collaborators (2005), using an 18G 1 $\frac{1}{2}$ " needle (Microlance™, BD). Blood was collected into EDTA containing sampling tubes (SARSTEDT ref. 41.1504.005) and centrifuged 10min at 1200G in a microcentrifuge (1-14, sigma, Germany). The plasma was transferred into a 1.5ml reaction tube, centrifuged again (1200G/10min) and transferred once more into a new reaction tube. These 2 centrifugation and transferring steps were used to have complete clear plasma.

The angiotensinogen concentration was determined using a mouse total angiotensinogen assay kit (JP27413, IBL, Germany) and the procedure was made following the manufacturer instructions. The assay was a sandwich ELISA that included 2 kinds of antibodies, the anti-mouse AGT (135) rabbit IgG Affinity Purity placed on a 96-well precoated plate and the labeled antibody (HRP conjugated anti-mouse AGT (405) rabbit

IgG Fab' Affinity Purify). The coloring agent (Chromogen) used was Tetra Methyl Benzidine and the sample measurements were done with a plate reader (infinite®-200 TECAN, Austria) at 450nm.

As recommended by the manufacturer the samples were diluted with EIA buffer (provided in the kit) before placing them on the 96-well plate. The plasma was diluted 1250 folds and to achieve these serial dilutions were performed. First 10µl plasma were added to 90µl EIA buffer, then from this dilution 10µl were added to 90µl buffer and finally from this second dilution, 20µl were added to 230µl buffer. For the angiotensinogen determination 100µl from the diluted samples were used in each well and from every sample the measurements were done in duplicate; also this was made with the standard and the reagent blank (only EIA buffer). The standard was prepared with the recombinant mouse angiotensinogen provided within the kit and serial dilutions were made to have the subsequent concentrations in ng/ml: 0, 0.16, 0.31, 0.63, 1.25, 2.5, 5 and 10, as mentioned in the assay manual. When the samples and the standard were ready, the general steps for the measurement were: 1) placing 100µl of sample per well of the precoated plate; 2) incubation for 1h at 37°C; 3) washing of the wells during 25s and repeated 10 times; 4) incubation with the labeled secondary antibody for 30min at 37°C, except the reagent blank wells; 5) washing as in step three but 9 times; 6) addition of 100µl from the Chromogen solution per well and incubation for 30min, at room temperature in the dark; 7) stopping the reaction with the provided 1N H₂SO₄ solution; 8) cleaning the bottom of the plate and verifying the absence of bubbles in each well; and 9) measuring at 450nm with the plate reader and obtaining the absorbance values.

The absorbance value from the test sample blank (only EIA buffer and labeled antibody) was subtracted from all the obtained values and the mean value from each pair of measurement was obtained. The standard curve was plotted and a linear regression was made because the high linearity of the standard curve between 0.16 and 10ng/ml reported by the developers of the mouse angiotensinogen ELISA assay (Kobori et al., 2008) and confirmed by the determined regression. To calculate the angiotensinogen concentration in the samples, the absorbance value from each sample and the slope and intercept obtained from the linear regression were used in a linear equation where the concentration, in ng/ml, was defined as:

$$[\text{concentration}] = (\text{absorbance} - \text{intercept})/\text{slope}$$

This method was used in addition to plot the standard curve on a log-log scale using the Origin software and reading the concentration for unknown samples. Finally, the concentrations obtained were multiplied by the dilution factor to get the angiotensinogen concentration in the plasma from every mouse.

4.2.6 Isolation of adult mouse cardiomyocytes and mouse cardiac fibroblast culture

The initial steps of the procedure for isolation of adult mouse cardiomyocytes (CMs) and cardiac fibroblasts (FBs) were basically the same. The resulting protocol is an adaptation from the isolation protocol learned in the laboratory from Prof. Peter Lipp (Homburg, Germany) during one of the *Spezialpraktika* from the Graduate School GK1326 ("Mouse cardiomyocytes isolation protocol for Ca²⁺ imaging experiments") in combination with published methods (Goshima, 1969 and 1974; Eghbali et al., 1988; Hilal-Dandan et al., 2000; Ostrom et al., 2003; O'Connell et al., 2003; Fredj et al., 2005; Nakayama et al., 2006; Brenner and Dolmetsch, 2007; Viero et al., 2008) and personal experience during the protocol establishment. In summary, the procedure consisted of heart isolation and cannulation, heart perfusion and tissue digestion, mechanical disruption of the tissue and cell separation, a summary of the cell isolation is presented in Figure m2.

Depending on the main isolated cell type and the final use of the cells (i.e. RNA isolation or fibroblast culture) there were some variations in critical steps like the digestion time of the heart and the washing steps of the cells; these steps are mentioned below. Also, it is useful to mention that not always all steps and solutions were required. The working solutions were prepared always fresh using autoclaved d-diH₂O and the bottles and materials were sterile when the intention was to culture cells. The main solution (solution A) used was modified Tyrode's buffer. Using solution A the following solutions were prepared: 1) Solution A+ gassed (~15min with O₂/CO₂) kept at room temperature for cleaning and stabilization of the heart. 2) Solution A kept at 37°C to solve the enzyme cocktail* (Liberase, Roche) for digestion of the heart. 3) Solution A++extra (O₂/CO₂ equilibrated) containing serum albumin and Ca²⁺ to inhibit the digestion enzymes. 4) Cold macrophage (MF) solution without serum and Ca²⁺ for a pre-plating step used to separate fibroblasts from macrophages since it was reported that with this conditions macrophages and not fibroblast can attach to a plastic surface facilitating the separation of both cell populations (Landeem et al., 2007).

* Until 2009 it was used the Liberase Blendzyme 4 from Roche (2mg in a final volume of 12ml) but because the product was replaced, the new product used was Liberase TM Research Grade (2mg in a final volume of 15ml).

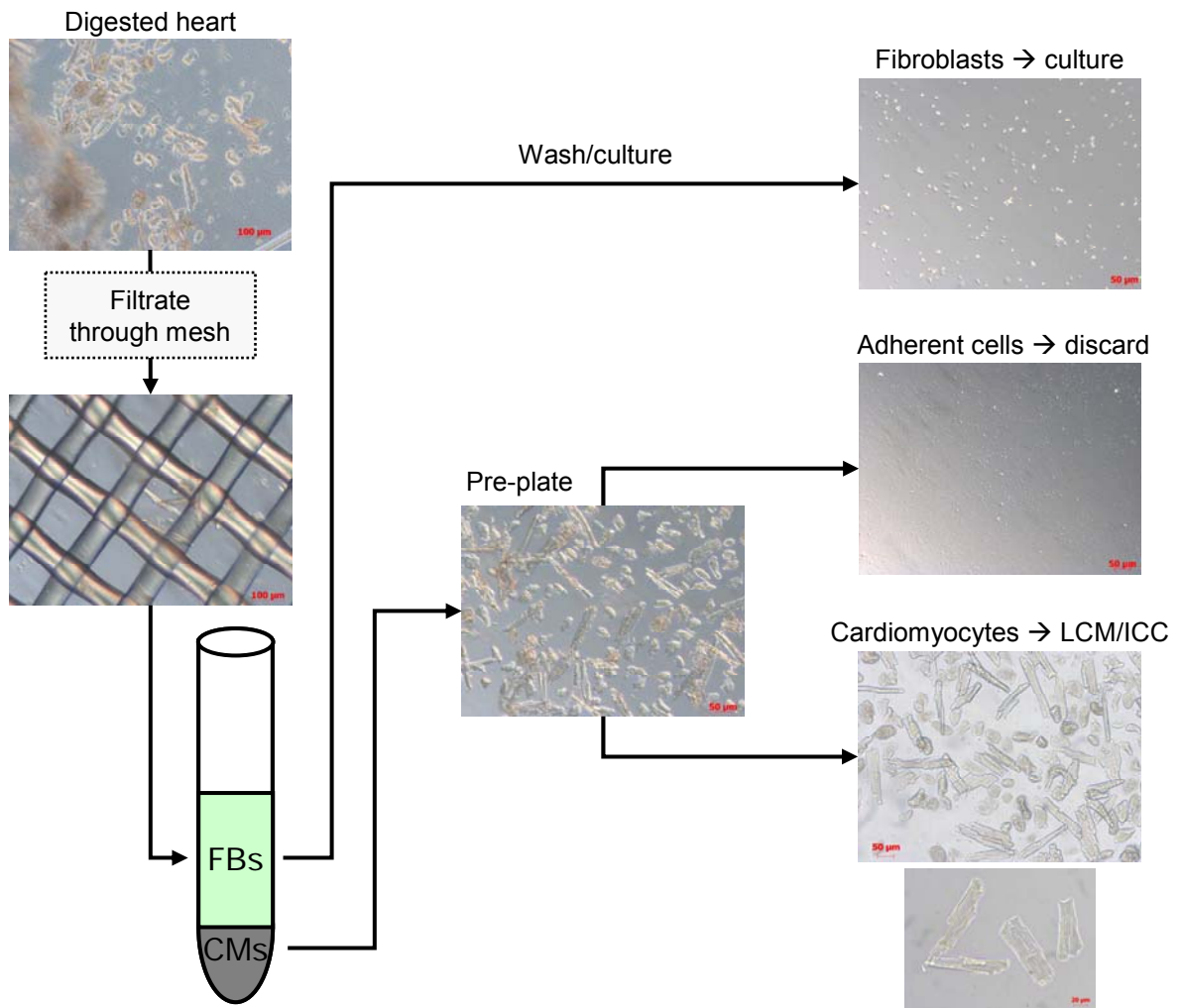


Figure m2. Summary of the isolation procedure used to obtain mouse cardiac fibroblasts and cardiomyocytes. After digestion of the heart the tissue is homogenized and passed through a nylon filter to remove remaining debris. The cardiomyocytes (CMs) are separated from other cardiac cells and fibroblasts (FBs) by decanting the cells suspension and/or centrifugation steps. The supernatant, rich in fibroblasts, is washed and cultured. The pellet is pre-plated to remove adherent cells (i.e fibroblasts or macrophages) and finally a cardiomyocyte enriched suspension is collected. LCM: Laser Capture Microdissection, ICC: Immunocytochemistry.

The perfusion system (Figure m3, A) was always rinsed with at least 1 liter of autoclaved d-diH₂O before and after its use. At the end of the preparation a cleaning step with 100ml EtOH 90% was also made with a final drying step of the tubing to avoid contamination of further preparations. The perfusion system was built with two independent tubes going into the cannula, one tube for the solution used to clean and stabilize the heart with the Tyrode's solution, and the second tube just to carry the digestion solution. When the tubing system was cleaned some solution A was passed first through the tube that carries the digestion solution (Liberase solution) in order to have this part of the tube filled with solution A to avoid air bubbles. The same was done with the other part of the perfusion system, but with solution A+ and this was made as second step, because in this way the

common end of the tubes contained only solution A+, that it was the first one used to perfuse the heart. After preparing the perfusion system, the warming bath was turned on (40°C to have at the end of the tube for Liberase solution 36.5°C, it depends on the tube size and length). It is important to calibrate the temperature in a way that at the end of the tubing the solution temperature is between 36 to 37°C.

Before excision of the heart the mouse was anesthetized with Avertin (i.p) and 20µl/g of Heparin (1000U/ml) were injected (i.p). Once there was no detectable reflex from the paw sole and the tip of the tail the mouse was placed on its back, the limbs were fixed and the abdomen and thorax were cleaned with abundant EtOH (70%). A transversal incision on the lower part of the abdomen was made, then two longitudinal incisions from the first one were done in direction to the head in order to perform a clam-shell bilateral thoracotomy, the ribs were removed and the heart was exposed. To facilitate the blood removing from the heart, a small incision was made on the renal artery and afterwards a paper tissue was placed on top to absorb the blood. The pericardium was removed gently and 1ml ice cold solution A was slowly injected inside the left ventricle to arrest the heart and to remove part of the blood. Before the heart explantation the valve from the perfusion system carrying solution A+ was opened (set to ~1drop/s).

The heart was rapidly excised with part of the aorta. This was done by pulling up gently the heart by fixing it from the tip and releasing the heart cutting first the pulmonary vein and artery from above and finally the aorta (close to the aortic arch) and vena cava. The heart was rapidly placed in ice cold solution A, where the excess of fat tissue around the aorta was removed. The aorta was cannulated, avoiding the damage of the aortic valve, with a self made 18G blunt cannula and fixed to it with two threads (USP 8/0 metric 0.4, Suprama, Germany). The heart was transferred to the perfusion system and was retrogradely perfused with the solution A+ at RT (previously equilibrated with O₂/CO₂) between 5-7 min, depending how fast the drops coming out were free of blood. The solution A+ was changed to the digestion solution (37°C and ~1drop/s) and the perfusion was carried out during 7-15 min*. This solution was recovered and recirculated during the perfusion. When the heart became "swollen and soft" it was removed from the cannula

* The perfusion time with the Liberase solution depends on the size of the heart, the age of the mouse, the appropriate cannulation and the designated use of the cells. Sufficient digestion of the heart is achieved when it becomes more pale and when the tissue from the ventricle is easily disrupted with forceps. When the digestion is too fast pay attention to the quality of the cells, can be that the Liberase concentration is too high. During this step check constantly the heart to avoid over-digestion of the tissue. If the interest is to get mainly fibroblast there is no problem that the heart is completely soft, but if the interest is to get a high percentage of healthy cardiomyocytes this digestion time is critical and has to be reduced to the minimum.

and placed into a sterile plastic Petri dish (35x10mm) containing ~2ml Liberase solution (37°C).

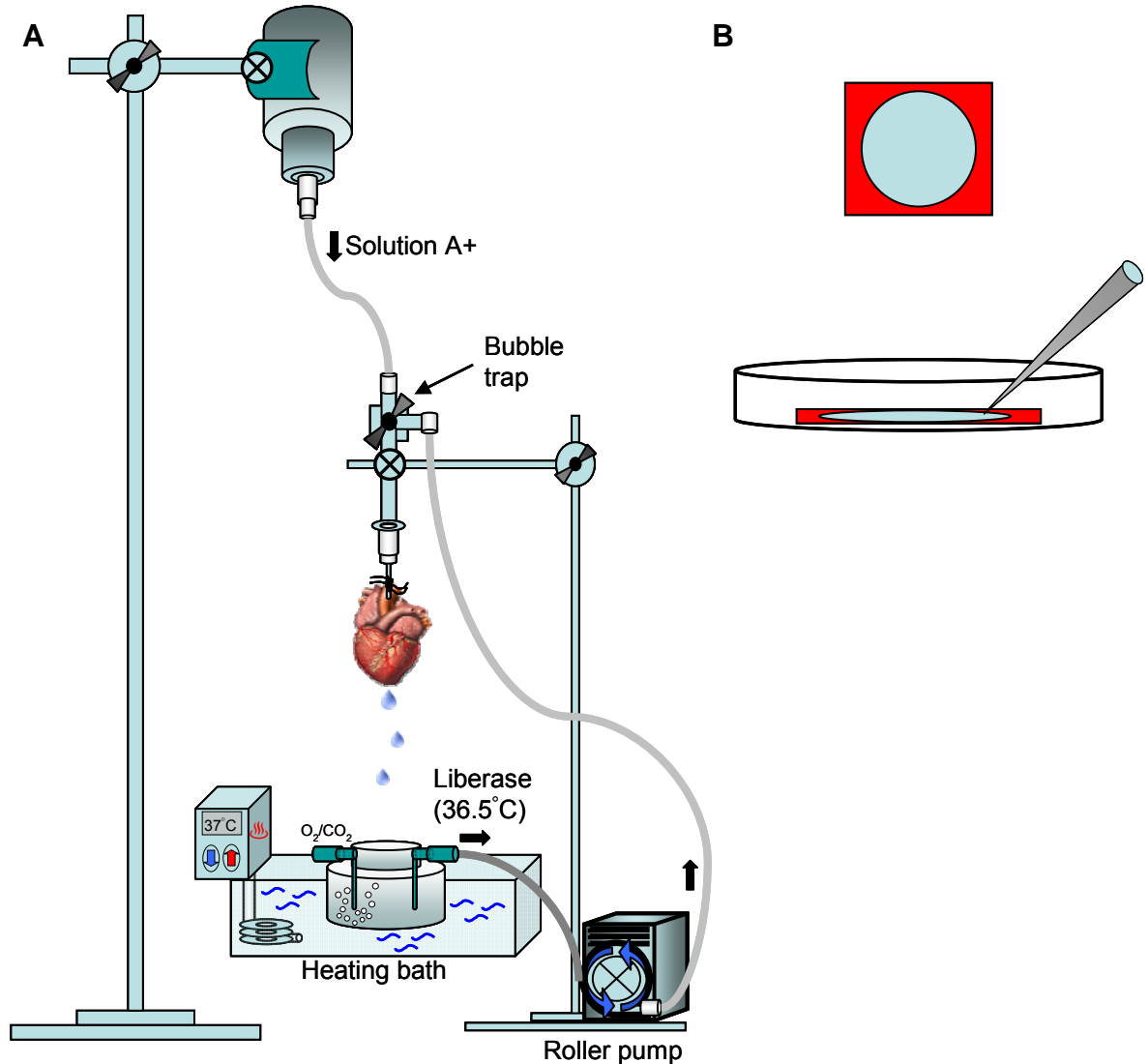


Figure m3. Perfusion system used for cardiac cell isolation and silicone isolators for fibroblast culture. (A) Diagram of the system used to retrogradely perfuse the mouse heart for the isolation of cardiomyocytes and fibroblasts. **(B)** Graphic showing the use of silicone isolators (red) on top of round glass coverslips (grey) to culture cardiac fibroblasts. To transfer the cells on coverslips with silicone isolators this is done by gently pipetting the cell suspension on one edge as depicted in B (lower picture); in this way the formation of bubbles is avoided.

The next steps, dissociation of cardiac cells and fibroblast culture, were done under the flow bench using sterile cell culture techniques. The ventricles were separated from the atria using fine scissors sterilized by flaming and they were transferred into a new Petri dish (35x10mm) containing 2ml A++extra solution (O_2/CO_2 equilibrated). The ventricles were minced into small pieces 2-3mm. The tissue was partially dissociated by gently

pipetting several times (~1min). The suspension was transferred into a 15ml polypropylene tube, the Petri dish was rinsed with 2ml solution A++extra and this was pooled with the suspension in the 15ml tube. Finally, solution A++extra was added to complete 10ml and the dissociation and homogenization of the tissue were continued for about 3 to 5 minutes until the suspension was homogeneous. The homogenate was filtered through a 150µm sterile filter (ref. 06-4-2319, CellTrics, Partec) and collected into a new 15ml polypropylene tube.

The cardiomyocytes were allowed to sediment (10min at 37°C). The supernatant rich in cardiac fibroblasts was transferred into a new 15ml polypropylene tube and centrifuged at 40G/1min/RT in order to retire remaining CMs. The supernatant was changed into a new 15ml tube. If there was interest to collect cardiomyocytes for immunocytochemistry (ICC), RNA isolation or Laser Capture Microdissection (LCM) the pellets containing CMs were pooled and solution A++extra was added to complete 10ml, this suspension was transferred into a plastic Petri dish (60x10mm) and the cells were pre-plated in a cell incubator 37°C, 5%CO₂ (HERA cell 150, Heraeus, Germany) to remove adherent cells like FBs. After 2h the cardiomyocytes were collected and counted manually using an improved Neubauer chamber (BRAND, Germany). The handling of the cardiomyocytes varied depending on their use, see below.

The FBs containing supernatant was centrifuged (250G/10min, RT) in a Jouan multifunction centrifuge (CR3i, Thermo Electron Corporation). The supernatant was discarded and the cell pellet was resuspended in 5ml M199 (Gibco, Invitrogen) supplemented with FCS, kanamycin and penicillin/streptomycin (M199-complete). The cell suspension was transferred into a 25cm² culture flask (vented cap, BD Biosciences) and kept during 2h in the cell incubator (37°C). After this period, the medium was removed and the flask was rinsed two times with medium (M199-complete) to remove non adherent cells and debris. Finally, the cells were cultured with 4ml of M199-complete, the medium was changed every 24h until they were confluent. Cells from one heart were usually confluent after 5-7 days of plating. The cells were regularly monitored with an inverted Nikon microscope (Eclipse TS100) using the 10X and 20X objectives (LWD 20X/0.40 Ph1 ADL ∞/1.2 and 10X/0.25 Ph1 ADL ∞/1.2 WD 6.2, Nikon).

In some preparations one differential plating step was used in between the FBs resuspension and its culture. The aim of this step was to reduce the population of macrophages in the culture as mentioned before. Instead of resuspending the cells in M199-complete, the cells were resuspended in 5ml cold MF-solution, placed into a Petri

dish (35x10mm) and incubated for 30 minutes (~6°C). After that period the non-adherent cells were recovered and 5ml solution A++extra were added (complete 10ml). The suspension was centrifuged (250G/10min). The supernatant was discarded and the cells were resuspended in M199-complete; the following steps were the same as mentioned in the previous paragraph.

Once the fibroblasts were confluent the cells were detached from the culture flask using Trypsin to split them for expansion of the culture or to transfer cells into coverslips. Briefly, for a 25cm² culture flask the medium was removed and the cells were rinsed with 5ml pre-warmed (37°C) DPBS Ca²⁺/Mg²⁺ free (Gibco, Invitrogen) supplemented with EDTA (0.2mM). The DPBS was removed and 1ml 1X Trypsin/EDTA solution was added, then the flask was placed back into the incubator during 3-5 minutes and 9ml of medium (M199-complete) were added to stop the Trypsin activity. The suspension was transferred into a polypropylene tube (15 or 50ml) and the cells were pelleted by centrifugation at 250G for 5min. The medium was removed and discarded, the cell pellet was resuspended into 2ml of medium and 10µl were taken to count the cells with the Neubauer chamber. Afterwards, 8ml medium (M199-complete) were added (or a different volume depending if the cells were going to be seeded into coverslips or were taken for RNA isolation) and the suspension was placed into a new 75cm² culture flask (vented cap, BD Biosciences) with 10ml medium. To increase the cell density on coverslips and the number of coverslips that can be obtained from one heart (20mm diameter), autoclaved silicone isolators (press to seal S7060-25EA, 1.0mm x 20mm, Sigma) on top of each glass coverslip were used (Figure m3, B). The coverslips used were sterilized by autoclaving and flamed before placing the isolator. Every coverslip with its isolator was placed inside a 35x10mm culture dish (Falcon, BD Biosciences). The final cell suspension volume used on each coverslips was 300µl. Cell culture medium was changed 24h after splitting to remove remaining Trypsin and cell debris. Medium was changed every 48h when the cells were cultured in flasks or 6-well plates, and every 24h when the cells were on coverslips with silicone isolators to avoid problems with the cells due to the reduced volume and the evaporation of the medium.

4.2.7 RNA isolation from cardiomyocytes and cardiac fibroblasts and RT-PCR

The cells used for RNA isolation (RT-PCR) were resuspended in cold DPBS Ca²⁺/Mg²⁺ free instead of culture medium. They were washed two times (250G/5min for fibroblasts or 40G/1min for cardiomyocytes), pelleted into a new sterile tube (1.5 or 2ml reaction tube)

and 300µl of RTL buffer (with 1% β-Mercaptoethanol) from the total RNA purification kit were added to each sample. The samples were used directly afterwards or kept at -80°C until RNA isolation. For RNA isolation the RNeasy Micro Kit (74004, Qiagen) was used. The procedure was done following the manufacture instructions and using RNase-free materials and reagents. Shortly, the volume was completed to 350µl with RTL buffer (with 1% fresh β-Mercaptoethanol), the samples were subjected to 30s vortex, 350µl 70% EtOH (prepared with sterile RNase-free water) were added and the solution was mixed well by pipetting. The complete solution was transferred into a RNeasy MinElute spin column placed into a 2ml collection tube and centrifuged for 25s at 9000G (microcentrifuge, 1-14, sigma, Germany). The flow-through collected in the 2ml tube was discarded, 350µl Buffer RW1 were added to the column and the column with collection tube were centrifuged at 9000G/25s, once more the flow-through was discarded. Thereafter, the DNase digestion step was included, for this the DNase was always prepared freshly by adding 10µl DNase I stock solution to 70µl RDD buffer per sample and it was mixed gently by inverting the tube. 80µl DNase solution were added directly on top of the spin column membrane and the sample was incubated for 15min at RT. Following the DNase treatment 350µl buffer RW1 were added to the column, it was centrifuged as before to wash the membrane and the column was placed into a new 2ml collection tube and the other tube containing the flow-through was discarded. Another two washing steps of the membrane were made, first by adding 500µl buffer RPE, centrifuging at 9000G for 25s and discarding the flow-through and the second, by adding 500µl of 80% EtOH, centrifuging 25s at 9000G, discarding carefully the flow-through and finalized with one additional centrifugation (9000G/25s) step and discarding of the collection tube. To dry the column, this was placed into a new 2ml collection tube, but the lid was not closed, then both were centrifuged for 2min at maximum speed (12470G or 13000rpm) and the collection tube was discarded. Finally, the elution of total RNA from the column was made by placing the column into a new 1.5ml collection tube, adding 41µl RNase-free water, centrifuging at maximum speed for 1min and the last two steps were repeated to get a final volume of 80µl. The samples were maintained on ice until the RNA quantification and RT-PCR and were kept for longer period at -20°C.

The RNA quantification was done with a NanoDrop spectrophotometer (NanoDrop-1000, peqlab). As blank for the measurements were used 2µl of the same RNase-free water applied for the RNA elution; to determine the concentration 2µl per sample were used. The software from the NanoDrop (ND-1000 v 3.5.2) provided directly the concentration data in µg/ml and the ratios between the absorbance at 260nm and 280nm, and between 260nm and 230nm to determine the purity of the RNA solutions.

The RT-PCR from left ventricular myocytes dissociated from hearts during Langendorff perfusion and from cultured cardiac fibroblasts was done using a one step kit (Super Script™ One Step RT-PCR with Platinum® Taq, Invitrogen). PCR products were obtained using spanning oligonucleotides as primers. The RT-PCR reactions were made in a final volume of 50µl where 25µl were from reaction mix, 1µl from each primer (10µM) and 1µl from the enzyme cocktail, and they were carried out in a thermocycler GeneAmp® PCR System 9700 (Applied Biosystems). The products were run in 2% agarose gels stained with Ethidium Bromide (15µl from a 1% stock solution in a 500ml gel) at 200mV during ~1.3h. To visualize the products and digitalize pictures from the PCR results a gel imaging system (GelDoc™, BioRad) was used. The primers and RT-PCR conditions are summarized in Table m2. As positive control RNA from mouse brain (10µl from a 1ng/µl solution) was used and as negative control a reaction replacing the RNA by an equivalent volume of a RNase-free water from the total RNA isolation kit plus PCR water was always included.

4.2.8 Laser Capture Microdissection of mouse cardiomyocytes

One application of the isolated mouse cardiomyocytes was the expression analysis by RT-PCR. Because the cardiomyocyte suspension obtained by the digestion of the heart is not completely pure (See results, Figure 21, C) the isolation and collection of single CMs by Laser Capture Microdissection (LCM) was chosen to obtain a pure population of cells for the expression analysis (Emmert-Buck et al., 1996).

After cardiomyocyte isolation and the pre-plating step mentioned previously, the cells were pelleted by centrifugation at 40G for 1.5min, then the CMs were resuspended into 2ml sterile and ice-cold DPBS (Ca²⁺/Mg²⁺-free) and the suspension was transferred into a new 15ml polypropylene tube. Once more the cells were pelleted by centrifugation (40G/1min), resuspended in cold PBS and this last step was done twice to wash the cells. Finally the CMs were resuspended in sterile and ice-cold DPBS at a concentration between 80-85 cells/µl. The isolated cardiomyocytes were cytospun on LCM glass slides (1mm PEN-membrane covered, Zeiss) pre-treated with UV light for 30min, to increase cell attachment, under a cell culture bench to avoid contamination of the slides.

Table m2 (A). Primers and conditions used for RT-PCR expression analysis of TRPs.

Gene	Primers (5'-3')	Product position	Expected product size (bp)
TRPC1	PH643 TGC AAA CG TTC TGA GTT ACC PH644 CGT CAG CAC AAT CAC AAC C	Exons 9-11	403
TRPC3	PH647 TAG AGA CAA ATG GCT CCC C PH648 TTT GAG GAC AAC AGA AGT CAC	Exons 7-8	337
TRPC4	KO-42 GCC TCT GCA GAT ATC TCT GGG KO-06 TCG TGC TGG GCT TTG ACA TTG	Exons 6-7	263
TRPC5	PH651 GTA TAA TGG TTC TCG TCC AAG G PH652 AGA GCG ACT GAA GGG TTT C	Exons 6-7	350
TRPC6	PH653 AAA AGT CAC ACT GGG GGA C PH654 ACC ATA CAG AAC GTA GCC G	Exons 6-8	424
TRPM4	IN-48 TCT TCA CAC TGC GCC TGC TG IN-49 GTC GGT AGA AGA CCC TGC GC	Exons 18-19	207
TMEM-2	UK79 CAG CTT TGG GAG GAC AAC G UK81 GCA GAA CTG GCC ACA AGG	Exons 6-10	397
HPRT-1	UW637 GCT CGA GAT GTC ATG AAG G UW638 AGT TGA GAG ATC ATC TCC ACC	Exons 2-3	225

Table m2 (B)

RT-PCR conditions		
Temperature	Time	Cycles
50°C	30min	1X
94°C	2min	1X
94°C	15s	40X
56°C	30s	
72°C	25s	
72°C	7min	1X
8°C	hold	

(A) Oligonucleotide sequences used for expression analysis of TRPs. All the primers were intron expanding. The predicted amplification and the expected product size are mentioned for each primer pair. **(B)** Conditions for the RT-PCR reaction for all the primer combinations.

The slides were mounted on pre-cleaned and cold (4°C) cyto-buckets (LT11175753, Thermo Electron Corporation), following the manufacture instructions, but with two modifications. First, instead of using grease in between the plastic block and the slide, it was used a rectangular piece of autoclaved Wathman paper with three holes fitting to the

holes of the plastic block. Second, the cells were not placed directly into the three holes of the plastic block but into 0.5ml sterile reaction tubes. Only two spaces of the plastic block were used to place two 0.5ml tubes because the PEN-membrane from the slides did not cover the complete surface of the slide. Inside each tube 150 μ l of the cardiomyocyte suspension were placed and a small hole was made on the tip of the tube with a 23G 1" needle (Microlance™, BD). After mounting the bucket with the cells, they were cytospun at 4°C (Jouan multifunction centrifuge CR3i, Thermo Electron Corporation) using 280G for 2.5 minutes. The slides were taken out of the buckets and directly fixed with increasing Ethanol concentrations (70%, 80%, 90% and 100% on minute each) or later with Methanol (100% 1 min). Immediately afterwards every slide was transferred inside a single sterile 50ml polypropylene tube to avoid complete drying of the samples and they were kept in ice until the isolation of cardiomyocytes.

The collection of the cells was made using a Zeiss P.A.L.M. LCM microscope (Zeiss/Microlaser Technologies) with a 20X magnification objective (Plan-Neofluar 0.5 ∞ /0.17). The cells were collected on the cap of 0.5ml LCM tubes (AdhesiveCap 500 opaque, Zeiss) as described by Schütze and Lahr (1998). The setting and controlling of the device were made by the incorporated software Palma®Robo Software v1.2.3. Robot LPC function was selected to cut and catapult the cells on the cap, the laser focus was set between 52 and 54, the laser energy for cutting was between 57 and 59% and the catapulting energy (LPC) was set around 83%. Once the setup was prepared, the slide was removed from the 50ml tube, placed into the microscope bench and let it dry for about 5min before starting. Then, the cap from the LCM tube was cut out from the tube and only was manipulated using pre-flamed forceps to avoid RNase contamination. The cap was placed facing down on the cap holder and approximated to the slide as much as possible, but avoiding any contact to the PEN membrane of the glass slide.

The cells were identified easily because their morphology; only well preserved cells, rod shaped and single placed were cut out of the slide. Between 40 and 170 mouse ventricular cardiomyocytes were collected on each cap, this number was time dependent. I determined to collect as much as possible cells in between 30min per slide, trying to reduce the exposure of the preparation. After catapulting the cells on the tube cap they were counted using the 4X magnification objective (Achromplan 4X/0.10 ∞ /-). The cap was carefully removed from the holder and it was used to close the tube that already contained 150 or 300 μ l RTL buffer (with 1% β -Mercaptoethanol) from the total RNA purification kit (RNeasy Micro Kit, Qiagen). 150 μ l RTL buffer were used when the cell number was ~50

cells, and 300 μ l when there were ~100 cells. After closing the tube, it was vortexed for 30s, placed on dry ice and stored at -80°C until the total RNA extraction

Total RNA extraction was made using the RNeasy Micro Kit (Qiagen). The procedure was similar except that before starting the isolation a carrier RNA was added (5 μ l per sample of a solution with 4ng/ μ l) for extraction of RNA from small number of cells. Elution volumes were variable (25 μ l, 46 μ l, 41 μ l 2X and 51 μ l 2X) depending on the amount of starting cells to get the maximum RNA from each preparation. The RT-PCR from these isolated cardiomyocytes was done also using the one step kit (Super Script™ One Step RT-PCR with Platinum® Taq, Invitrogen) and 50 μ l final reaction volume, from which usually 22 μ l were from the RNA solution. The RT-PCR and electrophoresis conditions were the same mentioned above and total RNA from brain was used as positive control and the elution water as negative control.

4.2.9 Characterization of cardiac fibroblast culture by immunocytochemistry

To characterize cultured mouse cardiac fibroblasts four different antibodies were selected according to Thum and collaborators (2008). The antibodies used were: rabbit anti-human prolyl-4-hydroxylase beta polyclonal (Acris) which is mentioned as fibroblast specific marker; mouse monoclonal anti-CD31 (Platelet Endothelial Cell Adhesion Molecule or PECAM1) clone P2B1 (abcam) used as endothelial marker; rabbit polyclonal against smooth muscle α 2-actin or ACTA2 (abcam) for smooth muscle cells; and mouse monoclonal anti- α -actinin (ACTN2) clone EA-53 (Sigma) used as cardiomyocyte marker. For characterization of the fibroblasts I selected the anti-P4HB rabbit polyclonal instead of the monoclonal (P4HB, clone 6-9H6, Acris) used by Thum and coworkers because the last one reacts with rat but no mouse fibroblasts. The secondary antibodies used were goat IgG anti-mouse conjugated to Alexa Fluor 594 and goat IgG anti-rabbit conjugated to Alexa Fluor 488 (Molecular Probes, Invitrogen). As positive control for the selected markers freshly isolated mouse cardiomyocytes isolated as described, freshly isolated ileum smooth muscle cells (iSMC) from the longitudinal muscle layer isolated by collagenase treatment (Tsvilovsky et al., 2009) and mouse aortic endothelial cells (MAEC) prepared in our laboratory as described were used (Suh et al., 1999; Freichel et al., 2001). Negative controls consisted of cells processed in the same way as positive controls but omitting the primary antibody.

All different cell types used (CMs, FBs, MAEC and iSMC) were placed on pre-cleaned round coverslips (20 or 25mm diameter, Nr. 0/1). Coverslips were cleaned by incubation for 2h in 2N NaOH at RT followed by extensive rinse in d-diH₂O; they were stored submerged in 70% EtOH and flamed before its use. Cardiac fibroblasts and endothelial cells were cultured on glass coverslips and they were used between passage 1 (P1) up to passage 3 (P3), but in some case acute isolated FBs were directly plated on glass coverslips. Cardiomyocytes were attached to coverslips by cytopsin; a similar procedure was followed as the one mentioned in the LCM procedure but instead of using glass slides, three coverslips were placed between the Wathman paper and the plastic block. CMs were resuspended for cytopsin in PBS at a concentration of 100CMs/ μ l and after cytopsinning them (280G for 2.5min at 4°C) they were rinsed with PBS to remove non attached cells or cell clumps and finally the coverslips were placed into 6 or 12-well polystyrene cell culture plates (Falcon, Becton Dickinson) and kept submerged in PBS at 4°C until cell fixation. Ileum smooth muscle cells were processed similarly to CMs but they were cytopsin by centrifuging at 250G/2min from a cell suspension containing 50 cells per μ l.

The immunostaining procedure was standardized for the positive controls in such way that at the end there were only small differences in primary antibody concentrations and the incubation times. This allowed the staining in parallel of different cell types and different cell markers to reduce the variability between preparations. Before cell fixation the samples were rinsed in cold PBS (pH 7.4, sterile and filtered). Cell fixation was done by incubation in 4% Paraformaldehyde (PFA) prepared in PBS (pH 7.4) over 10min at 4°C and subsequently the cells were washed two times for 5min by submerging them in cold PBS. The samples were transferred then into pre-chilled Acetone (-20°C) for exactly 5min (step omitted when CD31 was used) and washed after 3 times with cold PBS during 5min each time. To block unspecific binding, the samples were incubated for 1h (RT) in 1% BSA prepared in PBST (only PBS for CD31) including 0.3M Glycine which reduces the background by binding to free aldehyde groups. Between 50-100 μ l from the primary antibody solved in 1% BSA (PBST or only PBS for CD31) were added and the cells were incubated at RT, protected from light in a humid chamber. Concentration and incubation times used are depicted in Table m3. Three washing steps of 5min each with cold PBS were made followed by the incubation with the secondary antibodies (Table m3) at RT and protected from light. The secondary antibody mixtures were decanted and three 5min-washing steps with cold PBS were done. Samples were always protected from light. To stain the nuclei the cells were incubated for 5min at RT with DAPI 1.5 μ g/ml in PBS. Finally

the coverslides were mounted on glass slides using as an anti-fade mounting medium (Vectashield, Linaris) and were stored at 4°C protected from light until its analysis.

Table m3. Immunocytochemistry conditions used for characterization of cardiac fibroblast.

	anti-P4HB	anti-α-actinin	anti-α-SM actin	anti-CD31
positive control	fibroblasts	cardiomyocytes	iSMC	MAEC
acetone permeabilization	yes	yes	yes	no
blocking	1% BSA in PBST	1% BSA in PBST	1% BSA in PBST	1% BSA in PBS
concentration	1 μ g/ml (in PBST)	150 μ g/ml (in PBST)	10 μ g/ml (in PBST)	10 μ g/ml (in PBS)
incubation time	1h	2h	2h	2h
secondary antibody (2nd-ab)	anti-rabbit AlexaF488	anti-mouse AlexaF 594	anti-rabbit AlexaF488	anti-mouse AlexaF 594
2nd-ab dilution	1:1000 (in PBST)	1:200 (in PBST)	1:200 (in PBST)	1:200 (in PBS)
2nd-ab incubation time	1h	1h	1h	1h

iSMC: ileum smooth muscle cells, MAEC: Mouse aortic endothelial cells, PBS: Phosphate buffered saline, PBST: PBS-Tween 20 and Alexa-F: Alexa Fluor.

The analysis from stained cells was made using two different microscopes. One setup was an inverted TE2000-U microscope (Nikon, Japan) with a X-Cite®120 fluorescence illumination system (EXFO, Photonic Solutions Inc., Canada) coupled to a digital camera (DS5mc, Nikon). This setup was equipped with a FITC filter and a UV filter used to visualize signals from Alexa Fluor-488 conjugated antibodies and from the nuclear staining DAPI, respectively. The processing and digitalization from the pictures was made using the NIS-Elements software (F 2.30, Nikon). The second setup was an AxioVert 200M inverted microscope (Zeiss, Germany) equipped with a HXP120 fluorescence lamp (Kübler codex, Germany), a digital camera AxioCam MRm (Zeiss), filters for FURA (DAPI), GFP (Alexa Fluor-488) and Alexa-594 and the software used was AxioVision v4.7.2 (Zeiss). The imaging conditions, like exposition time, used in positive controls were the same for the negative controls.

4.2.10 Calcium imaging from mouse cultured cardiac fibroblasts

To measure changes in intracellular calcium concentration from isolated mouse cardiac fibroblasts the ratiometric calcium indicator FURA-2 for microfluorometric analysis was used. For measurements an inverted AxioObserver A.1 microscope (Zeiss, Germany) equipped with a polychromatic Xenon light source (Polychrome V, TILL Photonics, Germany) was utilized. A 20X magnification objective (FLUAR 20X/0.75 ∞ /0.17, ref.

420150-9900, Zeiss) was used and the recordings were obtained through a digital camera AxioCam MRm (Zeiss). Cells were alternately excited at 340 nm and at 380 nm and the exposure time varied from 60-400 milliseconds; pairs of frames were recorded every 0.2-5 seconds. Increase in intracellular calcium concentrations $[Ca^{2+}]_i$ led to an increase in the emitted fluorescence at 510 nm after 340 nm excitation and decreasing emission after 380 nm excitation. Changes in $[Ca^{2+}]_i$ levels over time were expressed in arbitrary units as fluorescence ratio between emission-340/emission-380 (Em340/Em380), calculated from regions of interest (ROI) that included complete cells. Settings of the setup and, recording and analysis of the data were done with the Physiology module from the AvioVision software (v4.8.1, Zeiss).

Mouse adult cardiac fibroblasts were cultured on sterile and round pre-cleaned (see section 4.2.9) glass slides (25mm diameter). To increase the density of cells, silicone isolators were used for plating. In some experiments cells were serum starved over night. The fibroblasts were incubated with 5 μ M FURA-2-AM (Molecular Probes, Invitrogen, Germany) in M199 (10% FCS or without when mentioned) at 37°C for 25-45min. The medium was removed, the cells were rinsed with physiological buffer and transferred into a stainless steel chamber (Attofluor® A-7816, Molecular Probes) coupled to a vacuum sucking system and a perfusion system to be washed with running buffer over 15-30min. As physiological solution was selected modified Tyrode's buffer containing 1.8mM $CaCl_2$, after trying other solutions found to be used in the literature like HEPES buffered saline (Ostrom et al., 2003) or Ringer solution (Shumilina et al., 2005). In some set of experiments of Calcium re-addition the Ca^{2+} -free solution contained 1mM EGTA.

Initial measurements were done at room temperature but during the standardization of the protocol it was established to measure at 37°C. To this end a dual automatic temperature control system (TC344 Heater Controller, Warner Instrument Corp. Harvard Apparatus Company, USA) was used with a heating tube for the perfusion solutions and a heating element connected to a home made aluminium support to keep the coverslip's chamber warm. After the de-esterification period (~30min) the recordings were done. First, a one minute period was recorded to obtain a basal calcium level; cells were then stimulated with different agonists such as Serotonin, Isoproterenol, human ATII (Sigma) or Thapsigargin. Agonists were prepared at the desired final concentration in Tyrode's buffer to perfuse the cells constantly with it. In most of the experiments different agonist were tested with washing steps in between. The data from the fluorescence ratios were exported with AxioVision and mean traces for groups of cells were made with Origin 8 (OriginLab Corporation, USA).

4.2.11 Surface ECG recording

ECG recordings were made under 2% isofluran anesthesia (in O₂/N₂O gas mixture 1:2). The mice were kept laying on their front on a warm plate at 37°C and three steel electrodes (29G, MLA1203, ADInstruments) were placed subcutaneously as described by Li and coworkers (2004a) but following the lead I configuration (positive electrode in left foreleg, negative electrode in right foreleg and ground electrode in left rear leg). The electrodes were connected to a BioAmp and a Power Lab/8S (ADInstruments). The ECGs were recorded at a rate of 4 KHz using high pass filtering 0.3Hz and low pass filtering 100Hz. The signal range was determined between 4 to 10mV. The analysis of ECG traces was made with the ECG analysis module from ChartPro v5.5.5 and LabChart 6.0 (ADInstruments). The ECG from each mouse was recorded for about 5 minutes and for the analysis a period of 1 minute was taken after the first minute of recording when the signal was completely stabilized. For analysis and detection of the ECG waves the option “mouse” in the ECG module and the option “rodent T wave” were selected. Additionally, an average trace (Figure m4) was made from ten beats and the QT interval correction was calculated using the formula $QTc=QT/\sqrt{RRx10}$ from Mitchell et al. (1998).

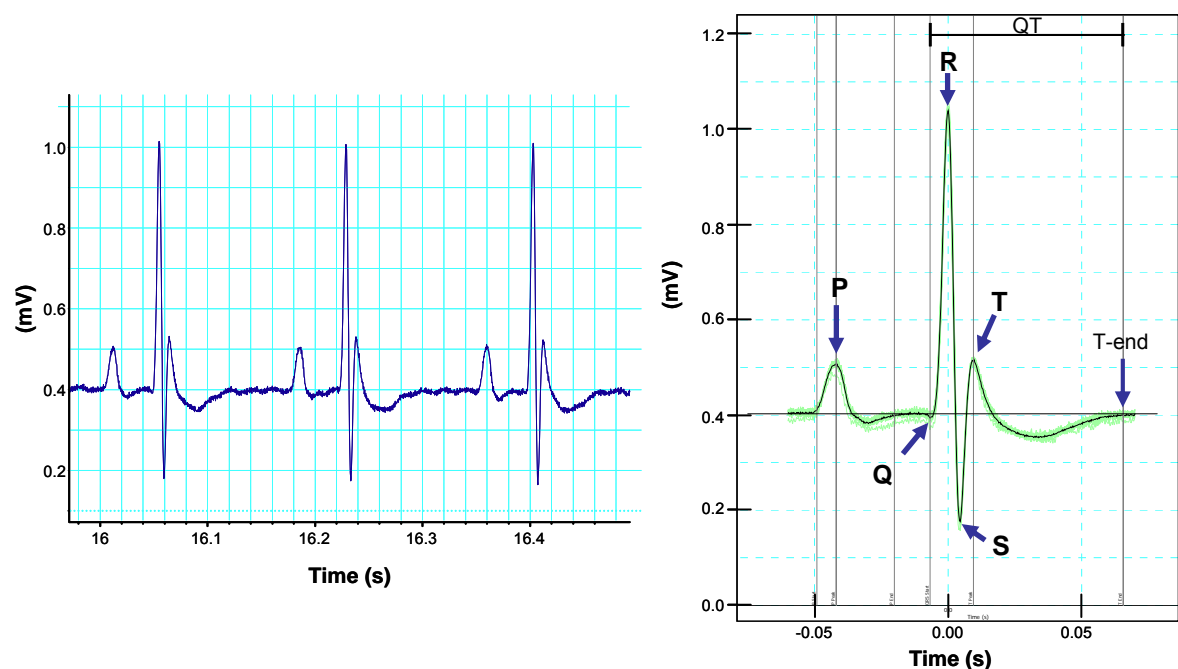


Figure m4. Surface ECG trace from mouse. Original trace of and ECG recording (left panel) from a mouse kept under isofluran anesthesia. On the right is shown an average ECG trace obtained from 10 heart beats where the different ECG waves and the Q-T interval limits are depicted.

At the end the detection of different waves and intervals was checked manually. Also the presence of irregular beatings was checked manually by scrolling through the recording. The following parameters and the corresponding units were obtained for each ECG measurement: RR Interval (s), Heart Rate (BPM), PR Interval (s), P Duration (s), QRS Interval (s), QT Interval (s), QTc (s), JT Interval (s), Tpeak-Tend Interval (s), P Amplitude (mV), Q Amplitude (mV), R Amplitude (mV), S Amplitude (mV), ST Height (mV), T Amplitude (mV).

4.2.12 Organ bath: spontaneously beating isolated right atria

Four atria were placed in the organ bath (5ml, FMI-Föhr Medical Instruments, Germany) to measure two atria per genotype simultaneously. To prepare the atrium the heart was quickly excised after the injection of 1ml Krebs-Henseleit (KH) into the left ventricle and was placed into a plastic Petri dish (Silicone pre-coated) containing KH solution constantly gassed (95% O₂ and 5% CO₂). The heart was gently fixed with a needle through the left ventricle with the posterior part of the heart facing up and the adhering fat close to the aorta was removed. The right atrium was partially dissected free from the heart by an incision close to the coronary vessels positioned parallel to it and by one cut made on the inferior vena cava; then, the excess from the superior vena cava was removed. A ~12cm thread (7/0 Suprama, Germany) with a small ring (~2mm diameter) at the end and spaced for 9.5cm to the knot point was fixed to the tip of the right atrium and the remaining thread distal to the ring was cut out (Figure m5, A). The needle fixing the heart was removed; the heart was turned down and fixed again through the left ventricle and finally the right atria was completely dissected free from the heart by cutting carefully the remaining tissue below it. Finally, a second thread was fixed to the remaining part of the inferior vena cava, this suture also had a small ring at the end but spaced only by ~3mm from the knot place. Special attention was taken when the second thread was closed to avoid closure of the atrial opening.

The atria were suspended in the organ bath using two threads, the short one attached to the lower hook and the long one to the hook below the transducer. Each isometric transducer (TIM-1030, FMI) was coupled to an amplifier (MIO-0501 DC, FMI) connected to a Power Lab 8S (ADInstruments) that allowed the digitalization and recording of the measurements with the LabChart software (ADInstruments). The organ bath chambers were filled with warmed (37°C) and constantly gassed (95% O₂ and 5% CO₂) KH solution. The atria were pre-loaded to 0.4g tension and were let to equilibrate for 1 hour until they reached a stable beating rate. This equilibration period included two washing steps in

between at minute 30 and 45. Once the beating rate was stable the cumulative concentration dose response experiments with different agonists were done. In a series of experiments Isoproterenol was applied first in a concentration range from 10pM to 1µM (Figure m5, B). After the last dose of isoproterenol three washing steps were made and the atria were let to recover to the basal beating rate for one hour with two additional washing steps (40 and 50min after last Isoproterenol dose). Then, Acetylcholine (ACh) dose response (10nM to 30µM) was carried out. After washing out ACh and getting the basal beating rate, a final 10nM Isoproterenol dose to test the atrial response at the end was used.

Angiotensin II dose responses (10pM to 10µM) were preceded by three washing steps with a recovery period of 20min between each step. After the last ATII dose four additional washing steps spaced each by ten minutes with a final recovery of 10-15 minutes were done. After this, increasing Phenylephrine concentrations (PE) (1nM to 300µM) were applied to test the normal response to this agonist. A final single application of Iso 10nM was done after washing out the PE and recovering to the basal beating rate. To analyze the data and to extract the values from the recordings the Dose Response module from the LabChart software (v7.1.2) was used. The dose response curves were made with a mean value of 30s from the beating rate when the maximum and stable response was achieved for every concentration.

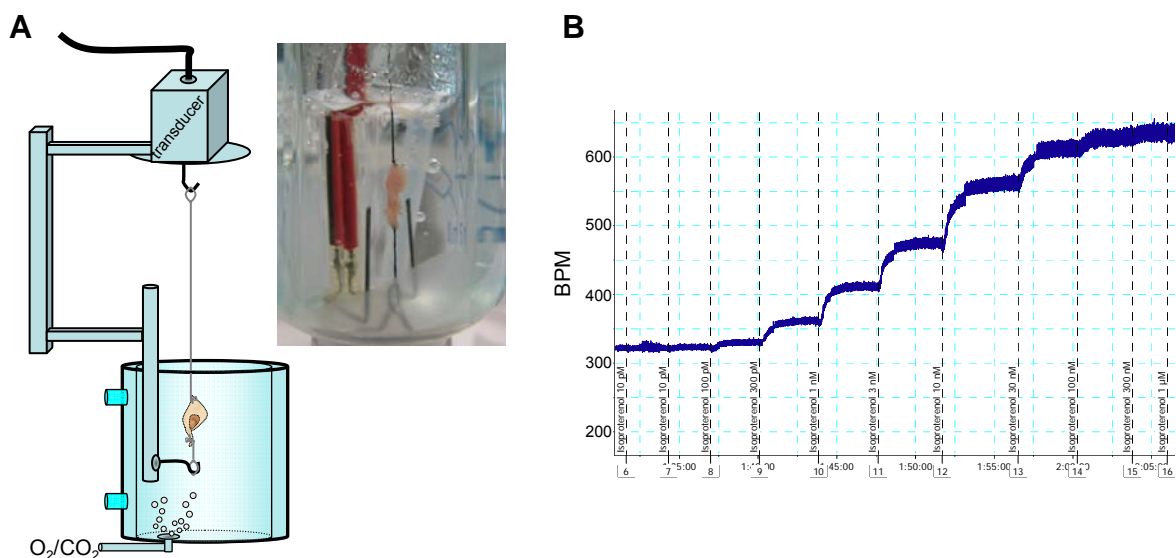


Figure m5. Mouse right atrial preparation for organ bath experiments. (A) Graphic representation and original picture from a mouse right atria hanging in the organ bath to quantify the spontaneous atrial beating rate. **(B)** Original trace from the spontaneous beating of a right atria exposed to increasing isoproterenol doses starting from 10pM up to 1µM.

4.3 *In vitro* analysis of platelets

4.3.1 Platelet counting

The manual platelet counting was made from diluted blood in a 1% Ammonium Oxalate solution prepared with d-diH₂O sterile and filtered (stored at 4°C) following the method described by Harrison and coworkers (2004). Before starting each preparation the Ammonium Oxalate solution was centrifuged for 15min at 1500G to remove debris. The blood was taken from conscious mice by submandibular bleeding using 18G 1¹/₂" needles (Microlance™, BD) and 50 to 70µl blood were collected into Heparin containing sampling tubes (SARSTEDT ref. 41.1503.005). To dilute the blood 50µl blood were added into 950µl 1% Ammonium oxalate solution to have a 1:20 dilution, the suspension was mixed for 15min at RT to lyse the erythrocytes and to keep the platelets intact. From the blood suspension 10µl were placed into an improved Neubauer counting chamber (BRAND, Germany). The chamber was placed into a moist Petri dish for 20min to allow the platelets to settle and afterwards the platelets were counted under an inverted Nikon microscope (Eclipse TS100) using a 40X magnification objective (LWD 40X/0.55 Ph1 ∞/1.2 WD 2.1, Nikon). The cells were counted from the smallest squares on the middle of the chamber (25 squares subdivided in 16 squares that are equivalent to 0.1µl) and a zigzag sequence between the squares was followed. At the end the number of cells per µl was calculated.

In addition to the manual counting, platelets numbers were obtained with a Coulter counter (AcT diff, Beckman Coulter). For this, blood samples were collected into EDTA containing sampling tubes (SARSTEDT ref. 41.1503.005). The blood was obtained by submandibular bleeding, mixed by repetitive inversion of the tube and kept at RT until the measurements. From each sample 12µl blood were taken by the counter.

4.3.2 Hematocrit quantification from mouse samples

Blood were taken from conscious mice by submandibular bleeding. Around 50µl blood (~5 drops) were collected into heparin containing sampling tubes (SARSTEDT ref. 41.1503.005). The blood was transferred into Hematocrit capillaries (Na-heparin, 7493-11, BRAND, Germany), the capillary end, where the blood was inserted, was sealed with yellow Plasticine and the tubes were centrifuged for 10 minutes at 13000rpm in a Hematocrit centrifuge (Type 2011-Hettich, Germany). At the end the total lengths of the sample contained in the tube and the red portion were measured with a ruler, and the

proportion in percentage of the red phase was calculated in relation with the total length to obtain the hematocrit value.

4.3.3 Isolation of mouse platelets and preparation of platelet rich plasma (PRP) and washed platelet (WP) suspensions

For both PRP and WP preparations the mice were anesthetized with Avertin given by an i.p injection (300-800 μ l depending on the mouse weight and genotype). After checking the absence of sensitivity from the paw sole and tip tail the blood was obtained by submandibular bleeding using an 18G 1 $\frac{1}{2}$ " needle (MicrolanceTM, BD). The resulting protocols to prepare PRP and WP were modifications from different published methods (Hechler et al., 1998; Fabre et al., 1999; Foster et al., 2001; Nieswandt et al., 2002; Cazenave et al., 2004).

Preparation of platelet rich plasma (PRP). To prepare PRP the blood was collected into 15ml polypropylene tubes containing 10 μ l of Na-heparin solution (1000U/ml). The blood from 4 to 8 mice from the same genotype and gender was pooled and Na-heparin (1000U/ml) was added to have a final concentration of 10U/ml heparin. The blood was centrifuged for 8min at 260G (RT); the supernatant represented the platelet rich plasma (PRP) and was transferred into a new 15ml polypropylene tube. Platelets from the PRP were counted from a diluted sample (1:10) made using 5 μ l PRP and 45 μ l sterile Sodium Chloride (0.9%) solution and placing 10 μ l into a Neubauer chamber for manual counting. The remaining blood was centrifuged once more for 15min at 2200G to obtain the platelet poor plasma (PPP) that was moved into another new 15ml tube. From the PPP 200 μ l were saved for the calibration of the aggregometer and the rest was used to dilute the PRP to a final concentration of 3x10⁸ platelets/ml. The PRP was kept at 37°C before and during the aggregation experiments.

Preparation of washed platelets (WP). To prepare washed platelets blood from 4 to 7 mice from the same genotype and gender was collected in 15ml polypropylene tubes containing 100 μ l of Acid-Citrate-Dextrose (ACD). Between blood collection from individual mice or when the volume reached around 900 μ l ACD (100 μ l) was added to have a final ratio 1:10 between ACD and blood. After adding ACD the blood was gently mixed; it was checked for clumps and the wall of the tubes was cleaned with a cotton bud rinsed with ACD. To each blood sample 0.75 volumes from the 1X Platelet's Buffer (pre-warmed at 37°C) were added, mixed well and centrifuged at 2300G during 10s per milliliter of final

volume. The supernatant, rich in platelets, was transferred carefully and without red cells into a new 15ml tube. Prostacyclin (PGI₂) was added to the platelet suspension (5µl per ml from a 0.1mM solution) and the cells were incubated in a warming bath for 5min at 37°C. After incubation PGI₂ was added once more as before (5µl/ml) to the cell suspension and this was centrifuged at 1000G for 5 minutes. The supernatant was discarded and the platelet pellet was resuspended in 2ml Platelet's Buffer where 5µl/ml PGI₂ (0.1mM) and 2µl/ml heparin (5000U/ml) were included. The suspension was incubated one more time at 37°C for 5 minutes; next 5µl/ml PGI₂ were added and the platelets were pelleted (1000G, 5 minutes). Then the supernatant was discarded, the cells were resuspended in 1ml Platelet's Buffer and were kept at 37°C. To count the cells a 5µl aliquot from the cell suspension was diluted in 195µl 0.9% NaCl, from this dilution 10µl were placed into a Neubauer chamber to determine the number of platelets. The platelet concentration was adjusted with Platelet's Buffer to 3x10⁸ platelets per milliliter (Walther et al., 2003) and 1µl per ml apyrase (0.2 or 0.02U/µl), which hydrolyses ATP and ADP into AMP, was added into the cell suspension to have final concentrations of 0.2U/ml or 0.02U/ml. The apyrase concentration was reduced specially to evaluate the platelet aggregation induced by thromboxane analogue U46619. TxA₂ and its analogues induce ADP release from platelets that amplifies platelet aggregation mediated by the TxA₂ receptor itself. Apyrase in a concentration of 0.2U/ml significantly reduced the U46619-induced aggregation, even at high concentrations such as 10µM (Figure m6, A). Finally, the platelets were incubated to recover for at least 30min at 37°C before starting the aggregation experiments.

4.3.4 Platelet aggregation: turbidimetric measurements

To evaluate the *in vitro* platelet aggregation of TRPC-deficient mice I established in our group a protocol for turbidimetric measurements using PRP and WP preparations (see 4.3.3). The principle of the method is described in the Figure m7. The aggregometer used was an APACT 4S Plus (Rolf Greiner BioChemica, Germany) which has the option to measure 4 samples in parallel at 37°C. It monitors the aggregation, measured by changes in the optical density (OD) at 740nm under constant stirring (1000 rpm) from samples placed in plastic cuvettes (400068, Micro-Planküvetten with mixer 1.0x4mm, Rolf Greiner BioChemica) that included a metallic mixer. In addition, the raw and graphic data from the aggregation were visualized and obtained with the APACT software AS-IS v1.21c (Rolf Greiner BioChemica). The software calculated the following parameters from each aggregation curve that were used for the aggregation analysis: Platelet Shape Change

(PSC) given in percentage of aggregation, maximum aggregation expressed in percentage of aggregation, area under the aggregation curve given in percentage of aggregation, and slope of the aggregation curve defined as the maximum slope during aggregation, in percentage of aggregation, over the time in minutes.

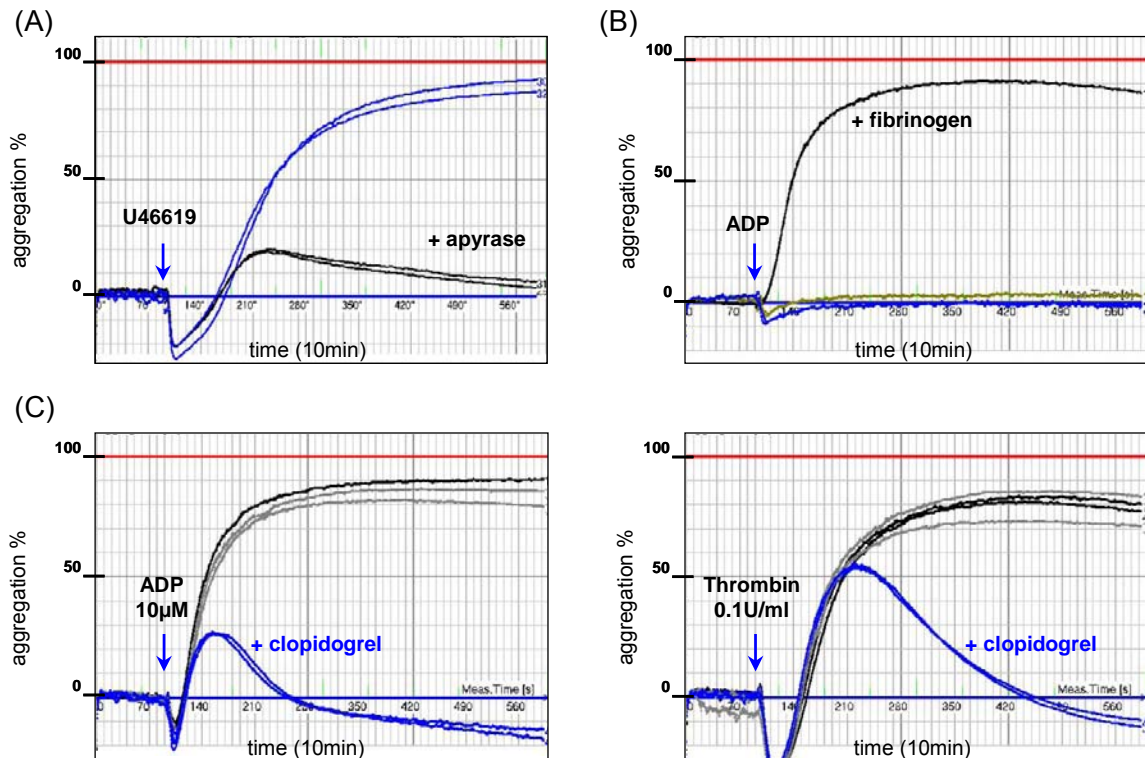


Figure m6. Effect of apyrase, fibrinogen or Clopidogrel in washed platelets preparations from wild type mice used for *in vitro* aggregation. (A) Platelet aggregation induced in washed platelets by 10 μ M U46619 in the absence (blue traces) or in the presence of 0.2U/ml (black traces) of Apyrase. (B) ADP-induced aggregation in washed platelets requires the presence of fibrinogen. Without adding fibrinogen ADP fails to induce aggregation in a concentration of 10 μ M (blue) or 20 μ M (orange); when fibrinogen (70 μ g/ml) was added 10 μ M ADP induced aggregation (black). (C) Platelets from mice pre-treated with Clopidogrel (o.p. 5mg/kg/day over 2 days) in blue, from mice receiving only vehicle (DSMO 1% and NaCl 0.009% in a 5% Saccharose solution) in gray or without any pre-treatment in black. The aggregation was induced by 10 μ M ADP (left panel) or by thrombin 0.1U/ml (right panel). There is no change in the aggregation compared between vehicle and non pre-treated mice. The arrows indicate the time of the agonist addition.

Around 20 min before starting the measurements the aggregometer was turned on because it was required to be pre-warmed at 37.4 $^{\circ}$ C for automatic calibration of the channels (without measuring cuvettes). Every channel was calibrated separately with a cuvette containing 200 μ l of platelet poor plasma (PPP) or 1X Platelet's Buffer depending if the experiments were done with platelet rich plasma or washed platelets, respectively. This calibration value was automatically set as equivalent to the maximum possible aggregation value (100% aggregation). Subsequently, four samples, two per genotype,

consisting each in 190 μ l platelets suspension were placed inside the measuring spaces and the basal value (0% aggregation) was set. Measurements were started with a time lag of ~8s between channels and a base line was recorded for 90s without stimulation. After the time point of 90s an aliquot of 10 μ l from the agonist was added to the platelet suspension of each channel and the aggregation was recorded up to 800s in case of Collagen, Thrombin or the TxA₂ analogue U46619 stimulation, and up to 600 for ADP stimulation.

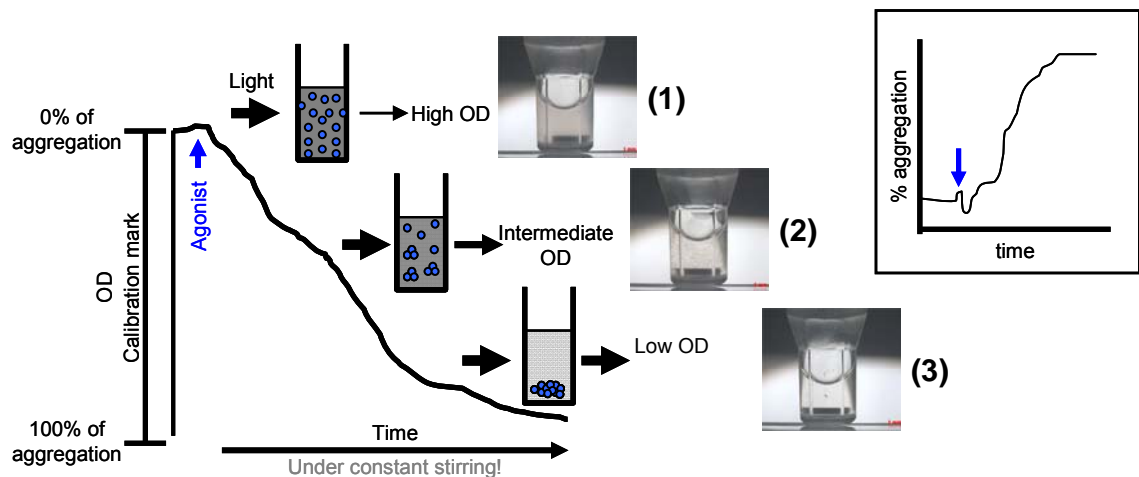


Figure m7. Turbidimetric aggregometry. The platelet suspension before stimulation **(1)** presents a high optical density (OD) which is set as the baseline level of aggregation (0%). After the addition of an agonist the platelets aggregate leading to a reduction in the optical density of the suspension **(2)** until the aggregation is completed **(3)**. The maximum aggregation (100%) reference is given by the resuspension buffer in case of WP or by the platelet poor plasma in case of PRP analysis. The inset shows the usual way to represent the aggregation curve (Modified from Jarvis, 2004).

All agonists were solved in sterile NaCl (0.9%) and were stored below -20°C. Only freshly thawed aliquots were used for every day of experiments. ADP-induced aggregation in washed platelets was done in the presence of human fibrinogen because, similar to experiments performed with washed platelets from humans (Park and Hourani, 1999) and mice (Varga-Szabo et al., 2008a), I observed no aggregation by adding ADP in washed platelet preparations from mice (Figure m6, B). The final fibrinogen concentration was 70 μ g/ml; 4 μ l from a fibrinogen solution (35mg/ml in 0.9% NaCl, sterile filtered) were added to each platelet sample around 4min before starting the OD aggregation experiments.

4.3.5 Platelet aggregation in platelets from mice pre-treated with Clopidogrel

To distinguish the aggregation response mediated by the two different ADP receptors expressed in mouse platelets (P2Y₁ and P2Y₁₂) Clopidogrel was used to selectively block P2Y₁₂ receptors. 24h and 2h before blood collection the mice received Clopidogrel orally (o.p.) at a dose of 5mg/kg (Savi et al., 1992) and at a volume of 10µl/g body weight. For peroral administration a curved reusable gavage feeding needle (PS/18, No.18061-50; F.S.T., Germany) was used. Clopidogrel was solved with DMSO to a concentration of 50mg/ml (stock solution kept at 4°C) and subsequently solved 1:1 with sterile saline (0.9%) solution to a concentration of 25mg/ml, this second dilution was made shortly before application to the mice. Saccharose 5% (w/v) solved in tap water was used as vehicle. The sweet water was used to avoid rejection and regurgitation of the drug by the mice and this was confirmed by the constant observation of the mice during the 15min subsequent to drug administration. In the first experiments with Clopidogrel a group of vehicle treated mice receiving the same proportion of DMSO and 0.9% NaCl was included (Figure m6, C). Because there was no obvious inhibition of platelet aggregation by these vehicle substances this vehicle control treatment was omitted later on. Preparation of washed platelets from Clopidogrel treated mice for *in vitro* aggregation experiments were performed as described (see 4.3.4).

4.3.6 RNA isolation from mouse platelets and RT-PCR

Total platelet RNA was extracted from washed platelet preparations. After a final washing step when platelets were resuspended in 1X Platelet's Buffer and counted, the cells were washed again 2 times with sterile and Ca²⁺/Mg²⁺ free DPBS. Briefly, the platelets were pelleted by centrifugation during 5min at 1000G and the supernatant was discarded, the platelets were resuspended into 2ml DPBS and were transferred into a sterile 2ml reaction tube where a second washing step with DPBS was performed. Finally, the pellet was obtained by centrifuging for 10min at 1200G into a microcentrifuge and it was resuspended in 300µl RTL Buffer provided with the RNA isolation kit. Cells were lysed by 30s shaking with the vortex. The samples were kept on ice if the total RNA isolation was made immediately or were kept at -80°C until RNA was extracted.

For extraction of total RNA the RNeasy Micro Kit (Qiagen) was used like for cardiac cells (see 4.2.7) and 6x10⁷ to 1x10⁹ platelets were used in each RNA extraction column. RNA was eluted two times in 41µl RNase-free water included in the kit. The RT-PCR from the

platelets was done also using the one step kit (Super Script™, Invitrogen) in 50µl final reaction volume, and between 20 to 60ng total RNA were used per RT-PCR reaction. The RT-PCR and electrophoresis conditions were the same mentioned already and total RNA from brain was used as positive control and the elution water as negative control.

4.3.7 Fluorescence-activated cell sorting (FACS) of mouse platelets

The sorting of mouse platelets was done with P.D Dr. Stephan Philipp from our Department and it was made as second *Spezialpraktika* from the GK 1326 (“Fluorescence Activated Cell Sorting (FACS) of mouse platelets for further expression analysis of TRPC channels”). This method served to sort platelets for RT-PCR analysis and also to evaluate the purity of the washed platelet preparation used for aggregometry and expression analysis.

Washed platelets were prepared as described using 2 to 3 mice, but 1X Platelet's Buffer without CaCl₂ was used during the platelet isolation. Platelet concentration was adjusted to 1x10⁸ platelets per ml and the cells were allowed to recover for 30min at 37°C before starting the experiments. An aliquot of 100µl (1x10⁷ platelets) was transferred into a 2ml sterile tube and 5µl from a monoclonal FITC-labeled antibody against mouse αIIbβ3 integrin (CD41/CD61) (Clone Leo.F2, emfret analytics, Germany) and 400µl of Platelet's Buffer containing 1mM CaCl₂ were added. The suspension was incubated at RT for 15 minutes in the dark and after the labeled cells were placed into ice and protected from the light until the sorting.

The cell sorting was done using a MoFlo fluorescence-associated cell sorter (Dako Cytomation Beckman Coulter, Germany) using a 488nm argon laser beam for excitation. After calibration of the sorting machine an aliquot of the non stained platelets was used to characterize the cell population using the forward scatter (FSC) and side scatter (SSC). Then, the stained platelets were compared to non stained platelets with respect to FSC, SSC and to the FITC fluorescence. A right shift of the FITC fluorescence was observed in the stained platelet samples. Finally the cells were sorted directly into PCR tubes in groups of 50, 200, 500 and 2000 per tube. When one 96-PCR rack was completed, this one was placed under a flow bench and the PCR tubes were rapidly closed to prevent sample evaporation. The tubes were transferred into dry ice and they were stored at minus 80°C. The RT-PCR was done using freshly thawed platelets and a one step kit

(Super Script™, Invitrogen) in 25µl final reaction volume. The RT-PCR primers and conditions were the same used for cardiac cells (Table m2).

4.3.8 Western blot from mouse isolated platelets

For isolation of protein fractions from platelets the blood from 4-6 mice was pooled and washed platelets were obtained as described. In addition to the procedure mentioned before, platelets were washed two times with sterile warm (37°C) DPBS (Ca²⁺/Mg²⁺ free) supplemented with Heparin (10U/ml final concentration). To wash the platelets a cell pellet was obtained by centrifugation (1000G/5min) and the cells were resuspended in 2ml DPBS (5µl/ml from a 0.1mM PGI₂ solution were added) the suspension was incubated 5min at 37°C, PGI₂ was added again (5µl/ml) and the cells were pelleted once more and resuspended in DPBS in the presence of PGI₂ (5µl/ml). Finally, the cells were incubated 5 minutes (37°C), a 5µl aliquot was taken to count the cells and the DPBS was removed by centrifugation. The pellet was kept on ice and the cells were homogenized with RIPA Lysis Buffer containing protease inhibitors (added before use); this material was used for expression analysis by western blots. Western blots were performed with help from Christine Wesely (AG Prof. Flockerzi) and home-made rabbit polyclonal antibodies against TRPC1 (unpublished), TRPC3 (unpublished), TRPC4 (Freichel et al., 2001), TRPC5 (unpublished), TRPC6 (Tsvilovskyy et al., 2009) and TRPM4 proteins (Mathar et al., 2010) were used.

4.4 Data analysis

The graphs presented in this work were made with Origin v7.0220 and v8.1.13.88 (OriginLab Corporation, USA). Inside the graphs error bars represent the Standard Error of the Mean (SEM). In case of data presented in tables or numbers inside text, bars or graphs the Standard Deviation (SD) was included. Statistical significances were depicted as *p<0.05; **p<0.01, ***p<0.001 and ns (not significant). Descriptive statistical values such as mean value, median, SEM and SD were calculated with Microsoft Office Excel (Office 2003, Microsoft Corporation) or with Origin. Other descriptive statistics like frequency count were done only with Origin. Specific data analysis procedures used are described under each topic (i.e. cardiac fibrosis).

For statistical analysis comparing mean values from two independent group, for example, comparison between maximal aggregation from WT and KO, the two samples independent Student's t-test was used. In some cases like comparing the weight before and after cardiac hypertrophy induction from the same group, the two-sample paired t-tests were computed. These tests and the probability values (p or p-value) were obtained either with Excel or with Origin and were made after determining if the data from the samples followed a normal distribution. The normality was tested with the Shapiro-Wilk Normality Test from Origin and assumed normal when the p-value was lower than 0.05.

When comparing three or more group mean values, for example aggregation from platelets from Clopidogrel pre-treated mice or cardiac hypertrophy indexes, the one-way analysis of variance (ANOVA) was used after testing if the data were normally distributed. One-way ANOVA calculations were made in Origin and within the calculation the Levene's test for equal variance was computed because one-way analysis of variance assumes that the sample data sets have been drawn from populations that follow a normal distribution with constant variance. In addition, the computations for actual power of the tests were done to assess the probability of successfully rejecting the null hypothesis (no difference between the mean values). When there were significant differences ($p < 0.05$) the Bonferroni *post hoc* mean comparisons were calculated also with Origin.

In addition to the one-way ANOVA when data from cardiac hypertrophy indexes from wild-type and knockout groups (HW/BW, HW/TL and others) were compared the two-way ANOVA (in Origin) was used because strictly some of these experiments followed an experimental design with two factors (variables) and each one had two levels. One factor was the genotype of the mice subdivided in two levels, WT and KO; the second factor was the treatment also with two levels, control treatment (saline) or treatment (Iso or ATII). With the Two-way ANOVA was tested if there were significant differences between the variables level means within a factor and the interactions between the factors. Also computations for Bonferroni *post hoc* means comparisons and for actual power were performed.

When the data did not follow a normal distribution the non-parametric statistic analysis Kruskal-Wallis was used to compare the results from the analyzed groups and the calculation were done manually. Briefly, all the data were organized from the smaller to the higher value and then were ranked with consecutive numbers starting from 1 up to n. Next, the rank sum (A_i) for each group ($A_1, A_2, A_3 \dots A_{ith}$) and the average rank for each group ($\bar{A}_i = A_i/n_i$) were computed. After that it was calculated the sum of squared deviations

between each sample group's average rank and the overall average rank, weighted by the sizes of the group. This calculation is a measure of variability between the observations and what it is expected if the hypothesis of no treatment effect is true; the equation used for this sum was:

$$D = n_1(\bar{A}_1 - \bar{A})^2 + n_2(\bar{A}_2 - \bar{A})^2 + \dots + n_i(\bar{A}_i - \bar{A})^2$$

Where, n_i refers to the number of observations of the i^{th} group and \bar{A} is the average rank of all the observations ($N = n_1 + n_2 + \dots + n_i$) and was equal to $(N+1)/2$. The value D was used to compute the Kruskal-Wallis test statistic H as follows:

$$H = D / (N(N+1)/12)$$

The null hypothesis of no difference between the mean values of the groups was rejected when the calculated H value was higher than the corresponding value with $k-1$ degrees of freedom from critical values for the χ^2 distribution, where k was the number of treatment groups. When there were significant differences between the means from the treatments the non-parametric multiple comparisons were done with the Dunn's test. For each pair of comparisons the Q value was calculated:

$$Q = (\bar{A}_1 - \bar{A}_2) / \sqrt{(N(N+1)/12) (1/n_1 + 1/n_2)}$$

Finally Q values were compared with the critical values of Q for nonparametric multiple comparison testing (Glantz, 2005) and the null hypothesis was rejected or accepted.

5. Results

5.1 Cardiac hypertrophy in TRPC deficient mice

5.1.1 Characterization of protocols for Isoproterenol- and Angiotensin II-induced cardiac hypertrophy in wild type mice

The neurohumorally induced cardiac hypertrophy was selected as method to test the role of TRPC channels for cardiac remodeling. Cardiac hypertrophy induction was done by chronic infusion of two different substances, the β -adrenergic agonist Isoproterenol (Iso) or the AT₁ receptor agonist angiotensin II (ATII). Both agonists were delivered into mice via micro-osmotic pumps. Isoproterenol was mainly given at a dose of 30mg/kg/day over 7 days (referred as Iso-30) but in one series of experiments it was tested a dose of 8.7mg/kg/day over 7 days. ATII was used in two doses, a pressor dose of 3mg/kg/day over 14 days (ATII-3) and a lower dose of 0.3mg/kg/day over 14 day (ATII-0.3).

Before it could be quantified whether the development of cardiac hypertrophy might be changed in TRPC knockout (KO) mice it was required to establish a reliable cardiac hypertrophy induction protocol and all related analysis steps. The protocol was established first in wild type (WT) mice from the first generation offspring between C57Bl6/N and 129SvJ mice because these mice have a genetic background that could be used as control for the TRPC deficient mouse lines available in our laboratory. The main readout of the initial experiments of neurohumoral induced hypertrophy in WT mice (Figure 1) were hypertrophy indexes such as heart weight/body weight (HW/BW) or heart weight/tibia length (HW/TL) ratios (Figure 1, Aa and Ba). The related percentage of increase of each index in relation to saline treated control mice were determined (Figure 1, Ab and Bb). From these data the Iso-induced increase in HW/BW was $20.25 \pm 8.41\%$ ($p < 0.001$), in the ATII-0.3 group the increment was $10.03 \pm 6.80\%$ ($p < 0.001$) and in the ATII-3 the increase was $38.12 \pm 15.49\%$ ($p < 0.001$). The increments in HW/TL were $26.89 \pm 9.30\%$ ($p < 0.001$) for the Iso group, $10.98 \pm 4.96\%$ ($p < 0.001$) for ATII-0.3 and $17.25 \pm 13.71\%$ ($p < 0.001$) for ATII-3. The variability in HW/BW and HW/TL was higher in the ATII-3-treated mice compared to those treated with Iso-30 or only saline as shown in the frequency distribution from both indexes (Figure 1, C and D).

Weight from lungs and liver were determined too as well as the corresponding values normalized to body weight or tibia length and the water content from both organs. An increase in lung weight ratios or in lung water content can be indicative of left ventricular

malfunction that ends into pulmonary congestion. In addition, liver weight ratios or the liver water content can be increased when right ventricular function is significantly impaired. Lung weight/body weight ratio (LW/BW) was increased in mice treated with ATII-3 (Figure 1, Ea) which is due to the fact that the ATII-3 dose led to weight loss (Figure 1, I) and not to water accumulation in lungs from mice treated with this ATII dose (Figure 1, G). Lung weight/tibia length ratio (LW/TL) was increased in Iso-treated mice (Figure 1, Eb). This increase was not due to an increment in lung water content caused by Iso-30 (Figure 1, G) and it was not evident with the LW/BW index probably because Iso-30 treatment produced a significant increase in body weight (Figure 1, I). ATII-3 treatment led to a significant increment of liver weight/body weight ratio (LivW/BW) but not of liver weight/tibia length ratio (LivW/TL), most likely due to weight loss caused by ATII-3 treatment instead of changes in right ventricular function (Figure 1, Fa). Liver water content was slightly increased only in mice that received the ATII-3 dose (Figure 1, H).

Because the body weight was an important parameter used to normalize organ weights and to know the effect of each protocol on it, mice were weighed before and at the end of cardiac hypertrophy induction and the change in body weight was calculated (Figure 1, I). Saline treatment alone induced minor and not significant increments in body weight after 7 ($2.29 \pm 4.64\%$) or 14 days ($3.81 \pm 5.10\%$) of infusion. In contrast, isoproterenol led to a $9.84 \pm 4.70\%$ increase in body weight that was significantly different ($p < 0.001$) to saline treated mice, and ATII-3mg led to a significant ($p < 0.001$) decrease in body weight of $13.70 \pm 6.77\%$. ATII-0.3mg treated mice showed a similar weight gain ($3.97 \pm 4.06\%$) as saline treated mice.

Tibia length was not affected by any neurohumoral treatment in comparison to saline treatment (saline: $17.48 \pm 0.43\text{mm}$; Iso-30: $17.45 \pm 0.50\text{mm}$; ATII-0.3: $17.50 \pm 0.21\text{mm}$, and ATII-3: $17.50 \pm 0.41\text{mm}$). Therefore, values normalized to body weight reflected more a systemic effect of the treatment and those values normalized to tibia length reflected changes in a determined organ.

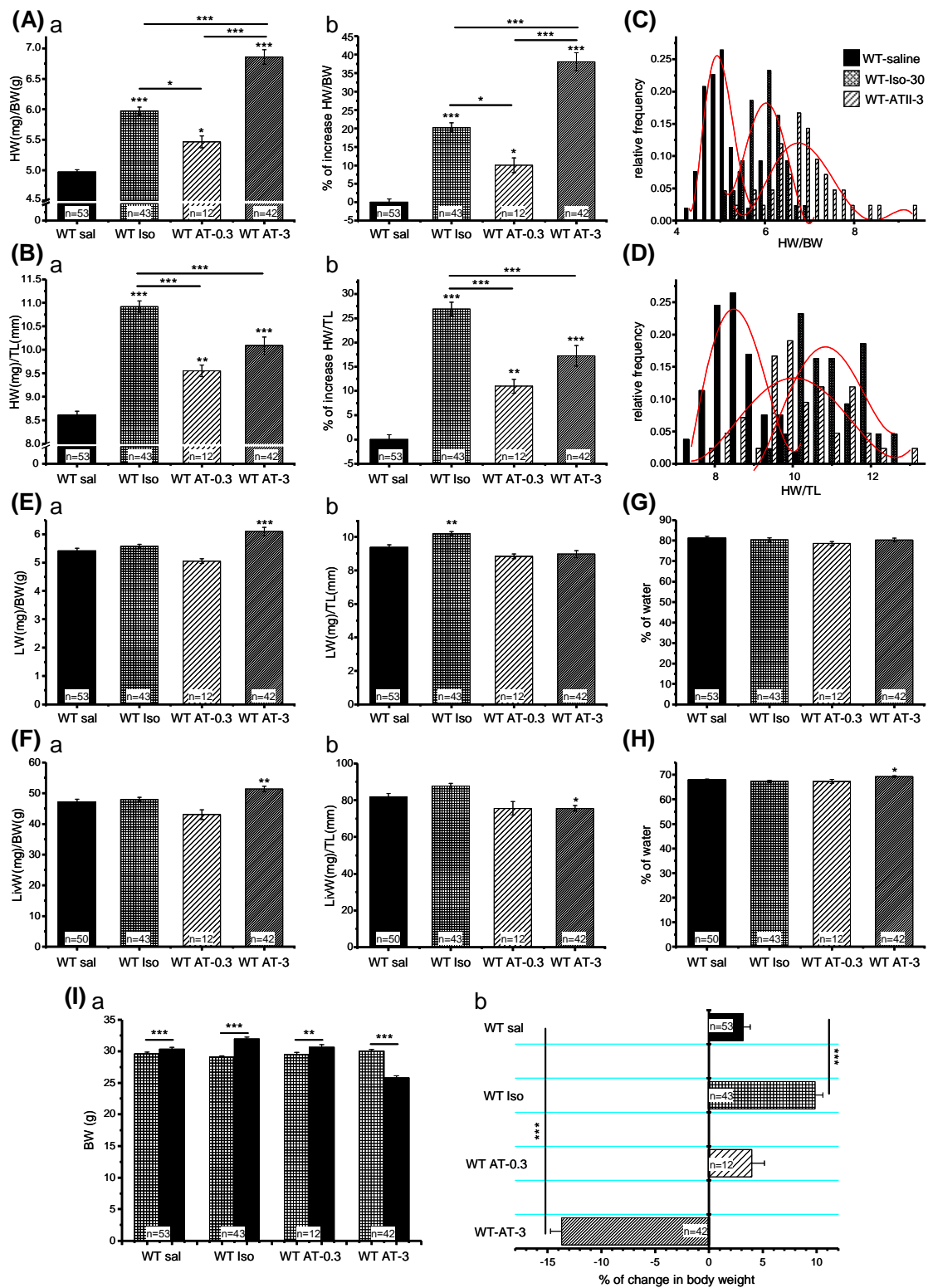


Figure 1. Neurohumoral-induced cardiac hypertrophy in wild type mice. Cardiac hypertrophy induced by infusion of Isoproterenol (Iso) at a dose of 30mg/kg/day (7 days) or angiotensin II (ATII) at doses of 3mg/kg/day or 0.3mg/kg/day over 14 days. Cardiac hypertrophy was evaluated using: **(A)** HW/BW index (a) and corresponding percentage of increase (b); **(B)** HW/TL (a) and corresponding percentage of increase (b); frequency distribution of **(C)** HW/BW and **(D)** HW/TL indexes. In addition, weight of lungs **(E)** and liver **(F)** normalized to BW (a) or TL (b) and the water content from both organs **(G-H)** were evaluated. **(I)** Body weight (a) before (hatched bars) and after (filled bars) hypertrophy induction and the percentage of change in body weight (b) are presented. BW: body weight, HW: heart weight, TL: tibia length, LW: lung weight, LivW: Liver weight, n=: number of mice. Error bars indicate SEM. * $p < 0.05$, ** $p < 0.01$ and *** $p < 0.001$ according to Bonferroni comparisons (A-H) or the paired Student's t-test (I).

Induction of cardiac hypertrophy with neurohumoral agents implies a complex effect on different organ systems and its development is mediated by other organs beyond the heart itself. In addition to cardiac hypertrophy indexes I measured with Ilka Mathar the effects of Iso-30 or ATII-3 on blood pressure from conscious mice because cardiac hypertrophy development can be mediated by changes in blood pressure. Wild type mice were implanted with telemetric blood pressure transmitters and after 7 days of recovery from the transmitter implantation basal mean arterial blood pressure (MAP) was continuously recorded during one week. Afterwards, micro-osmotic pumps were implanted and MAP was recorded until the end of the infusion. Isoproterenol led to a significant increase in MAP after two days of pump implantation (Figure 2, A and C). When the mean values before and during isoproterenol infusion were compared (Figure 2, E) no significant increment ($p=0.13138$) in blood pressure was identified by Iso infusion in this time period of seven days despite parameters for cardiac size increased significantly (Figure 1, A and B). On the other hand, ATII-3mg produced an immediate and significant rise in MAP that increased day by day until the end of the infusion on day 14th (Figure 2, B and D); the mean elevation of MAP produced by ATII during the complete period of treatment was 44.9mmHg compared to basal values (Figure 2, E).

To further characterize the hypertrophy protocol and in addition to hypertrophy indexes and blood pressure I analyzed the heart rate from both, telemetric blood pressure recordings and from ECG recordings at the day 6th of Iso infusion or day 13th of ATII infusion. From telemetric recordings we observed that during Iso-30 treatment the heart rate was significantly increased by about 143BPM, and during ATII-3 infusion the heart rate was also significantly increased by about 37BPM (Figure 2, F). From ECG recordings I observed that isoproterenol treated mice had a significantly ($p<0.001$) higher heart rate of 636 ± 46 BPM ($n=41$) compared to 486 ± 31 BPM ($n=16$) from saline treated mice. ATII-3mg produced a significant ($p<0.01$) elevation of heart rate (530 ± 58 BPM, $n=26$) compared to the saline infused mice (486 ± 42 BPM, $n=20$) despite was expected a reflexory bradycardia as response to the increment of MAP produced by ATII-3. Possibly, this was not observed because the ECG recordings were obtained under anesthesia. However, from the telemetric recordings we observed a reflexory bradycardia but only during the first two days of ATII-3mg infusion and the subsequent days the heart rate increased. ATII-0.3 dose did not affect significantly the heart rate (518 ± 58 BPM, $n=12$) ($p=0.05783$).

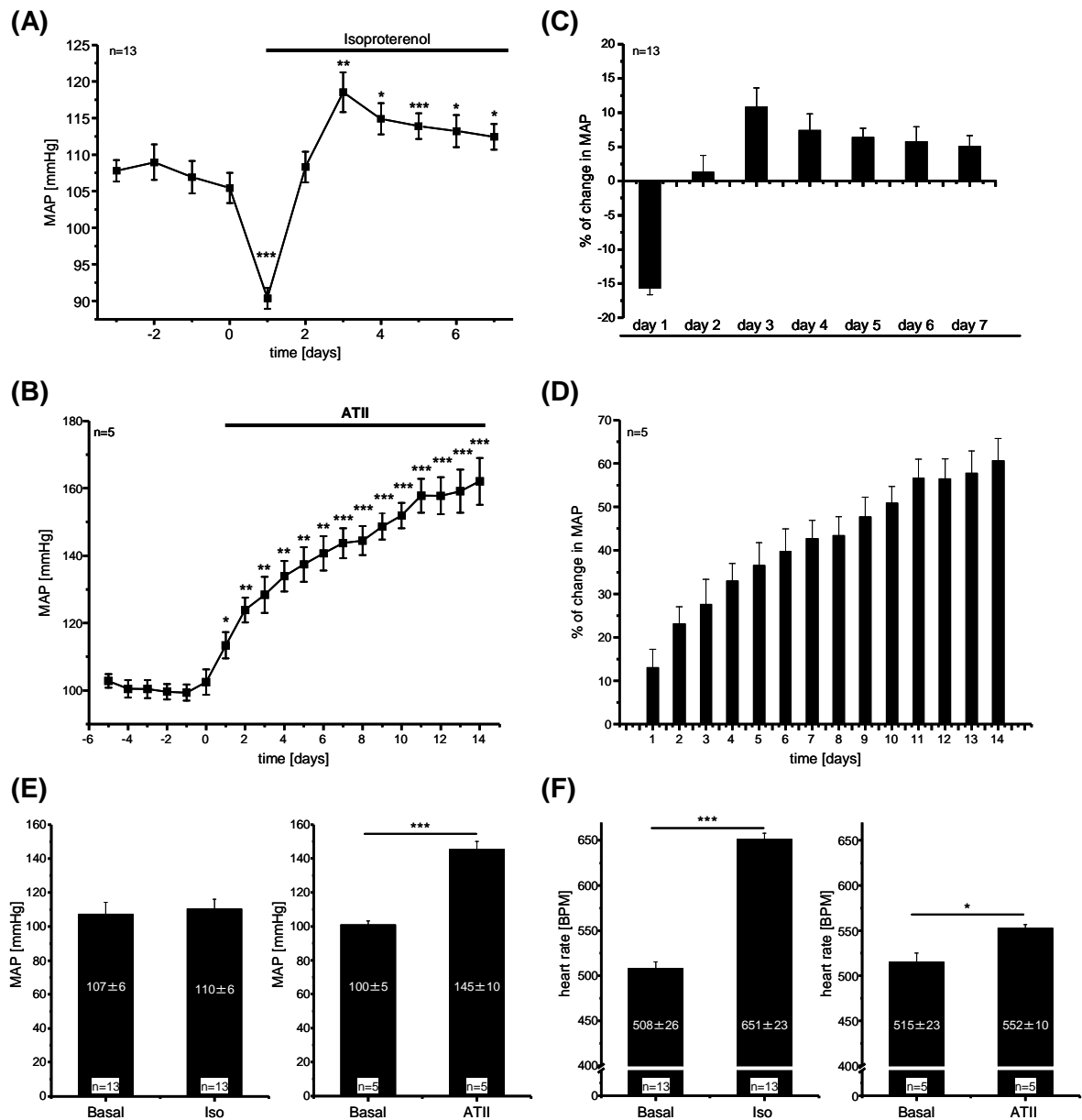


Figure 2. Effects of isoproterenol or ATII on blood pressure during cardiac hypertrophy induction. Mean arterial blood pressure (MAP) from conscious wild type mice before and during (A) Iso or (B) ATII treatment; day 1 corresponds to time point of osmotic pump implantation. The daily percentage of increase in MAP calculated relative to mean value before pump implantation is presented for (C) isoproterenol and (D) ATII treatments. Mean values from (E) MAP and (F) heart rate (F) before and during the isoproterenol (left panels) or ATII (right panels) treatments are shown. Basal mean blood pressure was calculated from measurements during 4 days before osmotic pump implantation. Mean MAP during Iso treatment was calculated from all days omitting the one were the osmotic pumps were implanted. Mean MAP during ATII infusion was calculated from all days of treatment. Iso was infused at a dose of 30mg/kg/day over 7 days and ATII at a dose of 3mg/kg/day during 14 days. ATII: angiotensin II, Iso: isoproterenol, n=: number of mice. Error bars indicate SEM. * $p < 0.05$, ** $p < 0.01$ and *** $p < 0.001$ according to the Student's t-test for paired samples.

5.1.2 Neurohumoral-induced cardiac hypertrophy in TRPC3/TRPC6 (-/-)² mice

Using RNA isolated from mouse cardiac cells I amplified transcripts from TRPC3 and TRPC6 (Figure 3, A). In addition, TRPC6 proteins of a size of ~120 kilodaltons (kDa) were detected by western blot analysis (made in collaboration with C. Wesely and Prof. V Flockerzi) with an antibody against a C-terminal fragment of TRPC6 (Tsvilovskyy et al., 2009) in heart preparations from wild type mice but not from TRPC6 deficient mice (Figure 3, B).

Isoproterenol-induced hypertrophy. Analysis of HW/BW and HW/TL indexes (Figure 3, Ca and Cb) revealed a significant isoproterenol effect ($p < 0.001$, two-way ANOVA) but no differences due to genotype, which implies no reduction in the isoproterenol-induced cardiac hypertrophy in TRPC3/TRPC6 (-/-)² mice. Analysis of LW/TL and LivW/TL indexes and the water content in lungs and liver (Figure 3, D) revealed no difference between wild type and TRPC3/TRPC6 (-/-)² mice.

ATII treatment. In experiments using the ATII-3 dose only 43% of TRPC3/TRPC6 (-/-)² mice survived until the end of the treatment whereas 86% of the ATII-treated wild type mice survived (Figure 3, E). The wild type survival rate calculated from all the experiments that I did during my thesis was 97%. In the surviving mice no difference was found in HW/BW or in water content from lungs and liver between genotypes (Figure 3, F). Statistical analysis of HW/TL index showed significant differences due to genotype ($p < 0.001$) and the values were 8.93 ± 0.34 mg/mm for WT-saline, 9.91 ± 0.53 mg/mm for WT-ATII-3, 7.43 ± 0.33 mg/mm for TRPC3/TRPC6 (-/-)²-saline and 8.76 ± 0.4 mg/mm for TRPC3/TRPC6 (-/-)²-ATII-3, the difference between genotypes in this index could be explained because of reduced values observed in TRPC3/TRPC6 (-/-)² mice. However no reduction in percentual increases of HW/TL between WT and TRPC3/TRPC6 (-/-)² mice was observed ($p < 0.24409$). Still the number of mice was quite low in this experimental series due to the mortality.

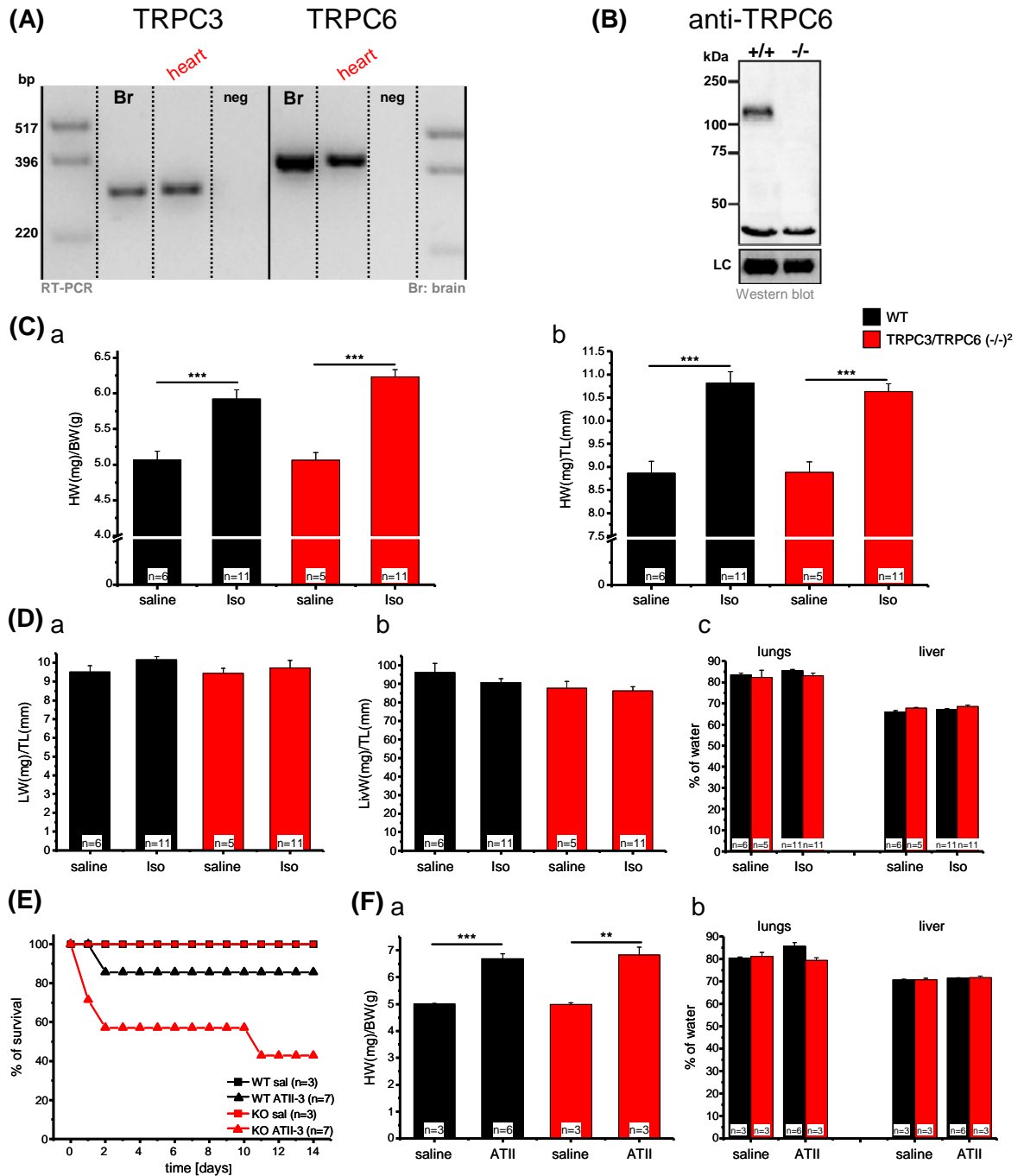


Figure 3. No reduction in cardiac hypertrophy response in TRPC3/TRPC6 (-/-)² mice after isoproterenol or angiotensin II treatment. (A) TRPC3 and TRPC6 transcripts from cardiac cells obtained by Langendorff perfusion. Products were amplified using intron spanning oligonucleotides as primers and single step RT-PCR amplification kit. Total RNA from brain (Br) was used as positive control and RNA free water was used as negative one. (B) Western blot with anti-TRPC6 using microsomal membrane protein fractions from WT (+/+) and TRPC6 deficient (-/-) mice. (C) HW/BW (a) and HW/TL (b) indexes from WT and TRPC3/TRPC6 (-/-)² mice after Iso-30 treatment (D) LW/TL (a), LivW/TL (b) and water content in lungs or liver (c) after Iso treatment. (E-F) ATII-induced cardiac hypertrophy in TRPC3/TRPC6 deficient mice. (E) Survival curve of ATII-3 treated WT and TRPC3/TRPC6 (-/-)² mice compared to saline (sal) treated mice of both genotypes. (F) HW/BW (a) and water content in lungs and liver (b) after ATII-3 treatment were analyzed. kDa: kiloDalton, BW: body weight, HW: heart weight, TL: tibia length, LW: lung weight, LivW: Liver weight, n=: number of mice. KO: knockout. Error bars indicate SEM. **p < 0.01 and ***p < 0.001 and ns (not significant) according to Bonferroni comparisons.

Because the high mortality triggered by ATII-3mg in TRPC3/TRPC6 (-/-)² mice I used a lower dose of ATII-0.3 to induce cardiac hypertrophy in these mice. No ATII-0.3 treated WT or TRPC3/TRPC6 (-/-)² mice die during the two independent performed experimental series. HW/BW and HW/TL indexes were not reduced in TRPC3/TRPC6 (-/-)² mice compared to wild type mice (Figure 4, Aa-b and Ba-b). The percentual increase for both indexes was not reduced rather increased in TRPC3/TRPC6 deficient mice (Figure 4, Ac and Bc). However the differences in the hypertrophy indexes were not observed between saline treated WT and TRPC3/TRPC6 (-/-)² mice in this study using AT-0.3 (Figure 3C). Analysis of LW/TL, LivW/TL and water content in lungs and liver showed no evidence of pulmonary or liver congestion in WT or TRPC3/TRPC6 (-/-)² mice (Figure 4, C). In addition, direct measurements of left ventricular function were obtained with a Mikro-Tip catheter under Isoflurane anesthesia but no differences were detected in parameters such as maximum pressure, change in pressure over time (dP/dt), contractility, exponential time constant of relaxation (τ) and pressure time index. Only a lower heart rate was observed in ATII treated TRPC3/TRPC6 (-/-)² mice compared to wild type (Table 1).

Table 1. No differences in left ventricular pressure in TRPC3/TRPC6 (-/-)² mice at the end of treatment with a low dose of angiotensin II.

Genotype/treatment		Heart Rate (BPM)	Max Pressure (mmHg)	Max dP/dt (mmHg/s)	Contractility Index (1/s)	τ (s)	Pressure Time Index (mmHg.s)
129B6F1/saline (n=4)	Mean	554.79	76.33	3979.34	135.11	0.0134	2.70
	SD	13.70	6.20	389.24	6.87	0.0010	0.27
129B6F1/ATII (n=10)	Mean	513.51	81.78	3807.6	119.74	0.0149	3.11
	SD	39.44	6.08	653.63	6.56	0.0013	0.67
TRPC3/C6 (-/-) ² /saline (n=5)	Mean	459.36	83.39	4105.6	135.49	0.0142	3.32
	SD	61.53	13.27	516.05	28.35	0.0019	0.56
TRPC3/C6 (-/-) ² /ATII (n=6)	Mean	466.62	94.42	4610.58	126.57	0.0164	3.94
	SD	47.34	17.91	1153.81	20.89	0.0040	0.88
Comparison ATII treatments	t-test (p)	0.01986	0.36316	0.69833	0.98012	0.46777	0.08426

The following parameters at the end of ATII-0.3 treatment were obtained: heart rate; maximum (Max) pressure; maximum change in pressure during systole (Max dP/dt); contractility index defined as the quotient of the Max dP/dt divided by the pressure on the time of Max dP/dt; exponential time constant of relaxation Tau (τ); and pressure time index or tension time index determined as the product between the average ventricular pressure during systole and the systolic duration. SD: Standard deviation; p: probability values from the Student's t-test; n= number of mice.

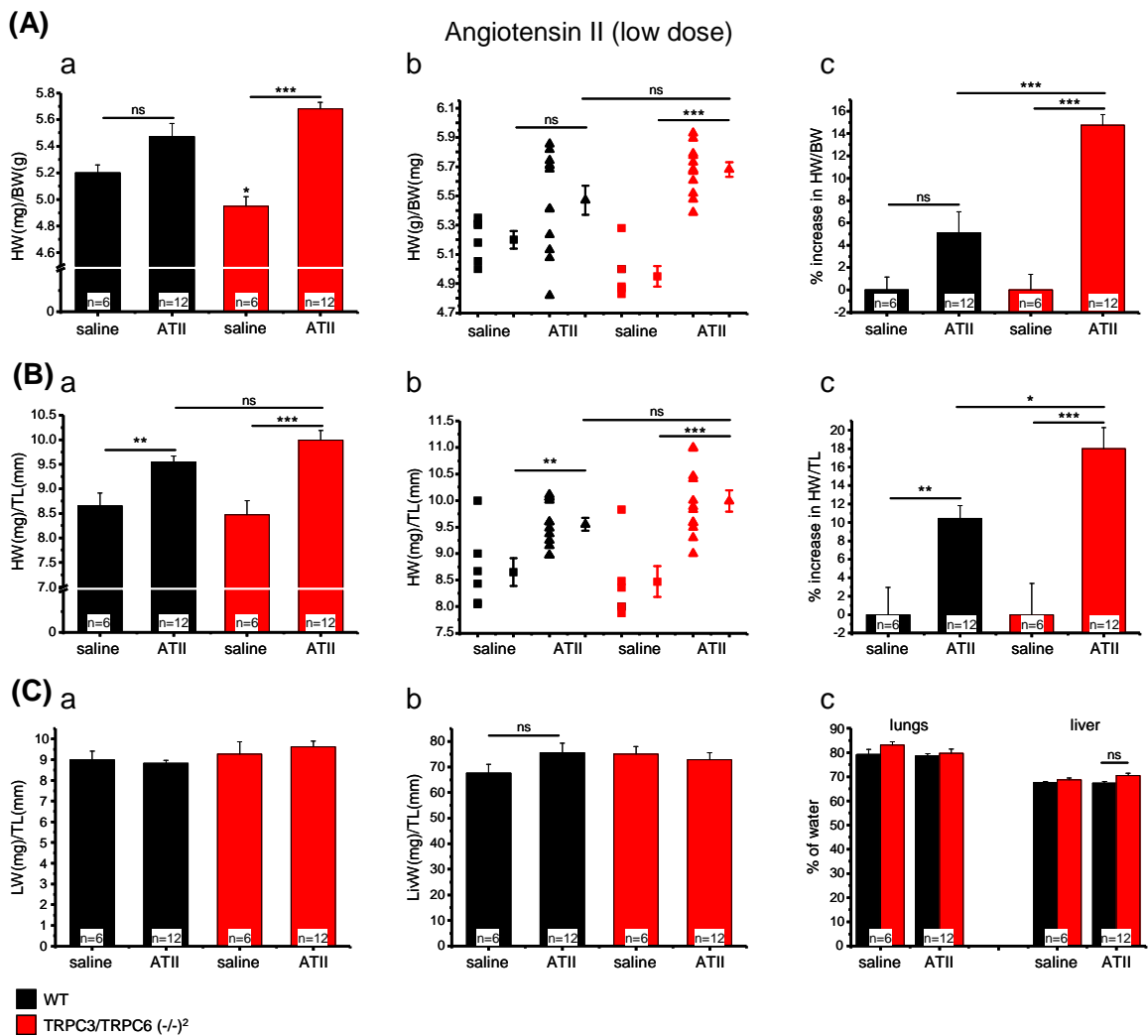


Figure 4. No reduction in cardiac hypertrophy response in TRPC3/TRPC6 (-/-)² mice after treatment with a low dose of angiotensin II. After ATII-0.3 treatment TRPC3/TRPC6(-/-)² mice did not show a reduction in the hypertrophic response compared to WT mice analyzed by: **(A)** HW/BW (a and b) and its percentual increase (c); **(B)** HW/TL (a and b) and its percentual increase (c); and **(C)** LW (a) and LivW (b) both normalized to TL, and water content from both organs (c). BW: body weight, HW: heart weight, TL: tibia length, LW: lung weight, LivW: Liver weight, n=: number of mice. Error bars indicate SEM. *p<0.05, **p<0.01, ***p<0.001 and ns (not significant) according to Bonferroni comparisons.

5.1.3 Reduced neurohumoral-induced cardiac hypertrophy in TRPC1/TRPC4 (-/-)² mice

Northern blot analysis revealed abundant expression of TRPC1 and possibly expression of TRPC4 transcripts (Freichel et al., 2004). The expression of TRPC1 and TRPC4 transcripts was confirmed by RT-PCR using total RNA from cardiac cells (Figure 6, A).

Isoproterenol-induced hypertrophy. Based on the expression data I made a pilot experiment to induce cardiac hypertrophy in TRPC1/TRPC4 (-/-)² mice. Mice were subjected to isoproterenol infusion at a dose of 60mg/kg/day during 7 days. Evaluation of

HW/BW and HW/TL revealed a significant reduction in cardiac hypertrophy development in TRPC1/TRPC4 (-/-)² mice (Figure 5, A and B), but no differences in LW/TL ratio were observed (Figure 5, C).

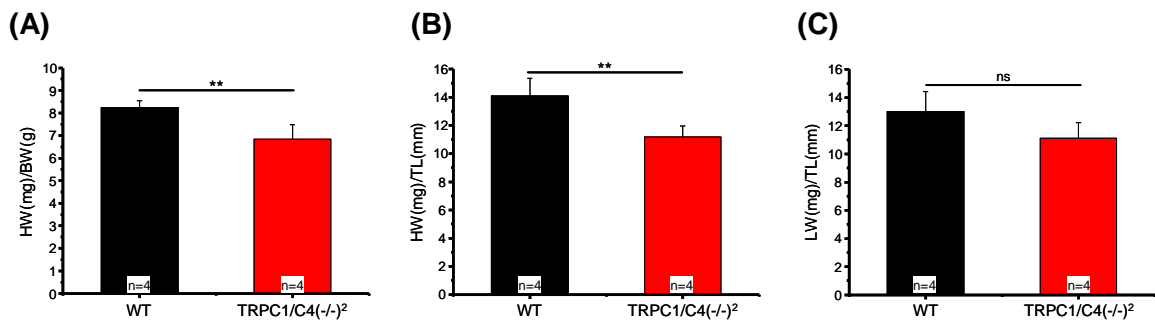


Figure 5. Pilot experiment showed a reduced cardiac hypertrophy development in TRPC1/TRPC4 (-/-)² after isoproterenol treatment. Evaluation of (A) HW/BW, (B) HW/TL and (C) LW/TL in WT (black) and TRPC1/TRPC4 (-/-)² mice (red) after isoproterenol infusion (60mg/kg/day) during 7 days. BW: body weight, HW: heart weight, TL: tibia length, LW: lung weight, n=: number of mice. Error bars indicate SEM. **p<0.01 and ns according to the Student's t-test.

Isoproterenol treatment. Effects on heart weight. All following experiments of isoproterenol induced hypertrophy were done using the Iso-30 dose (30mg/kg/day) because this dose is reported by many other groups in the literature and allows better comparison afterwards. After Iso-30 treatment there was also an obvious macroscopic increase in heart size in the wild type group and this hypertrophic response was also reduced in TRPC1/C4 knockout mice (Figure 6, B). Statistical analysis of HW/BW showed both, a significant isoproterenol effect (p<0.001) and a significant genotype effect (p<0.05). Also the percentual change in HW/BW was significantly reduced (p<0.05) in TRPC1/TRPC4 (-/-)² mice by about 40% (Figure 6, C). No differences in body weight between treatments (WT-Iso= 29.78 ±1.94g and TRPC1/TRPC4 (-/-)²-Iso= 29.59 ±2.60g; p=0.14808) or in the percentual change in body weight (WT-Iso= 7.67 ±2.92% and TRPC1/TRPC4 (-/-)²-Iso= 6.69 ±3.75%; p=0.40199) were observed. Similarly, the HW/TL index was reduced significantly by ~27% in TRPC1/TRPC4 (-/-)² mice (Figure 6, Dc).

Isoproterenol treatment. Effects on lung weight. Analysis of lung weight showed no significant differences in LW/BW index (Figure 6, Ea) due to isoproterenol (p=0.08943) or due to genotype (p=0.06138). From the analysis done with the LW/TL index (Figure 6, Eb) there was a significant effect of isoproterenol (p<0.001) on lung weight in WT that can not be attributed to an accumulation of water in the lungs because of the isoproterenol

treatment (Figure 6, Ec). In contrast, there was a difference in lung water content between genotypes being this value smaller in TRPC1/TRPC4 (-/-)² mice (Figure 6, Ec).

Isoproterenol treatment. Effects on liver weight. Isoproterenol had no significant effect on both LivW/TL ($p=0.18008$) and in the liver water content (Figure 6, Fb-c). It was remarkable that livers from TRPC1/TRPC4 deficient mice were smaller, either from absolute weight values or from values normalized to body weight ($p<0.001$) or to tibia length ($p<0.001$) independent of saline or isoproterenol treatment (Figure 6, Fa and b).

Isoproterenol treatment. Effects on cardiomyocyte size. To assess changes in cardiomyocyte size after Iso-30 treatment the cross sectional area from transversally sectioned left ventricular cardiomyocytes was quantified (Figure 7, A). Comparison of WT and TRPC1/TRPC4 (-/-)² mice treated either with saline or isoproterenol revealed a significant effect due to both, Iso-treatment ($p<0.001$) and to genotype ($p<0.001$). Also, a significant ($p<0.001$) reduction of 79% in the Iso-induced increase of cardiomyocyte cross sectional area was observed in TRPC1/TRPC4 (-/-)² mice (Figure 7, B). This difference can be appreciated by contrasting the frequency distribution from the cross sectional area of wild type (Figure 7, Ca) with the one from TRPC1/TRPC4 deficient mice (Figure 7, Cb), or by comparing the relative cumulative frequency from both genotypes that shows a left shift in the cell area from the TRPC1/TRPC4 (-/-)²-iso treated group versus the WT-Iso treated group (Figure 7, Cc).

Isoproterenol treatment. Effects on cardiac fibrosis. Isoproterenol-induced cardiac hypertrophy is not only associated with increment of cardiac mass or cardiomyocyte size, but also with changes in other cellular populations and tissue structure of the heart like an increase in collagen deposition by fibroblasts. Therefore the collagen content was measured in Sirius red stained cross heart sections from WT-saline, WT-Iso, TRPC1/TRPC4(-/-)²-saline and TRPC1/TRPC4(-/-)²-Iso treated mice (Figure 7, D). Isoproterenol generated a significant ($p<0.001$) increase of interstitial heart fibrosis in both genotypes, however, TRPC1/TRPC4 (-/-)² mice responded in lesser extent compared with wild type mice (Figure 7, E).

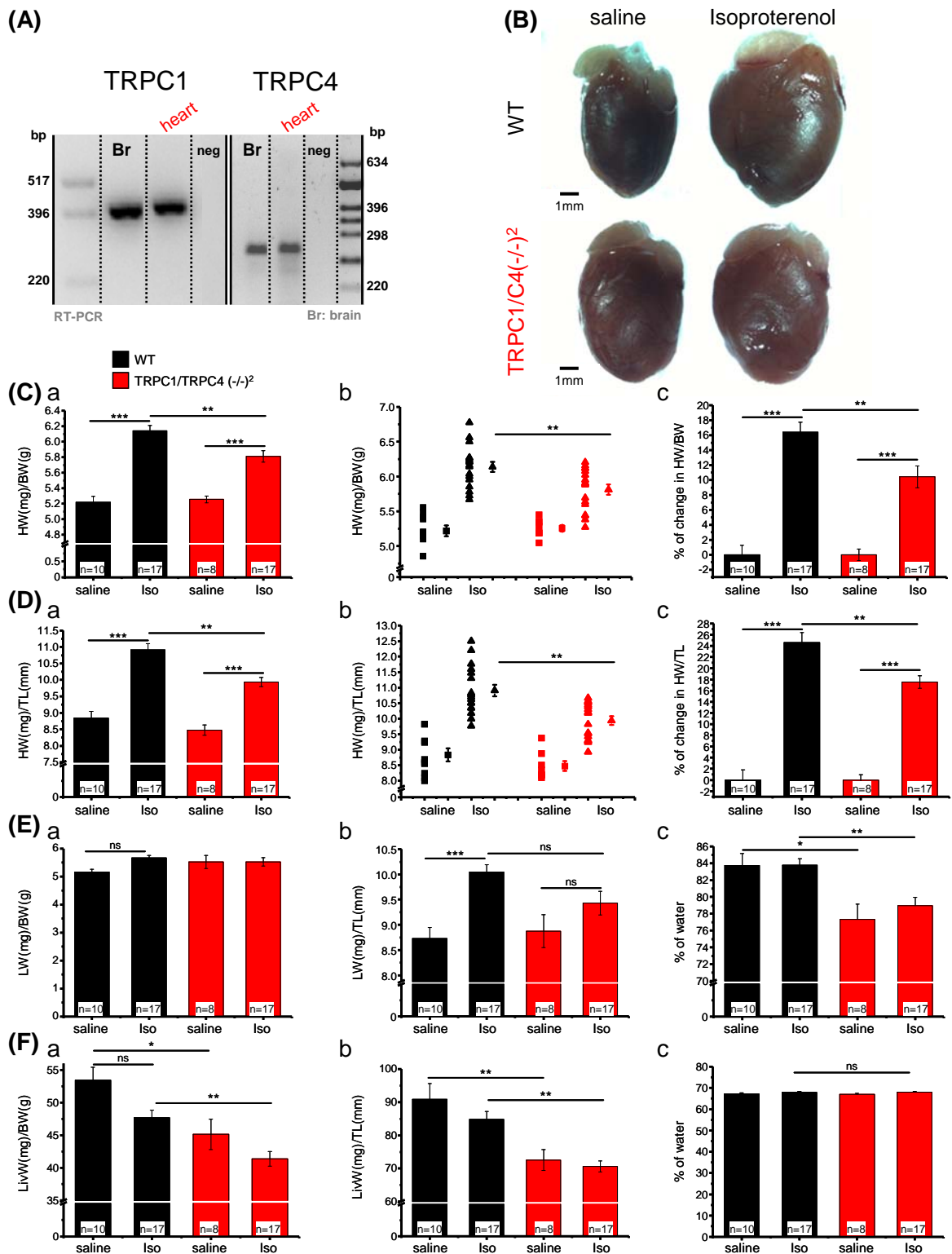


Figure 6. TRPC1/TRPC4 (-/-)² mice have reduced isoproterenol-induced cardiac hypertrophy. **(A)** TRPC1 and TRPC4 transcripts from cardiac cells isolated by Langerdorff perfusion. Total RNA from brain (Br) was used as positive control and RNA free water from the RNA isolation kit was used as negative control (neg). **(B-F)** Hypertrophy development after Iso-30 treatment. **(B)** Representative hearts from WT and TRPC1/TRPC4 (-/-)². **(C)** HW/BW (a and b) and percentage of change in HW/BW weight relative to the corresponding saline group (c) from WT and TRPC1/TRPC4 (-/-)² mice. **(D)** HW/TL (a and b) and percentage of change in HW/TL (c). **(E-F)** Evaluation of pulmonary or liver congestion. **(E)** LW/BW (a), LW/TL (b) and lung water content. **(F)** LivW/BW (a), LivW/TL (b) and liver water content. BW: body weight, HW: heart weight, TL: tibia length, LW: lung weight, LivW: Liver weight, n=: number of mice (pooled from three independent experiments). Error bars indicate SEM. **p<0.01, ***p<0.001 and ns (not significant) according to Bonferroni comparisons.

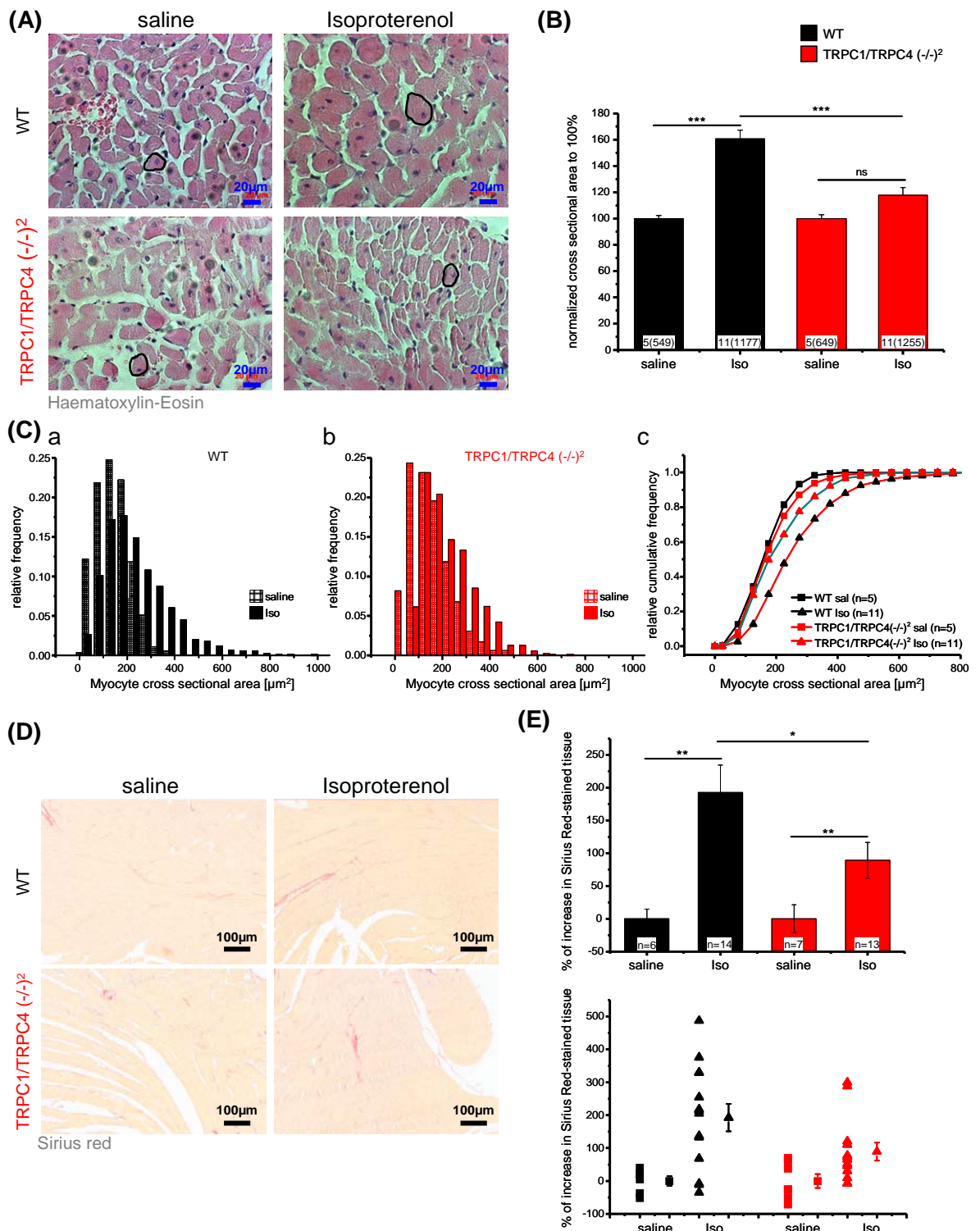


Figure 7. Isoproterenol-induced increase in cardiomyocyte size and in myocardial fibrosis are reduced in TRPC1/TRPC4 (-/-)² mice. Histopathological analysis of Iso-30-induced cardiac hypertrophy. **(A)** Representative paraffin heart sections (5 μm) from the left ventricle stained with Hematoxylin-Eosin; representative examples of analyzed cells are marked. **(B-C)** Statistical analysis of cardiomyocyte cross sectional area. **(B)** Comparison of cell areas normalized to the corresponding saline groups; the numbers represent number of mice and the number of cells (in parenthesis). **(C)** Relative frequency distribution (a-b) of the cell areas shown in B from saline and isoproterenol treated mice. In c, the relative cumulative frequency from the cross sectional area is shown. **(D)** Representative paraffin sections (5 μm) from the left ventricle stained with Sirius red. **(E)** Analysis of cardiac fibrosis measured as the percentage of increase in Sirius red staining compared to the corresponding saline control; lower panel shows the dot plot with single values from each mouse. n= number of mice. Error bars indicate SEM. * $p < 0.05$, ** $p < 0.01$ and *** $p < 0.001$ according to Bonferroni comparisons.

Analysis of cardiac hemodynamic functions. Measurements with the Millar tip catheter were carried out under two independent anesthetics, Avertin (2,2,2-tribromoethanol) or Isoflurane. Under Avertin, almost all calculated parameters, except for the exponential time constant of relaxation (τ), differed significantly in TRPC1/TRPC4 (-/-)² mice. But, under Isoflurane anesthesia there were no differences. A possible explanation for this discrepancy is that the heart rate was different between the two genotypes under Avertin but not under isoflurane narcosis (Table 2).

Table 2. Left ventricle pressure in TRPC1/TRPC4 (-/-)² mice at the end of isoproterenol treatment.

Genotype		Heart Rate (BPM)	Max Pressure (mmHg)	Max dP/dt (mmHg/s)	Contractility Index (1/s)	τ (s)	Pressure Time Index (mmHg.s)
129B6F1 (n=7) Avertin	Mean	629.44	99.41	5317.77	144.00	0.012	3.23
	SD	19.87	14.09	1037.02	22.62	0.002	0.058
TRPC1/C4 (-/-) ² (n=8) Avertin	Mean	583.09	74.77	3698.76	116.58	0.013	2.48
	SD	41.85	9.18	771.75	18.15	0.001	0.34
	t-test	0.0193	0.0013	0.0043	0.0218	0.3415	0.0085
129B6F1 (n=9) Isofluran	Mean	533.92	78.46	3631.64	109.91	0.015	2.96
	SD	49.14	30256	581.84	12.55	0.002	0.23
TRPC1/C4 (-/-) ² (n=5) Isofluran	Mean	513.77	74.60	3290.31	103.31	0.018	3.11
	SD	48.17	2.99	222.48	13.40	0.002	0.39
	t-test	0.4734	0.4937	0.2374	0.3752	0.0805	0.373

Hemodynamic Parameters obtained from mice under Avertin or isofluran anesthesia on the 7th day of Iso-30 treatment using a Millar catheter. The following parameters were measured: heart rate; maximum (Max) ventricular pressure; maximum change in pressure during systole (Max dP/dt); contractility index defined as the quotient of the Max dP/dt divided by the pressure on the time of Max dP/dt; exponential time constant of relaxation (τ); and pressure time index or tension time index determined as the product between the average ventricular pressure during systole and the systolic duration. SD: Standard deviation; p: probability values from the Student's t-test; n= number of mice.

Angiotensinogen plasma levels. I observed that livers from TRPC1/TRPC4 (-/-)² mice were considerably smaller compared to those from wild type mice (Figure 6, Fa-b). This observation was corroborated when the liver weight values of saline-treated mice from different experiments were analyzed together (Figure 8, inset). Angiotensinogen is produced and released into the circulation mainly by the liver and it is a substrate for renin, which can be increased by isoproterenol stimulation of the kidney. Therefore, angiotensinogen plasma levels were determined in untreated wild type and TRPC1/TRPC4 (-/-)² mice, but they were not different (Figure 8).

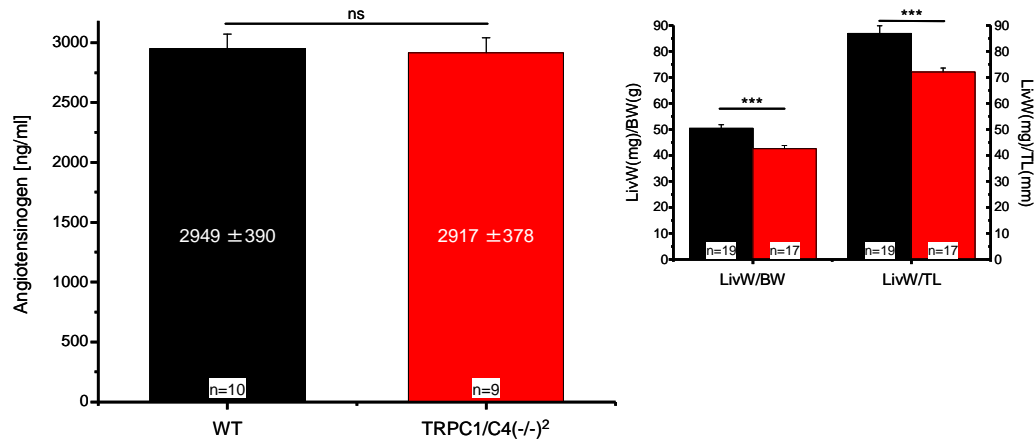


Figure 8. Angiotensinogen plasma levels are not different in TRPC1/TRPC4 (-/-)² mice despite the smaller liver size. Angiotensinogen plasma levels determined by a sandwich ELISA from wild type (black) and TRPC1/TRPC4 (-/-)² (red). The right inset shows liver weight normalized to body weight (left bars) or tibia length (right bars). n= number of mice. Error bars indicate SEM. ***p<0.001 and ns (not significant) according to the Student's t-test.

Regulation or renal renin secretion in TRPC1/TRPC4(-/-)² mice. β-adrenergic stimulation by isoproterenol leads to renin secretion that could affect ATII plasma levels and subsequently cardiac hypertrophy development. In collaboration with Prof. Frank Schweda from Regensburg we observed in isolated kidneys that the isoproterenol-induced renin production was not impaired in TRPC1/TRPC4 deficient mice; as well, the inhibition of renin secretion by ATII in both wild type and TRPC1/TRPC4(-/-)² mice was similar.

ATII-induced hypertrophy. The decreased hypertrophic response in TRPC1/TRPC4(-/-)² mice after isoproterenol treatment could be due to changes upstream or downstream of the ATII production. Therefore I induced cardiac hypertrophy in wild type and TRPC1/TRPC4 (-/-)² mice with the ATII.

ATII. Effects on cardiomyocyte size and cardiac fibrosis. The histopathological examination of cardiomyocyte cross sectional area from Hematoxylin-eosin stained heart sections (Figure 9, A) showed both, a significant ATII effect (p<0.0001) and a significant genotype effect (p<0.05). ATII-induced increase in cardiomyocyte area in TRPC1/TRPC4 deficient mice was 71% less compared with ATII-treated wild type mice (Figure 9, B). Additionally, the relative collagen content was quantified from Sirius red stained heart sections (Figure 9, C). ATII treatment augmented significantly cardiac fibrosis (p<0.001) and the cardiac fibrosis development was significantly reduced in TRPC1/TRPC4 (-/-)² mice (Figure 9, D).

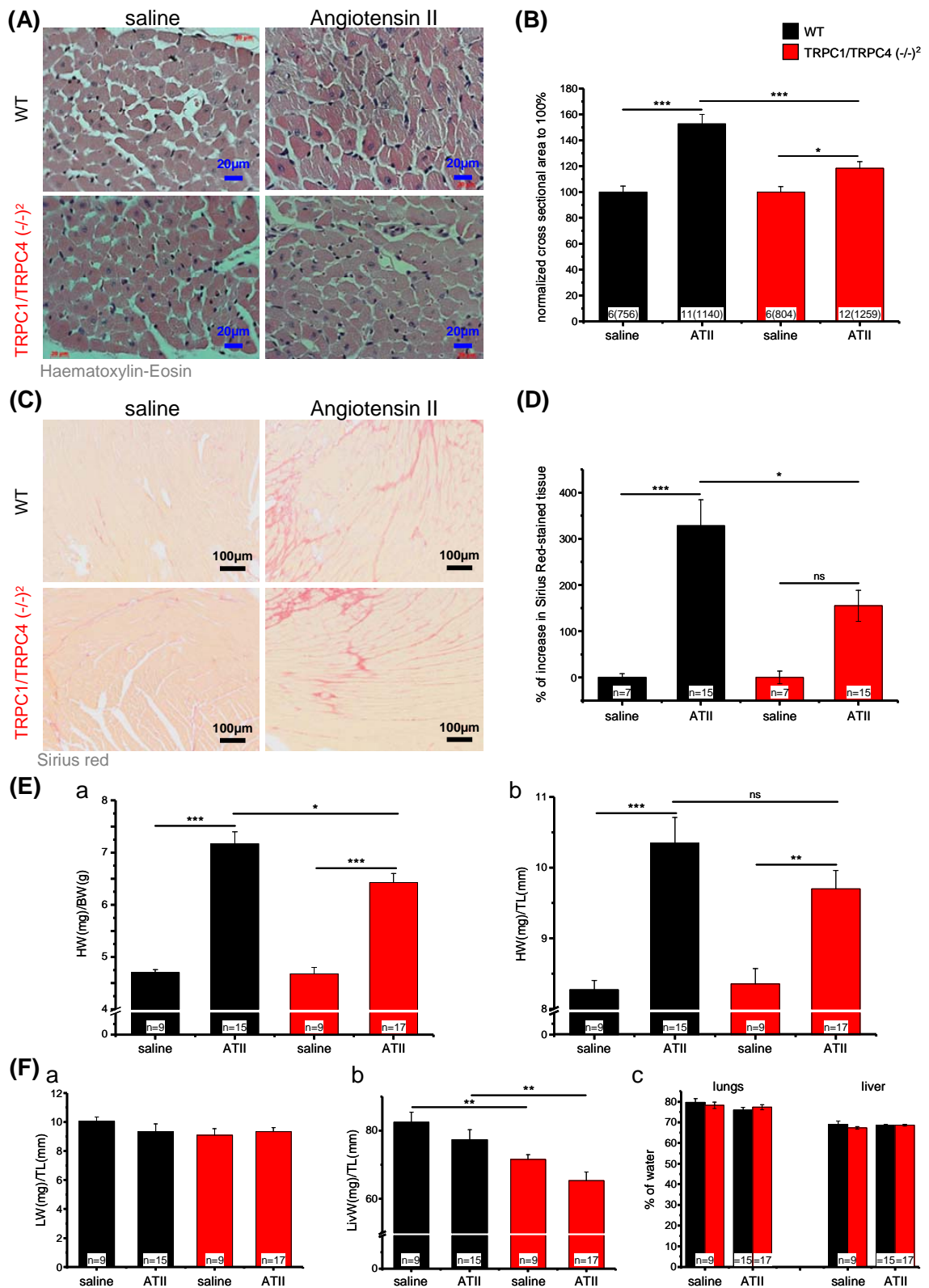


Figure 9. TRPC1/TRPC4 (-/-)² mice presented reduced angiotensin II-induced cardiac hypertrophy. Hypertrophy development after ATII-3 II treatment. **(A)** Representative paraffin heart sections (5µm) from the left ventricle. **(B)** Cardiomyocyte cross sectional area normalized to the corresponding saline group; numbers represent number of mice and number of cells (in parenthesis). **(C)** Representative paraffin sections (5µm) from the left ventricle. **(D)** Percentage of increase in Sirius red staining compared to the corresponding saline control. **(E)** HW/BW (a) and HW/TL (b). **(F)** LW/TL (a) and LivW/TL (b), and water content in lungs or liver (c). BW: body weight, HW: heart weight, TL: tibia length, LW: lung weight, LivW: Liver weight, n=: number of mice. Error bars indicate SEM. *p<0.05, **p<0.01, ***p<0.001 and ns (not significant) according to Bonferroni comparisons.

ATII. Effects on body weight and hypertrophy indexes. No significant changes in body weight were observed in wild type ($3.91 \pm 6.52\%$) or TRPC1/TRPC4 $(-/-)^2$ ($2.67 \pm 3.68\%$) mice treated with saline. ATII produced a significant reduction in body weight that was similar between both genotypes (WT: $-13.47 \pm 5.23\%$ and TRPC1/TRPC4 $(-/-)^2$: $-10.24 \pm 4.84\%$). HW/BW was significantly reduced in TRPC1/TRPC4 $(-/-)^2$ mice after ATII treatment (Figure 9, Ea). This corresponds to a 28% reduced hypertrophy response in TRPC1/TRPC4 $(-/-)^2$ mice. The HW/TL index revealed a significant effect of ATII ($p < 0.001$) but no significant difference with respect to genotype ($p = 0.35432$) although the average reduction in HW/TL was ~36% in TRPC1/TRPC4 $(-/-)^2$ mice (Figure 9, Eb). Analysis of other indexes such as lung weigh/tibia length, liver weight/tibia length and water content of lungs or liver showed no differences between WT and TRPC1/TRPC4 deficient mice and no differences caused by ATII treatment. Only the reduced liver size previously observed in TRPC1/TRPC4 $(-/-)^2$ mice was confirmed (Figure 9, F).

Isoproterenol treatment. Effects on heart rate and blood pressure. Heart rate was calculated from surface ECG recordings obtained under Isoflurane anesthesia and from telemetric blood pressure recordings. Analysis of surface ECG recordings under anesthesia at day 6 of isoproterenol infusion showed that HR was significantly increased in both wild type and TRPC1/TRPC4 deficient mice ($p < 0.001$). The absolute heart rate and its increase were significantly reduced in TRPC1/TRPC4 $(-/-)^2$ mice (Figure 10, A).

HR measurement obtained from telemetric blood pressure recordings from WT and TRPC1/TRPC4 $(-/-)^2$ conscious mice under isoproterenol treatment confirmed that the increase in HR produced by Iso-treatment is significantly reduced in TRPC1/TRPC4 $(-/-)^2$ mice (Figure 10, Bc). A similar small elevation in the mean arterial pressure in both genotypes was observed (Figure 10, B). Comparison of HW/BW and HW/TL from mice with blood pressure transmitters showed that TRPC1/TRPC4 $(-/-)^2$ mice developed less cardiac hypertrophy (Figure 10, E and F). The increase in body weight was similar in both genotypes (Figure 10, D). There was no evidence of pulmonary or hepatic congestion and the reduced liver size in TRPC1/TRPC4 $(-/-)^2$ mice was still evident (Figure 10, G).

ATII treatment. Effects on heart rate. ATII treatment (3mg/kg/day) produced a significant increase in heart rate (Figure 2, F). Therefore, I analyzed heart rate from surface ECGs obtained under anesthesia at the end of ATII-3 treatment. In WT mice heart rate was significantly increased. However, no significant increase was observed in TRPC1/TRPC4 $(-/-)^2$ mice treated with ATII and treated with saline (Figure 10, H).

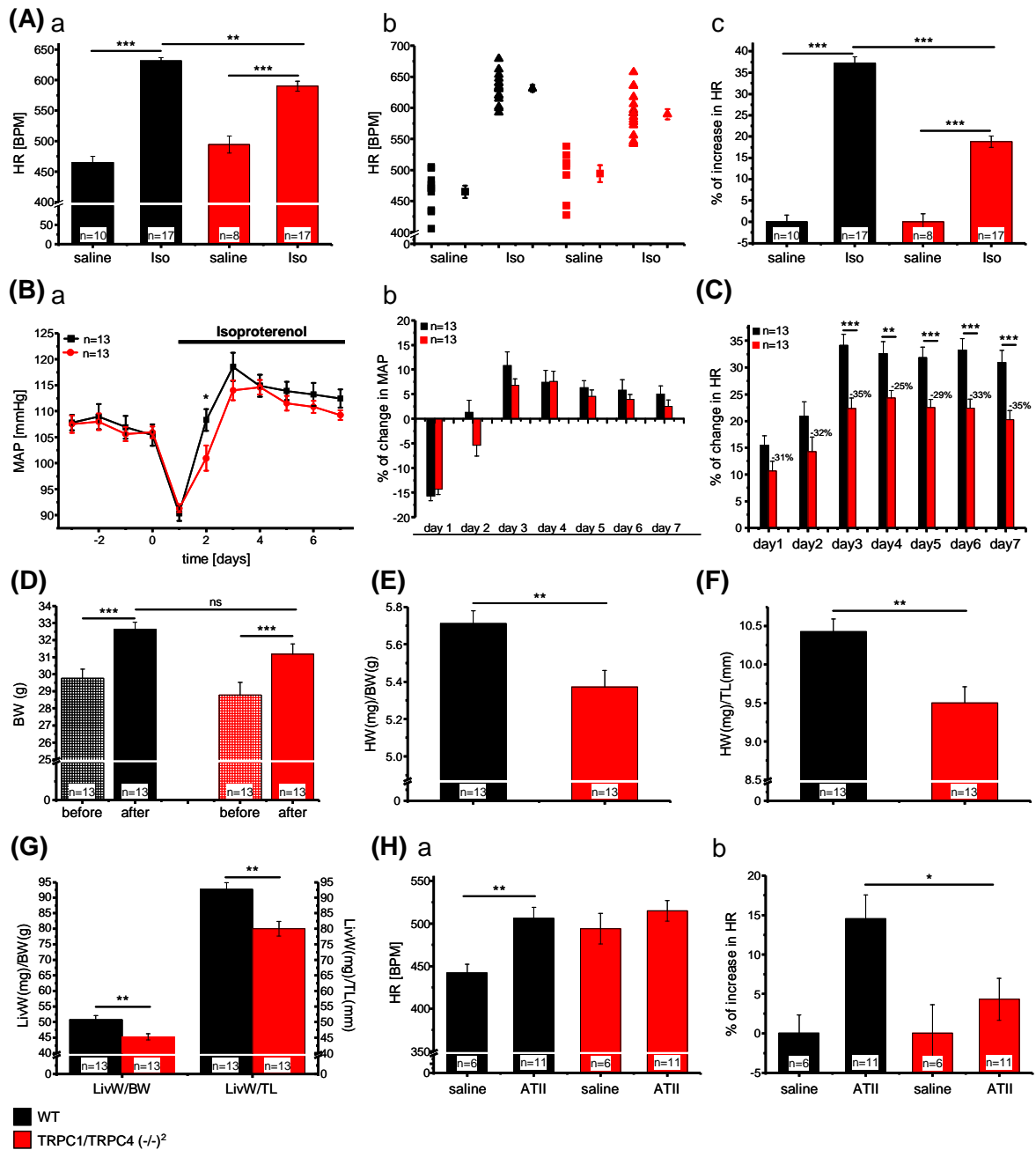


Figure 10. Heart rate and mean arterial pressure during isoproterenol infusion in TRPC1/TRPC4 (-/-)² mice. TRPC1/TRPC4 (-/-)² mice have reduced isoproterenol-induced increase in heart rate but no differences in MAP compared with wild-type control mice. **(A)** Mean values (a) dot plot (b) and percentual increase (c) of heart rate (HR) measured from surface ECG recordings on 6th day of Iso-30 treatment. **(B, a)** Mean arterial blood pressure (MAP) from conscious mice before and during isoproterenol treatment and **(B, b)** daily percentages of increase in MAP calculated from the mean value before pump implantation; day 1 corresponds to time point of osmotic pump implantation. **(C)** Daily percentage of increase in heart rate from conscious mice. From these mice **(D)** weight before and after isoproterenol treatment is presented as well as the cardiac hypertrophy indexes **(E)** HW/BW and **(F)** HW/TL and **(G)** liver weight normalized to body weight or tibia length. **(H)** Mean values (a) and percentual increase (c) of heart rate (HR) measured from surface ECG recordings at the end of ATII treatment. n= number of mice. Error bars indicate SEM. *p<0.05, **p<0.01, ***p<0.001 and ns (not significant) according to the Student's t-test.

Heart rate regulation in isolated right atria. To further examine the observed differences in regulation of heart rate between wild type and TRPC1/TRPC4 (-/-)² mice during Iso-30 and ATII-3 treatments I analyzed the beating frequency of isolated spontaneously beating right atria to evaluate the regulation of the pacemaking activity in both genotypes. I analyzed the effect of the β -adrenergic receptor agonist isoproterenol, the AT₁ receptor agonist angiotensin II, the muscarinic receptor agonist Acetylcholine (Ach), and the α_1 -adrenergic receptor agonist Phenylephrine on atrial preparations. For all agonists cumulative concentration responses were performed and the absolute beating rate, the change in beating compared to basal beating rate and the percentual change in beating rate were analyzed. Right atria from TRPC1/TRPC4 deficient mice responded to the same extent as wild type atria to stimulation with isoproterenol and Acetylcholine (Figure 11, A and B). However, the response positive chronotropic response to ATII was reduced in atria from TRPC1/TRPC4 (-/-)² mice in terms of absolute beating rate and beating rate normalized to basal level, but not when normalized to the maximal response (Figure 11, C). Similarly, the positive chronotropic response to Phenylephrine was significantly reduced in TRPC1/TRPC4 deficient atria in all three dose-response analysis (Figure 11, D).

5.1.3.1 Isoproterenol-induced cardiac hypertrophy in TRPC1^{-/-} and TRPC4^{-/-} mice

Reduced cardiac hypertrophy development in TRPC1/TRPC4 deficient mice after isoproterenol or angiotensin II treatment could be solely due to inactivation either of TRPC1 or TRPC4. Therefore I analyzed development of hypertrophy, in single TRPC1^{-/-} and TRPC4^{-/-} mice, by treatment with Iso-30 treatment and also ATII-3 (see section 5.1.3.2).

TRPC1^{-/-} mice. Iso-30 treatment had a significant effect ($p < 0.001$) on both hypertrophy indexes, HW/BW and HW/TL from wild type and TRPC1^{-/-} mice (Figure 12, A-B), but no reduction in the cardiac hypertrophy was observed in TRPC1^{-/-} mice (Figure 12, A). Interestingly, the HW/TL ratio in TRPC1 deficient mice was increased compared to wild type mice (Figure 12, B). The percentual increase in HW/BW from TRPC1^{-/-} mice ($23.36 \pm 9.83\%$) was also significantly ($p < 0.05$) higher compared to the increase produced in wild type mice ($14.16 \pm 8.45\%$). However, the percentual increment produced in HW/TL from wild type mice ($27.99 \pm 9.04\%$) was not different to the increment produced in TRPC1 deficient mice ($32.66 \pm 8.80\%$). There were no effects of isoproterenol treatment or differences between genotypes on lung weight/tibia length ratio (Figure 12, C) and on

water content in lungs or liver (Figure 12, E). Isoproterenol had no effect on liver weight/tibia length ratio (Figure 12, D).

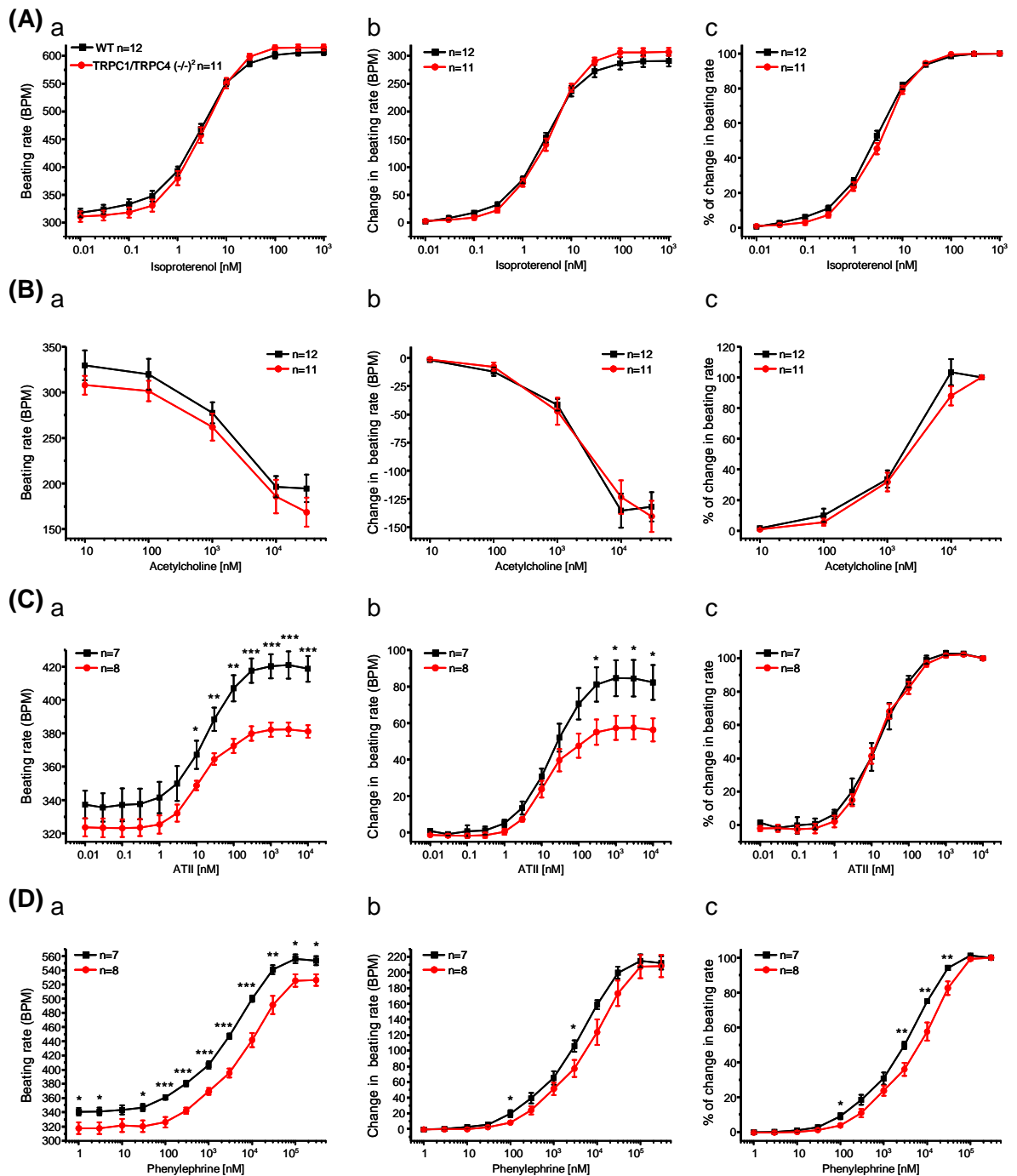


Figure 11. Reduced chronotropic response in isolated right atria from TRPC1/TRPC4 (-/-)² mice after ATII stimulation but not after Isoproterenol stimulation. Different dose-response curves from agonist-induced chronotropic effect on beating isolated right atria from wild type (black) and TRPC1/TRPC4 (-/-)² (red) mice. The tested agonists were **(A)** isoproterenol, **(B)** Acetylcholine (ACh), **(C)** angiotensin II (ATII) or **(D)** Phenylephrine (PE). From each agonist the absolute values of beating rate (a panels), the change in beating rate normalized to the basal values (b panels) and the percentage of change in beating rate normalized to the maximum response (c panels) are shown. n= number of mice. Error bars indicate SEM. *p<0.05, **p<0.01, ***p<0.001 and ns according to the Student's t-test.

TRPC4 $-/-$ mice. The effect of Iso-30 on HW/BW and HW/TL was significant ($p < 0.001$) for both wild type and TRPC4 $-/-$ mice; comparisons of these two indexes between both genotypes showed no differences (Figure 13, A and B). Iso-30 produced a similar percentual increase in HW/BW in wild type ($16.40 \pm 5.34\%$) and in TRPC4 $-/-$ mice ($14.60 \pm 6.45\%$). Percentual increase of HW/TL in wild type ($24.81 \pm 7.23\%$) and in TRPC4 $-/-$ mice ($22.64 \pm 6.93\%$) were also comparable. In both animal groups isoproterenol had a similar effect on LW/TL, on LivW/TL and on water content from lungs and liver (Figure 13, C-E).

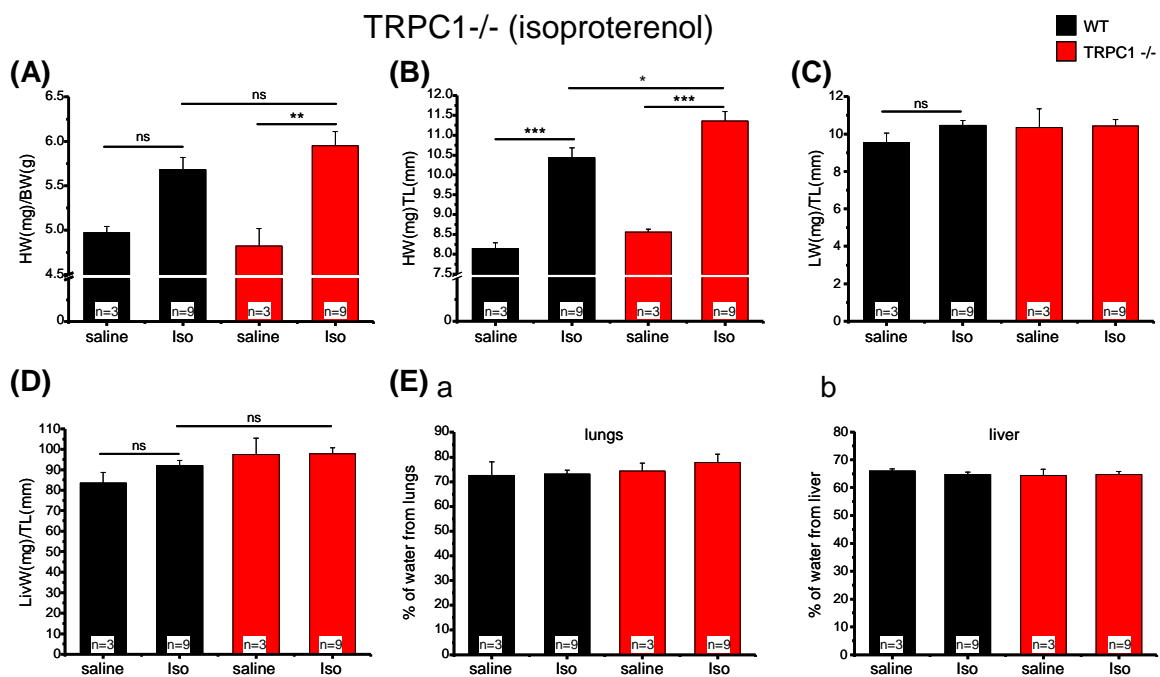


Figure 12. Isoproterenol-induced cardiac hypertrophy is not reduced in TRPC1 $-/-$ mice. Cardiac hypertrophy induced in wild type and TRPC1 deficient mice by Iso-30 treatment. Cardiac hypertrophy indexes (A) HW/BW and (B) HW/TL were analyzed. Additionally, (C) LW/TL, (D) LivW/TL and (E) water content in lungs (a) and in liver (b) are included. BW: body weight, HW: heart weight, TL: tibia length, LW: lung weight, LivW: Liver weight, n= number of mice. Error bars indicate SEM. * $p < 0.05$, ** $p < 0.01$, *** $p < 0.001$ and ns (not significant) according to Bonferroni comparisons.

5.1.3.2 Angiotensin II-induced cardiac hypertrophy in TRPC1 $-/-$ and TRPC4 $-/-$ mice

TRPC1 $-/-$ mice. ATII-3 produced a significant increase ($p < 0.001$) of both hypertrophy indexes HW/BW and HW/TL in a similar manner in wild type and TRPC1 $-/-$ mice (Figure 14, A and B). No difference caused by ATII treatment or by genotype was observed on the LW/TL (Figure 14, C). ATII treatment reduced LivW/TL in both genotypes but had no influence on liver or lung water content (Figure 14, D-E).

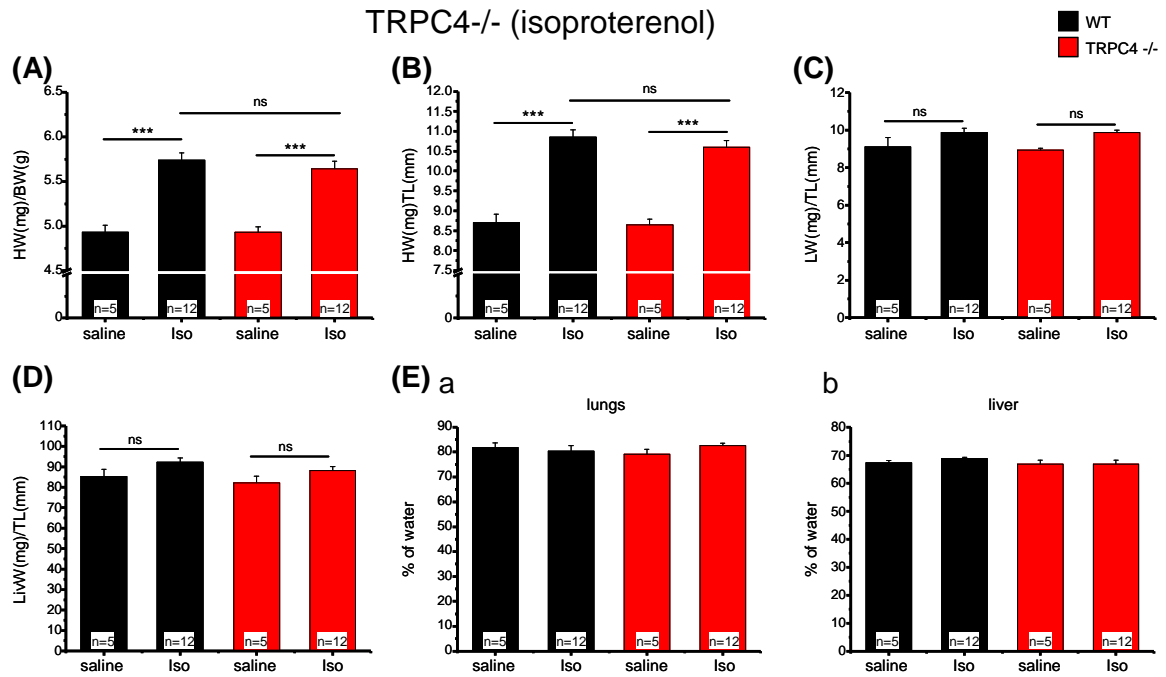


Figure 13. Isoproterenol-induced cardiac hypertrophy is not reduced in TRPC4^{-/-} mice. Cardiac hypertrophy induced in wild type and TRPC4 deficient mice by Iso-30 treatment. Cardiac hypertrophy indexes **(A)** HW/BW and **(B)** HW/TL were analyzed. Additionally, **(C)** LW/TL, **(D)** LivW/TL and **(E)** water content in lungs (a) and in liver (b) are included. BW: body weight, HW: heart weight, TL: tibia length, LW: lung weight, LivW: Liver weight, n= number of mice. Error bars indicate SEM. *p<0.05, **p<0.01, ***p<0.001 and ns (not significant) according to Bonferroni comparisons.

TRPC4^{-/-} mice. In experiments with TRPC4^{-/-} mice ATII-3 treatment produced a significant (p<0.001) increase in HW/BW and HW/TL that was similar to the increase in wild type mice (Figure 15, A and B). LW/TL, LivW/TL and water content from lungs and liver were not different between genotypes (Figure 15, C-E). In this group ATII-3 treatment decreased LivW/TL index in TRPC4^{-/-} mice (Figure 15, Eb). This was the only experimental case where a significant increase in water content in the liver was observed.

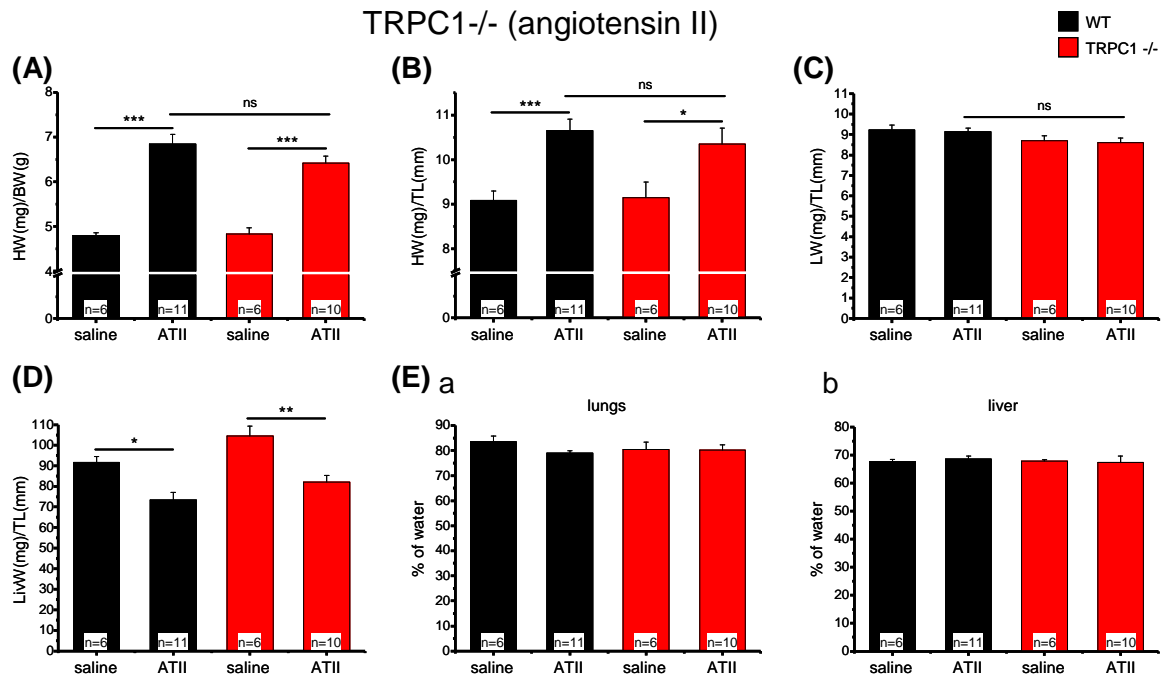


Figure 14. Angiotensin II-induced cardiac hypertrophy is not reduced in TRPC1^{-/-} mice. Cardiac hypertrophy induced in wild type and TRPC1 deficient mice by ATII-3 treatment. Cardiac hypertrophy indexes (A) HW/BW and (B) HW/TL were analyzed. Additionally, (C) LW/TL, (D) LivW/TL and (E) water content in lungs (a) and in liver (b) are included. BW: body weight, HW: heart weight, TL: tibia length, LW: lung weight, LivW: Liver weight, n= number of mice. Error bars indicate SEM. *p<0.05, **p<0.01, ***p<0.001 and ns (not significant) according to Bonferroni comparisons.

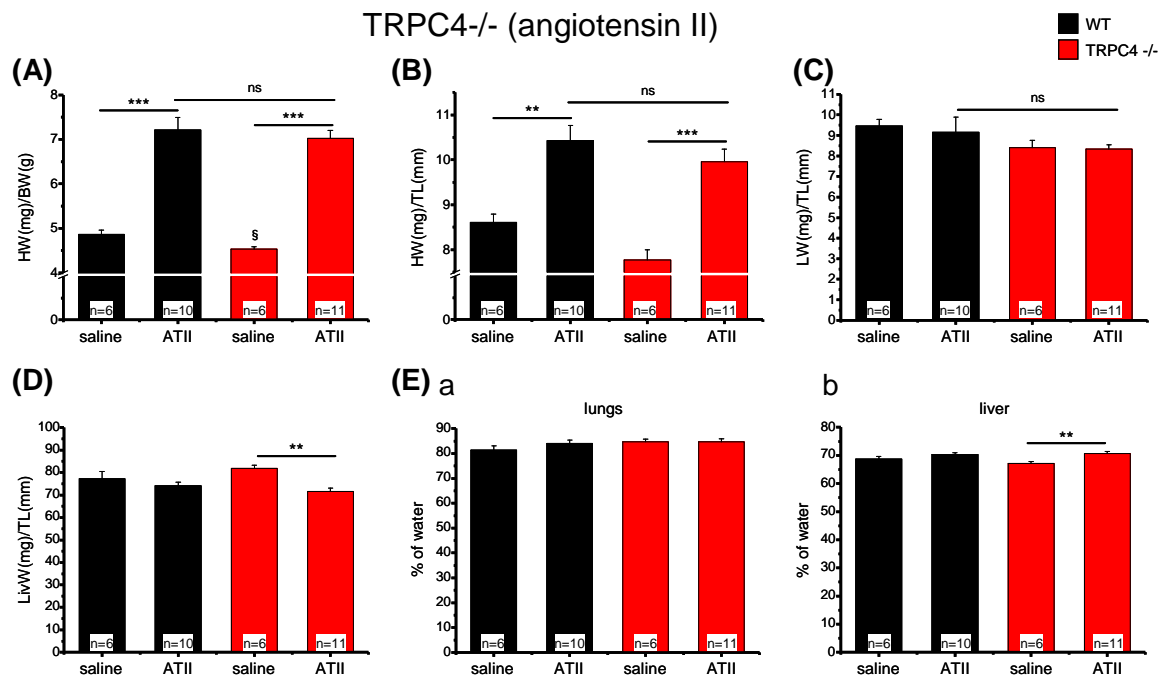


Figure 15. Angiotensin II-induced cardiac hypertrophy is not reduced in TRPC4^{-/-} mice. Cardiac hypertrophy induced in wild type and TRPC4 deficient mice by ATII-3 treatment. Cardiac hypertrophy indexes (A) HW/BW and (B) HW/TL were analyzed. Additionally, (C) LW/TL, (D) LivW/TL and (E) water content in lungs (a) and in liver (b) are included. BW: body weight, HW: heart weight, TL: tibia length, LW: lung weight, LivW: Liver weight, n= number of mice. Error bars indicate SEM. *p<0.05, **p<0.01, ***p<0.001 and ns (not significant) according to Bonferroni comparisons.

5.1.4 TRP expression analysis in isolated adult mouse cardiomyocytes

Analysis of the development of cardiac hypertrophy revealed a reduced Iso- and ATII-induced increase in collagen content in cardiac tissue sections from TRPC1/TRPC4 (-/-)² mice (Figure 7, D and Figure 9, D). Nevertheless, comparison of absolute values of basal fibrosis levels in heart sections showed a significantly higher proportion of Sirius red stained tissue in TRPC1/TRPC4 (-/-)² mice compared to WT mice (Figure 16). Also, the reduced hypertrophy development and increase of cardiomyocyte cross sectional area observed in TRPC1/TRPC4 deficient mice may not only be a result of a direct action of isoproterenol or angiotensin II on cardiomyocytes, but could also be mediated by other cell types within the heart (see Figure i1). The differences in the content of cardiac collagen, which is mainly defined by the function of cardiac fibroblasts, as well as the observed cardiomyocyte growth after neurohumoral stimulation, prompted me to study the expression of TRPC channels in these cell types.

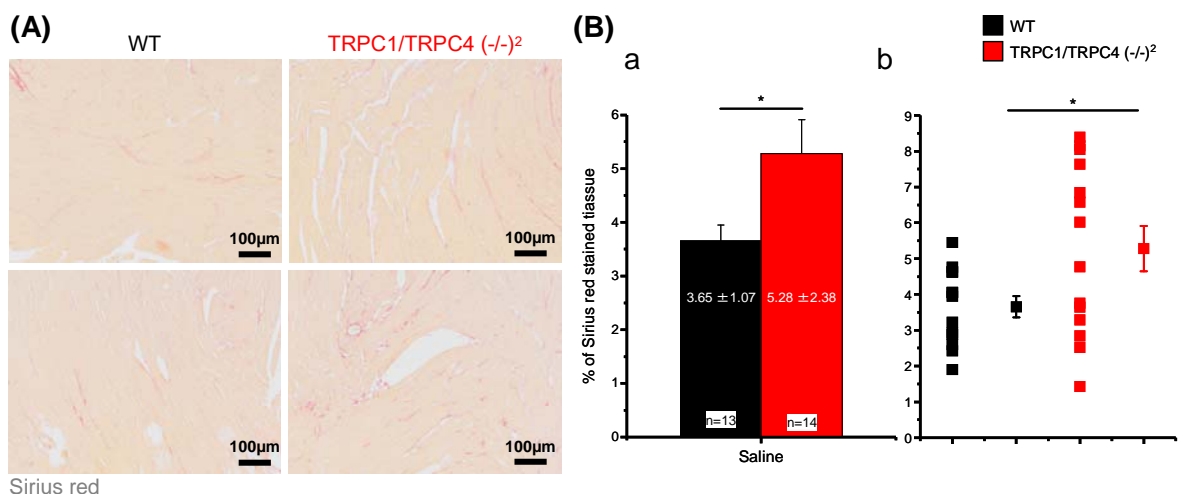


Figure 16. Basal levels of cardiac fibrosis are higher in TRPC1/TRPC4 (-/-)² mice. Cardiac fibrosis quantified from Sirius red stained tissue sections from wild-type and TRPC1/TRPC4 (-/-)² mice. **(A)** Representative paraffin sections (5µm) from the left ventricle stained with Sirius red from saline treated mice. **(B)** Analysis of cardiac fibrosis determined as the percentage of tissue stained with Sirius red, mean values (a) and single values from each analyzed mouse (b) are presented. n= number of mice. Error bars indicate SEM. *p<0.05 according to the Student's t-test.

Cardiomyocytes from adult wild type mice were isolated by digestion of hearts in Langendorff preparations and separated by centrifugation and differential plating steps. The major proportion of these cell suspensions which were used until now for RT-PCR analysis as those shown in Figure 17 (A) was cardiomyocytes, but this suspension also contained other cell types including endothelial cells, macrophages, smooth muscle cells and a large number of cardiac fibroblast, as I observed later when cells were stained for

the fibroblast marker P4HB in cardiomyocyte preparations (Figure 19, D). From RNA isolated from these cellular preparations termed “Langendorff suspension” I amplified transcripts specific for TRPC1, TRPC3, TRPC4 and TRPC6 (Figure 17, Ab). These results were reproduced and we also detected transcripts of genes encoding TRPM4, TMEM-2 (a gene close to TRP family), L-type voltage-gated calcium auxiliary subunit $Ca_v\beta 2$ (Meissner et al., 2011) and the Hypoxanthine Phosphoribosyltransferase-1 (HPRT-1) (see Table 3, in the column “Langendorff suspension”). TRPC5 was not included in this analysis because it could never be amplified from two independent Langendorff preparations (Table 3), which is in line with observations from others that did not detect TRPC5 expression in mouse heart by northern blot analysis (Okada et al., 1998).

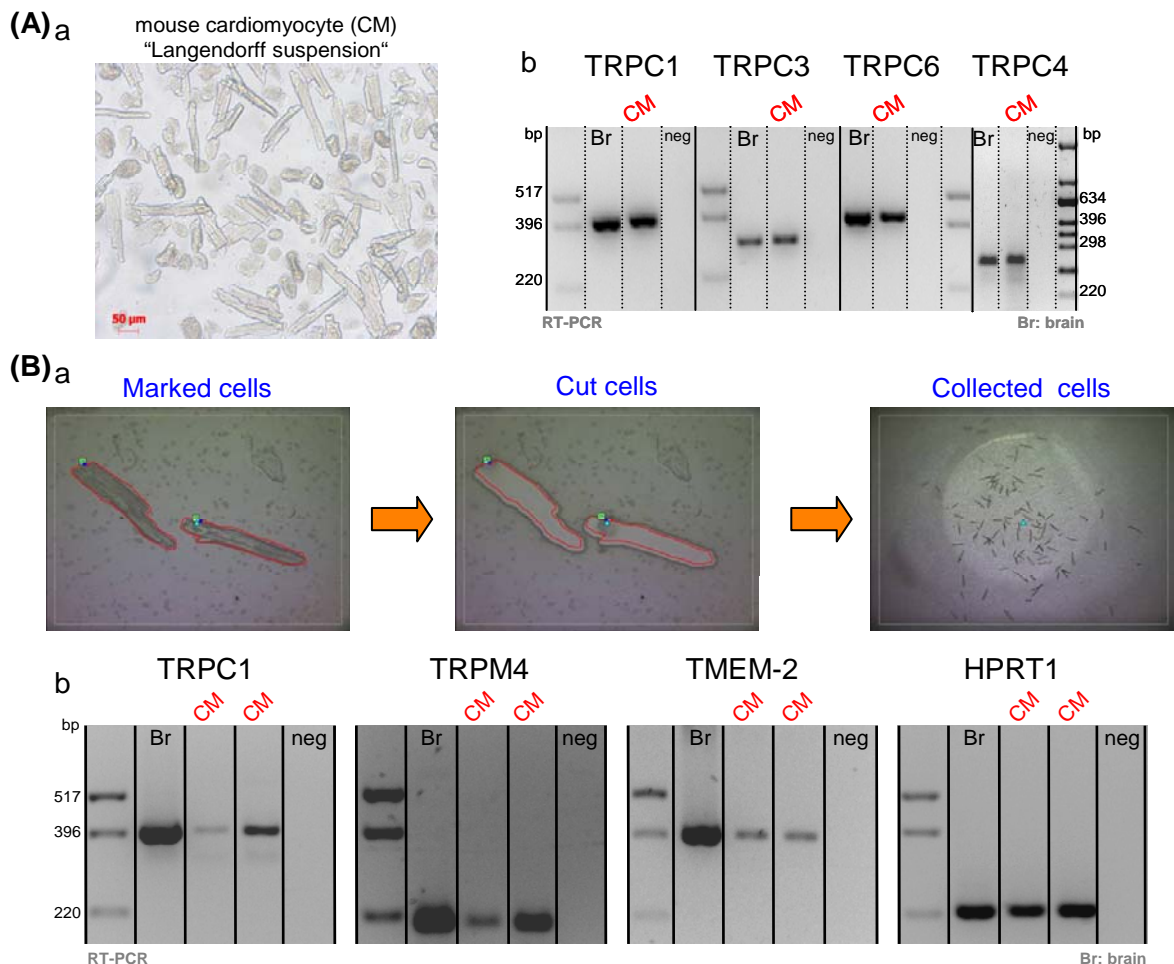


Figure 17. Expression of TRPs in isolated mouse cardiomyocytes analyzed by RT-PCR. Different TRPs transcripts amplified from total RNA obtained from either cell suspensions isolated by **(A, a)** heart digestion according to the Langendorff perfusion system (“Langendorff suspension”) or **(B, a)** from mouse cardiomyocytes (CM) collected by Laser Capture Microdissection (LCM). Representative agarose gels showing **(A, b)** the expression of TRPC1, TRPC3, TRPC6 and TRPC4 in RNA from “Langendorff suspension” and gels showing **(B, b)** the expression in LCM-collected cardiomyocytes of TRPC1, TRPM4, TMEM-2 and HPRT-1 that was used as control for the RNA quality obtained from the LCM-isolated cardiomyocytes. Total RNA from brain was used as positive control (Br) and RNA free water from the RNA isolation kit was used as negative control (neg). bp: base pair.

To circumvent contamination by other cell types and to obtain a pure cardiomyocyte fraction out of the cell population obtained after Langendorff digestion of the heart for RT-PCR analysis, I decided to selectively isolate cardiomyocytes by Laser Capture Microdissection (LCM). With this procedure, single cardiomyocytes were collected on a special glass slide (Figure 17, Ba) for RNA isolation. From this material I amplified transcripts of TRPC1, TRPM4, TMEM-2 and HPRT-1 (Figure 17, Bb) and I amplified only once TRPC3 from five experiments and once TRPC4 from ten experiments. TRPC6 transcripts were never amplified (Table 3, in the column "LCM-Cardiomyocytes").

Table 3. Summary of TRP expression analysis in mouse cardiomyocytes and cultured cardiac fibroblasts by RT-PCR.

gene	Langendorff suspension				LCM-cardiomyocytes				Cultured cardiac fibroblasts			
	# Cell preps	# RNA preps	# PCRs	positive amplification/reactions	# Cell preps	# RNA preps	# PCRs	positive amplification/reactions	# Cell preps	# RNA preps	# PCRs	positive amplification/reactions
TRPC1	6	6	5	10/10	4	7	9	7/9	3	3	4	4/4
TRPC3	5	5	4	5/7	4	5	5	1*/5	3	3	4	4/4
TRPC4	5	5	5	7/10	5	10	10	1*/10	3	3	5	8/8
TRPC5	2	2	2	0/2	1	1	1	0/1	3	3	3	3/3
TRPC6	5	5	3	5/5	5	12	14	0/14	3	3	3	3/3
TRPM4	1	1	1	1/1	3	3	3	3/3	1	1	1	1/1
TMEM-2	4	4	1	4/4	3	4	4	4/4	nt	nt	nt	nt
Ca _v β2	nt	nt	nt	nt	1	1	1	1/1	1	1	1	1/1
HPRT-1	6	6	3	6/6	5	8	8	8/8	3	3	3	3/3

The expression of distinct TRPs was analyzed using RNA from three different sources (1) cell suspensions isolated by Langendorff heart preparation, (2) cardiomyocytes isolated by Laser Capture Microdissection (LCM), and (3) from cultured cardiac fibroblasts. In the table are included the number of cell preparations (# Cell preps) equivalent to independent mice, the number of independent RNA isolations (# RNA preps), the number of independent RT-PCR experiments (# PCRs) and the amplification results expressed as the number of positive amplifications related to the number of RT-PCR reactions carried out (positive amplifications/reactions). Results from amplification of transcripts of TRPM4, TMEM-2, Ca_vβ2 subunit and HPRT-1 (Hypoxanthine Phosphoribosiltransferase) are also given. nt: not tested and *: weak bands, observed only once.

In addition to the expression analysis described above we carried out a systematic procedure using cardiomyocytes isolated by LCM. Four independent cell preparations, corresponding to four mice were prepared and around 300 cardiomyocytes per preparation were collected to obtain four separate RNA preparations. RT-PCR experiments were performed with each RNA preparation and the results are summarized in Figure 18, where only transcripts from TRPC1, TRPM4 and TMEM2 were detected, which is in correspondence with the analysis described above. However, TRPC3, TRPC4 and TRPC6 transcripts were not detected in any of the four independent LCM preparations of

cardiomyocytes. TRPC5 was not included in this analysis because it could never be amplified from the initial cell suspensions obtained by Langendorff preparations.

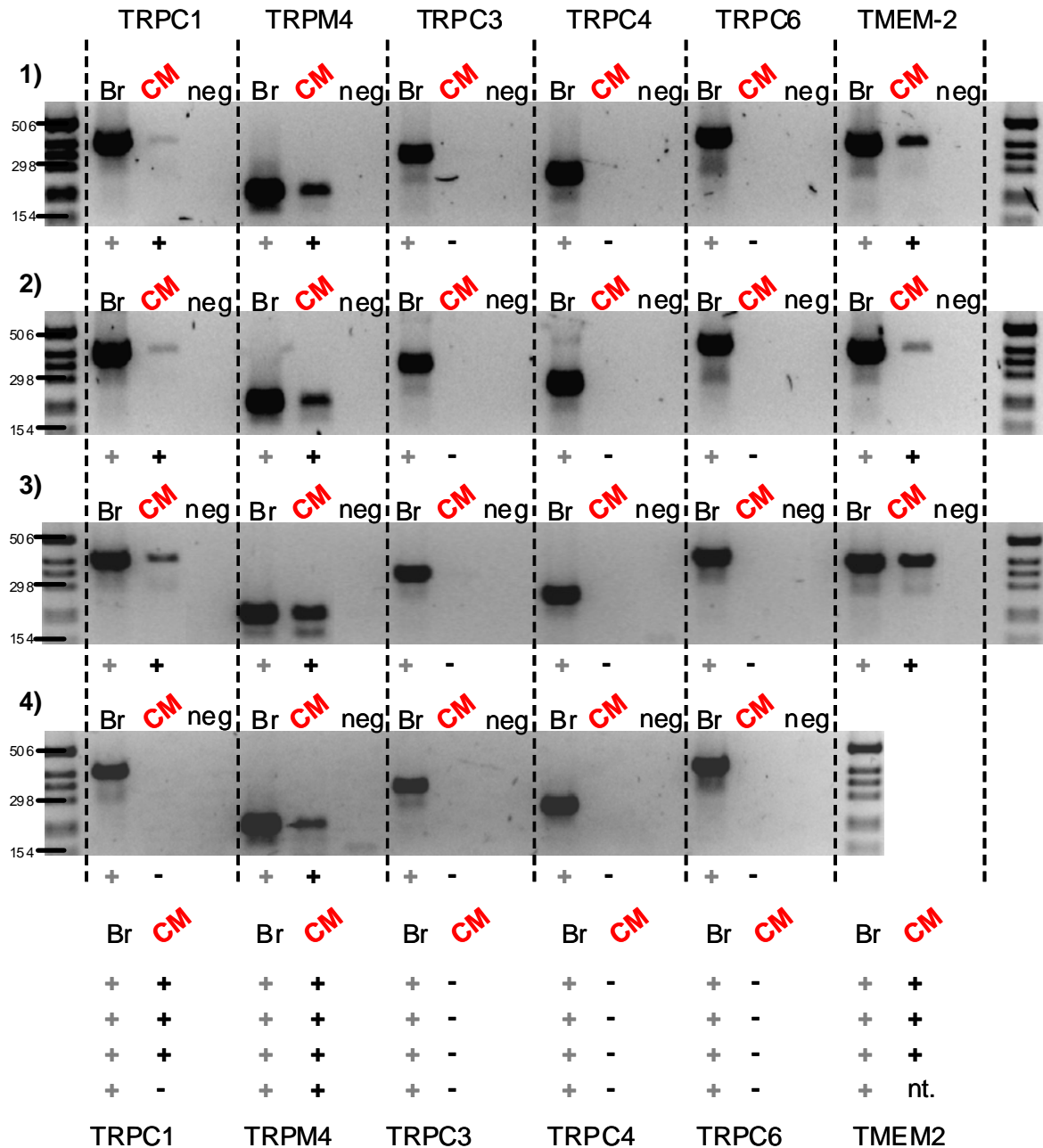


Figure 18. Systematic RT-PCR expression analysis of TRPs in LCM-isolated mouse cardiomyocytes. Transcripts from different TRPs amplified from total RNA obtained from mouse cardiomyocytes (CM) collected by Laser Capture Microdissection (LCM). Representative agarose gels (1- 4) after RT-PCR amplification showing the expression TRPC1, TRPM4, TRPC3, TRPC4, TRPC6 and TMEM-2 transcripts in total RNA from LCM-isolated cardiomyocytes. Each gel corresponds to an independent experiment and to an independent mouse. On the bottom the amplification results are summarized. Positive amplifications are coded with a plus symbol (+) and negative amplifications with a minus symbol (-). Total RNA from brain was used as positive control (Br) and PCR water was used as negative control (neg). bp: base pair, nt: not tested.

5.1.5 Isolation, culture and characterization of adult mouse cardiac fibroblasts

In order to study the expression and functional contribution of cardiac fibroblasts in the development of cardiac hypertrophy mediated by TRPC channels, it was required to establish a method to isolate cardiac fibroblasts and to characterize the obtained cell population by immunostaining using markers for different cardiac cell types.

5.1.5.1 Characterization of cardiac fibroblast culture by immunocytochemistry

There are only a few reports about culturing primary cardiac fibroblasts. Most of them are from rats (Colston et al., 2002; Ostrom et al., 2003; Olson et al., 2008) and only a few from mice (Jaffré et al., 2009). Based on information from the reported methods I established a protocol to culture fibroblasts from mouse heart. To isolate these cells hearts were perfused according to the Langendorff preparation, but were digested more rigorously than for cardiomyocyte isolation. From these preparations most of the cardiomyocytes were separated by centrifugation steps and the remaining cells were subjected to differential plating to get a population mostly composed of fibroblasts. An example of cultured cells from different time points after plating is shown in Figure 19 (A). Once a reproducible culture protocol was determined and it was observed that the cells had a typical reported cardiac fibroblasts morphology (Wang et al., 2003; Haudek et al., 2006; Landeen et al., 2007), samples from different preparations between the first and third passage were used to demonstrate the expression profile of markers of different cardiac cell types by Immunocytochemistry (ICC) methods.

To characterize the cultured fibroblasts four markers were used according to Thum and collaborators (2008): 1) P4HB (Prolyl-4-hydroxylase) as marker for fibroblasts; 2) CD-31 (or PECAM-1) used as endothelial marker; 3) α -smooth muscle 2-actin (or ACTA2) for identification of smooth muscle cells or myofibroblasts, and 4) α -actinin (ACTN2) used as cardiomyocyte marker. A representative staining using these markers to characterize cultured cardiac fibroblasts is shown in Figure 19 (B). The cultured cells were positive for PH4B and negative for α -actinin, α 2-actin and for CD-31. In a few cells an un-specific staining close to the nucleus was observed. Also markers were tested with positive controls using established isolation procedures. Freshly isolated cardiomyocytes were only positive for α -actinin. Positive controls for α -smooth muscle actin and for CD-31 were freshly isolated ileum smooth muscle cells (Tsvilovskyy et al., 2009) and cultured mouse aortic endothelial cells (Freichel et al., 2001), respectively.

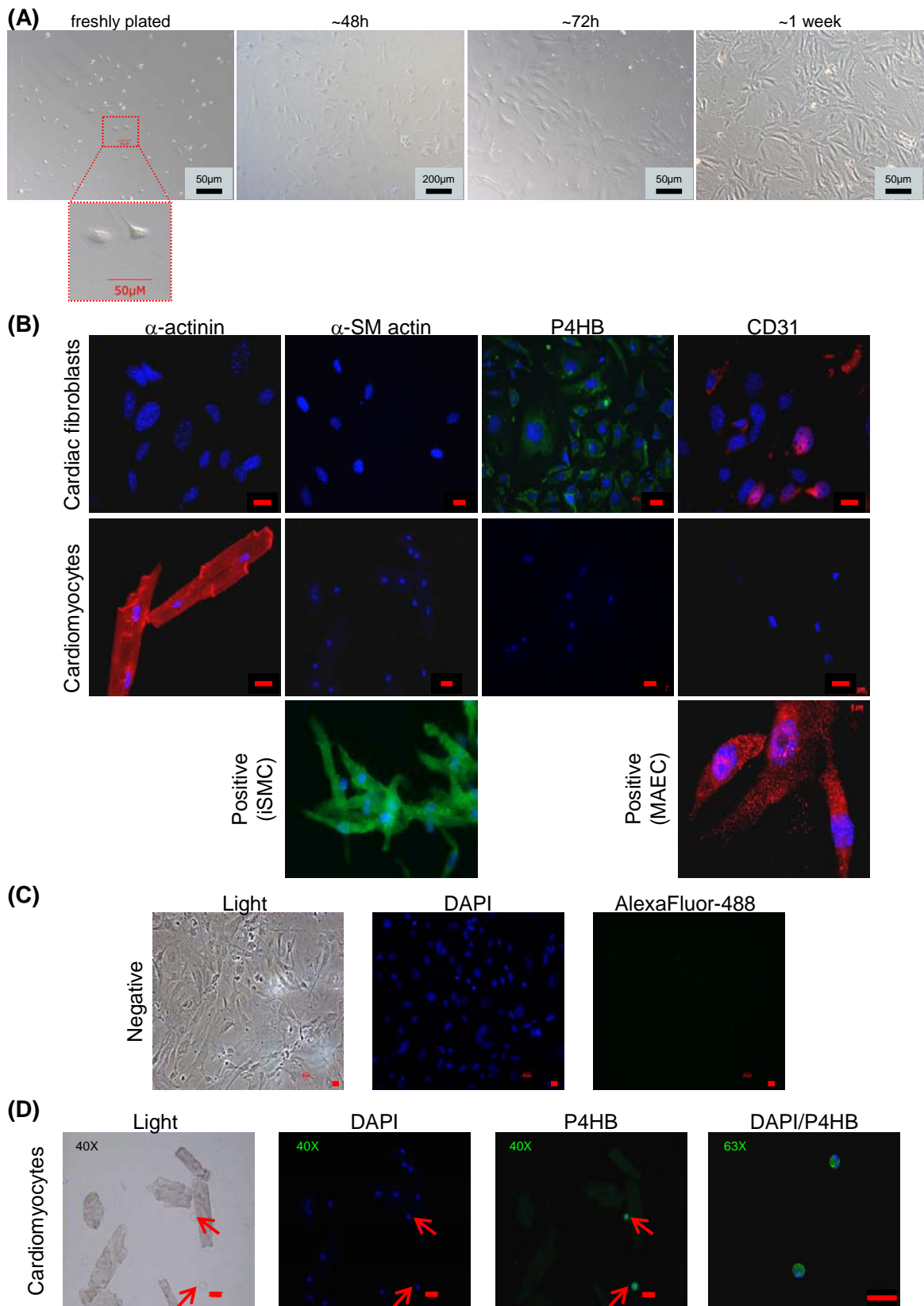


Figure 19. Characterization of cultured mouse cardiac fibroblasts. **(A)** Phase contrast photographs of cultured cardiac fibroblasts at different time points of culture. The inset shows two selected cells from the first hours after plating. **(B)** Representative immunocytochemical staining of cultured cardiac fibroblasts (Passage 1) and cardiomyocytes with DAPI (blue) and antibodies against α -actinin (red), α -smooth muscle actin (α -SM actin, green), prolyl 4-hydroxylase (P4HB, green) and CD31 (red). Isolated mouse ileum smooth muscle cells (iSMC) and mouse aortic endothelial cells (MAEC) were used as positive controls for α -SM actin and CD31 respectively. Similar staining patterns were obtained in at least one preparation from the second and third

passages. **(C)** A representative example of negative controls without the first antibody is included for the secondary antibody Alexa fluor-488 (green). **(D)** Positive cells for P4HB (green) found in preparations of freshly isolated cardiomyocytes are shown with red arrows. Higher magnification microphotographs from these cells stained with anti-P4HB (green) and nuclear staining DAPI (blue) are included. Red scale bars in B and C and corresponds to 20 μ m.

As negative control all cell types were processed similarly but the primary antibody was omitted, as shown for cardiac fibroblasts and the secondary antibody Alexa Fluor-488 (Figure 19, C). To quantify the number of P4HB positive cells in the cardiac fibroblasts culture the number of positive cells for P4HB was determined in comparison with the number of nuclei (DAPI staining) in at least three independent cell preparations between the first and third passage. From these quantifications about 95% of the cells were P4HB stained.

5.1.5.2 TRP expression analysis in adult mouse cardiac fibroblasts

Using cultured cardiac fibroblasts characterized by ICC we made a systematic expression analysis of TRPCs by RT-PCR. Cells were harvested between the first and third passage when they were confluent. From different preparations corresponding to independent mice we amplified transcripts from TRPC1, TRPC3, TRPC4, and also from TRPC5 and TRPC6 (Figure 20) that were not detected in any preparation of isolated cardiomyocytes. Beyond these genes, we could also detect transcripts from TRPM4 and the control gene HPRT-1. The results are summarized in Table 3 (under "Cultured cardiac fibroblasts" title).

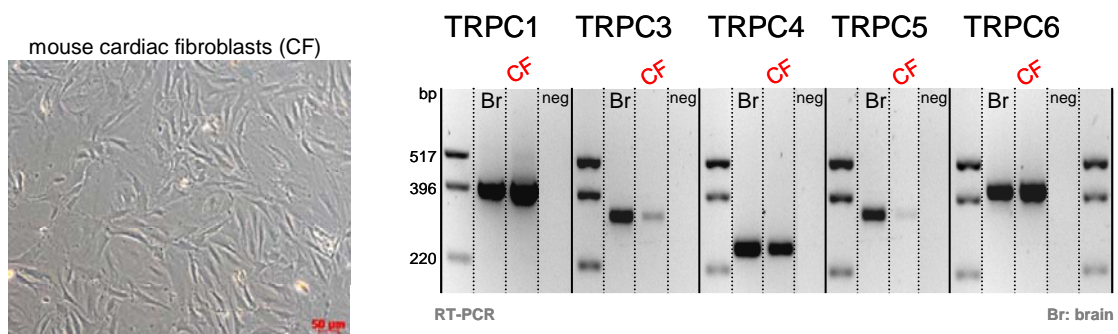


Figure 20. TRPC expression in cultured adult mouse cardiac fibroblasts. Transcripts from different TRPCs amplified from total RNA obtained from cultured mouse cardiac fibroblasts (CF) as those shown in the left picture. On the right, a representative agarose gel after RT-PCR amplification showing the expression of TRPC1, TRPC3, TRPC4, TRPC5 and TRPC6 in RNA from cultured fibroblasts. Total RNA from brain was used as positive control (Br) and RNA free water from the RNA isolation kit was used as negative control (neg). bp: base pair.

5.1.5.3 Calcium microfluometry from mouse cardiac fibroblasts

The reduced isoproterenol- and angiotensin II-induced cardiac hypertrophy development in TRPC1/TRPC4 (-/-)² mice might be due to impaired secretion of hypertrophy inducing factors from cardiac fibroblasts after Iso or ATII stimulation (Jaffré et al., 2009). Since these stimuli are known to increase the intracellular Ca²⁺ concentration in cardiac fibroblasts I started Ca²⁺ microfluometric analyses from cardiac fibroblasts lacking TRPC1 and TRPC4 proteins, which are able to form cation channels in other cell types (Freichel et al., 2001; Liu et al., 2007). Different agonists including isoproterenol, angiotensin II or serotonin were applied. There is not much information in the literature about calcium measurements in mouse cardiac fibroblasts; therefore, it was required to settle a reproducible protocol using our cultured fibroblasts.

First attempts to detect changes in [Ca²⁺]_i by agonist stimulation at room temperature were not successful. When the measurements were performed at 37°C by heating the perfusion solutions with a temperature control system the response rate improved significantly. An example comparing some of the firsts experiments performed at room temperature or with a pre-warmed physiological solution (~37°C) using isoproterenol as stimulus is shown in Figure 21 (A).

Several agonists like isoproterenol, serotonin and angiotensin that are related with cardiac hypertrophy development and secretion of hypertrophy inducing factors from cardiac fibroblasts were tested. I obtained fast responses after stimulation with all three agonists, but the responses were heterogeneous in terms of magnitude and also because not all cells responded to all agonist (Figure 23, B). Also, differences in response depending on the confluence state of the cells, time after splitting and serum deprivation (as mentioned in the literature) were observed (data not shown).

Due to the observed high variability in the responses, I decided to apply a more common protocol used to test calcium entry triggered by depletion of intracellular Ca²⁺ stores with Thapsigargin stimulation and analyzed changes in fluorescence in fibroblasts from wild type and TRPC1/TRPC4 deficient mice. Fibroblasts in calcium free solution were stimulated with 1µM Thapsigargin that produced a fast increase in the fluorescence FURA-2 ratio comparable between both genotypes (Figure 21, C and D, middle panels).

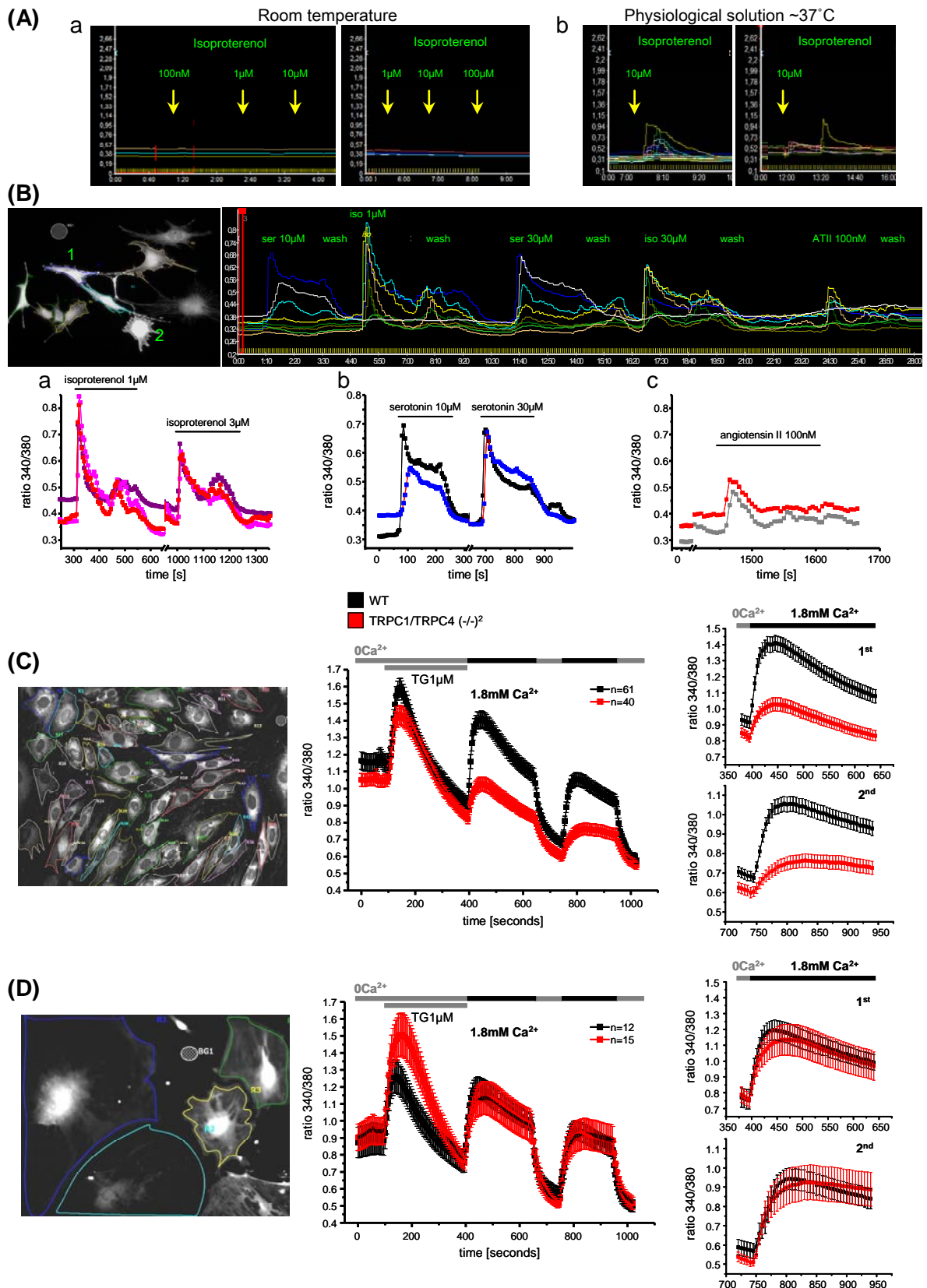


Figure 21. First Ca²⁺ imaging experiments TG with cultured adult mouse cardiac fibroblasts. Changes in intracellular calcium concentration in cultured cardiac fibroblasts loaded with Fura-2 (5 μ M) were expressed as changes in the fluorescence ratio (Em340/Em380). **(A)** First measurements where isoproterenol was applied at room temperature **(a)** or at **(b)** 37°C; each panel corresponds to different set of experiments and arrows indicate the time of isoproterenol addition. **(B)** Agonist induced increase in [Ca²⁺]_i concentration. Upper left a picture from fibroblasts that were stimulated with serotonin (ser), isoproterenol (iso) and angiotensin II (ATII) and on the right the corresponding original trace from the fluorescence ratio. As can be observed, the responses were

variable and not all cells were responded to all agonists. For example serotonin and isoproterenol evoked a change in fluorescence ratio but in case of cell 2 the response was observed only after stimulation with serotonin and not after isoproterenol. On the lower panels are depicted examples of evoked- Ca^{2+} transients by stimulation with iso (a), ser (b) and AII (c) from the upper cells. **(C-D)** Calcium re-addition protocol where Thapsigargin ($1\mu\text{M}$) was applied in Ca^{2+} -free (1mM EGTA) external solution to deplete the stores and then 1.8mM external Ca^{2+} was added as indicated. Left pictures show representative pictures from the cells used for the experiments. **(C)** Cells with the typical fibroblast morphology in culture highly confluent. **(D)** Larger cells with a myofibroblast morphology. The middle panels show changes in fluorescence ratios from these two types of analyzed cells and the right insets correspond to the two steps of Ca^{2+} addition showed in the middle panels. Black traces are from WT cells and red traces from TRPC1/TRPC4 $(-/-)^2$ cells. n = number of cells from two independent preparations from passage 1.

After recovering to the base line, calcium (1.8mM) was re-added by changing to a calcium containing solution, and a second increase in the fluorescence ratio was observed corresponding to calcium entry; after some minutes the calcium was removed and re-added to monitor once more the calcium entry.

From two independent series I observed that TRPC1/TRPC4 knockout cells presented a reduced increase in the fluorescence ratio in the two calcium re-addition phases (Figure 21, C). The difference was observed in highly confluent cells with a characteristic fibroblasts morphology (Figure 21, A, left panel) but not in those cell populations that were less confluent and showed a myofibroblast-like morphology (Figure 21, D). Morphological differences related with the density of the cells have been already observed in corneal fibroblasts from rabbit (Masur et al., 1996). In the future this morphological difference will be further analyzed by staining the α -smooth muscle to evaluate whether the cells shown in Figure 21 (D) are myofibroblasts. Changes of intracellular Ca^{2+} concentration after stimulation with physiological agonists in cells of different states of differentiation will be analyzed in both genotypes. Additional experiments are required to characterize the observed phenotype after Thapsigargin addition, as well as the impact of changes in the intracellular calcium concentration for the secretion of hypertrophy inducing factors in TRPC1/TRPC4 $(-/-)^2$ mice.

5.2 Platelet aggregation in TRPC deficient mice

To investigate whether TRPC proteins are relevant for platelet aggregation I performed *in vitro* aggregation experiments with mouse platelets from different TRPC single and compound knockout mouse lines using several platelet activating agonists (Table 4). Additionally, the expression of different TRPs in mouse platelets has been analyzed.

Table 4. Overview of platelet aggregometry screening with TRPC deficient mouse lines.

Mouse model		Agonist tested			
		ADP	Thrombin	Collagen	U46619
TRPC1 <i>-/-</i>	♀	X	X	X	X
	♂	X	—	—	—
TRPC3 <i>-/-</i>	♀	—	X	—	—
	♂	—	X	X	—
TRPC5 <i>-/-</i>	♀	—	—	—	—
	♂	X	X	X	X
TRPC6 <i>-/-</i>	♀	X	X	X	X
	♂	X	X	X	X
TRPC1/C4 (<i>-/-</i>) ²	♀	—	X	X	—
	♂	—	—	—	—
TRPC1/C6 (<i>-/-</i>) ²	♀	X	X	X	X
	♂	X	X	X	X
TRPC4/C6 (<i>-/-</i>) ²	♀	X	X	X	X
	♂	X	X	X	X
TRPC3/C6 (<i>-/-</i>) ²	♀	X	X	X	X
	♂	X	X	X	X
TRPC1/C4/C6 (<i>-/-</i>) ³	♀	X	X	X	X
	♂	—	—	—	—
TRPC1/C3/C6 (<i>-/-</i>) ³	♀	X	X	X	X
	♂	—	—	—	—

In the table is listed which of the four agonists (ADP, thrombin, collagen or TxA2 analogue U46619) were tested in different TRPC deficient mouse lines. The systematic screening was performed with platelets isolated either from male or female mice. Platelets from mouse lines that presented significant differences for a determined agonist are highlighted in blue; — indicates that the condition has been not tested yet.

As one of the initial steps in the analysis of platelet function we determined platelet numbers in male mice using whole blood from some mouse lines mentioned in Table 4, as well as from three of the wild type mouse lines used in our group. Platelet counts in 129SvJ mice were significantly lower in comparison with C57BL/6N mice or with mice first generation (F1) offspring from these two mouse lines (Figure 22, A). Platelet counts were comparable to corresponding controls in TRPC6, TRPC3/TRPC6, TRPC1/TRPC4 and

TRPC4/TRPC6 deficient male mice (Figure 22, B-E). In addition, I counted manually platelets from wild type and TRPC4/TRPC6 $(-/-)^2$ male and female mice and there were also no differences between wild type and TRPC4/TRPC6 $(-/-)^2$ mice. Only differences in platelet counts due to the gender were observed. Platelet counts between WT male and female mice were significantly different ($p < 0.001$) as well as counts between TRPC4/TRPC6 $(-/-)^2$ male and female mice ($p < 0.001$). These platelet counts expressed as 10^3 platelets/ μl were 1235 ± 315 and 1221 ± 144 for WT ($n=11$) and TRPC4/TRPC6 $(-/-)^2$ ($n=11$) male mice, respectively; and they were 944.5 ± 153 and 872 ± 189 for WT ($n=10$) and TRPC4/TRPC6 $(-/-)^2$ ($n=10$) female mice, respectively.

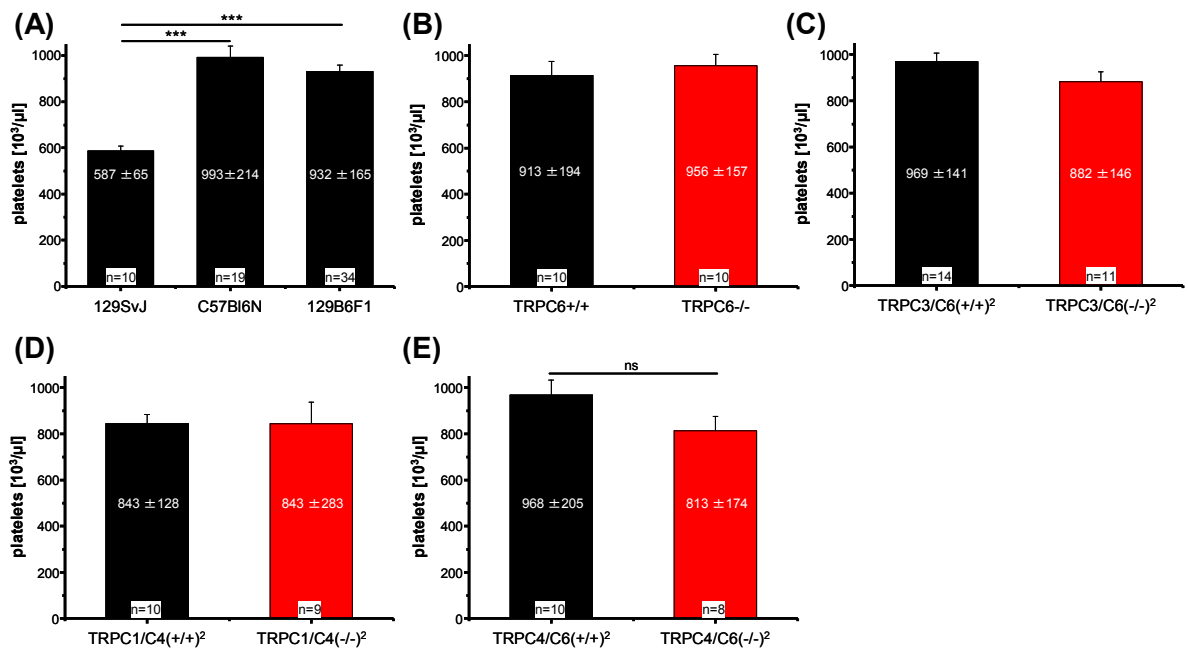


Figure 22. Whole blood platelet counts are not altered in different TRPC deficient mouse lines. Platelet counts from (A) wild type male mice from three mouse lines, and platelet counts from (B) TRPC6 $-/-$, (C) TRPC3/TRPC6 $(-/-)^2$, (D) TRPC1/TRPC4 $(-/-)^2$ and (E) TRPC4/TRPC6 $(-/-)^2$ male mice were determined with a Coulter counter AcT diff (Beckman) and compared to appropriate wild type controls. In addition, values for Error bars indicate SEM. *** $p < 0.001$ and ns (not significant) according to the Student's t-test.

5.2.1 TRP expression analysis in isolated mouse platelets

For analysis of TRPC protein expression in isolated mouse platelets we used antibodies directed against TRPC1 (unpublished) TRPC3 (unpublished), TRPC4 (Freichel et al., 2001), TRPC5 (unpublished), TRPC6 (Tsvilovsky et al., 2009) and TRPM4 proteins (Mathar et al., 2010) that has been generated by Prof. V. Flockerzi and coworkers. Using the antibody ab861 against a C-terminal fragment of the murine TRPC6, proteins of

~120kDa in platelet protein preparations from wild type mice but not from TRPC6 $-/-$ mice were detected (Figure 23, A). So far, using antibodies directed against TRPC1, TRPC3, and TRPC4 the observed protein patterns detected by western blot analysis did not differ between protein preparations from wild type and the corresponding knockout controls (data not shown). We did not detect TRPC5 proteins in mouse platelets with antibodies against TRPC5 that detected TRPC5 proteins in brain preparations from wild type mice but not from TRPC5 $-/-$ mice (data not shown). With the antibody Ak578 directed against the amino-terminal end of mouse TRPM4, proteins of ~138kDa in platelet protein preparations from wild type mice but not from TRPM4 $-/-$ mice were detected (Figure 23, B). In addition, using RT-PCR analysis, I amplified transcripts from TRPC1 and TRPC6 using total RNA isolated from wild type mouse platelets (Figure 23, C). Moreover, I also amplified transcripts from TRPM4, TMEM-2, and the housekeeping genes, HPRT-1 and GAPDH (Glyceraldehyde 3-phosphate dehydrogenase). With our protocol that produced amplification products with RNA from other tissues no transcripts from TRPC3, TRPC4 or TRPC5 were detected so far (Table 5).

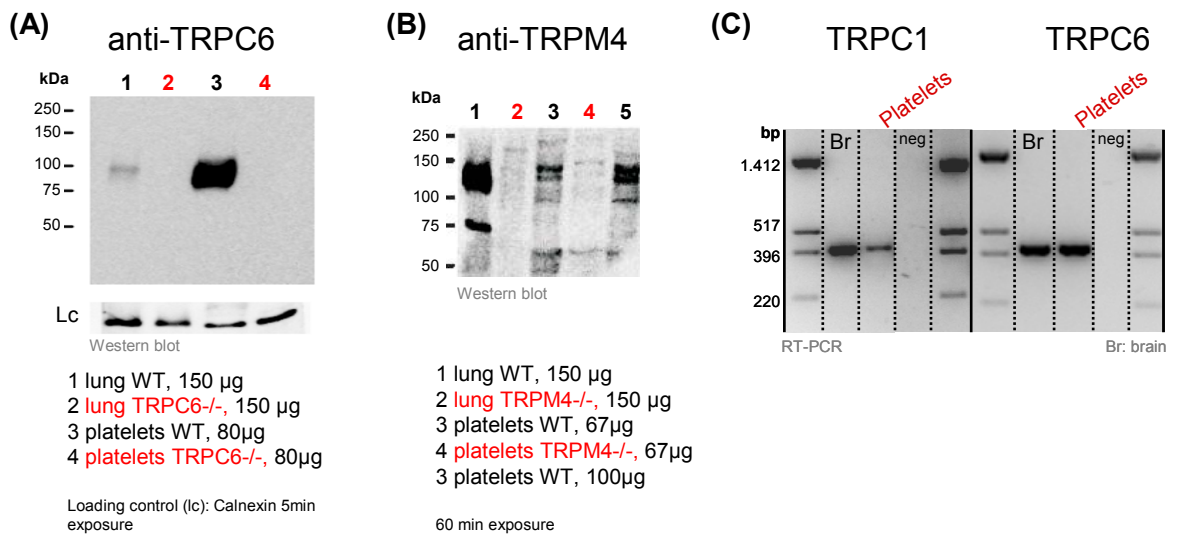


Figure 23. Expression analysis of TRPs in mouse platelets. (A) Western blot with the antibody 861 against TRPC6 proteins using platelet protein fractions from wild type (line 3) and TRPC6 deficient mice (line 4). (B) Western blot with the antibody Ak578 against TRPM4 proteins using platelet protein fractions from wild type (line 3) and TRPM4 deficient mice (line 4). (A-B) Lung protein preparations from wild type (lines 1) and from corresponding TRP-deficient mice (lines 2) were used as control. (C) Detection of transcripts of TRPC1 and TRPC6 in isolated platelets. Total RNA from brain was used as positive control (Br) and RNA free water from the RNA isolation kit was used as negative control (neg). kDa: kiloDalton, bp: Base pair.

Table 5. Summary of TRP expression analysis in mouse platelets by RT-PCR.

gene	Platelets			# PCRs	positive amplification/reactions
	# Cell preparations	# RNA preparations	FACS preparations		
TRPC1	5	4	1	6	7/12
TRPC3	6	5	1	4	0/8
TRPC4	3	2	1	3	0/6
TRPC5	1	nt.	1	1	0/2
TRPC6	4	3	1	5	10/10
TRPM4	1	nt.	1	2	4/7
TMEM-2	2	1	1	2	4/4
HPRT-1	2	2	nt.	2	2/2
GAPDH	1	1	nt.	1	1/1

The expression of different TRPs was analyzed in isolated mouse platelets. In the table the number of cell preparations equivalent to independent mice, the number of independent RNA isolations, the number of independent RT-PCR experiments (# PCRs) and the amplification results expressed as the number of positive amplifications related to the number of RT-PCR reactions carried out (positive amplifications/reactions) are mentioned. Preparations from sorted platelets by FACS were used directly for RT-PCR without RNA extraction. Amplifications of transcripts of a TRP relative TMEM-2, of HPRT-1 (Hypoxanthine Phosphoribosiltransferase) and of GAPDH (Glyceraldehyde 3-phosphate dehydrogenase) were used as positive control for RNA integrity. #: number, nt: not tested.

5.2.2 Turbidimetric aggregometry and characterization of the platelet preparation

For analyzing of the role of TRPC proteins for platelet aggregation I decided for the turbidimetric method or optical aggregometry as an *in vitro* assay of platelet function. Because platelet expression analysis and aggregation experiments were made using isolated washed platelets, we determined the purity of the preparation by flow cytometry. The size and complexity of the cells in the platelet suspension were characterized using the forward scatter (FSC) and side scatter (SSC) (Figure 24, A). The analyzed platelet population was more than 99.5% homogeneous (See values of region 35 in upper right table from Figure 24, A) and this homogeneity was observed in two independent platelet preparations. To corroborate that the cells were indeed platelets, we incubated platelets with an antibody against mouse α IIb β 3 integrin (CD41/CD61) FITC-labeled used as specific platelet marker. We characterized the stained sample by FSC and SSC and the observed pattern was identical to the one from the non-stained sample with more than 99.5% homogeneity (Figure 24, Ab).

When the samples were analyzed by fluorescence intensity, there was a right switch into the fluorescence signal in comparison with the non stained platelet sample (compare Figure 24, Ba and Bb). It was determined that >99.9% of the cells expressed the α IIb β 3 integrin (Figure 24, see values from regions 12 and 14 for stained platelets in B) indicating the high purity of the preparation. This observation was confirmed in two independent preparations. Additionally, we sorted stained platelets in groups of 50, 200, 500 and 2000 platelets in single PCR reaction tubes and after freezing the samples I made RT-PCR directly with these platelets. From these samples I amplified transcripts from TRPC1, TRPC6, TRPM4 and TMEM-2 (Table 5).

Because calcium is an important component of platelet function and its extracellular presence is needed to obtain platelet aggregation due to its requirement for fibrinogen binding and for maintaining the platelet signaling by its influx into platelets, I did aggregometry experiments with platelets from wild type mice in the presence and in the absence of extracellular calcium. When washed platelets from wild type were stimulated with agonists like ADP, thromboxane A₂ receptor agonist (U46619), thrombin or collagen in the presence of 2mM extracellular Ca²⁺, a rapid aggregation response was observed with all four agonist. When the same stimuli were used with platelets in a calcium free solution containing 2mM EGTA (Weber et al., 1999), no aggregation was observed and only an increase in the optical density of the suspension, corresponding to the called platelet shape change (PSC), was evident for stimulation with ADP, U46619 or collagen (Figure 24, C).

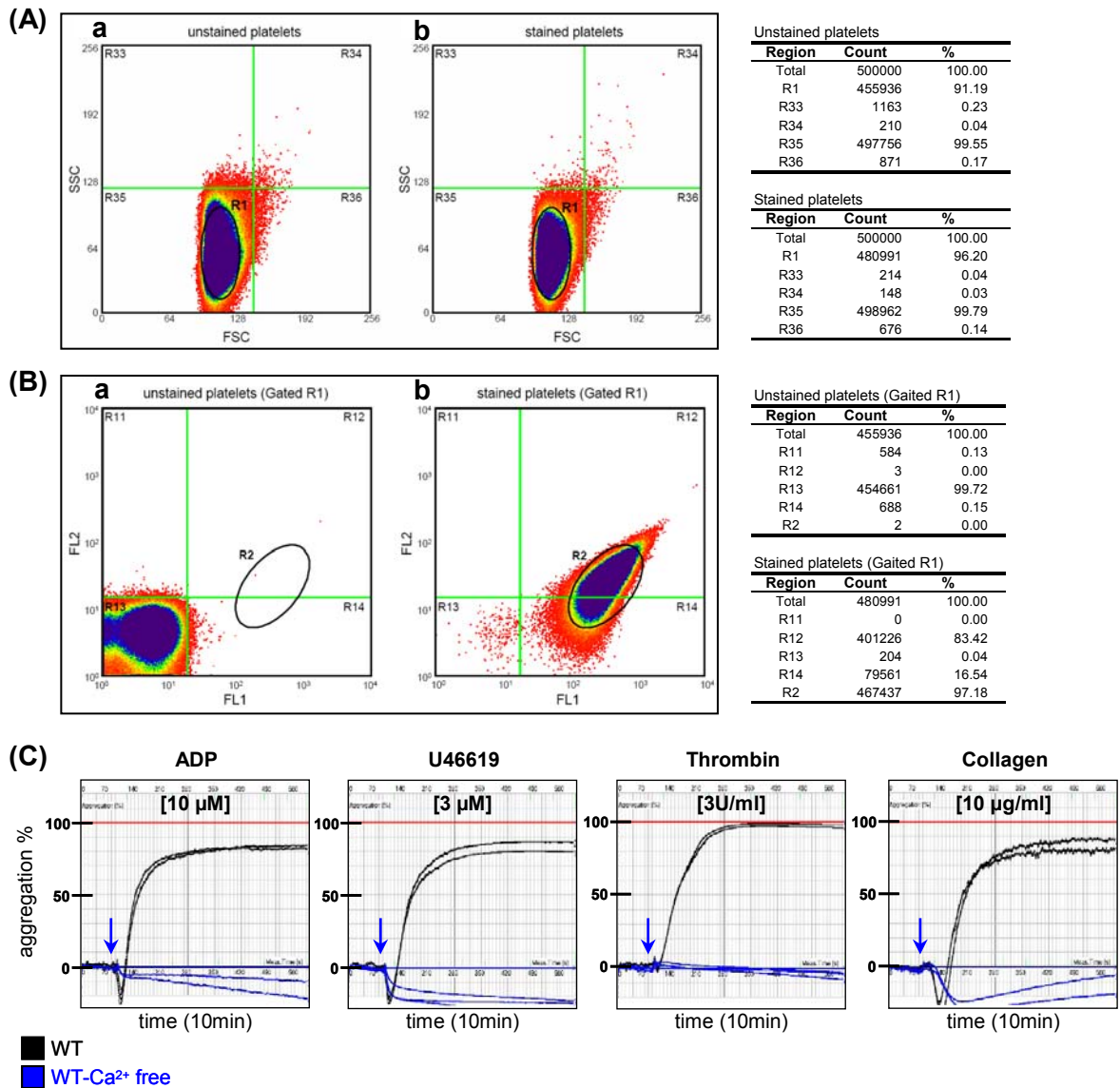


Figure 24. Washed platelet preparation is 99.9% pure and Ca²⁺ is required for platelet aggregation. **(A)** Flow cytometric analysis of mouse isolated platelets. Unstained platelet's sample (a) and platelets incubated with FITC-conjugated anti integrin $\alpha_{IIb}\beta_3$ (b) were analyzed by side scatter (SSC; y axis) and forward scatter (FSC; x axis). Platelets were identified in region 1 (R1, lower left quadrant). **(B)** Single color flow cytometric analysis of mouse isolated platelets. Unstained platelets (a) and platelets incubated with FITC-conjugated anti-integrin $\alpha_{IIb}\beta_3$ (b) were gated by FSC/SSC characteristics and the fluorescence was analyzed. The platelet population incubated with the anti-integrin $\alpha_{IIb}\beta_3$ shows a right shift in the fluorescence, compare region 2 (R2) between right and left panels. Data tables on the right contain number of analyzed platelets and percentage of events for each region. **(C)** Representative original traces from aggregation experiments performed in washed platelets from wild type (WT) male mice. Aggregation was induced by application (arrow) of ADP, Thromboxane A₂ receptor agonist analogue U46619, thrombin or collagen. Aggregation from platelets of WT mice in the presence of 2mM Ca²⁺ (black traces) or with 2mM EGTA (blue traces) are given.

5.2.3 ADP-, Thromboxane A₂ analogue U46619-, Thrombin- and Collagen-induced aggregation in platelets from wild type mice

Four different agonists were used for the analysis of platelet aggregation to cover a variety of activation mechanisms and cascades involved in platelet activation: ADP, Thromboxane A₂ analogue U46619, thrombin or Collagen, agonists that stimulate P2Y₁/P2Y₁₂, TP, PAR4 and GPVI receptors, respectively. I analyzed four parameters from aggregation traces: 1) the platelet shape change (PSC) that corresponds to the fast negative inflection in the aggregation curve observed after agonist addition; 2) the maximum aggregation that is defined as the maximum percentage value reached during aggregation; 3) the area under the aggregation curve, defined as the integral of the aggregation curve over the time period corresponding to the aggregation phase; and 4) the maximum slope of the aggregation curve, defined in percentage of aggregation per minute.

For the aggregation assays I used platelets from male or female mice because it has been reported that platelets from female mice are more sensitive to agonists than platelets from male mice (Leng et al., 2004). A comparison between agonist-induced platelet aggregation in platelets from wild type female and male mice was made (Figures 25 and 26). ADP produced a significantly higher maximal aggregation in female platelets at 3 μ M and 10 μ M compared to platelets from male mice, also the area under the aggregation curve was significantly higher for 30 μ M in female platelets. No differences in PSC or in the aggregation slope between both genders were detected (Figure 25, A). After stimulation with U46619 only the PSC at two concentrations in platelets from female mice was increased (Figure 25, B).

Thrombin stimulation induced a small but significantly augmented maximal aggregation and aggregation area at a concentration of 1U/ml in platelets from female mice; interestingly, in these platelets the aggregation slope at 0.1U/ml thrombin was higher, but smaller at 3U/ml compared to platelets from males (Figure 26, A). Collagen induced in platelets from females a significantly increased maximal aggregation and aggregation area at a concentration of 10 μ g/ml; however, no difference was observed in PSC or in the maximal slope (Figure 26, B).

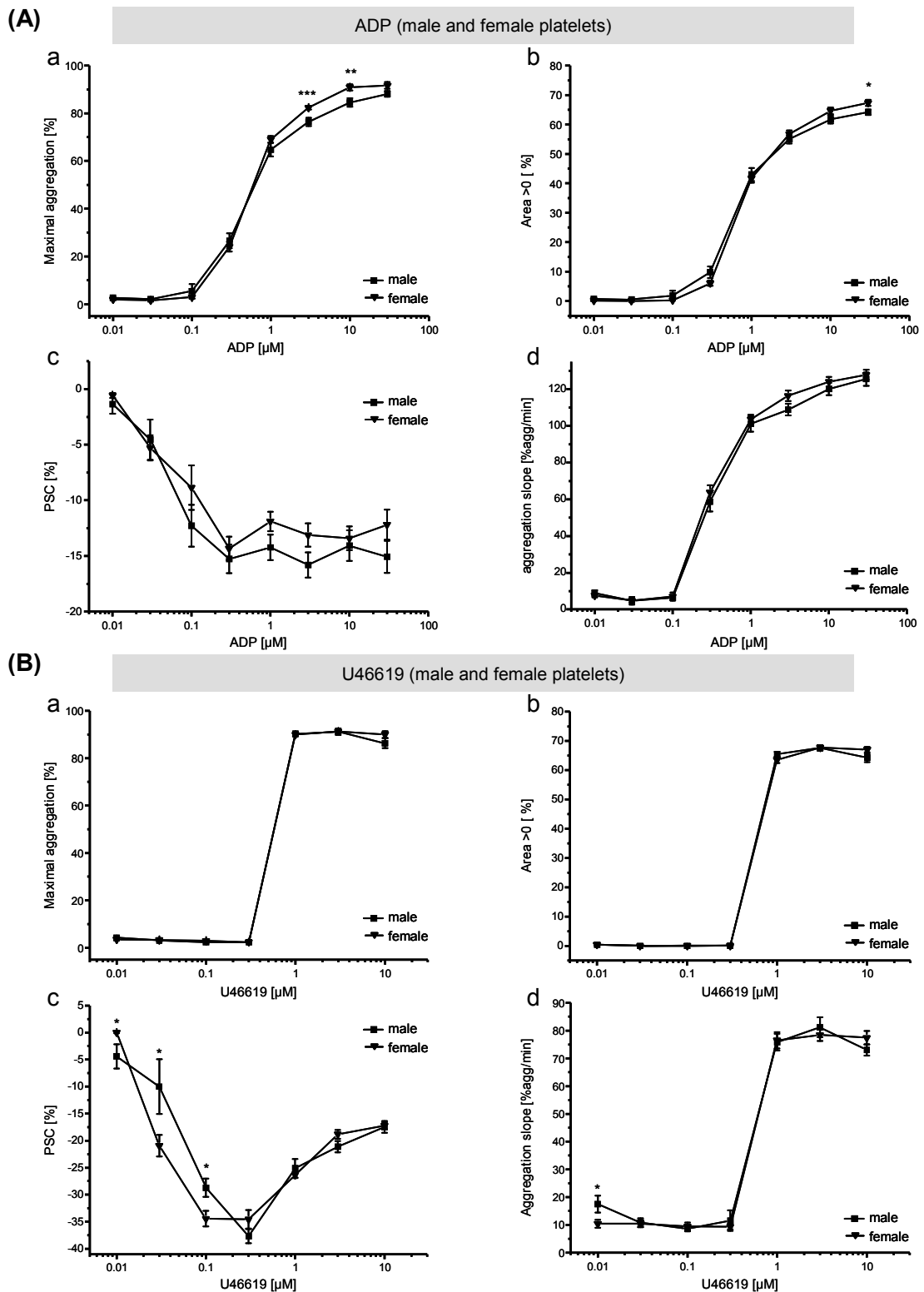


Figure 25. *In vitro* platelet aggregation in male and female wild type platelets induced by ADP or by U46619. Concentration-response curves from platelets stimulated with: **(A)** ADP or **(B)** Thromboxane A₂ analogue U46619 where maximal aggregation (a), area under the aggregation curve (b), platelet shape change (PSC, c) and maximal slope during aggregation (d) were analyzed. Numbers of measurements per ADP concentration for males were: 0.01 μM =12, 0.03 μM =14, 0.1 μM =26, 0.3 μM =38, 1 μM =42, 3 μM =30, 10 μM =24 and 30 μM =25, and for females were: 0.01 μM =22, 0.03 μM =24, 0.1 μM =31, 0.3 μM =51, 1 μM =62, 3 μM =45, 10 μM =46 and 30 μM =28. Numbers of measurements per U46619 concentration for males were: 0.01 μM =10, 0.03 μM =8, 0.1 μM =13, 0.3 μM =15, 1 μM =44, 3 μM =17 and 10 μM =10, and for females were: 0.01 μM =16, 0.03 μM =18, 0.1 μM =21, 0.3 μM =27, 1 μM =78, 3 μM =35 and 10 μM =22. Error bars indicate SEM. * p <0.05, ** p <0.01 and *** p <0.001 according to the Student's t-test.

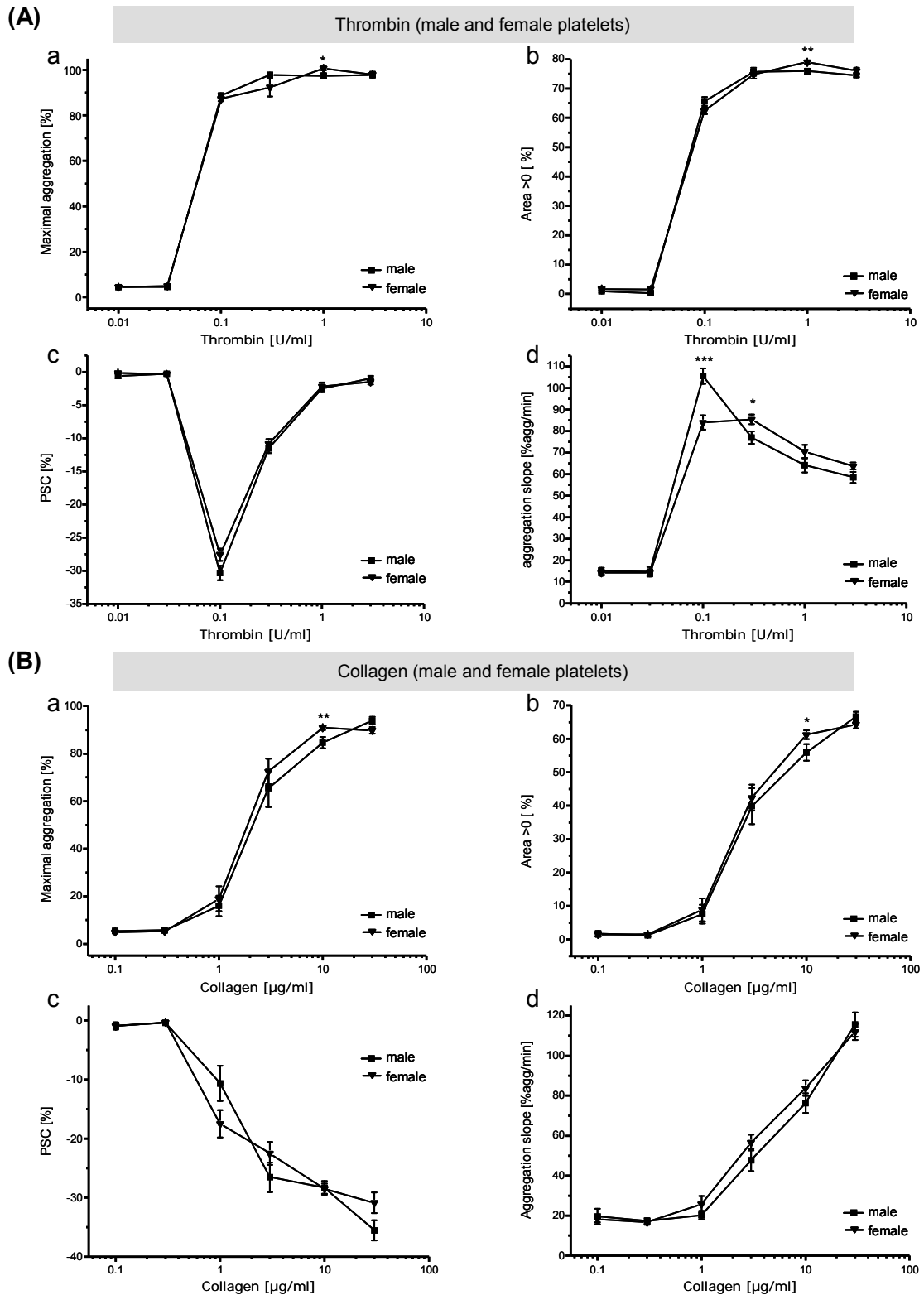


Figure 26. *In vitro* platelet aggregation in male and female wild type platelets induced by thrombin or by collagen. Concentration-response curves from platelets stimulated with: **(A)** Thrombin or **(B)** collagen where maximal aggregation **(a)**, area under the aggregation curve **(b)**, platelet shape change (PSC, **c**) and maximal slope during aggregation **(d)** were analyzed. Numbers of measurements per thrombin concentration for males were: 0.01U/ml=9, 0.03U/ml=10, 0.1U/ml=21, 0.3U/ml=20, 1U/ml=14 and 3U/ml=17, and for females: 0.01U/ml=15, 0.03U/ml=14, 0.1U/ml=36, 0.3U/ml=22, 1U/ml=18 and 3U/ml=19. Numbers of measurements per collagen concentration for males were: 0.1 μ g/ml=8, 0.3 μ g/ml=8, 1 μ g/ml=21, 3 μ g/ml=20, 10 μ g/ml=23 and 30 μ g/ml=17, and for females were: 0.1 μ g/ml=9, 0.3 μ g/ml=19, 1 μ g/ml=29, 3 μ g/ml=31, 10 μ g/ml=32 and 30 μ g/ml=22. Error bars indicate SEM. * p <0.05, ** p <0.01 and *** p <0.001 according to the Student's t-test.

5.2.4 Screening of TRPC deficient platelets by turbidimetric aggregometry

It has been reported that different TRPCs are expressed in platelets and we were able to detect the expression of TRPC1 and TRPC6. Although, so far the expression analysis, as first step in studying the role of TRPCs in platelets, is hampered due to lack of appropriate antibodies and to restricted mRNA content in platelets. In addition, there are still no specific agonists or antagonist for these channels available. Therefore, I compared agonist-induced aggregation in platelets from different single and compound TRPC deficient mouse lines. A summarized description of my observations from aggregation experiments is contained in Tables 6 and Table 7 for results from female and male mice, respectively.

TRPC6 *-/-* mice. Based on our expression analysis I focused on studying platelets obtained from TRPC6 deficient female or male mice bred with two different genetic backgrounds (C57BL/6N or the F1 offspring of C57BL/6Nx129SvJ intercrosses). No difference in maximal aggregation using different concentrations of ADP, Thrombin, Collagen or U46619 between platelets from wild type and TRPC6^{-/-} mice was observed (Tables 6A and 7A); a detailed description of these results is presented below under section 5.2.4.1.

TRPC1 *-/-* mice. Aggregation in washed platelets from TRPC1^{-/-} mice induced by thrombin, collagen or U46619 showed no difference in the maximal aggregation between wild type and TRPC1 deficient platelets from female mice (Table 6A). In experiments performed with platelet rich plasma (PRP) the ADP-induced maximal aggregation was similar between platelets from wild type and TRPC1^{-/-} mice (Table 6A).

TRPC3 *-/-* mice. Other groups reported the expression of TRPC3 in platelets (see Table i4). I analyzed platelet aggregation in platelets from TRPC3 deficient mice. Maximal aggregation after thrombin or ADP stimulation was similar between platelets from wild type and TRPC3^{-/-} female mice at the tested concentrations (Table 6A). Using platelets from TRPC3^{-/-} male mice no differences in aggregation were detected at one collagen concentration (Table 7A); however, the thrombin-induced aggregation was slightly but significantly reduced at the concentrations of 0.3/Uml (-14%) and 1U/ml (-11%) in platelets from TRPC3^{-/-} male mice (Table 7A).

TRPC5 *-/-* mice. Also the expression of TRPC5 in platelets has been reported (see Table i4). In experiments comparing platelet aggregation between wild type (F1) and TRPC5 deficient platelets no difference was observed in the maximal aggregation after thrombin,

collagen or U46619 stimulation. The ADP induced aggregation was significantly reduced in platelets from TRPC5^{-/-} male mice when compared to the response from F1 mice (Table 7A). For TRPC5^{-/-} mice of a mixed genetic background litter-matched controls from heterozygous breedings were available. In two experimental series using these mice I observed no difference in aggregation induced by ADP, thrombin, collagen and U46619 (Table 7A). Then, the observed difference in the ADP response between TRPC5^{-/-} and F1 mice could be explained by differences in the genetic background and not due to the TRPC5 deletion.

TRPC compound knock out mice. It has been proposed that TRPC channels can form heteromeric channel complexes. The loss of one channel or channel subunit could be compensated by others; for that reason I performed experiments with platelets from TRPC1/TRPC6 and TRPC3/TRPC6 compound deficient mice. Both mouse lines were generated by intercrossing between corresponding single TRPC deficient mouse lines. TRPC1/TRPC6 and TRPC3/TRPC6 mice were fertile and show no obvious sign of disease. The most striking finding from these experiments was an impaired ADP-induced platelet response in platelets from both genotypes (Table 6B) and was extensively analyzed in platelets from TRPC1/TRPC6 and TRPC3/TRPC6 female (Table 6B) and male (Table 7B) mice. These results are described in detail under sections 5.2.4.2 and 5.2.4.3, respectively.

TRPC1/TRPC4/TRPC6 (-/-)³ mice. TRPC1/TRPC4/TRPC6 deficient mice were fertile and show no obvious sign of disease. Platelets from TRPC1/TRPC4/TRPC6 deficient female mice showed no differences in aggregation after stimulation with several collagen doses (Table 6B). But, platelets from these mice had a reduced response after stimulation with different ADP concentrations, and a significant ($p < 0.01$) reduction of about 43% in the maximal aggregation after stimulation with 1 μ M U46619 and a significant ($p < 0.05$) reduction of 34% in maximal aggregation induced by 0.1U/ml thrombin were observed (Table 6B).

TRPC4 deficiency in platelets. Since TRPC4 was reported in platelets (see Table i4) I also analyzed TRPC4/TRPC6 deficient mice. No difference in thrombin- induced aggregation was observed in platelets from TRPC4/TRPC6 (-/-)² mice (Tables 6B and 7B). After stimulation with 1 μ M U46619 was observed a 23% reduction in maximal aggregation only in platelets from TRPC4/TRPC6 deficient male mice (Table 7B). ADP-induced aggregation was tested in PRP preparations but revealed no difference in aggregation of platelets from TRPC4/TRPC6 (-/-)² male mice (Table 7B). An small

impairment in platelet aggregation in platelets from TRPC4/TRPC6 (-/-)² female mice was observed (Table 6B). Finally, regarding platelets from TRPC1/TRPC4 (-/-)² mice no differences after collagen or thrombin stimulation were observed in one experimental series (Table 6B) and this corresponded to the observations mentioned for TRPC1/TRPC4/TRPC6 (-/-)³ platelets (Table 6B).

Table 6A. Summary of platelet aggregometry results from different single TRPC deficient mouse lines analyzed in platelets from female mice.

TRP	Aggregation from female mice																			
	ADP (PRP)				ADP (WP)				Thrombin (WP)				Collagen (WP)				U46619 (WP)			
	#prep	#exp	µM	Obs.	#prep	#exp	µM	Obs.	#prep	#exp	U/ml	Obs.	#prep	#exp	µg/ml	Obs.	#prep	#exp	µM	Obs.
TRPC1	—	—	1	—	—	—	0.01	—	1x	2	0.01	no ≠	—	—	0.1	—	—	—	0.01	—
	1x	2	5	no ≠	—	—	0.03	—	2x	4	0.03	no ≠	1x	2	0.3	no ≠	—	—	0.03	—
	1x	2	10	no ≠	—	—	0.1	—	2x	4	0.1	i.r.	1x	3	1	no ≠	—	—	0.1	—
	—	—	50	—	—	—	0.3	—	3x	4	0.3	no ≠	2x	3	3	no ≠	—	—	0.3	—
	—	—	—	—	—	—	1.0	—	1x	2	1	no ≠	2x	4	10	i.r.	1x	1	0.5	no ≠
	—	—	—	—	—	—	3.0	—	1x	2	3	no ≠	1x	2	30	no ≠	—	—	1	—
	—	—	—	—	—	—	10	—	—	—	—	—	1x	2	50	no ≠	2x	2	2	no ≠
	—	—	—	—	—	—	30	—	—	—	—	—	—	—	—	—	—	—	3	—
—	—	—	—	—	—	—	—	—	—	—	—	—	—	—	—	—	—	10	—	
TRPC3	—	—	1	—	—	—	0.01	—	—	—	0.01	—	—	—	0.1	—	—	—	0.01	—
	1x	1	5	no ≠	—	—	0.03	—	—	—	0.03	—	—	—	0.3	—	—	—	0.03	—
	1x	2	10	no ≠	—	—	0.1	—	1x	1	0.1	no ≠	—	—	1	—	—	—	0.1	—
	—	—	50	—	—	—	0.3	—	1x	4	0.15	no ≠	—	—	3	—	—	—	0.3	—
	—	—	—	—	—	—	1.0	—	—	—	0.2	—	—	—	10	—	—	—	1	—
	—	—	—	—	—	—	3.0	—	—	—	0.3	—	—	—	30	—	—	—	3	—
	—	—	—	—	—	—	10	—	1x	4	1	no ≠	—	—	50	—	—	—	10	—
	—	—	—	—	—	—	30	—	—	—	3	—	—	—	—	—	—	—	—	—
TRPC6-C57	—	—	1	—	—	—	0.01	—	1x	3	0.01	no ≠	—	—	0.1	—	—	—	0.01	—
	—	—	5	—	—	—	0.03	—	2x	4	0.03	no ≠	1x	2	0.3	no ≠	—	—	0.03	—
	—	—	10	—	—	—	0.1	—	1x	3	0.1	no ≠	—	—	1	—	—	—	0.1	—
	—	—	50	—	1x	3	0.3	no ≠	2x	6	0.3	no ≠	2x	4	3	no ≠	1x	2	0.3	no ≠
	—	—	—	—	1x	3	1.0	no ≠	—	—	1	—	2x	4	10	no ≠	2x	6	1	no ≠
	—	—	—	—	1x	3	3.0	no ≠	1x	3	3	no ≠	2x	4	30	no ≠	2x	7	3	no ≠
	—	—	—	—	1x	3	10	no ≠	—	—	—	—	—	—	50	—	1x	2	10	no ≠
	—	—	—	—	1x	4	30	no ≠	—	—	—	—	—	—	—	—	—	—	—	—
TRPC6-F1	—	—	1	—	3x	8	0.01	no ≠	1x	2	0.01	no ≠	2x	7	0.1	no ≠	1x	2	0.01	no ≠
	—	—	5	—	3x	9	0.03	no ≠	1x	2	0.03	no ≠	3x	9	0.3	no ≠	1x	2	0.03	no ≠
	—	—	10	—	4x	11	0.1	no ≠	4x	7	0.1	no ≠	3x	9	1	no ≠	2x	4	0.1	no ≠
	—	—	50	—	4x	15	0.3	no ≠	1x	3	0.15	no ≠	3x	7	3	no ≠	2x	4	0.3	no ≠
	—	—	—	—	4x	13	1.0	no ≠	4x	9	0.3	no ≠	4x	9	10	no ≠	4x	10	1	no ≠
	—	—	—	—	4x	10	3.0	no ≠	3x	9	1	no ≠	2x	4	30	no ≠	3x	10	3	no ≠
	—	—	—	—	3x	9	10	no ≠	2x	7	3	no ≠	—	—	50	—	3x	6	10	no ≠
	—	—	—	—	2x	4	30	no ≠	—	—	—	—	—	—	—	—	—	—	—	—
	—	—	—	—	—	—	—	—	—	—	—	—	—	—	—	—	—	—	—	—
	—	—	—	—	—	—	—	—	—	—	—	—	—	—	—	—	—	—	—	—

Platelets from single deficient mouse lines were analyzed after stimulation with ADP, thrombin, collagen or the Thromboxane A₂ receptor agonist U46619 in platelet rich plasma (PRP) or washed platelets (WP) as indicated. For each agonist concentration the number of independent preparations (#prep) and the number of experiments (#exp) are given. Differences in maximal aggregation are mentioned in the observation (Obs.) columns. The suffixes -F1 or -C57 refers to the background of the mouse line, either from a mixed background (129SvJ x C57BL6N) or from a single C57BL6N background, respectively. no≠: not significantly different, ≠: different (*p<0.05; **p<0.01, and ***p<0.001 according to the Student's t-test), ≠?: possible difference, but reduced number of data to perform proper statistical analysis, and i.r.: inconsistent results.

Table 6B. Summary of platelet aggregometry results from different compound TRPC deficient mouse lines analyzed in platelets from female mice.

TRP	Aggregation from female mice																			
	ADP (PRP)				ADP (WP)				Thrombin (WP)				Collagen (WP)				U46619 (WP)			
	#prep	#exp	μM	Obs.	#prep	#exp	μM	Obs.	#prep	#exp	U/ml	Obs.	#prep	#exp	μg/ml	Obs.	#prep	#exp	μM	Obs.
TRPC3/C6	—	—	1	—	3x	6	0.01	no ≠	2x	5	0.01	no ≠	1x	2	0.1	no ≠	3x	7	0.01	no ≠
	—	—	5	—	3x	6	0.03	no ≠	2x	4	0.03	no ≠	2x	4	0.3	no ≠	3x	7	0.03	no ≠
	—	—	10	—	4x	8	0.1	no ≠	4x	9	0.1	≠*	2x	4	1	no ≠	3x	6	0.1	no ≠
	—	—	50	—	6x	18	0.3	no ≠	1x	2	0.15	i.r.	3x	6	3	no ≠	3x	6	0.3	no ≠
					6x	25	1.0	≠***	3x	7	0.3	no ≠	3x	5	10	no ≠	8x	38	1	≠***
					5x	12	3.0	≠**	2x	4	1	no ≠	2x	4	30	no ≠	4x	11	3	≠*
					4x	10	10	≠*	2x	6	3	no ≠	—	—	50	—	1x	2	5	no ≠
				4x	9	30	no ≠									3x	6	10	no ≠	
TRPC4/C6	1x	1	0.01	no ≠	—	—	0.01	—	—	—	0.01	—	3x	5	0.1	no ≠	1x	1	0.25	no ≠
	1x	1	0.5	no ≠	—	—	0.03	—	—	—	0.03	—	2x	6	0.3	no ≠	2x	3	0.5	no ≠
	3x	6	1	no ≠	—	—	0.1	—	—	—	0.1	—	3x	6	1	no ≠	1x	1	0.75	no ≠
	2x	4	3	no ≠	—	—	0.3	—	1x	2	0.3	no ≠	4x	10	3	≠*	1x	2	2	no ≠
	5x	10	5	no ≠	—	—	1.0	—	1x	3	1	no ≠	6x	12	10	no ≠	—	—	0.01	—
	4x	10	10	≠?*	—	—	3.0	—	—	—	3	—	4x	8	30	no ≠	—	—	0.03	—
	2x	4	20	no ≠	1x	1	10	—					—	—	50	—	—	—	0.1	—
	1x	2	50	no ≠	—	—	30	—									1x	2	0.3	no ≠
	1x	2	100	no ≠													2x	4	1	no ≠
																	1x	2	3	no ≠
																1x	2	10	no ≠	
TRPC1/C6	—	—	1	—	3x	7	0.01	no ≠	3x	6	0.01	no ≠	2x	4	0.1	no ≠	2x	4	0.01	no ≠
	—	—	5	—	4x	9	0.03	no ≠	3x	6	0.03	no ≠	3x	6	0.3	no ≠	3x	6	0.03	no ≠
	—	—	10	—	5x	11	0.1	no ≠	4x	10	0.1	no ≠	4x	10	1	no ≠	3x	6	0.1	no ≠
	—	—	50	—	8x	16	0.3	≠***	3x	6	0.3	no ≠	4x	8	3	no ≠	3x	6	0.3	no ≠
					7x	16	1.0	≠***	3x	6	1	no ≠	4x	9	10	no ≠	7x	17	1	≠**
					6x	12	3.0	≠***	3x	8	3	no ≠	4x	8	30	no ≠	3x	6	3	no ≠
					5x	13	10	no ≠							50		3x	6	10	no ≠
				4x	9	30	no ≠													
TRPC1/C3/C6	—	—	1	—	2x	4	0.01	no ≠	—	—	0.01	—	—	—	0.1	—	—	—	0.01	—
	—	—	5	—	3x	5	0.03	no ≠	—	—	0.03	—	—	—	0.3	—	—	—	0.03	—
	—	—	10	—	3x	9	0.1	no ≠	2x	4	0.1	≠?	—	—	1	—	—	—	0.1	—
	—	—	50	—	3x	10	0.3	≠***	1x	2	0.3	no ≠	—	—	3	—	1x	2	0.3	no ≠
					3x	8	1.0	≠*	1x	2	1	no ≠	2x	4	10	≠?	3x	15	1	≠*
					3x	6	3.0	no ≠	—	—	3	—	1x	2	30	no ≠	2x	5	3	≠?
					3x	6	10	≠?					—	—	50	—	1x	2	10	no ≠
				2x	5	30	≠?													
TRPC1/C4/C6	—	—	1	—	—	—	0.01	—	—	—	0.01	—	—	—	0.1	—	1x	2	0.01	no ≠
	—	—	5	—	—	—	0.03	—	1x	2	0.03	no ≠	1x	2	0.3	no ≠	1x	2	0.03	no ≠
	—	—	10	—	—	—	0.1	—	3x	9	0.1	≠*	1x	4	1	no ≠	1x	2	0.1	no ≠
	—	—	50	—	1x	2	0.3	no ≠	1x	2	0.15	no ≠	2x	4	3	no ≠	2x	4	0.3	no ≠
					2x	8	1.0	≠***	1x	4	0.3	no ≠	3(4)x	7	10	no ≠	4x	13	1	≠***
					2x	6	3.0	≠***	1x	2	1	no ≠	1(2)x	6	30	no ≠	6x	16	3	no ≠
					2x	6	10	≠*	1x	2	3	no ≠			50	—	1x	2	10	no ≠
				1x	1	30	—													
TRPC1/C4	—	—	1	—	—	—	0.01	—	—	—	0.01	—	—	—	0.1	—	—	—	0.01	—
	—	—	5	—	—	—	0.03	—	—	—	0.03	—	—	—	0.3	—	—	—	0.03	—
	—	—	10	—	—	—	0.1	—	1x	2	0.1	no ≠	1x	2	1	no ≠	—	—	0.1	—
	—	—	50	—	—	—	0.3	—	1x	2	0.3	no ≠	1x	3	3	no ≠	—	—	0.3	—
					—	—	1.0	—	1x	2	1	no ≠	1x	2	10	no ≠	—	—	1	—
					—	—	3.0	—	1x	2	3	no ≠	1x	2	30	no ≠	—	—	3	—
					—	—	10	—					—	—	50	—	—	—	10	—
				—	—	30	—													

Platelets from compound deficient mouse lines were analyzed after stimulation with ADP, thrombin, collagen or the Thromboxane A₂ receptor agonist U46619 in platelet rich plasma (PRP) or washed platelets (WP) as indicated. For each agonist concentration the number of independent preparations (#prep) and the number of experiments (#exp) are given. Differences in maximal aggregation are mentioned in the observation (Obs.) columns. no≠: not significantly different, ≠: different (*p<0.05; **p<0.01, and ***p<0.001 according to the Student's t-test), ≠?: possible difference, but reduced number of data to perform proper statistical analysis, and i.r.: inconsistent results.

Table 7A. Summary of platelet aggregometry results from different single TRPC deficient mouse lines analyzed in platelets from male mice.

TRP	Aggregation from male mice																			
	ADP (PRP)				ADP (WP)				Thrombin (WP)				Collagen (WP)				U46619 (WP)			
	#prep	#exp	μM	Obs.	#prep	#exp	μM	Obs.	#prep	#exp	U/ml	Obs.	#prep	#exp	μg/ml	Obs.	#prep	#exp	μM	Obs.
TRPC3	—	—	1	—	—	—	0.01	—	1x	2	0.01	no ≠	—	—	0.1	—	—	—	0.01	—
	—	—	5	—	—	—	0.03	—	1x	2	0.03	no ≠	—	—	0.3	—	—	—	0.03	—
	—	—	10	—	—	—	0.1	—	2x	4	0.1	no ≠	—	—	1	—	—	—	0.1	—
	—	—	50	—	—	—	0.3	—	—	—	0.15	—	—	—	3	—	—	—	0.3	—
	—	—		—	—	—	1.0	—	1x	4	0.2	no ≠	—	—	10	—	—	—	1	—
	—	—		—	—	—	3.0	—	2x	4	0.3	≠**	2x	5	30	no ≠	—	—	3	—
	—	—		—	—	—	10	—	3x	8	1	≠***	—	—	50	—	—	—	10	—
—	—		—	—	—	30	—	2x	6	3	no ≠	—	—		—	—	—		—	
TRPC5 litter-matched	—	—	1	—	1x	2	0.01	no ≠	—	—	0.01	—	—	—	0.1	—	—	—	0.01	—
	—	—	5	—	1x	4	0.03	no ≠	—	—	0.03	—	—	—	0.3	—	—	—	0.03	—
	—	—	10	—	2x	6	0.1	no ≠	2x	4	0.1	no ≠	—	—	1	—	—	—	0.1	—
	—	—	50	—	2x	7	0.3	no ≠	1x	2	0.3	no ≠	1x	5	3	no ≠	1x	4	0.3	no ≠
	—	—		—	2x	8	1.0	no ≠	1x	4	1	no ≠	2x	7	10	no ≠	2x	9	1	no ≠
	—	—		—	2x	7	3.0	no ≠	—	—	3	—	1x	2	30	no ≠	1x	2	3	no ≠
	—	—		—	1x	3	10	no ≠	—	—		—	—	—	50	—	—	—	10	—
—	—		—	1x	4	30	no ≠	—	—		—	—	—		—	—	—		—	
TRPC5	—	—	1	—	—	—	0.01	—	—	—	0.01	—	—	—	0.1	—	—	—	0.01	—
	—	—	5	—	—	—	0.03	—	—	—	0.03	—	—	—	0.3	—	—	—	0.03	—
	—	—	10	—	1x	2	0.1	no ≠	1x	4	0.1	no ≠	1x	4	1	no ≠	—	—	0.1	—
	—	—	50	—	1x	3	0.3	≠***	1x	2	0.3	no ≠	1x	2	3	no ≠	—	—	0.3	—
	—	—		—	1x	4	1.0	≠*	—	—	1	—	1x	2	10	no ≠	1x	2	1	no ≠
	—	—		—	1x	3	3.0	≠*	—	—	3	—	1x	2	30	no ≠	1x	2	3	no ≠
	—	—		—	1x	2	10	no ≠	—	—		—	—	—	50	—	—	—	10	—
—	—		—	1x	2	30	no ≠	—	—		—	—	—		—	—	—		—	
TRPC6-C57	—	—	1	—	—	—	0.01	—	3x	9	0.01	no ≠	4x	11	0.1	no ≠	2x	4	0.01	no ≠
	—	—	5	—	—	—	0.03	—	4x	10	0.03	no ≠	2x	7	0.3	no ≠	1x	2	0.03	no ≠
	—	—	10	—	1x	2	0.1	no ≠	7x	15	0.1	no ≠	5x	9	1	no ≠	1x	3	0.1	no ≠
	—	—	50	—	1x	2	0.3	no ≠	3x	6	0.15	no ≠	5x	14	3	no ≠	2x	6	0.3	no ≠
	—	—		—	2x	9	1.0	no ≠	5x	10	0.3	no ≠	7x	13	10	no ≠	5x	15	1	no ≠
	—	—		—	2x	5	3.0	no ≠	8x	16	1	no ≠	6x	10	30	no ≠	4x	13	3	no ≠
	—	—		—	2x	6	10	no ≠	3x	8	3	no ≠	—	—	50	—	3x	6	10	no ≠
—	—		—	2x	9	30	no ≠	—	—		—	—	—		—	—	—		—	
TRPC6-F1	—	—	1	—	—	—	0.01	—	—	—	0.01	—	—	—	0.1	—	—	—	0.01	—
	—	—	5	—	—	—	0.03	—	1x	3	0.03	no ≠	2x	4	0.3	no ≠	—	—	0.03	—
	—	—	10	—	1x	4	0.1	no ≠	3x	11	0.1	no ≠	1x	3	1	no ≠	—	—	0.1	—
	—	—	50	—	1x	4	0.3	i.r.	1x	2	0.15	no ≠	4x	8	3	no ≠	4x	7	0.3	no ≠
	—	—		—	1x	4	1.0	no ≠	3x	9	0.3	no ≠	3x	11	10	no ≠	4x	15	1	no ≠
	—	—		—	1x	4	3.0	no ≠	1x	2	1	no ≠	1x	2	30	no ≠	3x	7	3	no ≠
	—	—		—	1x	4	10	no ≠	—	—	3	—	—	—	50	—	1x	2	5	i.r.
—	—		—	—	—	30	—	—	—		—	—	—		—	—	—	10	—	

Platelets from single deficient mouse lines were analyzed after stimulation with ADP, thrombin, collagen or the Thromboxane A₂ receptor agonist U46619 in platelet rich plasma (PRP) or washed platelets (WP) as indicated. For each agonist concentration the number of independent preparations (#prep) and the number of experiments (#exp) are given. Differences in maximal aggregation are mentioned in the observation (Obs.) columns. The suffixes -F1 or -C57 refers to the background of the mouse line, either from a mixed background (129SvJ x C57BL6N) or from a single C57BL6N background, respectively. no≠: not significantly different, ≠: different (*p<0.05; **p<0.01, and ***p<0.001 according to the Student's t-test), ≠?: possible difference, but reduced number of data to perform proper statistical analysis, and i.r.: inconsistent results.

Table 7B. Summary of platelet aggregometry results from different compound TRPC deficient mouse lines analyzed in platelets from male mice.

TRP	Aggregation from male mice																				
	ADP (PRP)				ADP (WP)				Thrombin (WP)				Collagen (WP)				U46619 (WP)				
	#prep	#exp	μM	Obs.	#prep	#exp	μM	Obs.	#prep	#exp	U/ml	Obs.	#prep	#exp	μg/ml	Obs.	#prep	#exp	μM	Obs.	
TRPC3/C6			1	—	3x	7	0.01	no ≠	4x	9	0.01	no ≠	3x	5	0.1	no ≠	2x	4	0.01	no ≠	
			5	—	3x	7	0.03	no ≠	5x	10	0.03	no ≠	3x	6	0.3	no ≠	2x	4	0.03	no ≠	
			10	—	5x	10	0.1	no ≠	9x	25	0.1	≠**	4x	9	1	no ≠	2x	6	0.1	no ≠	
			50	—	5x	13	0.3	≠**	5x	12	0.15	≠*	6x	13	3	no ≠	4x	6	0.3	no ≠	
					5x	15	1.0	no ≠	8x	17	0.3	no ≠	7x	13	10	no ≠	8x	19	1	≠*	
					5x	10	3.0	no ≠	7x	16	1	≠*	5x	13	30	no ≠	4x	9	3	≠*	
					5x	10	10	no ≠	5x	14	3	no ≠	—	—	50	—	3x	6	10	no ≠	
					5x	11	30	≠**													
TRPC4/C6	—	—	0.01	—	—	—	0.01	—	1x	2	0.01	no ≠	1x	2	0.1	—	—	—	0.01	—	
	—	—	0.5	—	—	—	0.03	—	1x	2	0.03	no ≠	1x	2	0.3	—	—	—	0.03	—	
	2x	3	1	no ≠	—	—	0.1	—	1x	2	0.1	no ≠	2x	6	1	—	1x	1	0.1	—	
	1x	1	3	no ≠	—	—	0.3	—	1x	2	0.15	no ≠	3x	5	3	≠**	1x	3	0.3	no ≠	
	1x	2	5	no ≠	—	—	1.0	—	2x	5	0.3	no ≠	2x	5	10	≠*	1x	3	1	≠?	
	3x	7	10	no ≠	—	—	3.0	—	2x	5	1	no ≠	2x	5	30	≠*	1x	2	3	no ≠	
	—	—	20	—	—	—	10	—	2x	3	3	no ≠	—	—	50	—	—	—	10	—	
	—	—	50	—	—	—	30	—													
	—	—	100	—																	
TRPC1/C6	—	—	1	—	2x	4	0.01	no ≠	2x	4	0.01	no ≠	1x	3	0.1	no ≠	2x	4	0.01	no ≠	
	—	—	5	—	2x	4	0.03	no ≠	2x	4	0.03	no ≠	1x	3	0.3	no ≠	2x	4	0.03	no ≠	
	—	—	10	—	4x	10	0.1	no ≠	2x	4	0.1	no ≠	2x	4	1	no ≠	2x	4	0.1	no ≠	
	—	—	50	—	6x	14	0.3	≠**	2x	4	0.3	no ≠	3x	6	3	no ≠	2x	4	0.3	no ≠	
					6x	14	1.0	no ≠	2x	5	1	no ≠	3x	6	10	no ≠	5x	15	1	≠**	
					4x	12	3.0	no ≠	2x	5	3	no ≠	2x	4	30	no ≠	3x	7	3	no ≠	
					3x	6	10	no ≠					—	—	50	—	2x	4	10	no ≠	
					3x	11	30	no ≠													

Platelets from compound deficient mouse lines were analyzed after stimulation with ADP, thrombin, collagen or the Thromboxane A₂ receptor agonist U46619 in platelet rich plasma (PRP) or washed platelets (WP) as indicated. For each agonist concentration the number of independent preparations (#prep) and the number of experiments (#exp) are given. Differences in maximal aggregation are mentioned in the observation (Obs.) columns. no≠: not significantly different, ≠: different (*p<0.05; **p<0.01, and ***p<0.001 according to the Student's t-test), ≠?: possible difference, but reduced number of data to perform proper statistical analysis.

5.2.4.1 Agonist-induced *in vitro* platelet aggregation in TRPC6^{-/-} platelets

The experiments below are pooled from at least 3 independent experimental series and obtained with platelets from female TRPC6^{-/-} mice and F1 controls. Similar results were obtained in platelets from male mice as well as from mice of both genders bred under C57BL6/N background (see summary of all experiments in Tables 6A and 7A).

ADP-induced aggregation in platelets from TRPC6^{-/-} mice was not impaired at all tested concentrations (Figure 27, A). Aggregation analyzed by maximal aggregation, area of the aggregation curve, PSC or aggregation curve slope in all ADP concentrations was comparable between wild type and TRPC6^{-/-} platelets (Figure 27, A). The Thromboxane A₂ analogue U46619 produced also similar aggregation responses (Figure 27, B). Neither thrombin- (Figure 28, A) nor collagen-induced (Figure 28, B) aggregation in platelets from TRPC6 deficient mice presented impaired responses.

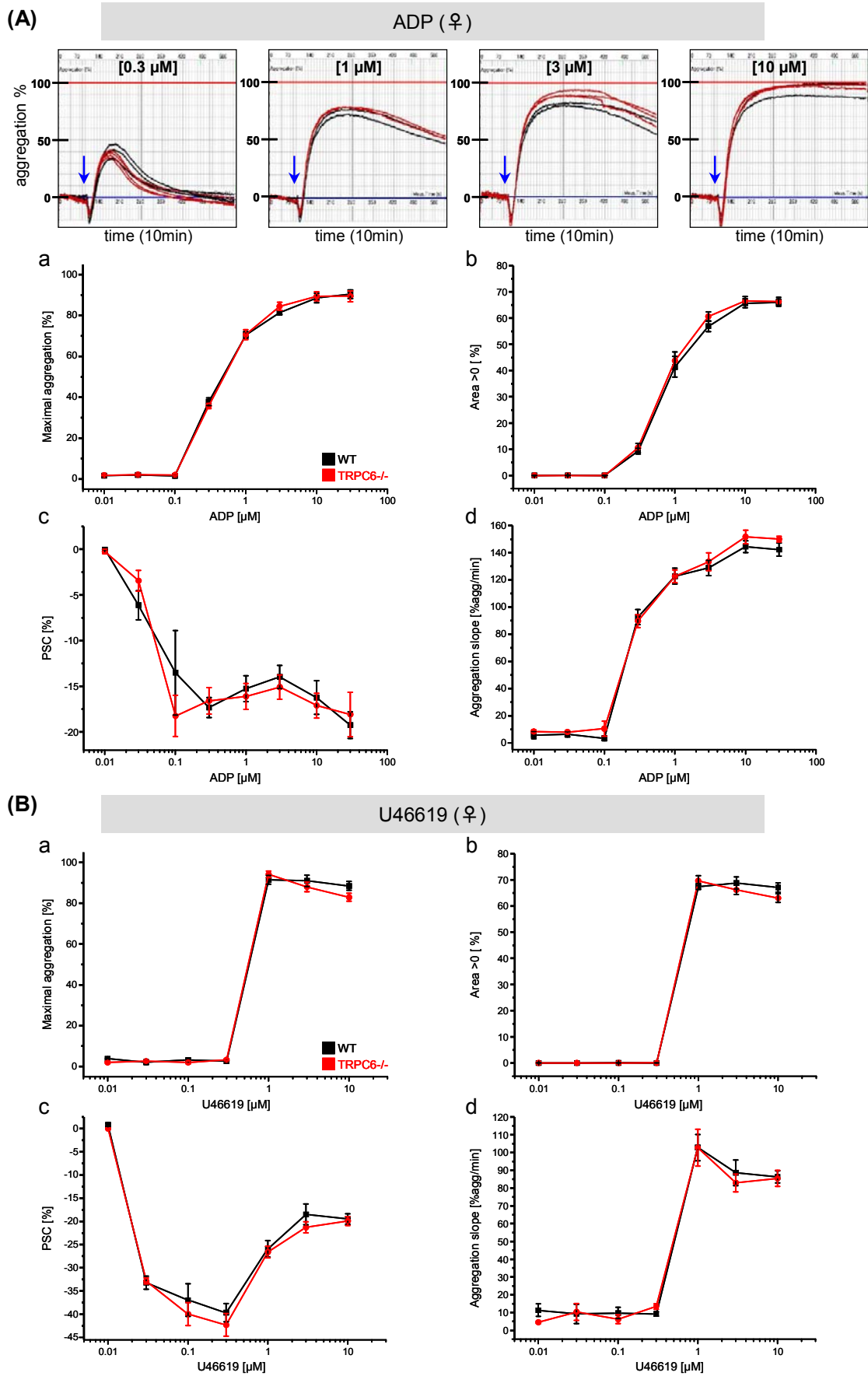


Figure 27. ADP- and U46619-induced platelet aggregation in washed platelets from wild type and TRPC6^{-/-} mice. Representative original aggregation curves of ADP-induced aggregation in wild type (black) and TRPC6^{-/-} platelets where ADP application is indicated by an arrow (A, upper panels). Concentration-response curves from platelets stimulated with: (A) ADP or (B)

Thromboxane A₂ analogue U46619 where maximal aggregation (**a**), area under the aggregation curve (**b**), platelet shape change (PSC, **c**) and maximal slope during aggregation (**d**) were analyzed. Numbers of measurements per ADP concentration for wild type were: 0.01μM=6, 0.03μM=7, 0.1μM=10, 0.3μM=10, 1μM=8, 3μM=8, 10μM=6, 30μM=4, and for TRPC6^{-/-} were: 0.01μM=8, 0.03μM=9, 0.1μM=11, 0.3μM=15, 1μM=13, 3μM=10, 10μM=9, 30μM=4. Numbers of measurements per U46619 concentration for wild type were: 0.01μM=2, 0.03μM=2, 0.1μM=4, 0.3μM=4, 1μM=8, 3μM=7, 10μM=6, and for TRPC6^{-/-} were: 0.01μM=2, 0.03μM=2, 0.1μM=4, 0.3μM=4, 1μM=10, 3μM=10, 10μM=6. Error bars indicate SEM.

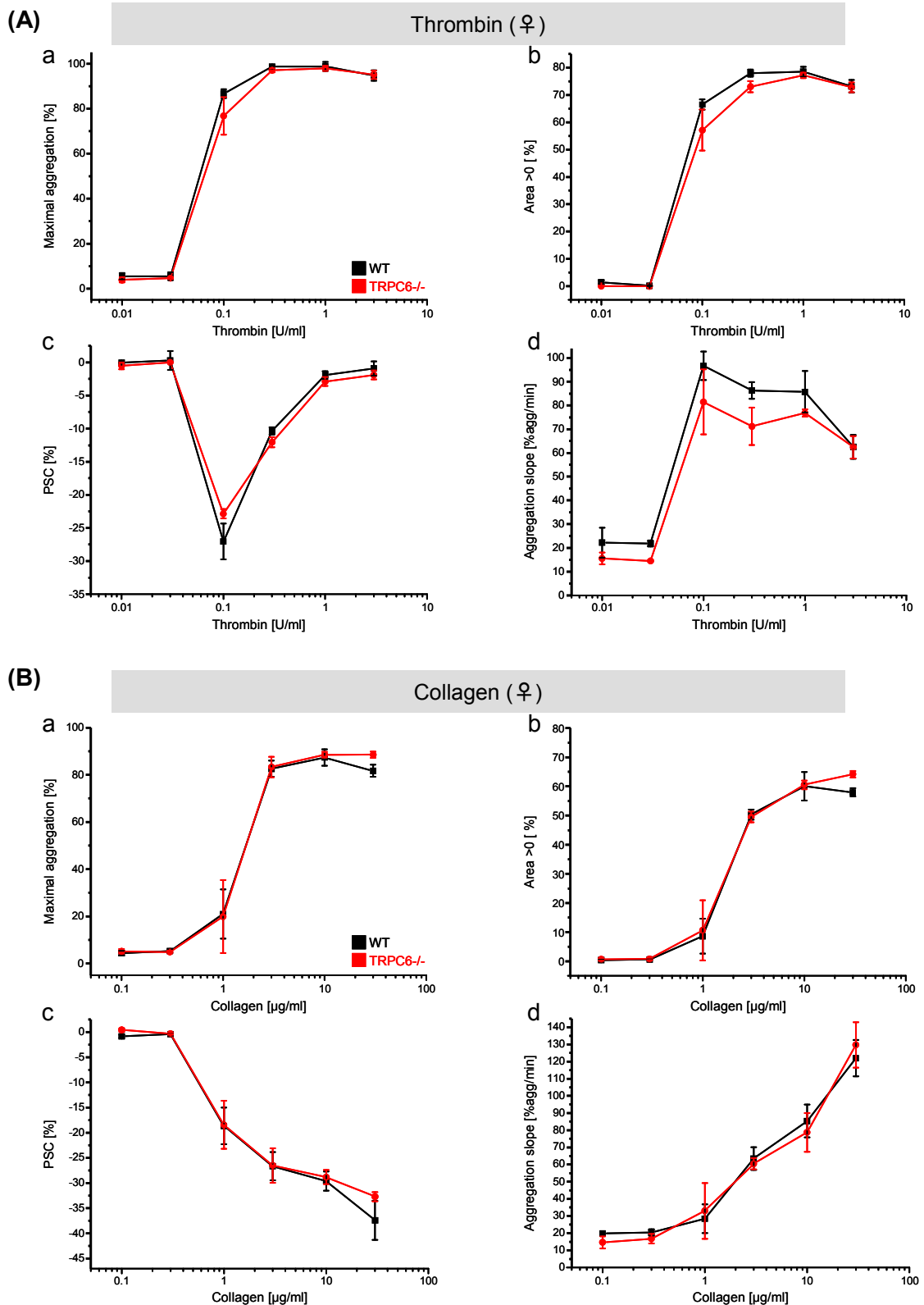
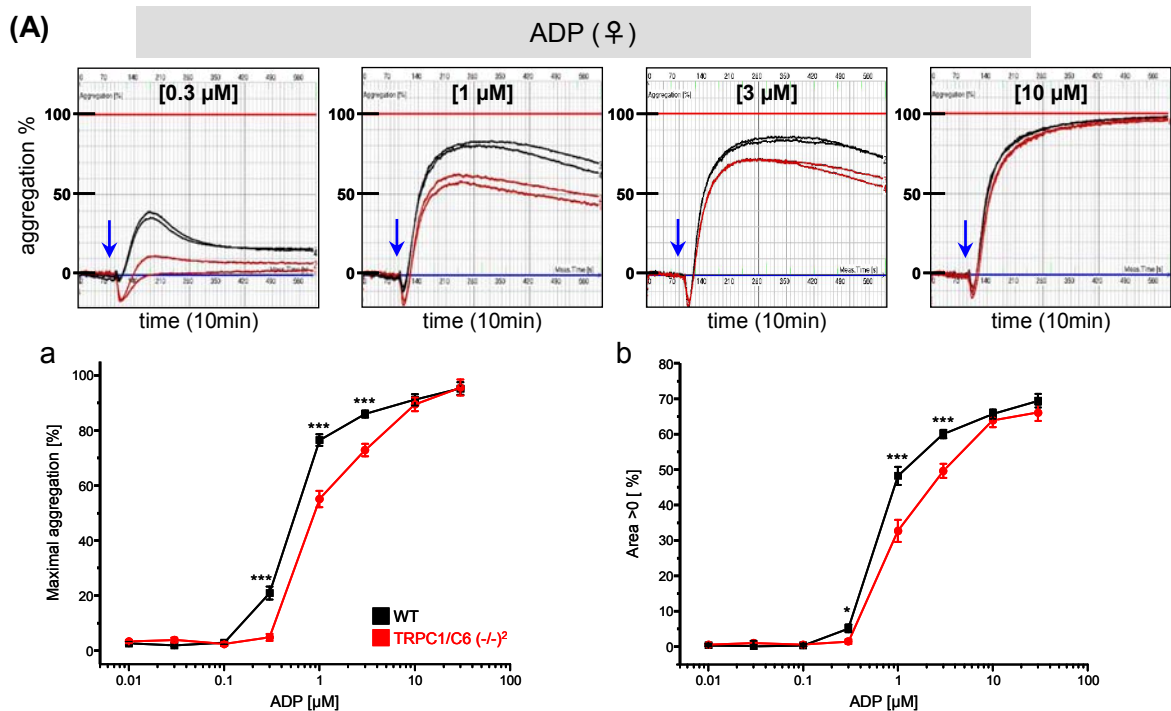


Figure 28. Thrombin- and collagen-induced platelet aggregation in washed platelets from wild type and TRPC6^{-/-} mice. Concentration-response curves from wild type (WT) and TRPC6^{-/-} platelets stimulated with: **(A)** thrombin or **(B)** collagen where maximal aggregation (**a**), area under the aggregation curve (**b**), platelet shape change (PSC, **c**) and maximal slope during aggregation (**d**) were analyzed. Numbers of measurements per thrombin concentration for wild type were: 0.01U/ml=2, 0.03U/ml=2, 0.1U/ml=5, 0.3U/ml=6, 1U/ml=4, 3U/ml=4, and for TRPC6^{-/-} were: 0.01U/ml=2, 0.03U/ml=2, 0.1U/ml=7, 0.3U/ml=6, 1U/ml=6, 3U/ml=7. Numbers of measurements per collagen concentration for wild type were: 0.1µg/ml=2, 0.3µg/ml=4, 1µg/ml=8, 3µg/ml=4, 10µg/ml=6, 30µg/ml=4, and for TRPC6^{-/-} were: 0.1µg/ml=5, 0.3µg/ml=7, 1µg/ml=6, 3µg/ml=4, 10µg/ml=6, 30µg/ml=4. Error bars indicate SEM.

5.2.4.2 Agonist-induced *in vitro* platelet aggregation in TRPC1/TRPC6^(-/-) platelets

In platelets from TRPC1/TRPC6^(-/-) female mice a right shift in ADP dose response of both the maximal aggregation and the area under the aggregation curve was observed (Figure 29, Aa-b). Also, ADP-induced aggregation was slower in TRPC1/TRPC6^(-/-) platelets as measured by the slope of the aggregation curve (Figure 29, Ad). No differences were observed in platelet shape change (Figure 29, Ac). Similar results were obtained in platelets from male mice. After 0.3µM ADP stimulation the maximal aggregation, the aggregation area, the slope of the aggregation curve, and also the PSC were significantly reduced in TRPC1/TRPC6^(-/-) platelets (Figure 29, B).



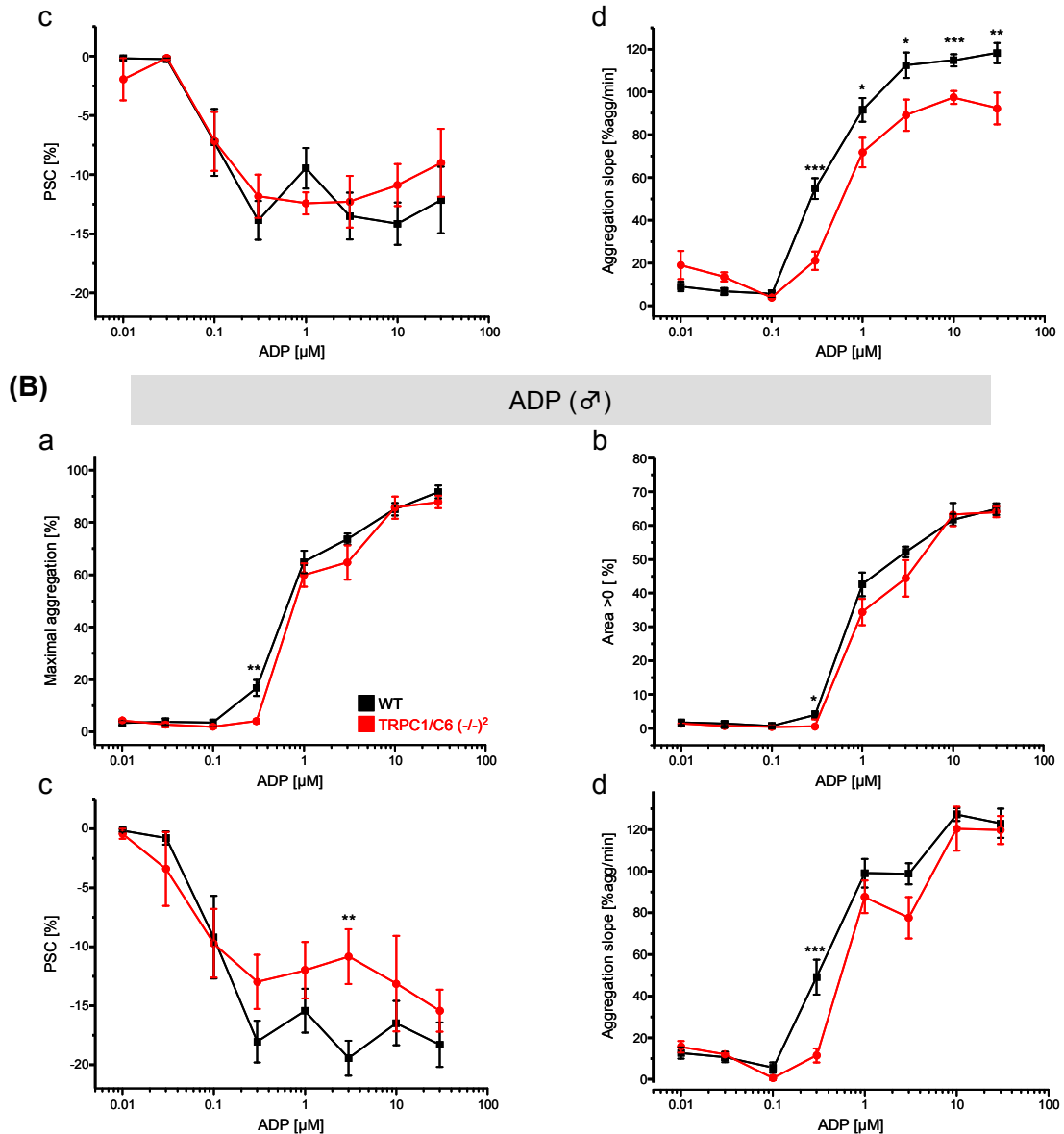
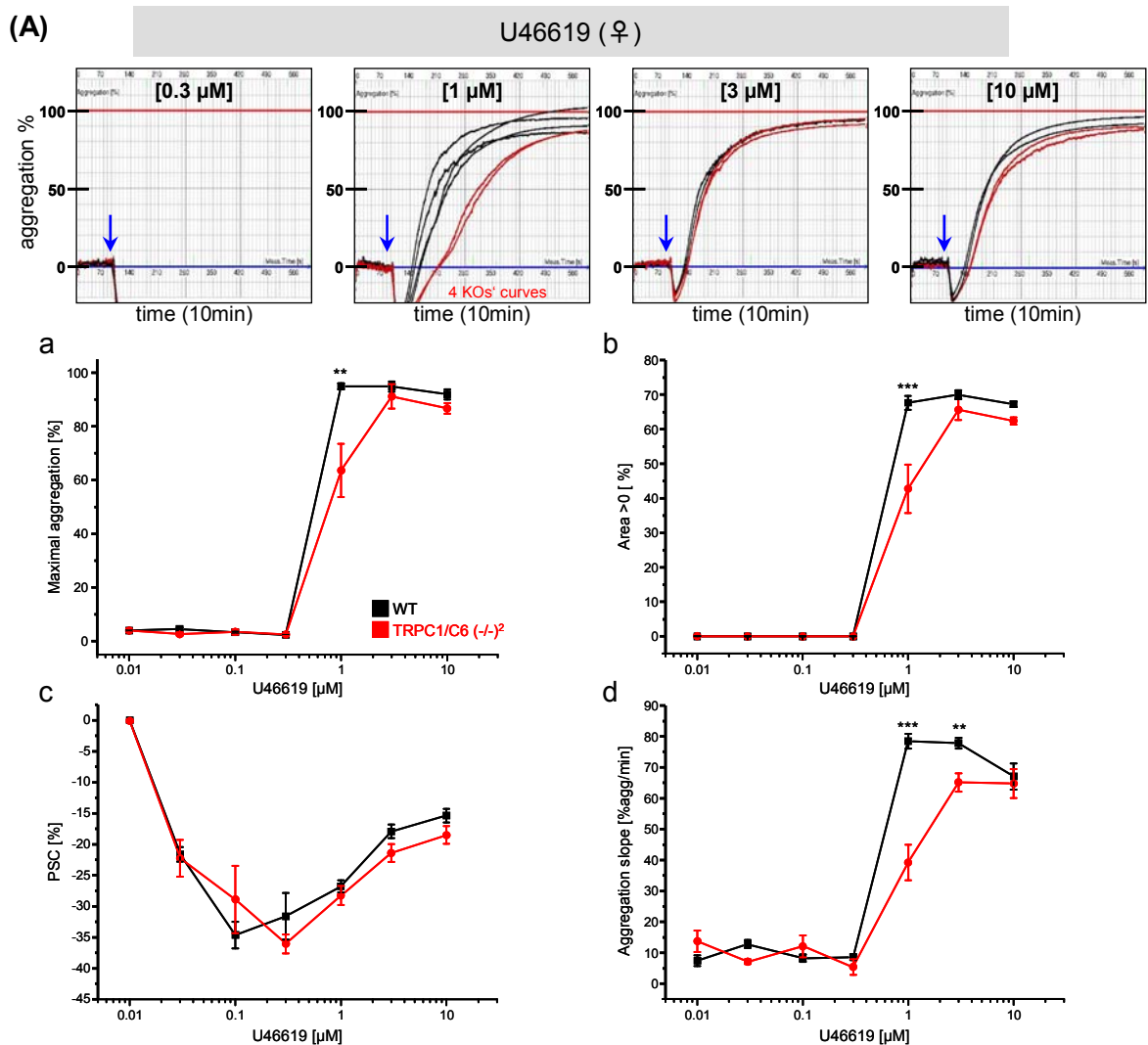


Figure 29. ADP-induced platelet aggregation in washed platelets from wild type and TRPC1/C6 (-/-)² mice. Platelet aggregation was compared between wild type and TRPC1/TRPC6 (-/-)² platelets from (A) female and (B) male mice. Representative original aggregation curves of ADP-induced aggregation in wild type and TRPC1/TRPC6 (-/-)² platelets where ADP application is indicated by an arrow (A, upper panels). Concentration-response curves where maximal aggregation (a), area under the aggregation curve (b), platelet shape change (PSC, c) and maximal slope during aggregation (d) were analyzed. Numbers of measurements per ADP concentration for wild type females were: 0.01μM=8, 0.03μM=9, 0.1μM=13, 0.3μM=23, 1μM=20, 3μM=15, 10μM=18, 30μM=11; for TRPC1/TRPC6 (-/-)² females were: 0.01μM=7, 0.03μM=9, 0.1μM=11, 0.3μM=16, 1μM=16, 3μM=12, 10μM=13, 30μM=9; for wild type males were: 0.01μM=5, 0.03μM=6, 0.1μM=9, 0.3μM=19, 1μM=22, 3μM=13, 10μM=9, 30μM=9; and for TRPC1/TRPC6 (-/-)² males were: 0.01μM=4, 0.03μM=4, 0.1μM=10, 0.3μM=14, 1μM=14, 3μM=12, 10μM=6, 30μM=11. Error bars indicate SEM. *p<0.05, **p<0.01 and ***p<0.001 according to the Student's t-test.

Induction of platelet aggregation with 1μM U46619 revealed a prominent reduction in platelets from TRPC1/TRPC6 (-/-)² mice of both genders. The maximal aggregation was significantly reduced by 33% in platelets from TRPC1/TRPC6 (-/-)² female mice by 31% in

males (Figure 30, Aa and Ba). The area under aggregation curve and the slope of the aggregation curve were also significantly reduced in platelets from TRPC1/TRPC6 $(-/-)^2$ mice at 1 μM U46619 (Figure 30, A and B). PSC was only different at 3 μM only in platelets from male mice (Figure 30, Ac and Bc).

Thrombin experiments with TRPC1/TRPC6 $(-/-)^2$ platelets from female or male mice showed no difference at any tested concentration in maximal aggregation, area under aggregation curve and PSC (Figure 31, Aa-c and Ba-c). Only the slope of the aggregation curve was significantly diminished at 0.1U/ml thrombin in platelets from with TRPC1/TRPC6 $(-/-)^2$ male mice, and it was reduced at three concentrations in platelets from with TRPC1/TRPC6 $(-/-)^2$ female mice (Figure 31, Ad and Bd).



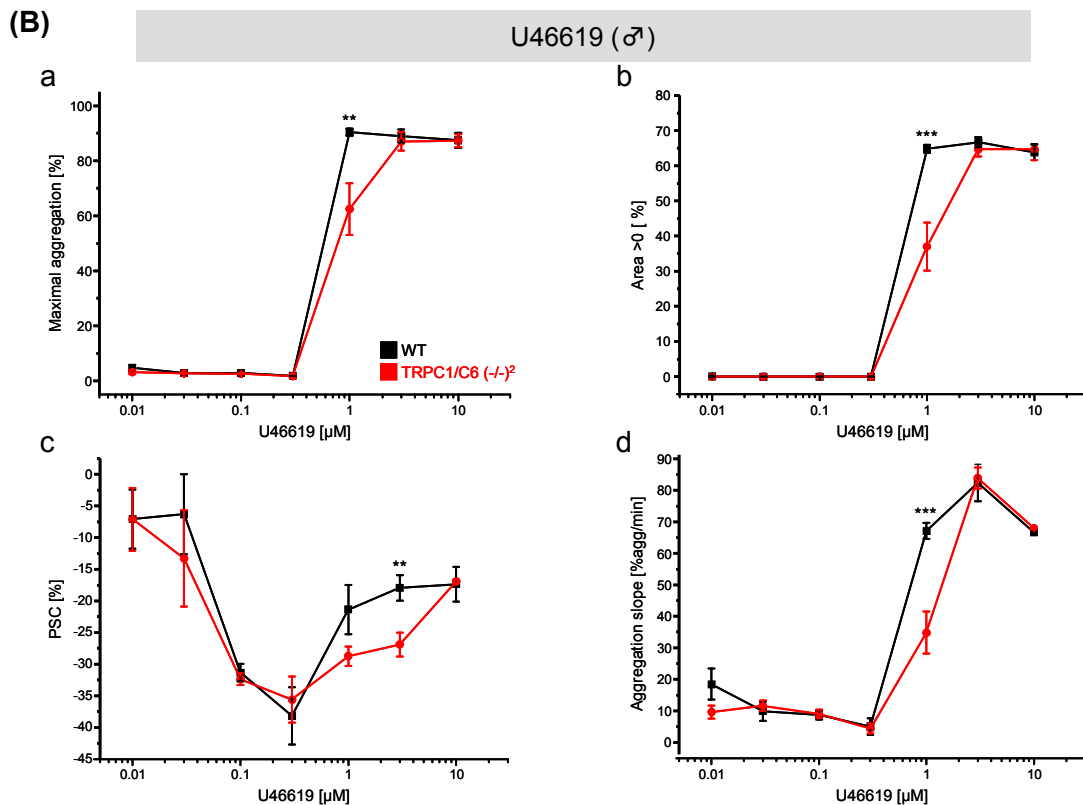


Figure 30. U46619-induced platelet aggregation in washed platelets from wild type and TRPC1/C6 (-/-)² mice. Platelet aggregation was compared between wild type and TRPC1/TRPC6 (-/-)² platelets from **(A)** female and **(B)** male mice. Representative original aggregation curves of U46619-induced aggregation in wild type and TRPC1/TRPC6 (-/-)² platelets where U46619 application is indicated by an arrow (**A**, upper panels). At 1 μ M U46619 not all four traces from TRPC1/TRPC6 deficient platelets are visible because there was no aggregation in some of them. Concentration-response curves where maximal aggregation **(a)**, area under the aggregation curve **(b)**, platelet shape change (PSC, **c**) and maximal slope during aggregation **(d)** were analyzed. Numbers of measurements per U46619 concentration for wild type females were: 0.01 μ M=4, 0.03 μ M=7, 0.1 μ M=8, 0.3 μ M=10, 1 μ M=22, 3 μ M=7, 10 μ M=6; for TRPC1/TRPC6 (-/-)² females were: 0.01 μ M=4, 0.03 μ M=6, 0.1 μ M=6, 0.3 μ M=6, 1 μ M=17, 3 μ M=6, 10 μ M=6; for wild type males were: 0.01 μ M=6, 0.03 μ M=4, 0.1 μ M=4, 0.3 μ M=4, 1 μ M=18, 3 μ M=8, 10 μ M=4; and for TRPC1/TRPC6 (-/-)² males were: 0.01 μ M=4, 0.03 μ M=4, 0.1 μ M=4, 0.3 μ M=4, 1 μ M=15, 3 μ M=7, 10 μ M=4. Error bars indicate SEM. **p<0.01 and ***p<0.001 according to the Student's t-test.

Collagen-induced platelet aggregation evaluated by maximum aggregation, area under aggregation curve, PSC and aggregation curve slope was unchanged in platelets from TRPC1/TRPC6 deficient mice (Figure 32).

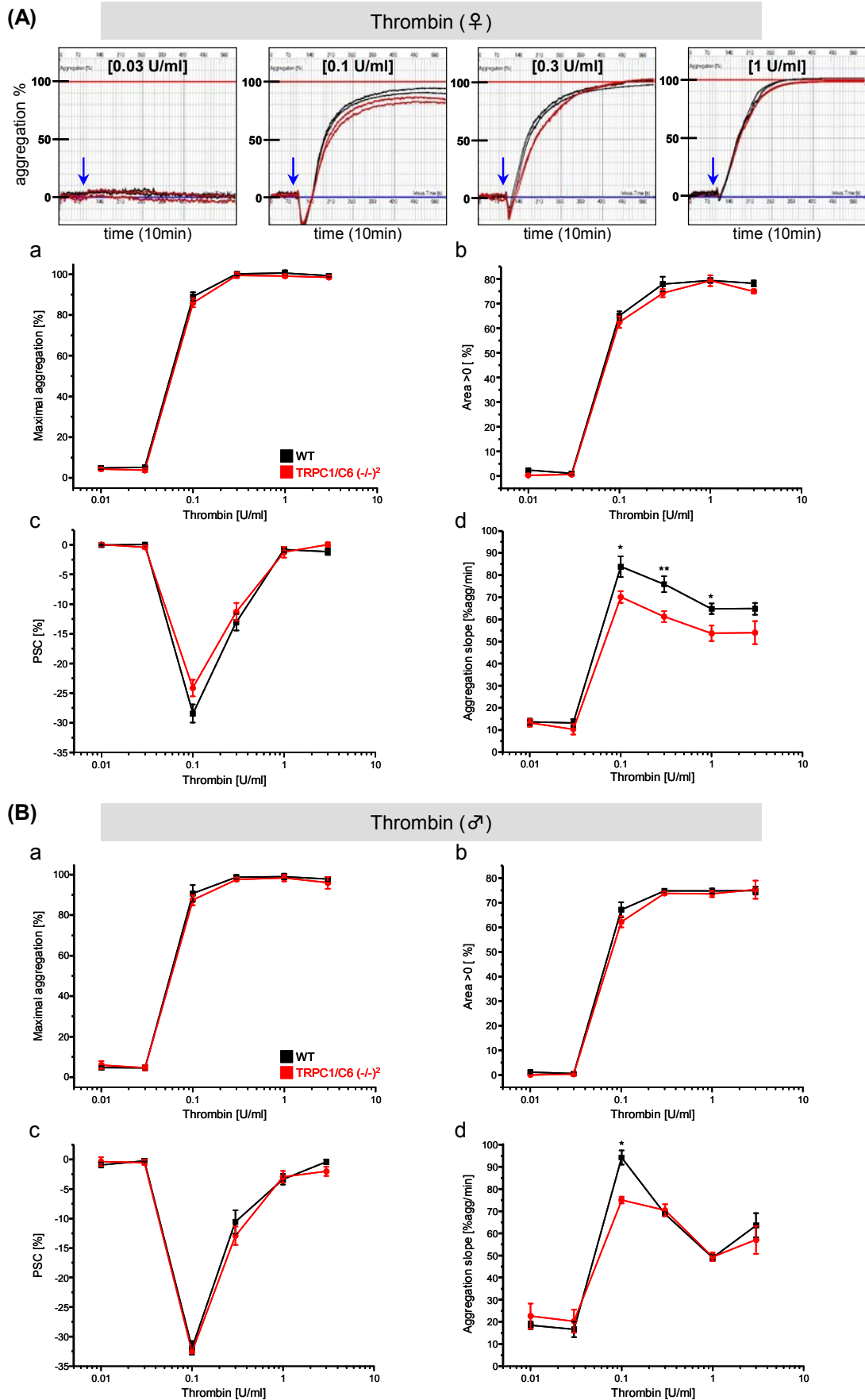
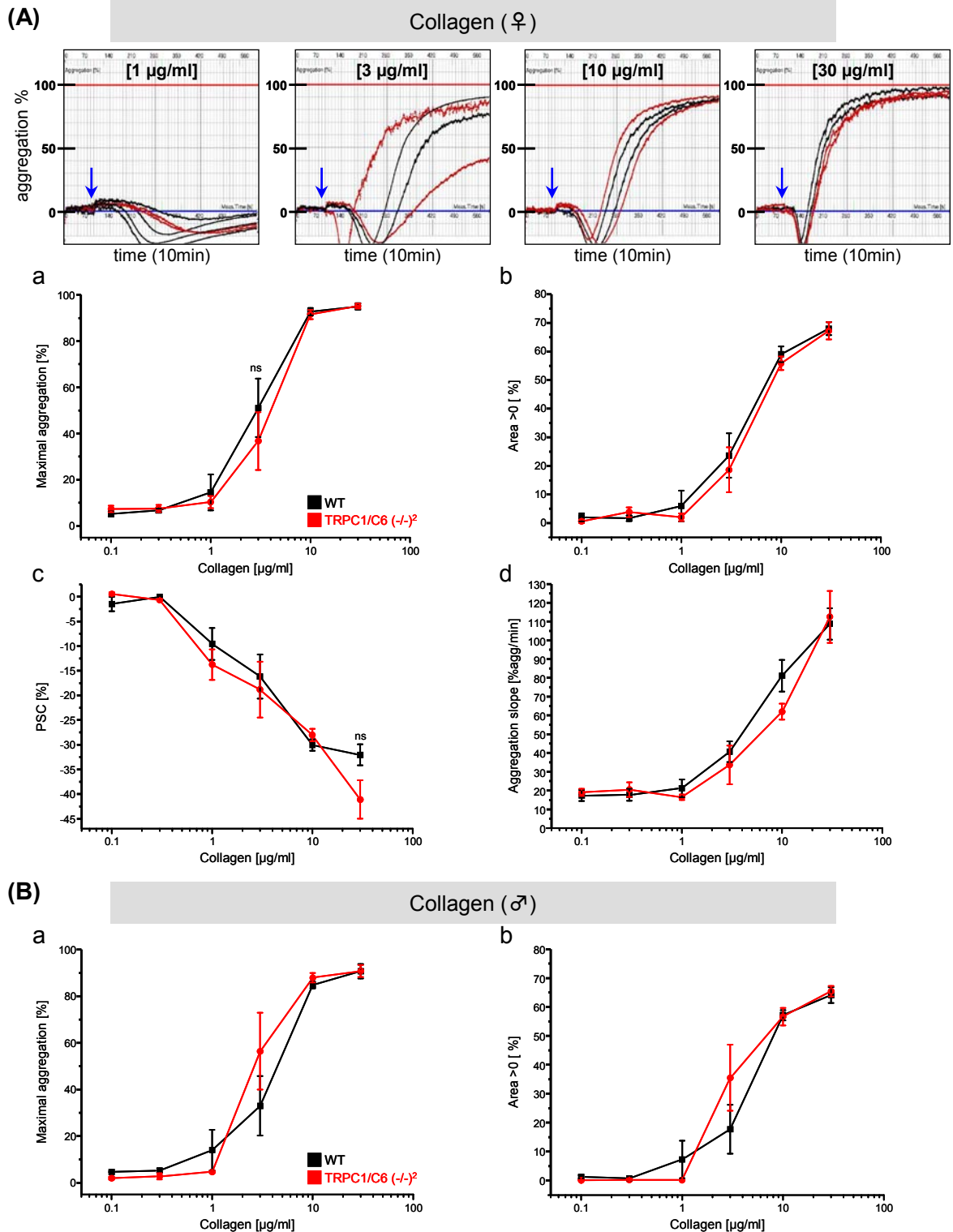


Figure 31. Thrombin-induced platelet aggregation in washed platelets from wild type and TRPC1/C6 (-/-)² mice. Platelet aggregation was compared between wild type and TRPC1/TRPC6 (-/-)² platelets from (A) female and (B) male mice. Representative original aggregation curves of thrombin-induced aggregation in wild type and TRPC1/TRPC6 (-/-)² platelets where thrombin

application is indicated by an arrow (**A**, upper panels). Concentration-response curves where maximal aggregation (**a**), area under the aggregation curve (**b**), platelet shape change (PSC, **c**) and maximal slope during aggregation (**d**) were analyzed. Numbers of measurements per thrombin concentration for wild type females were: 0.01U/ml=9, 0.03U/ml=6, 0.1U/ml=12, 0.3U/ml=6, 1U/ml=7, 3U/ml=9; for TRPC1/TRPC6 $(-/-)^2$ females were: 0.01U/ml=6, 0.03U/ml=6, 0.1U/ml=10, 0.3U/ml=6, 1U/ml=6, 3U/ml=8; for wild type males were: 0.01U/ml=4, 0.03U/ml=5, 0.1U/ml=3, 0.3U/ml=6, 1U/ml=4, 3U/ml=6; and for TRPC1/TRPC6 $(-/-)^2$ males were: 0.01U/ml=4, 0.03U/ml=4, 0.1U/ml=2, 0.3U/ml=4, 1U/ml=5, 3U/ml=5. Error bars indicate SEM. * $p < 0.05$ and ** $p < 0.01$ according to the Student's t-test.



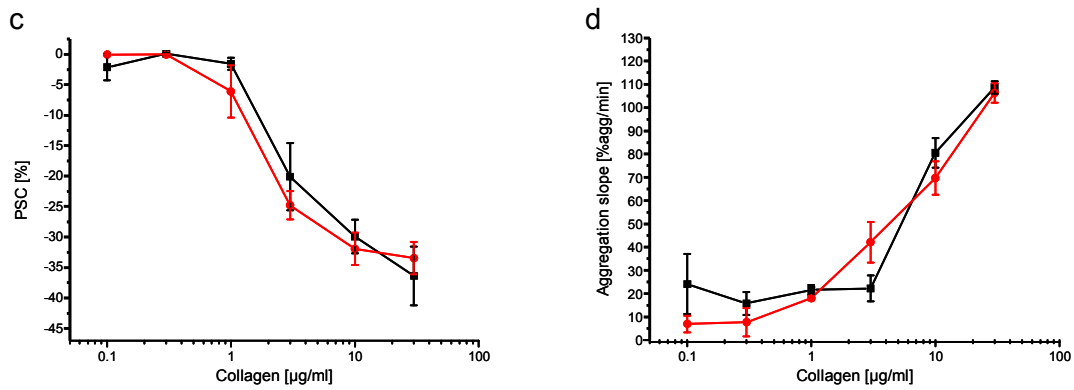


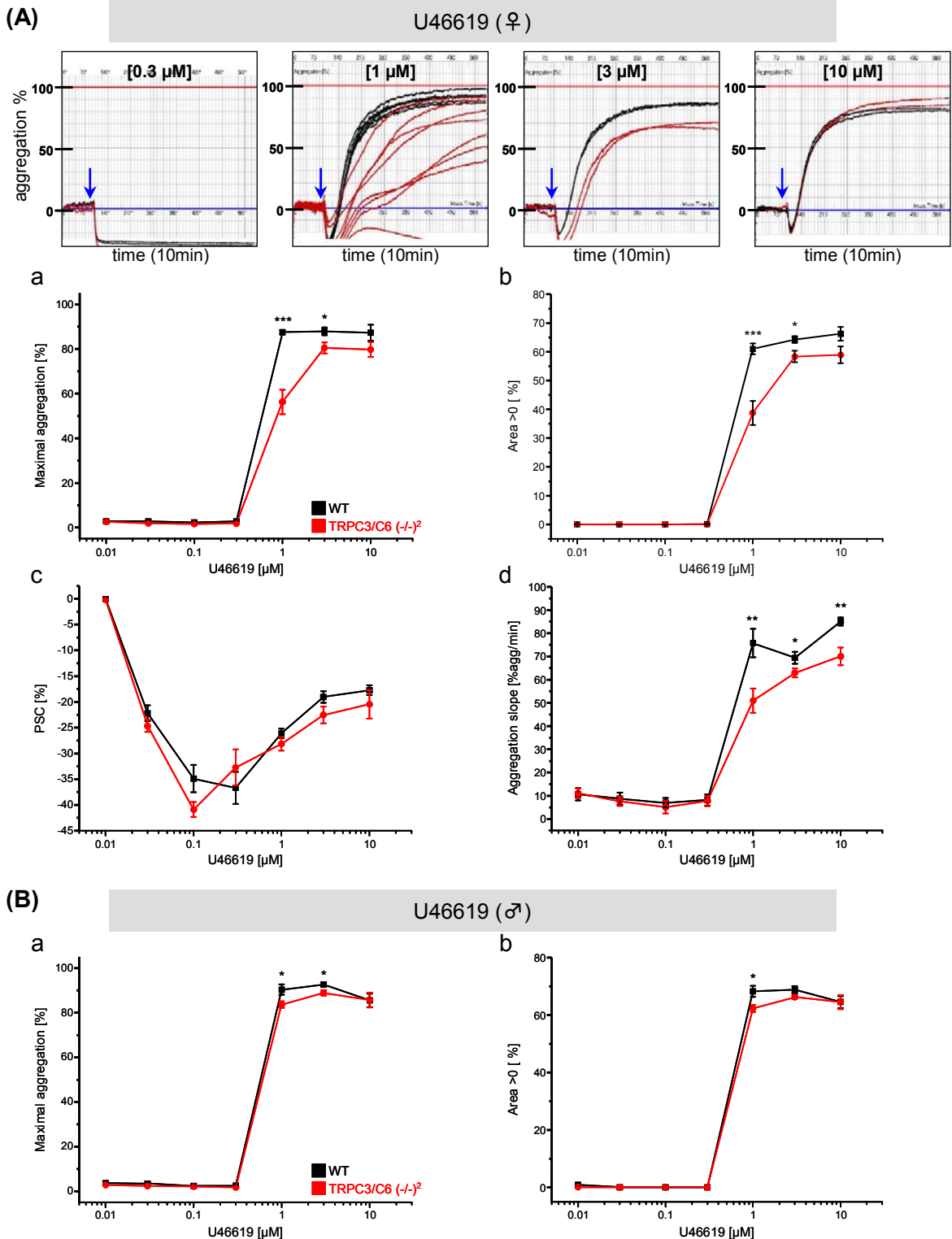
Figure 32. Collagen-induced platelet aggregation in washed platelets from wild type and TRPC1/TRPC6 (-/-)² mice. Platelet aggregation was compared between wild type and TRPC1/TRPC6 (-/-)² platelets from (A) female and (B) male mice. Representative original aggregation curves of collagen-induced aggregation in wild type and TRPC1/TRPC6 (-/-)² platelets where collagen application is indicated by an arrow (A, upper panels). Concentration-response curves where maximal aggregation (a), area under the aggregation curve (b), platelet shape change (PSC, c) and maximal slope during aggregation (d) were analyzed. Numbers of measurements per collagen concentration for wild type females were: 0.1 µg/ml=4, 0.3 µg/ml=6, 1 µg/ml=11, 3 µg/ml=11, 10 µg/ml=9, 30 µg/ml=8; for TRPC1/TRPC6 (-/-)² females were: 0.1 µg/ml=4, 0.3 µg/ml=6, 1 µg/ml=10, 3 µg/ml=8, 10 µg/ml=9, 30 µg/ml=8; for wild type males were: 0.1 µg/ml=2, 0.3 µg/ml=2, 1 µg/ml=6, 3 µg/ml=8, 10 µg/ml=8, 30 µg/ml=4; and for TRPC1/TRPC6 (-/-)² males were: 0.1 µg/ml=3, 0.3 µg/ml=3, 1 µg/ml=4, 3 µg/ml=6, 10 µg/ml=6, 30 µg/ml=4. Error bars indicate SEM. ns (not significant) according to the Student's t-test.

5.2.4.3 Agonist-induced *in vitro* platelet aggregation in TRPC3/TRPC6 (-/-)² platelets

The analysis of platelets from TRPC3/TRPC6 (-/-)² mice was of particular interest because it has been reported that TRPC3 expression is upregulated in TRPC6^{-/-} mice which leads to a functional compensation of that of TRPC6 proteins (Dietrich et al., 2005). ADP-induced platelet aggregation response was diminished in platelets from TRPC3/TRPC6 deficient female and male mice. Analysis of maximal aggregation, area under the aggregation curve and slope of the aggregation curve showed a right shift in the dose-responses from TRPC3/TRPC6 (-/-)² platelets and the differences were significant for several ADP doses (Figure 33). Also, PSC was significantly reduced in platelets from TRPC3/TRPC6 (-/-)² mice at various ADP concentrations (Figure 33, Ac and Bc).

U46619-induced platelet aggregation in platelets from TRPC3/TRPC6 (-/-)² mice was also impaired. At a concentration of 1 µM U46619 maximal aggregation was significantly reduced by 36% and 7% in platelets from female and male TRPC3/TRPC6 (-/-)² mice, respectively, and a significant reduction was also observed at 3 µM U46619 (Figure 34, Aa and Ba). The aggregation area and the slope of the aggregation curve were also reduced in platelets from TRPC3/TRPC6 (-/-)² female mice (Figure 34, A).

indicated by an arrow (A, upper panels). Concentration-response curves where maximal aggregation (a), area under the aggregation curve (b), platelet shape change (PSC, c) and maximal slope during aggregation (d) were analyzed. Numbers of measurements per ADP concentration for wild type females were: 0.01 μ M=8, 0.03 μ M=8, 0.1 μ M=8, 0.3 μ M=16, 1 μ M=23, 3 μ M=12, 10 μ M=11, 30 μ M=10; for TRPC3/TRPC6 (-/-)² females were: 0.01 μ M=6, 0.03 μ M=6, 0.1 μ M=8, 0.3 μ M=18, 1 μ M=25, 3 μ M=12, 10 μ M=10, 30 μ M=9; for wild type males were: 0.01 μ M=7, 0.03 μ M=8, 0.1 μ M=11, 0.3 μ M=13, 1 μ M=15, 3 μ M=10, 10 μ M=12, 30 μ M=13; and for TRPC3/TRPC6 (-/-)² males were: 0.01 μ M=7, 0.03 μ M=7, 0.1 μ M=10, 0.3 μ M=13, 1 μ M=15, 3 μ M=10, 10 μ M=10, 30 μ M=11. Error bars indicate SEM. *p<0.05, **p<0.01, ***p<0.001 and ns (significant) according to the Student's t-test.



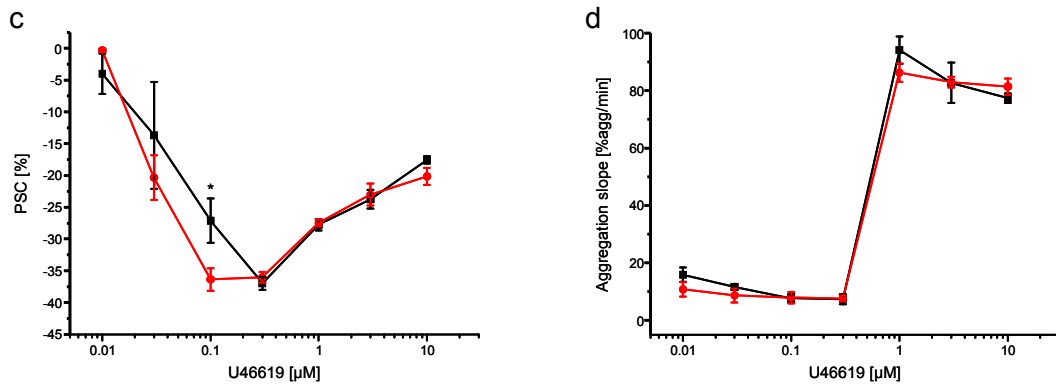


Figure 34. U46619-induced platelet aggregation in washed platelets from wild type and TRPC3/TRPC6 (-/-)² mice. Platelet aggregation was compared between wild type and TRPC3/TRPC6 (-/-)² platelets from (A) female and (B) male mice. Representative original aggregation curves of U46619-induced aggregation in wild type and TRPC3/TRPC6 (-/-)² platelets where U46619 application is indicated by an arrow (A, upper panels). Concentration-response curves where maximal aggregation (a), area under the aggregation curve (b), platelet shape change (PSC, c) and maximal slope during aggregation (d) were analyzed. Numbers of measurements per U46619 concentration for wild type females were: 0.01µM=8, 0.03µM=7, 0.1µM=7, 0.3µM=7, 1µM=29, 3µM=9, 10µM=6; for TRPC3/TRPC6 (-/-)² females were: 0.01µM=7, 0.03µM=7, 0.1µM=6, 0.3µM=6, 1µM=38, 3µM=11, 10µM=6; for wild type males were: 0.01µM=4, 0.03µM=4, 0.1µM=6, 0.3µM=6, 1µM=14, 3µM=6, 10µM=6; and for TRPC3/TRPC6(-/-)² males were: 0.01µM=4, 0.03µM=4, 0.1µM=6, 0.3µM=6, 1µM=13, 3µM=6, 10µM=6, Error bars indicate SEM. *p<0.05, **p<0.01 and ***p<0.001 according to the Student's t-test.

The maximal aggregation induced by thrombin was diminished by ~34% in TRPC3/TRPC6 (-/-)² platelets at a concentration of 0.1U/ml thrombin (Figure 35, Aa and Ba). In platelets from TRPC3/TRPC6 (-/-)² female mice the aggregation area at 0.1U/ml thrombin and the slope of the aggregation curve at several thrombin concentrations were significantly reduced (Figure 35, A). Similar results were seen in platelets from male mice (see Table 7B). PSC was not different between genotypes (Figure 35, Ac and Bb). The difference observed in thrombin aggregation was reduced when apyrase concentration was increased ten fold. Apyrase hydrolyses ATP and ADP into AMP; therefore part of the difference in thrombin aggregation could be explained as an impaired ADP-induced aggregation produced by the secreted ADP during thrombin stimulation (Figure 35, Ba and Bc).

Collagen-induced platelet aggregation was not essentially impaired in TRPC3/TRPC6 deficient platelets of females (Figure 36, A) and males (Figure 36, B).

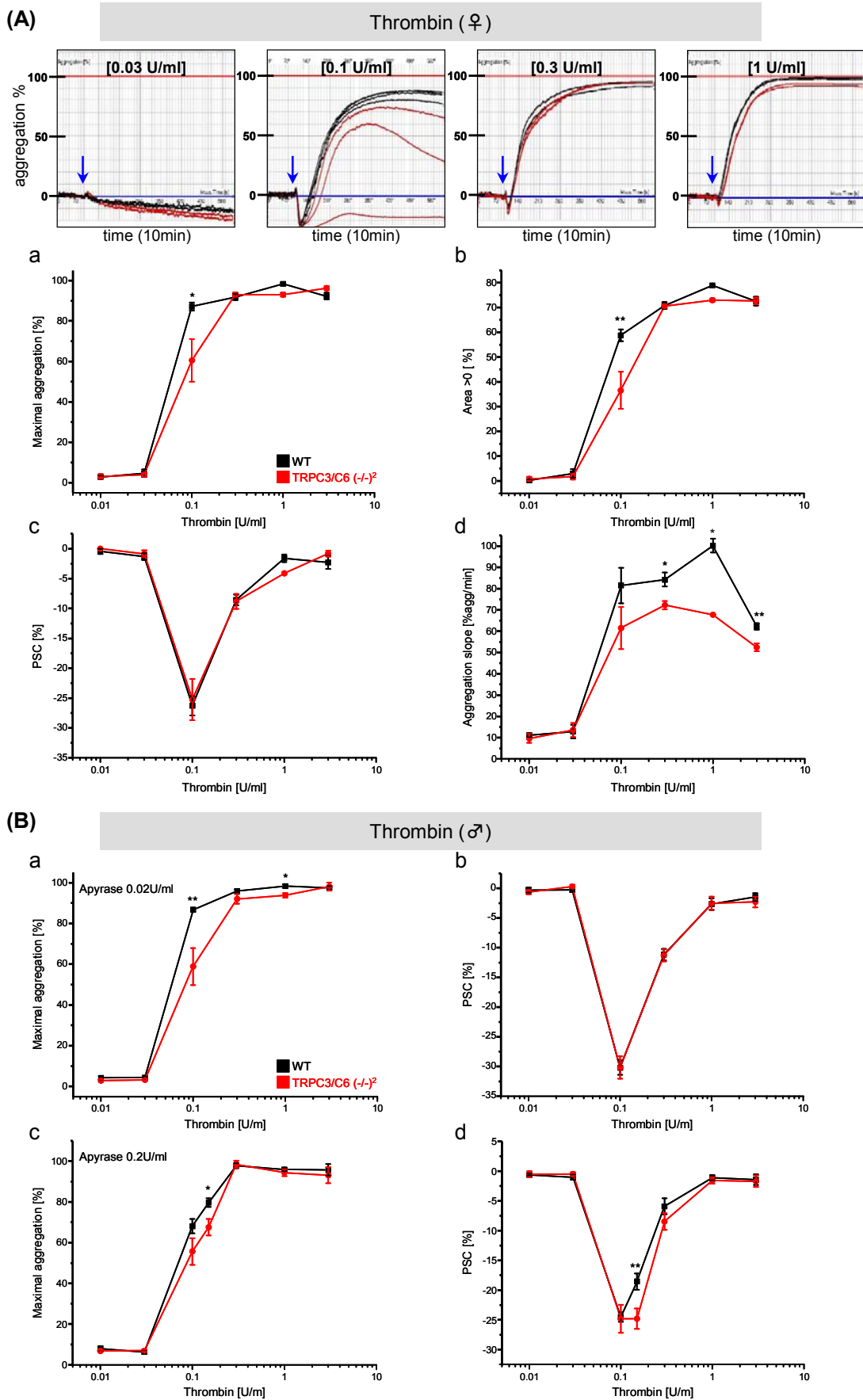
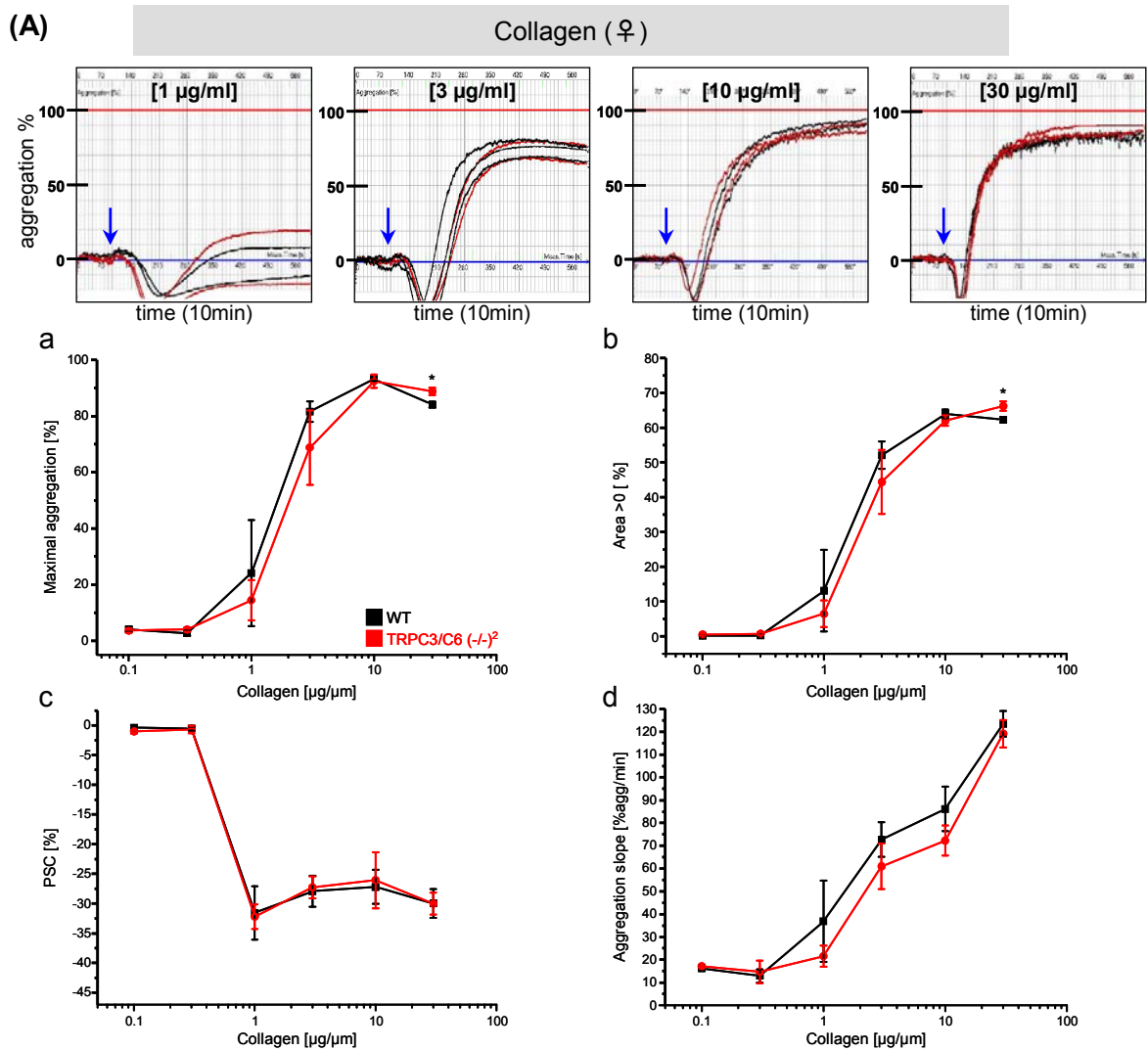


Figure 35. Thrombin-induced platelet aggregation in washed platelets from wild type and TRPC3/C6 (-/-)² mice. Platelet aggregation was compared between wild type and TRPC3/TRPC6 (-/-)² platelets from **(A)** female and **(B)** male mice. Representative original aggregation curves of

thrombin-induced aggregation in wild type and TRPC3/TRPC6 $(-/-)^2$ platelets where thrombin application is indicated by an arrow (**A**, upper panels). In **A** concentration-response curves where maximal aggregation (**a**), area under the aggregation curve (**b**), platelet shape change (PSC, **c**) and maximal slope during aggregation (**d**) were analyzed. In **B** are shown maximal aggregation (**a** and **c**) and PSC (**b** and **d**) for experiments in the presence of 0.02U/ml (upper panels) or 0.2U/ml (lower panels) apyrase. Numbers of measurements per thrombin concentration for wild type females were: 0.01U/ml=4, 0.03U/ml=4, 0.1U/ml=12, 0.3U/ml=4, 1U/ml=2, 3U/ml=4; for TRPC3/TRPC6 $(-/-)^2$ females were: 0.01U/ml=5, 0.03U/ml=4, 0.1U/ml=9, 0.3U/ml=4, 1U/ml=2, 3U/ml=4; for wild type males (**a** and **b**) were: 0.01U/ml=5, 0.03U/ml=5, 0.1U/ml=12, 0.3U/ml=6, 1U/ml=6, 3U/ml=9; for TRPC3/TRPC6 $(-/-)^2$ males (**a** and **b**) were: 0.01U/ml=4, 0.03U/ml=4, 0.1U/ml=12, 0.3U/ml=6, 1U/ml=6, 3U/ml=7; for wild type males (**c** and **d**) were: 0.01U/ml=6, 0.03U/ml=6, 0.1U/ml=12, 0.15U/ml=15, 0.3U/ml=10, 1U/ml=10, 3U/ml=8; and for TRPC3/TRPC6 $(-/-)^2$ males (**c** and **d**) were: 0.01U/ml=5, 0.03U/ml=6, 0.1U/ml=14, 0.15U/ml=12, 0.3U/ml=11, 1U/ml=10, 3U/ml=7. Error bars indicate SEM. * $p < 0.05$ and ** $p < 0.01$ according to the Student's t-test.



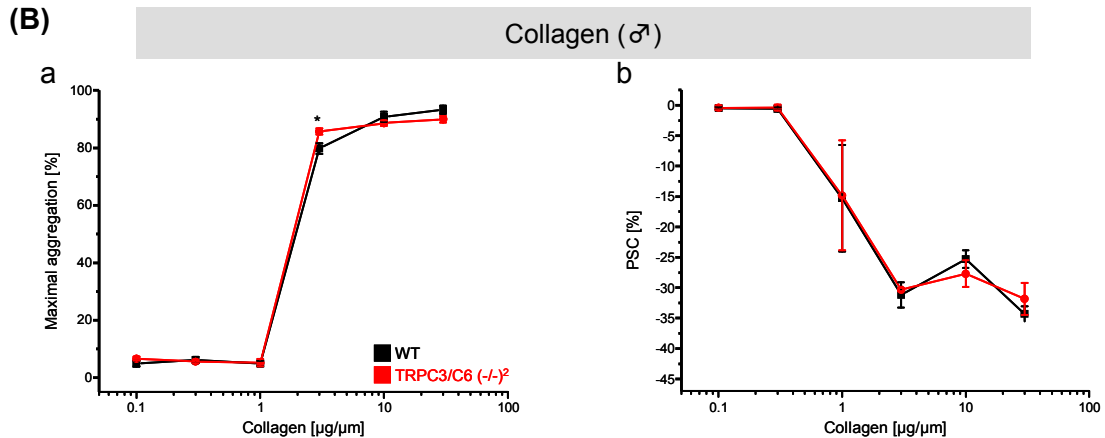


Figure 36. Collagen-induced platelet aggregation in washed platelets from wild type and TRPC3/C6 (-/-)² mice. Platelet aggregation was compared between wild type and TRPC3/TRPC6 (-/-)² platelets from (A) female and (B) male mice. Representative original aggregation curves of collagen-induced aggregation in wild type and TRPC3/TRPC6 (-/-)² platelets where collagen application is indicated by an arrow (A, upper panels). In A concentration-response curves where maximal aggregation (a), area under the aggregation curve (b), platelet shape change (PSC, c) and maximal slope during aggregation (d) were analyzed. Numbers of measurements per collagen concentration for wild type females were: 0.1µg/ml=2, 0.3µg/ml=4, 1µg/ml=4, 3µg/ml=8, 10µg/ml=6, 30µg/ml=4; for TRPC3/TRPC6 (-/-)² females were: 0.1µg/ml=2, 0.3µg/ml=4, 1µg/ml=4, 3µg/ml=6, 10µg/ml=5, 30µg/ml=4; for wild type males (a and b) were: 0.1µg/ml=4, 0.3µg/ml=4, 1µg/ml=4, 3µg/ml=4, 10µg/ml=4, 30µg/ml=7; for TRPC3/TRPC6(-/-)² males (a and b) were: 0.1µg/ml=4, 0.3µg/ml=4, 1µg/ml=4, 3µg/ml=4, 10µg/ml=6, 30µg/ml=7; for wild type males (c and d) were: 0.1µg/ml=4, 0.3µg/ml=2, 1µg/ml=4, 3µg/ml=12, 10µg/ml=11, 30µg/ml=8; and for TRPC3/TRPC6(-/-)² males (c and d) were: 0.1µg/ml=1, 0.3µg/ml=2, 1µg/ml=5, 3µg/ml=9, 10µg/ml=7, 30µg/ml=6. Error bars indicate SEM. *p<0.05 according to the Student's t-test.

5.2.4.4 Comparison of ADP-induced *in vitro* platelet aggregation in TRPC1/TRPC6 and TRPC3/TRPC6 deficient platelets

In figures 37 and 38 the ADP-induced aggregation responses from TRPC1/TRPC6 (-/-)² and TRPC3/TRPC6 (-/-)² mice was a mixed background are compared. In this comparison the results from wild type mice used as control for both genotypes were pooled.

Female mice. Platelets from females from both mouse lines had similar maximal aggregation responses, but reduced in comparison to wild type platelets after stimulation with ADP in a concentration range from 0.3µM to 3µM for both genotypes, and up to 30µM for TRPC3/TRPC6 (-/-)² platelets. The percentual reduction of maximal aggregation were between 7 to 76% depending on the dose (Figure 37, A). The slope of the aggregation area was not different between platelets from TRPC1/TRPC6 and TRPC3/TRPC6 deficient female mice, but it was significantly reduced when compared to wild type mice in a broad range of ADP concentrations (Figure 37, D). In contrast, the reduction in the

aggregation area was more prominent in platelets from TRPC3/TRPC6 (-/-)² female mice than in platelets from TRPC1/TRPC6 (-/-)² females, for example at 1 μ M ADP where the reduction was 57% and 22%, respectively (Figure 37, B).

Male mice. In platelets from TRPC1/TRPC6 (-/-)² and TRPC3/TRPC6 (-/-)² male mice the reduction in the aggregation response was also observed (Figure 38), but it was less prominent than in platelets from females. Maximal aggregation, area under aggregation curve and slope of the aggregation curve were significantly reduced in TRPC1/TRPC6 and TRPC3/TRPC6 deficient platelets at various ADP concentrations (Figure 38, A,B and D). PSC was significantly reduced only in TRPC3/TRPC6 (-/-)² platelets.

TRPC1/TRPC3/TRPC6 (-/-)³ mice. TRPC1/TRPC3/TRPC6 (-/-)³ mice were also fertile and show no obvious sign of disease. These mice were produced specially to assess whether the deletion of TRPC1, TRPC3 and TRPC6 together would produce more prominent differences than those observed in platelets from TRPC1/TRPC6 (-/-)² and TRPC3/TRPC6 (-/-)² mice. After stimulation with various collagen or thrombin concentrations no difference in aggregation was observed in platelets from TRPC1/TRPC3/TRPC6 (-/-)³ mice. In contrast, the ADP response, as well as the response to 1 μ M U46619 were reduced (Table 6B). However, the ADP- and U46619-induced aggregation responses in platelets from TRPC1/TRPC3/TRPC6 (-/-)³ mice were around the same extent as those in TRPC1/TRPC6 (-/-)² and TRPC3/TRPC6 (-/-)² mice.

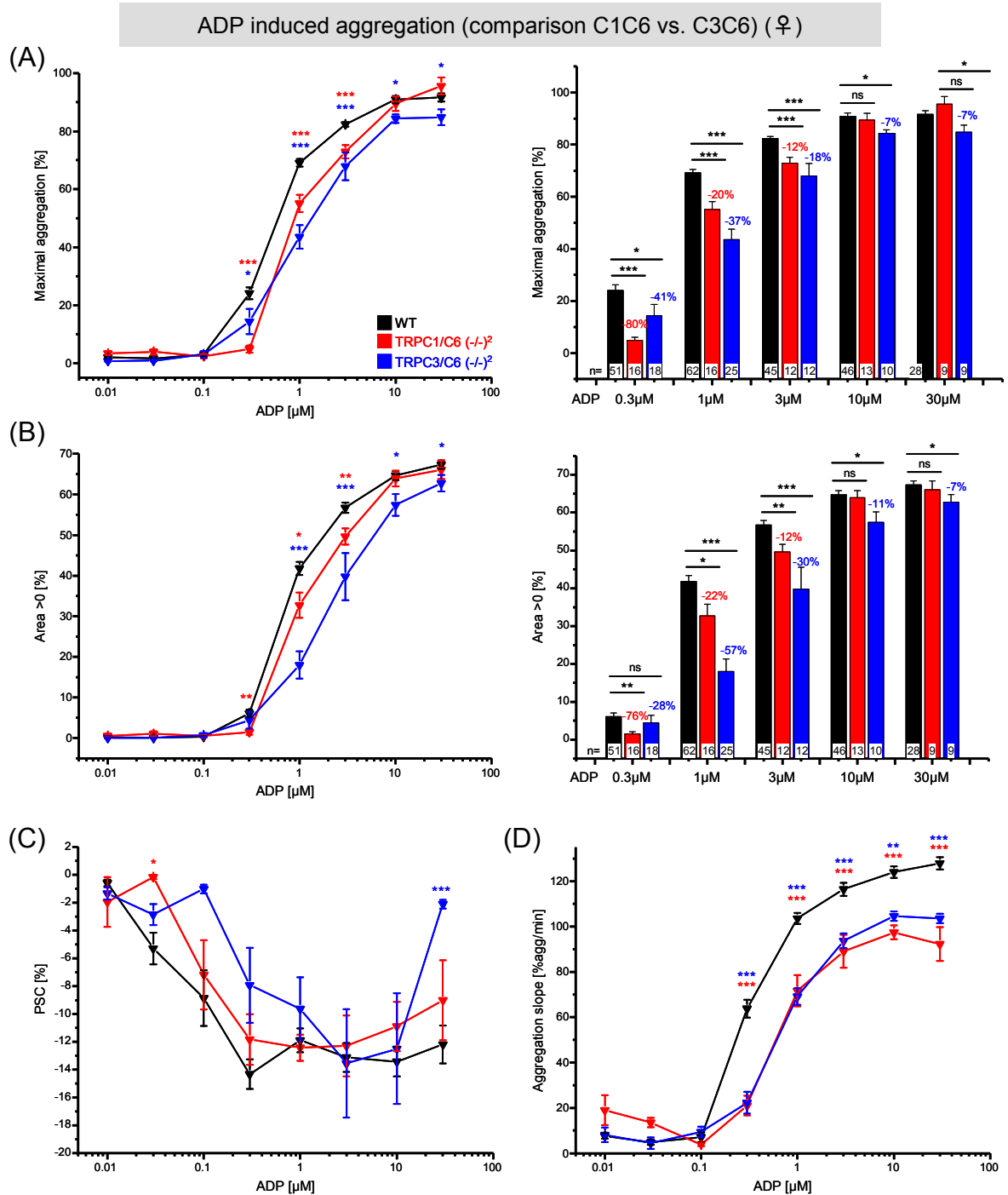


Figure 37. Comparison of ADP-induced platelet aggregation in TRPC1/C6 $(-/-)^2$ and TRPC3/C6 $(-/-)^2$ platelets from female mice. Concentration-response curves where (A) maximal aggregation, (B) area under the aggregation curve, (C) platelet shape change (PSC) and (D) maximal slope during aggregation were analyzed. Bar graphs from the maximal aggregation (A, right) and from the area under the aggregation curve (B, right) include the percentage of reduction in comparison with the wild type response. Numbers of measurements per ADP concentration for wild type mice were: 0.01 μM =22, 0.03 μM =24, 0.1 μM =31, 0.3 μM =51, 1 μM =62, 3 μM =45, 10 μM =46, 30 μM =28; for TRPC1/TRPC6 $(-/-)^2$ mice were: 0.01 μM =7, 0.03 μM =9, 0.1 μM =11, 0.3 μM =16, 1 μM =16, 3 μM =12, 10 μM =13, 30 μM =9; and for TRPC3/TRPC6 $(-/-)^2$ mice were: 0.01 μM =6, 0.03 μM =6, 0.1 μM =8, 0.3 μM =18, 1 μM =25, 3 μM =12, 10 μM =10, 30 μM =9. Error bars indicate SEM. * $p < 0.05$, ** $p < 0.01$, *** $p < 0.001$ and ns (not significant) according to the Student's t-test from comparisons against WT values.

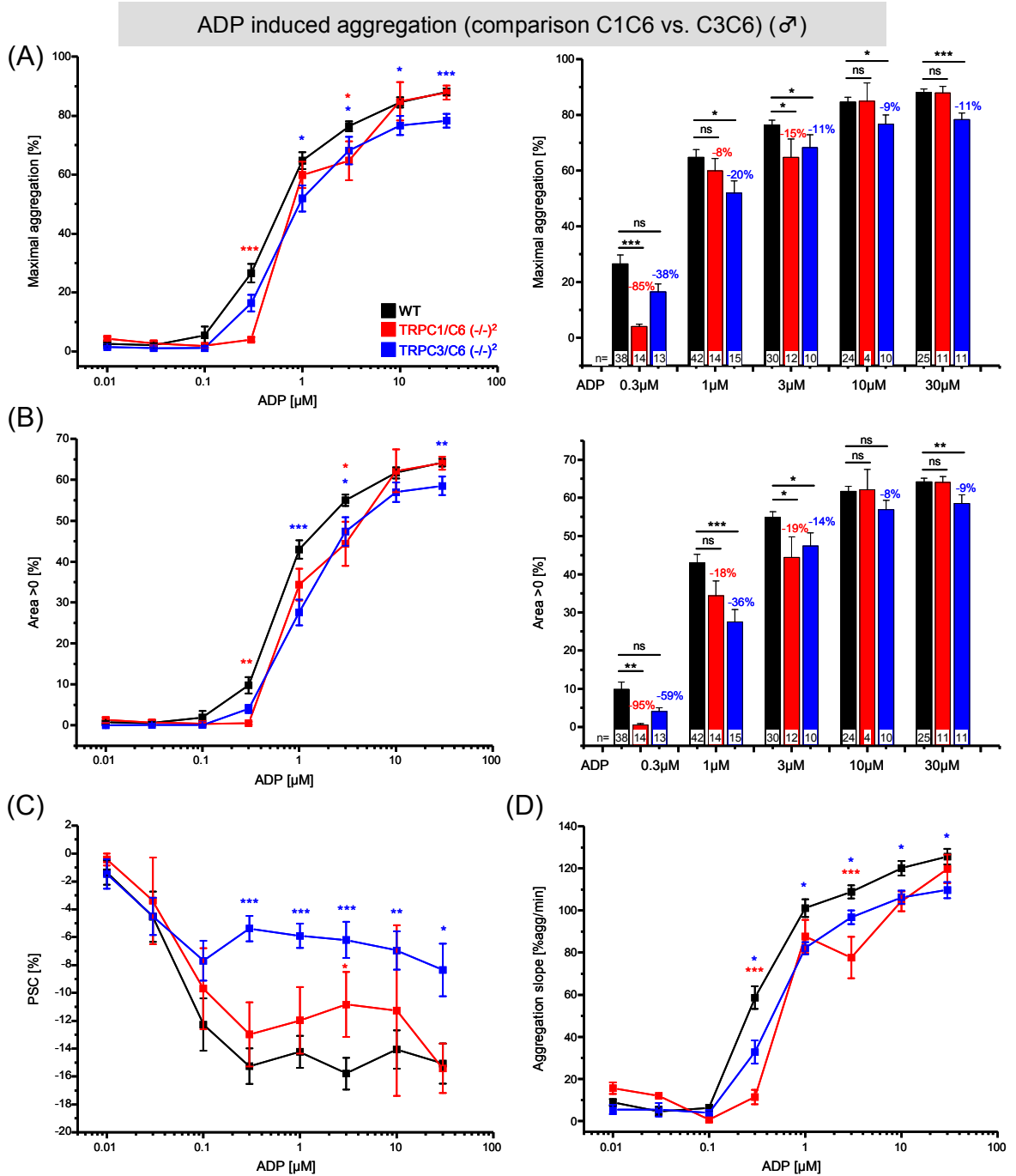


Figure 38. Comparison of ADP-induced platelet aggregation in TRPC1/C6 (-/-)² and TRPC3/C6 (-/-)² platelets from male mice. Concentration-response curves where (A) maximal aggregation, (B) area under the aggregation curve, (C) platelet shape change (PSC) and (D) maximal slope during aggregation were analyzed. Bar graphs from the maximal aggregation (A, right) and from the area under the aggregation curve (B, right) include the percentage of reduction in comparison with the wild type response. Numbers of measurements per ADP concentration for wild type mice were: 0.01 μM =12, 0.03 μM =14, 0.1 μM =26, 0.3 μM =38, 1 μM =42, 3 μM =30, 10 μM =24, 30 μM =25; for TRPC1/TRPC6 (-/-)² mice were: 0.01 μM =4, 0.03 μM =4, 0.1 μM =10, 0.3 μM =14, 1 μM =14, 3 μM =12, 10 μM =4, 30 μM =11; and for TRPC3/TRPC6 (-/-)² mice were: 0.01 μM =7, 0.03 μM =7, 0.1 μM =10, 0.3 μM =13, 1 μM =15, 3 μM =10, 10 μM =10, 30 μM =11. Error bars indicate SEM. * p <0.05, ** p <0.01, *** p <0.001 and ns (not significant) according to the Student's t-test from comparisons against WT values.

5.2.5 *In vitro* aggregation in platelets from Clopidogrel pre-treated mice

ADP activates in mouse platelets two differently coupled receptors, P2Y₁ and P2Y₁₂ receptors coupled to G_{α_q} and G_{α_i} proteins, respectively. To distinguish between the ADP-induced responses mediated by these receptors I did experiments with platelets from mice pre-treated with Clopidogrel (5mg/kg/day, orally over 2 days). Clopidogrel is a pro-drug and its active metabolite is an irreversible P2Y₁₂ antagonist. With its use we evaluated the ADP pathway leading to activation of the P2Y₁-G_{α_q}-PLC pathway which leads to elevation of intracellular Ca²⁺ concentration in platelets and might involve TRPC channels.

5.2.5.1 Effect of Clopidogrel in aggregation of platelets from wild type mice

Before performing comparative analysis between wild type and knockout mice using Clopidogrel, I compared the *in vitro* aggregation in platelets isolated from wild type female mice treated with vehicle solution or Clopidogrel. Platelets from vehicle pre-treated mice aggregated normally after ADP stimulation (Figure 39); therefore the vehicle control could be omitted in further experiments. ADP-induced aggregation in platelets from Clopidogrel treated mice was significantly reduced in a broad range of ADP concentrations (Figure 39) and the maximal aggregation was reduced between 67% up to 97%. Clopidogrel also reduced maximal aggregation induced by 10µg/ml collagen or by 1µM U46619, in 22% (89 ± 2 % vs. 70 ± 8%; n=3-5) and 21% (85 ± 3% vs. 67 ± 8%; n=3-5), respectively, indicating that TxA₂- and collagen-induced aggregation are partially mediated by ADP release.

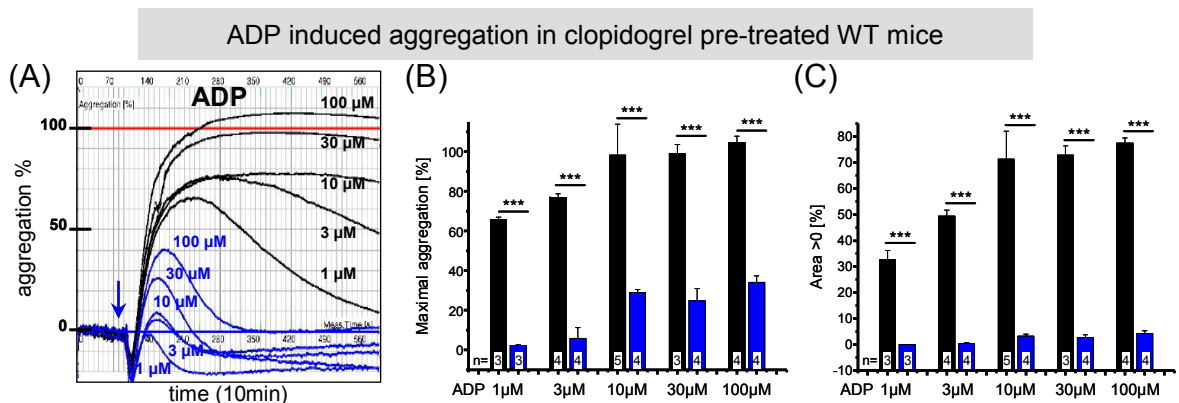


Figure 39. ADP-induced aggregation in platelets from Clopidogrel pre-treated wild type female mice. ADP-induced platelet aggregation was compared between platelets from wild type mice pre-treated either with vehicle (in black) or with Clopidogrel (in blue). **(A)** Original traces of platelet aggregation where ADP application is indicated by an arrow. Statistical analysis from **(B)** maximal aggregation and **(C)** area under the aggregation curve. Mice (n=5) received Clopidogrel orally at a dose of 5mg/kg/day over 2 days. n=number of aggregation curves. Error bars indicate SEM. ***p<0.001 according to the Student's t-test.

5.2.5.2 Aggregation in TRPC1/TRPC6 (-/-)² and TRPC3/TRPC6 (-/-)² platelets from Clopidogrel pre-treated mice

The differences in ADP-induced platelet aggregation in both TRPC1/TRPC6 (-/-)² and TRPC3/TRPC6 (-/-)² female mice became much more prominent in mice that received Clopidogrel (Figures 40) compared to untreated mice (Figures 37 and 38). A similar result was obtained when ADP-induced aggregation from TRPC3/TRPC6 (-/-)² male mice treated with Clopidogrel (Figure 41) or untreated (Figure 33B) was compared.

Female mice. In comparison to wild type platelets the maximal aggregation was reduced between 34% to 82% in TRPC1/TRPC6 deficient platelets, and reduced between 44% and 78% in TRPC3/TRPC6 deficient platelets (Figure 40, A). The aggregation area after ADP stimulation was reduced between 60% to 98% in TRPC1/TRPC6 (-/-)², and between 72% to 100% in TRPC3/TRPC6 (-/-)² platelets (Figure 40, B). Comparisons of maximal aggregation only between TRPC1/TRPC6 (-/-)² and TRPC3/TRPC6 (-/-)² platelets revealed a significant ($p < 0.05$) difference at 30 μ M ADP. Similar differences were observed in area under the aggregation curve (Figure 40, A and B). PSC was only changed at 0.3 μ M ADP in TRPC1/TRPC6 deficient platelets (Figure 40, C). Maximal aggregation slope was reduced in platelets from both TRPC deficient platelet groups to similar extent contrasted with wild type (Figure 40, D).

Male mice. Platelets from TRPC3/TRPC6 (-/-)² Clopidogrel pre-treated male mice presented a robust impaired *in vitro* aggregation for a wide range of ADP concentrations (0.3 μ M-100 μ M). Results from two pooled independent series showed that platelets from TRPC3/TRPC6 (-/-)² male mice presented significantly reduced maximal aggregation, reduced area under the aggregation curve and reduced slope of the aggregation curve (Figure 41, A, B and D). In these experiments no differences were detected in PSC between wild type and TRPC3/TRPC6 deficient platelets (Figure 41, C).

In addition to ADP I tested other agonists that induce ADP release with platelets from mice treated with Clopidogrel. U46619-induced platelet aggregation was impaired in TRPC1/TRPC6 (-/-)² and TRPC3/TRPC6 (-/-)² platelets not only at 1 μ M U46619, as already observed (Figures 30 and 34), but additionally at 3 μ M in TRPC3/TRPC6 (-/-)² platelets (Table 8). This implies that the reduced U46619-induced aggregation in TRPC3/TRPC6 (-/-)² mice is at least in part due to changes in ADP-induced aggregation response.

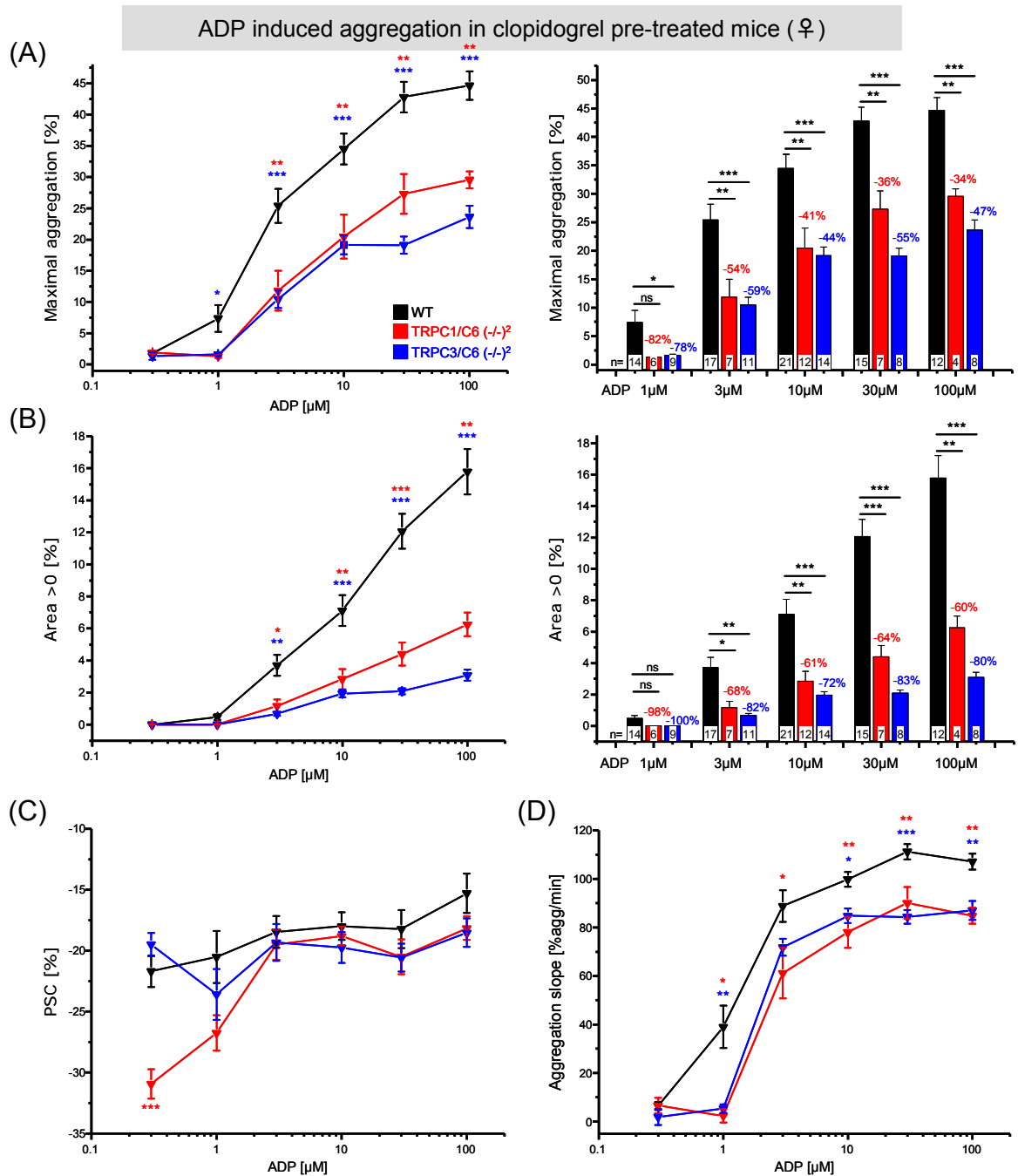


Figure 40. Platelet aggregation in washed platelets from Clopidogrel pre-treated TRPC1/C6 and TRPC3/C6 deficient female mice. ADP concentration-response curves where (A) maximal aggregation, (B) area under the aggregation curve, (C) platelet shape change (PSC) and (D) maximal slope during aggregation were analyzed. Bar graphs from the maximal aggregation (A, right) and from the area under the aggregation curve (B, right) for selected ADP concentrations include the percentage of reduction in comparison with the wild type response. Numbers of measurements per ADP concentration for wild type mice were: 0.3 μ M=10, 1 μ M=14, 3 μ M=17, 10 μ M=21, 30 μ M=15, 100 μ M=12; for TRPC1/TRPC6 (-/-)² mice were: 0.3 μ M=6, 1 μ M=6, 3 μ M=7, 10 μ M=12, 30 μ M=7, 100 μ M=4; and for TRPC3/TRPC6 (-/-)² mice were: 0.3 μ M=5, 1 μ M=9, 3 μ M=11, 10 μ M=14, 30 μ M=8, 100 μ M=8. Error bars indicate SEM. * <0.05, **<0.01 and ***p<0.001 according to the Student's t-test. Mice received Clopidogrel orally in a dose of 5mg/kg/day over 2 days. Data pooled from two independent series.

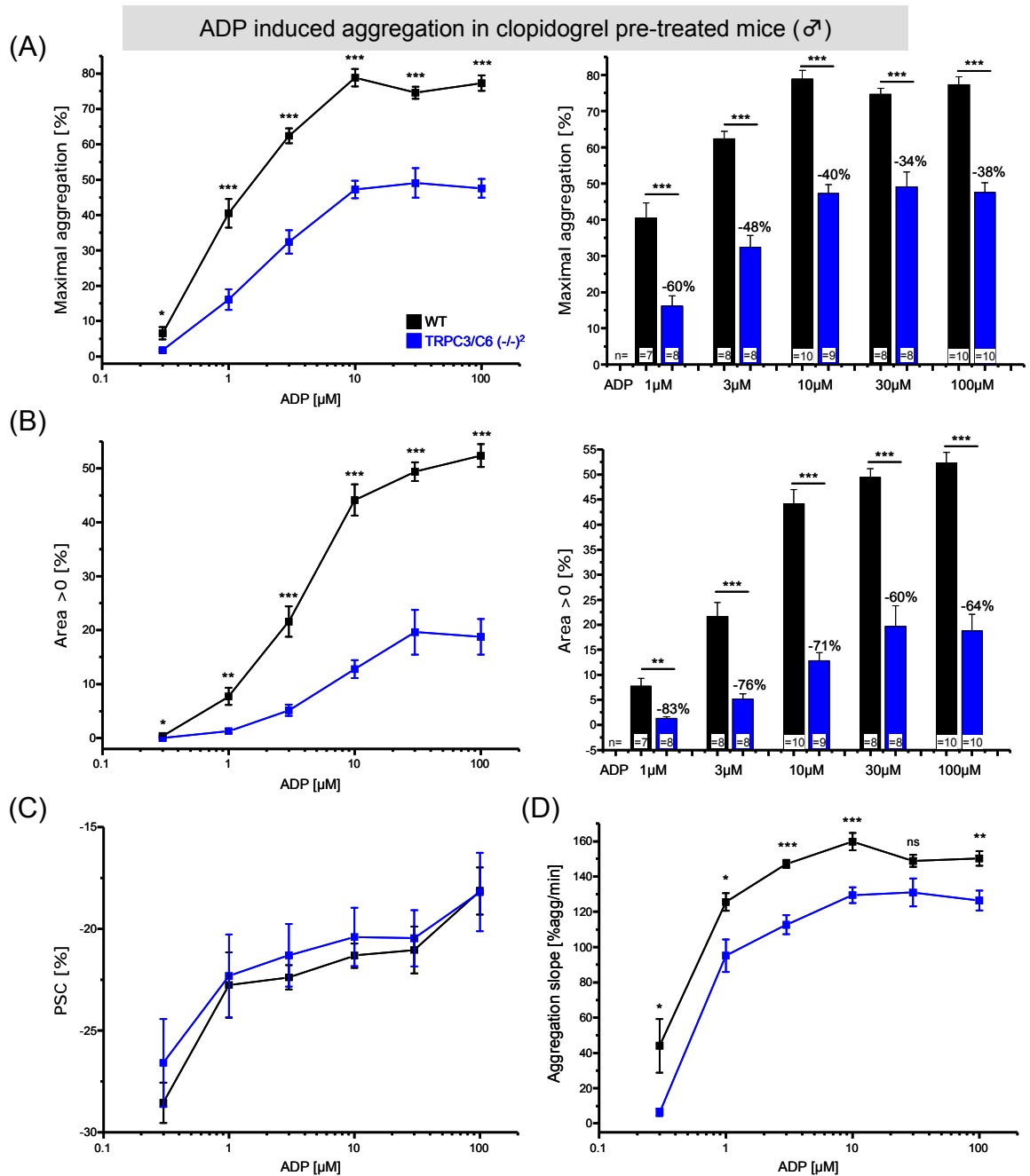


Figure 41. Platelet aggregation in washed platelets from Clopidogrel pre-treated TRPC3/C6 deficient male mice. ADP concentration-response curves where (A) maximal aggregation, (B) area under the aggregation curve, (C) platelet shape change (PSC) and (D) maximal slope during aggregation were analyzed. Bar graphs from the maximal aggregation (A, right) and from the area under the aggregation curve (B, right) for selected ADP concentrations include the percentage of reduction in comparison with the wild type response. Numbers of measurements per ADP concentration for wild type mice were: 0.3 μM =9, 1 μM =7, 3 μM =8, 10 μM =10, 30 μM =8, 100 μM =10; and for TRPC3/TRPC6 $(-/-)^2$ mice were: 0.3 μM =9, 1 μM =8, 3 μM =8, 10 μM =9, 30 μM =8, 100 μM =10. Error bars indicate SEM. * < 0.05, ** < 0.01, *** p < 0.001 and ns (not significant) according to the Student's t-test. Mice received Clopidogrel orally in a dose of 5mg/kg/day over 2 days. Data pooled from two independent series.

After stimulation with thrombin (0.1U/ml) no differences were observed in platelets from TRPC3/TRPC6 (-/-)² female mice. However, in platelet from TRPC3/TRPC6 deficient male mice the thrombin response was significantly reduced (Table 8), but not in a higher extent than in platelets from TRPC3/TRPC6 (-/-)² mice that did not received Clopidogrel (Figure 35). No differences in maximal aggregation were observed after 0.3U/ml thrombin in any group of Clopidogrel pre-treated mice (Table 8).

Platelet aggregation induced by 10µg/ml collagen was reduced in similar extent in platelets from wild type, TRPC1/TRPC6 (-/-)² and TRPC3/TRPC6 (-/-)² female mice. In males wild type and TRPC3/TRPC6 (-/-)² male mice no reduction in collagen-induced aggregation was observed by Clopidogrel treatment (Table 8). These observations suggest that the efficacy of the inhibitory action of Clopidogrel on aggregation is lower in male mice or that higher doses are required in males.

Table 8. Platelet aggregation in washed platelets from Clopidogrel pre-treated TRPC1/C6 and TRPC3/C6 deficient mice.

	U46619 [1µM]		U46619 [3µM]		Thrombin [0.1U/ml]		Thrombin [0.3U/ml]		Collagen [10µg/ml]	
	Max. agg. [%]	n=	Max. agg. [%]	n=	Max. agg. [%]	n=	Max. agg. [%]	n=	Max. agg. [%]	n=
Females										
Wild type	13.4 ± 13	11	71.2 ± 9.5	10	27.6 ± 22		92.7 ± 4.0	8	53.6 ± 35	11
TRPC1/TRPC6 (-/-) ²	2.7 ± 1.9 *	9	62.3 ± 0.3	4	—		95.1 ± 3.8	4	55.6 ± 21	5
TRPC3/TRPC6 (-/-) ²	2.4 ± 1.1	4	49.2 ± 13 ***	8	22.3 ± 17		94.2 ± 3.4	5	53.8 ± 34	4
Males										
Wild type	86.1 ± 7.2	10	91.3 ± 6.3	6	89.6 ± 16	9	99.3 ± 11	6	92.1 ± 2.9	4
TRPC3/TRPC6 (-/-) ²	2.11 ± 1.2***	8	78.9 ± 5.6*	4	59.7 ± 9.3**	4	96.8 ± 3.0	4	94.9 ± 2.6	3

Values of maximal platelet aggregation (Max. agg.) after stimulation with different agonist are presented. Mice received Clopidogrel orally in a dose of 5mg/kg/day over 2 days. Error (±) indicates SD. Number of experiments (n=) are indicated. *p<0.05, **p<0.01 and ***p<0.001 according to the Student's t-test against the corresponding wild type control.

6. Discussion

6.1 Role of TRPC-channels in cardiac hypertrophy: Analysis of TRPC-deficient mice

To analyze whether TRPC proteins are causally involved in the development of cardiac hypertrophy induced by neurohumoral mechanisms that contribute to comparable pathologies in humans I established in our group a protocol for isoproterenol- and ATII-induced cardiac hypertrophy. This protocol allowed us to have a reproducible hypertrophy induction in TRPC-deficient mouse lines and the corresponding wild type controls of a mixed 129SvJ/C57Bl6 genetic background.

Iso and ATII-induced cardiac hypertrophy protocols produced different cardiac and systemic effects in wild type mice. With our protocol Iso and ATII infusion produced in wild type mice a significant increment of heart weight. In terms of HW/BW the ATII-3 dose produced the higher values, followed by Iso-30 and ATII-0.3. In terms of HW/TL Iso-30 produced higher hypertrophy values compared to both ATII doses. The systemic application of Iso or ATII not only affects the heart but also other organ systems that may influence cardiac growth and function. With the ATII-0.3 dose no significant changes in body weight were observed. However, after Iso-30 treatment the mice gained significantly weight and this phenomenon has been already reported in mice treated with Iso during one or two weeks and it was associated with gain of brown fat and muscle, and higher food intake (Kudej et al., 1997; Friddle et al. 2000). On the contrary, the ATII-3 dose produced in wild type mice a reduction in body weight and this body weight reduction during ATII treatment has been reported by others using a similar model (Tozakidou et al., 2010).

The HW/BW index is a measure related more to the systemic effect of the treatment because their values are also determined by the changes in body weight that can be produced during hypertrophy induction. Assuming that tibia length is not changed by a one- or two-week treatment HW/TL index gives more specific information about changes in cardiac mass. Therefore, the observed increase in body weight after Iso-30 and the decrease in body weight after ATII-3 explain the small increase in HW/BW value in mice after Iso-30 compared to the HW/BW value from mice treated with ATII-3. No differences in tibia length among any group were observed; therefore, from comparison of the HW/TL index the cardiac hypertrophy induced by Iso-30 produced a larger increase in cardiac mass compared to the ATII-3 and ATII0.3 treatment. I observed a 25% increment in

HW/TL by Iso-30 in wild type mice which is comparable with other studies using the same dose (Keys et al., 2002; Maass et al., 2004; Wang et al., 2005; Jafreé et al., 2009). With the ATII-3 treatment we obtained similar increase in HW/BW as Tokudome and coworkers (2008), but a 50% higher increase in HW/BW than Song and coworkers (2006); HW/TL was not reported in these studies. The ATII-0.3 dose produced an increase of HW/TL around 11% whereas Pillai and coworkers (2006) reported an increase of 20% with the same treatment.

Overall, the variability of the increase in hypertrophy indexes is quite high in the literature which could be also be due to genetic variability of the mouse lines used in different studies. For instance there are reports showing that after the same ATII treatment C57Bl/6 and not BALBc wild type mice presented increased HW/BW (Francois et al., 2004). Therefore, this was the main reason to characterize the neurohumoral-induced cardiac hypertrophy with the appropriate wild type line that serves as control for the TRPC-deficient mouse lines that are available.

The effects of Iso-30 and ATII-3 on cardiomyocyte size and cardiac fibrosis were also analyzed in wild type mice (see Figures 7 and 9). Iso-30 produced a bigger increase of the myocytes cross sectional area compared to ATII-3. In contrast, ATII-3 increased the collagen content more than Iso-30 in wild type hearts, which was expected as ATII is one of the main stimuli that trigger cardiac fibrosis (Brown et al., 2005). The development of fibrosis with Iso-30 has been reported (Wang et al., 2005), as well as with several ATII doses (see section 3.2.2). With Iso-30 we observed 61% increase in cardiomyocyte size and similar results were reported by Iaccarino and coworkers (1999) who used the same Iso dose and reported a 67% increase. The ATII-3 dose produced increments in cardiomyocyte size of about 50%. This value is much higher than values reported in mice between 15 and 30% with other ATII protocols and mentioned in section 3.2.2, but the differences could be explained by the use of different doses or mice with different genetic background.

One important systemic effect of our neurohumoral-induced cardiac hypertrophy protocols evaluated by us was the effect on blood pressure. From telemetric blood pressure recording in conscious mice Iso-30 did not change MAP significantly. This agrees with other reports where Iso 30mg/kg/day (5 day) did not change MAP at the end of the treatment compared to base line (Monassier et al., 2008). In contrast, ATII-3 treatment led to a profound increment in MAP of 45mmHg which is in the range between 37 and 46mmHg reported with ATII doses of 1.44 mg/kg/day (Crowley et al., 2006) and

4.6mg/kg/day (Tozakidou et al., 2010), respectively, and measured with a telemetric system in conscious mice.

It is a striking observation that even with the notable effect of ATII on blood pressure the increase in cardiac weight produced by ATII is smaller when compared with the increase in cardiac mass produced by isoproterenol, which has a very small effect on blood pressure. From this result it can be concluded that the blood pressure is only a minor determinant in our hypertrophy models. In addition, ATII-induced hypertrophy seems to be independent of blood pressure *per se* since in mice some doses of ATII can increase cardiac mass without affecting blood pressure (Brancaccio et al., 2003); and, the ATII-induced cardiac mass increase in mice was prevented by a Serotonin receptor 5-HT_{2B}R antagonist independently of the hypertension produced by ATII (Monassier et al., 2008).

I also analyzed the effect of both Iso-30 and ATII-3 on heart rate from telemetric and from ECG recordings. Both treatments produced a significant elevation of heart rate that was almost four times higher with the Iso-30 dose compared to the ATII-3. The effect of Iso-30 corresponds to the sympathetic cardiac activation through β -adrenergic receptors in the heart with the corresponding positive chronotropic effect. This effect and a similar increment were reported in mice using the Iso-30 dose (Jaffré et al., 2009).

ATII had also a positively chronotropic effect. This was unexpected taking into account the blood pressure increase produced by ATII-3 which could lead to a reflex bradycardia (Xue et al., 2003). It has also been reported that ATII in mice produced no changes of heart rate (Kuriso et al., 2003;) or can lower the heart rate (Larkin et al., 2004; Kinoshita et al., 2010); but these measurements were done under anesthesia which can alter cardiovascular parameters in mice (Janssen et al., 2004). From telemetric recordings it was reported that ATII (1.2mg/kg/day) lowered heart rate in female but not in male mice (Xue et al., 2005). In conclusion, chronic ATII application effect on heart rate is variable and depends on doses, measurement conditions and on the mouse lines.

An additional characteristic of our hypertrophy protocols was the absence of edema evidence after the infusion of either isoproterenol or both ATII doses in lungs and liver which can occur when there is heart failure (Heineke and Molkentin, 2006). In contrast to aortic constriction protocols no deterioration of cardiac output was observed from measurements with Millar catheter. From this it can be concluded that our Iso and ATII protocols induce cardiac remodeling without heart failure.

TRPC3 and TRPC6 proteins are not necessary for the development of cardiac hypertrophy induced by Iso or ATII in mice. We showed the expression of TRPC6 proteins in heart from wild type but not from TRPC6^{-/-} mice giving strong evidence of the specificity of our antibody and the abundance of TRPC6 proteins in the heart. Testing of antibody specificity is very important since we have been analyzing the expression of other TRPC proteins in murine heart, like TRPC3, and so far with our antibodies we detected the same protein patterns in heart preparations from wild type and corresponding TRPC-deficient mice. By RT-PCR analysis using freshly isolated cardiac cells from Langendorff preparations and cultured cardiac fibroblasts we amplified transcripts from both TRPC3 and TRPC6 channels. However, from isolated cardiomyocytes by LCM we could not consistently detect TRPC3 or TRPC6 transcripts. In agreement with our expression analysis it has been published that TRPC3 and TRPC6 channels are expressed in the murine heart (Table i1). Nevertheless, any of the reported protein expression analysis of TRPC3 and TRPC6 proteins showed unequivocally the expression of these proteins in cardiomyocytes, and moreover, no validation of antibody specificity using cells or tissue from TRPC3 or TRPC6 deficient mice was presented. Therefore it can not be ruled out that the observed expression results from non cardiomyocytes.

Because there are no specific agonists or antagonists for individual TRPC proteins and to test the causative role of these proteins in cardiac hypertrophy I evaluated this concept by analyzing the development of cardiac hypertrophy in mouse lines lacking TRPC3 and TRPC6. Interestingly, the deletion of TRPC6 leads to a compensatory up-regulation of TRPC3 in some cells (Dietrich et al., 2005; Weissmann et al., 2006) and these proteins could form heteromultimeric units (Hofmann et al., 2002). In contrast to the initial hypothesis, the isoproterenol- and the angiotensin II-induced hypertrophic responses tended to be rather increased in compound TRPC3/TRPC6 (-/-)² mice, but certainly were not reduced. Furthermore, ATII-3 dose produced an increased mortality in TRPC3/TRPC6 deficient mice compared to WT mice. We can not exclude that this effect is linked with hypertrophy development or other cardiac dysfunction. However, my experiments pointed the possibility that it is more related to the deficiency of TRPC3 and not TRPC6 because no TRPC6^{-/-} mice died during ATII infusion, but some TRPC3 deficient mice did it during the ATII treatment (data not shown). In the ATII experiments using single TRPC3 or TRPC6 deficient there was also no evidence of ameliorated hypertrophy response, similarly as in one isoproterenol-induced hypertrophy experiment with TRPC3^{-/-} mice. Due to the impact of the ATII-3 dose on the survival of TRPC3/TRPC6 (-/-)² mice I evaluated the cardiac hypertrophy in these mice using a lower ATII dose and again no hypertrophy reduction was observed. On the contrary, the percentual increase in

hypertrophy indexes was significantly higher in TRPC3/TRPC6 (-/-)² mice, but without obvious differences in cardiac contractility between genotypes at the end of ATII treatment.

There is evidence from *in vitro* and transgenic overexpressing models pointing TRPC3 and TRPC6 proteins as positive mediators of cardiomyocyte hypertrophy. Nevertheless, the postulated function of these proteins might not necessarily be reflected in the *in vivo* situation. Using *in vivo* models it was shown recently that specific cardiomyocyte overexpression of either TRPC3 or TRPC6 in mice leads to an increase of cardiomyocyte size, cardiac mass and heart failure (Kuwahara et al. 2006; Nakayama et al. 2006), and the crossing between the TRPC3 transgenic mice with a cardiomyocyte specific transgenic PMCA4b mice produced a rescue effect on the hypertrophic phenotype (Wu et al., 2009), suggesting that increased cation entry in cardiomyocytes via TRPC3 and TRPC6 channels causes cardiac hypertrophy (Kuwahara et al. 2006; Nakayama et al. 2006). On the other hand, mice with specific cardiomyocyte overexpression of dnTRPC3 or dnTRPC6 showed reduced pathologic cardiac hypertrophy (Wu et al., 2010b). However, from our data we found no evidence that TRPC3 and TRPC6 channels are positive regulators of the neurohumoral induced hypertrophy. I used TRPC deficient mice and analyzed the systemic effect of its deletion in the cardiac hypertrophy development, and so far, the *in vivo* published observations about TRPC3 or TRPC6 are based on mouse models with cardiomyocyte specific overexpression of the expression of these two proteins. This strategy could be difficult to interpret since it was shown that the sole overexpression of GFP under an α -MHC promoter can lead in some mouse lines to dilated cardiomyopathy (Huang et al., 2000) and the hypertrophic response is a result of the interaction among several cell types and organs. Not only differences in cardiac hypertrophy induction models used by others or mouse lines may explain the different findings. It has to be taken into account that TRPC3 and TRPC6 channels are expressed in other cardiac cells like fibroblasts (see Figure 20 and Table i3) that can regulate the cardiac hypertrophy development in a different manner. For example, it has been shown that TRPC6 channels are negative regulators of the myofibroblast formation, being then TRPC6 a suppressor of the fibrotic response in cardiac fibroblasts (Nishida et al., 2007). These cell types can regulate the cardiomyocyte hypertrophy through secretion of growing factors and the collagen deposition during pathological conditions (Souders et al., 2009).

Concomitant inactivation of TRPC1 and TRPC4 proteins ameliorates the development of cardiac hypertrophy induced by Iso or ATII in mice. In addition to

TRPC3 and TRPC6 we also found expression of TRPC1 and TRPC4 transcripts in cardiac cells, which is in agreement with results our group made by northern blot analysis with mouse heart (Freichel et al., 2004) and from reported observations (Table i1). Also, I was able to detect specific TRPC1 but not TRPC4 transcripts in isolated adult cardiomyocytes, and I detect transcripts from both TRPC1 and TRPC4 in cultured cardiac fibroblasts, which can explain partially the different expression pattern between heart and cardiomyocytes. A complementary explanation is that in the heart there are other cell types including smooth muscle cells, endothelial cells, macrophages and cardiac mast cells among others, that indeed express different TRPCs. The expression of TRPC1 proteins in mouse heart was shown by others with an antibody against TRPC1 that detected this protein in heart preparations from wild type mice but not from TRPC1^{-/-} mice (Seth et al., 2009). We could not detect TRPC4 expression in purified cardiomyocytes. This differs from the TRPC4 protein expression reported in purified adult mouse cardiomyocytes (Nakayama et al., 2006); however, the specificity of the used anti-TRPC4 antibody has not been proven yet and the purity of the used preparation was not assessed. There could be also limitations regarding in our detection method by RT-PCR regarding limited amounts of mRNA due to the number of cells that might be still low to detect transcripts of low abundance.

Based on our initial expression analysis in mouse heart I studied mouse lines deficient for TRPC1, TRPC4, and TRPC1/TRPC4 (-/-)². I found clear evidence that in TRPC1/TRPC4 deficient mice the neurohumoral-induced cardiac hypertrophy generated either by isoproterenol or ATII infusion is significantly reduced. This reduced response required the deletion of both TRPC1 and TRPC4 proteins because no diminished hypertrophic responses in TRPC1^{-/-} and TRPC4^{-/-} mice were observed after isoproterenol and ATII treatments. One plausible option could explain that the phenotype was evident only in TRPC1/TRPC4 (-/-)² mice and not in single deficient mice. If both TRPC1 and TRPC4 proteins have overlapping functions regarding the mechanisms of heart hypertrophy development, then the deletion of one protein may be compensated by other (Dietrich et al., 2005). There is evidence that TRPC1 and TRPC4 proteins interact in heterologous and native systems (Hofmann et al., 2002; Goel et al., 2002) and could have overlapping functions (Sours-Brothers et al., 2009). But this can not be generalized and would depend on the cell type and type of stimulation.

After Iso-induced hypertrophy TRPC1/TRPC4 (-/-)² mice showed a significant reduction in both cardiac hypertrophy indexes and the corresponding percentual increments. In these experiments LW/TL from both genotypes was increased, but this was not associated to

edema in the lungs. In addition, no differences caused by isoproterenol treatment on liver weight or its water content were detected. Additionally, no differences were observed in left ventricular function parameters from WT and TRPC1/TRPC4 deficient mice at the end of the isoproterenol treatment. We can conclude that in these mice the hypertrophy was produced without obvious evidence of heart failure. Not only hypertrophy indexes like HW/BW in TRPC1/TRPC4 deficient mice were reduced after Iso treatment, also the cardiomyocyte cross sectional area and the increment in interstitial fibrosis were smaller in TRPC1/TRPC4 (-/-)² mice. This is an indication of the participation of both TRPCs in cardiomyocyte growth and fibroblast collagen formation produced by systemic isoproterenol application; although, the mechanisms behind this differences remain to be elucidated.

Basal angiotensinogen levels are not different in TRPC1/TRPC4 (-/-)² mice. Beyond a direct effect of isoproterenol on the heart, there are other systemic effects that can be involved in the Iso-induced cardiac hypertrophy. Isoproterenol can activate the kidney renin-angiotensin-Aldosterone system (RAAS), by stimulating the renin production and finally the concomitant increase of ATII levels, either in plasma (Leenen et al., 2001) or also local ATII production in the heart (Nagano et al., 1992). Since we observed that TRPC1/TRPC4 deficient mice had smaller livers, and the liver is the main source of angiotensinogen which is the substrate for ATI synthesis, one possibility was that TRPC1/TRPC4 (-/-)² mice had reduced circulating angiotensinogen that could end in reduced ATII levels during isoproterenol infusion and in a reduced hypertrophy development. However, this is unlikely because the angiotensinogen levels between wild type and TRPC1/TRPC4 (-/-)² mice were not different.

Renin secretion in TRPC1/TRPC4 (-/-)² mice is not altered. In collaboration with Prof. Frank Schweda (Regensburg) we observed that the isoproterenol-induced renin secretion and the ATII inhibition of the renin secretion in isolated kidneys from wild type and TRPC1/TRPC4 deficient mice were comparable, ruling out an impaired renal renin secretion under isoproterenol stimulation. From these experiments I conclude that the reduced response of TRPC1/TRPC4 in the Iso-induced experiments is not due to differences in renin secretion stimulated by Iso or due to differences in basal plasma levels of angiotensinogen. Still it is required to measure circulating and cardiac components of the RAAS under isoproterenol infusion to analyze their contribution to the hypertrophy development in TRPC1/TRPC4 (-/-)² mice.

The reduced hypertrophic response in TRPC1/TRPC4 (-/-)² could be due to and impaired response to ATII. There is evidence pointing the importance of systemic and local RAAS during the Iso-induced hypertrophy. There are contradictory results regarding the role of ATII during Iso-induced hypertrophy. In rats, the isoproterenol-induced cardiac hypertrophy was not prevented by both the AT₁R-blocker Losartan and the ACE inhibitor Quinapril (Leenen et al., 2001). In contrast, in a similar model isoproterenol-induced hypertrophy was prevented by the ACE inhibitor Trandolapril but not by bilateral nephrectomy (Nagano et al., 1992), suggesting that sympathetic activity is one of the regulators of the cardiac RAAS and hypertrophic response. Mice deficient for the AT_{1A}-R were not able to develop cardiac hypertrophy after 11 days of isoproterenol infusion (Zhang et al., 2007). In addition, the AT₁-R antagonist Olmesartan prevented the isoproterenol-induced cardiac hypertrophy in mice (Zhang et al., 2007).

To test if the reduced hypertrophy observed in TRPC1/TRPC4 (-/-)² mice after isoproterenol treatment was mediated by ATII, I induced cardiac hypertrophy in these mice by ATII infusion. After ATII treatment, the hypertrophy indexes, that are more variable with this protocol, as well as the cardiomyocyte size and the fibrosis increment were reduced in TRPC1/TRPC4 (-/-)² mice in a similar proportion compared to the reduction registered after isoproterenol treatment. In addition, no evidence of cardiac congestion in wild type and TRPC1/TRPC4 (-/-)² mice was detected in these experiments. From these results we can affirm that as well to the isoproterenol-induced hypertrophy, also the ATII hypertrophy response was reduced in TRPC1/TRPC4 knockout mice. It is conceivable that Iso- and ATII-induced hypertrophy share mechanisms that could be linked to the regulation of cardiomyocyte growth and fibrosis development. However, impaired pathways mediated through the kidney could also explain the reduced hypertrophy development in TRPC1/TRPC4 (-/-)² mice because angiotensin II-induced hypertrophy was abolished completely in mice deficient for the AT_{1A}-R in the kidneys independently of the presence of the receptors in the rest of the body (Crowley et al., 2006).

Reduced Iso-induced hypertrophy in TRPC1/TRPC4 (-/-)² mice is not explained by change in blood pressure. Isoproterenol has many other systemic including stimulation of Renin secretion and ATII production. It could also produce changes in blood pressure either by direct stimulation of β -receptors on the vessels causing vasodilatation or by secondary effects due to changes on heart rate. From analysis of wild type mice the isoproterenol effects on blood pressure were minor and it is unlikely that the small changes in blood pressure during isoproterenol infusion do significantly contribute to the

observed cardiac hypertrophy. However, because it was observed in our group that TRPC1/TRPC4 (-/-)² mice have reduced basal MAP (Mathar, 2010) and this could contribute to the differences observed in the Iso-induced hypertrophy, we measured blood pressure in TRPC1/TRPC4 deficient mice during the isoproterenol infusion but no differences were found in MAP before and during isoproterenol treatment. One explanation why the reduced basal MAP was not observed anymore in TRPC1/TRPC4 deficient mice is a difference in environmental conditions including housing. Unchanged blood pressure levels between wild type and TRPC1/TRPC4 (-/-)² mice were confirmed in three independent series. From these mice the Iso-induced hypertrophy was also diminished, discarding an obvious effect of the implantation of osmotic minipumps together with the blood pressure on the hypertrophy development. Taken together this results, it can be ruled out that differences in blood pressure regulation between wild type and TRPC1/TRPC4 (-/-)² during isoproterenol infusion can explain the reduced hypertrophy response of TRPC1/TRPC4 deficient mice.

The reduced hypertrophic response of TRPC1/TRPC4 (-/-)² mice could be related to diminished effects of ATII on heart rate. Isoproterenol also has a positive chronotropic effect on the heart. The heart rate during isoproterenol infusion measured from independent experimental groups and with two different methods, ECG recordings and telemetric recordings, showed a consistent reduced response in TRPC1/TRPC4 (-/-)² mice. In order to clarify this effect of isoproterenol on heart rate we did the experiments using isolated right atria, and isoproterenol or Acetylcholine at different concentrations produced comparable positive and negative chronotropic effects respectively, on atria from wild type and from TRPC1/TRPC4 (-/-)² mice. The isoproterenol effects have been reported in isolated mouse atrial preparations by others, but with smaller increases in a similar range of concentration, possibly due to differences in mouse lines (Vandecasteele et al., 1999). On the other hand, the absolute values and the increase in beating frequency after stimulation by different ATII concentrations were smaller in TRPC1/TRPC4 deficient mice. Therefore it can be speculated that the observed reduction of the isoproterenol-induced heart rate increase could be a secondary effect of an impaired response to the stimulation of the heart by ATII produced during isoproterenol infusion. This is also in agreement with the observation that during ATII infusion the increment in heart rate observed in wild type mice was not detected in TRPC1/TRPC4 deficient mice. It is plausible that part of the increment in heart rate triggered by isoproterenol is caused by direct stimulation ATII direct on the heart since in mice the AT₁-R antagonist Valsartan was able to decrease the isoproterenol-induced change in heart rate, but not changes in systolic blood pressure (Barki-Harrington et al., 2003). Moreover,

in mice the AT₁-R antagonist Olmesartan prevented the isoproterenol-induced cardiac hypertrophy (Zhang et al., 2007).

ATII receptors are coupled to G_q proteins which have signaling cascades that are proposed to activate TRPC channels (Clapham, 2003; Venkatachalam and Montell, 2007). Additional evidence to impaired G_q signaling in TRPC1/TRPC4 deficient mice is that the positive chronotropic response to Phenylephrine in isolated atria was also reduced, and Phenylephrine acts through α 1-adrenergic receptors which are also coupled to G_q proteins (Wettschureck and Offermanns, 2005). Therefore, it is possible that part of the mechanisms behind the reduced hypertrophy response of TRPC1/TRPC4 (-/-)² mice involves differences in heart rate regulation and ATII stimulation of the heart independent of blood pressure. Heart rate could be an important component of the diminished observed hypertrophy in TRPC1/TRPC4 deficient mice, since sustained changes in beating frequency can alter basal calcium levels and trigger hypertrophic responses (Tavi et al., 2004).

We ruled out that single deletion of TRPC1 or TRPC4 were responsible for the diminished hypertrophy responses observed after isoproterenol or ATII treatments, because from various independent experimental series we were not able to observe reduced responses in the hypertrophy indexes between wild type and TRPC1-/- or TRPC4-/- mice. Our results regarding TRPC1-/- mice are contradictory with recent observations using TRPC1 deficient mice but with a 129Sv genetic background. It was shown that TRPC1-/- mice have a minor increment of cardiac mass induced by TAC and also that they have about 58% ameliorated HW/BW increase after infusion of ATII at a dose of 1.44mg/kg/day during 28 days (Seth et al., 2009). It is difficult to explain this result compared with ours, some explanations could be differences in protocols, like the ATII concentration and duration, or the genetic background of the mice, but beyond this there are no more obvious differences that explain that other group reported that TRPC1 deficient mice have reduced heart hypertrophy and we were not able to detect reductions by two different protocols in different experimental groups. In this study it is also intriguingly that only TRPC1 is responsible for the reduced response, although TRPC3, TRPC4 and TRPC6 were shown to be expressed in the heart and they could be involved in hypertrophy development. Regarding TRPC4, recently it was published that mice expressing a dominant negative TRPC4 with an α -MHC promoter had less cardiac hypertrophy after aortic banding. Likewise very similar effects on hypertrophy were obtained also with overexpression of two other dominant-negative TRPC isoforms (Wu et al., 2010b). This

approach strongly relies on the specificity of the overexpressed protein which is difficult to demonstrate.

The expression pattern of TRPCs in the heart pointed a role on non-cardiomyocytes in TRPC1/TRPC4 mediated hypertrophy. The Iso- and ATII induced fibrotic increase in TRPC1/TRPC4 (-/-)² mice was reduced, but from comparison of control groups we observed that TRPC1/TRPC4 deficient mice had slightly significant increased basal fibrosis levels. For this reason and in order to identify cardiac cell types involved in the reduced cardiac hypertrophy observed in TRPC1/TRPC4 (-/-)² mice, the expression of different TRPC channels was analyzed in mouse heart, cardiac cells isolated from Langendorff preparations, isolated mouse cardiomyocytes by LCM and cultured cardiac fibroblasts, and some findings were discussed above. From heart Langendorff preparations we amplified transcripts from TRPC1, TRPC3, TRPC4 and TRPC6, but not transcripts from TRPC5 in agreement with northern blot expression analysis of TRPC5 in mouse heart reported by others (Okada et al., 1998). In isolated cardiomyocytes we were only able to detect TRPC1 transcripts. On the other hand, transcripts from TRPC1, TRPC3, TRPC4, TRPC5 and TRPC6 were obtained from cultured mouse cardiac fibroblasts. The differences in the expression pattern between cell pellets from Langendorff preparations and isolated cardiomyocytes can be explained by the presence of other cells different than cardiomyocytes on the Langendorff preparations. Indeed, I showed the presence of positive cells for a fibroblast marker (P4HB) in this kind of preparations (Figure 19, D). Other possible explanation is that the amount of RNA from LCM-cardiomyocytes was not sufficient to detect low abundance transcripts. Although, I tried with independent preparations and different cell numbers and the results were consistent, and the method worked to detect several other transcripts, for example TRPM4 or TMEM-2. It can also be possible that there are differences in the expression between species. We consider that the isolation of cardiomyocyte previous to selection of the cells by LCM is sufficient strategy to obtain a pure population for cell specific expression analysis. From the literature describing TRPC expression analysis in the heart, most of the data came from complete heart preparations or enriched cell pellets. Only the expression of TRPC1 proteins in the heart using hearts from TRPC1^{-/-} mice was shown so far (Seth et al., 2009) as we showed for TRPC6 proteins. So far, no specific TRPC expression in adult wild type cardiomyocytes has been reported. Immunocytochemistry experiments with adult mouse ventricular cardiomyocytes (Kuwahara et al., 2006) or mouse sinoatrial cells (Ju et al., 2007) using antibodies which have not been rigorously tested for their specificity were reported.

TRPC1/TRPC4 proteins contribute to Ca²⁺ entry in mouse cardiac fibroblasts. I studied cardiac fibroblasts to get a hint of their contribution for the neurohumoral-induced cardiac hypertrophy. I established in our group a protocol for the isolation and culture mouse cardiac fibroblasts. The purity of the fibroblast culture (~95%) assed by positive P4HB stained cells was comparable with other groups using the same cellular marker (Thum et al., 2008) or using other fibroblasts markers like vimentin (Jaffré et al., 2009). In addition, the tested fibroblasts were negative for α -SM actin and α -actinin, arguing against differentiation to a myofibroblasts phenotype during the first passages, and that there were no cardiomyocyte cells present. Few cells showed an unspecific perinuclear staining were stained with CD31. Cardiac fibroblasts have their origin in various cell lineages and tissue niches which explains the limitation of the current markers to characterize these cells (Snider et al., 2009; Zeisberg and Kalluri, 2010). For example, Vimentin is a common marker used to characterize cardiac fibroblasts that is also found in endothelial cells and in macrophages, cells commonly obtained in the first steps of the fibroblast culture that can reduce culture purity (Landeem et al., 2007; Jaffré et al., 2009).

With these P4HB-positive cells I started the establishment of a protocol to measure changes in intracellular calcium concentrations after agonist stimulation using fluorescence methods with the calcium indicator FURA-2, since changes in intracellular calcium concentration may affect the release of hypertrophy inducing agonists. After testing different conditions in wild type cells were obtained rapid responses after stimulation with isoproterenol, ATII or serotonin. The variability of these agonist responses among cells was too high, possibly explained by loss of expression of the corresponding receptors during culture. Therefore, I used a simpler protocol to test the calcium entry triggered by store depletion using Thapsigargin treatment in the absence of extracellular calcium, and re-adding Ca²⁺ to the extracellular solution to measure Ca²⁺ entry, as it was done in many cell types by others to characterize the TRPC functionality (Liu et al., 2007). From the first results I observed that the calcium release from internal stores was not impaired in cells from TRPC1/TRPC4 (-/-)² mice, but the calcium entry component produced after including Ca²⁺ in the extracellular medium was considerably reduced in a population of cells with a characteristic fibroblast morphology and not in larger cells with a morphology resembling myofibroblasts.

Even, if the reduced Store-Operated Ca²⁺-Entry could be assigned to a specific fibroblast subtype it would be necessary to determine if there is a functional defect in cells deficient for TRPC1 and TRPC4 channels after stimulation by cardiac fibroblasts-specific and/or hypertrophy inducing agonists. Moreover, in this case will be helpful to test if the release

of cytokines or growth factors is affected after isoproterenol or AII stimulation in cardiac fibroblasts from TRPC1/TRPC4 deficient mice since this is a proposed mechanism mediating the hypertrophy development through non-myocyte cells (Jaffré et al., 2009).

6.2 Role of TRPC channels in platelet aggregation: Analysis of TRPC-deficient mice

To study if TRPC proteins play a functional role in mouse platelets I established in our group protocols to isolate mouse platelets for expression and *in vitro* aggregation analysis. The use of several mouse lines deficient for different TRPC proteins allowed us to circumvent the lack of specific TRPC agonist and antagonist and to test anti-TRPC antibodies for specificity. We included in our platelet aggregation study TRPC compound knockout mouse lines because of three reasons; first, it has been reported that TRPC channels form functional units composed by different TRPC proteins (Strübing et al., 2001; Ambudkar et al., 2006) and that different TRPC proteins could interact in platelets (Brownlow and Sage, 2005); second, the deletion of one TRPC can be compensated by up regulated expression of other TRPC (Dietrich et al., 2005; Sel et al., 2008); and third, the use of compound deficient mouse lines facilitates the phenotype screening and reduces the number of mice used to obtain blood, an special issue for platelet studies in mice where the amount of blood is a limiting factor in case of mice.

Different TRPs are expressed in murine platelets. Using murine platelets from wild type mice we identified TRPC6 proteins that were not present in preparations from TRPC6 deficient mice. In similar experiment we detected also TRPM4 proteins in murine platelets. I amplified transcripts from TRPC1 and TRPC6 using RNA isolated from washed platelets. Also, transcripts from these two channels in addition to TRPM4 and TMEM-2 were amplified using platelets sorted by FACS. Because platelets have small amounts of mRNA (McRedmond et al., 2004) it was required to isolate high number of cells for RNA isolation and RT-PCR. From FACS experiments we determined that the platelet preparation was highly pure (>99.9%) and with platelets sorted by FACS the expression pattern of TRPC channels was not different compared to the obtained from RNA isolated from washed platelets. Therefore, we can assume that our RT-PCR expression analysis using RNA isolated from high number of washed platelets corresponds to the expression pattern in platelets. We did not amplify transcripts of other TRPC channels beyond TRPC1 and TRPC6. It does not mean indeed that they are not expressed in platelets because a limitation of this approach is that platelets are anucleated fragments that do not synthesize RNA restricting the detection of platelet's transcripts. On the other hand, the expression of

other TRPC proteins analyzed by western blot and various anti-TRPC antibodies produced similar protein patterns between platelet preparations from wild type and the corresponding TRPC-deficient control. Or, like in case of TRPC5 we did not detect TRPC5 proteins in platelet preparations using antibodies that have been proven to detect TRPC5 proteins specifically in other cellular or tissue preparation. Despite the power of protein detection by western blot using control samples from knockout mice this method is constricted to the generation of specific antibodies which is a time and effort consuming process. The expression of several TRPC proteins has been reported in the literature in mouse and human platelets (Table i4) and specific functions are proposed for these proteins in these channels in these cells, especially for TRPC1 and TRPC6 (Authi, 2007). In most cases the reported expression experiments did not include proper controls of antibody specificity and this issue has been discussed specifically for TRP expression in platelets due to controversial published results (Sage et al., 2002; Authi et al., 2002; Authi, 2007; Varga-Szabo et al., 2008b). Only in one report the protein expression of TRPC1 and TRPC6 proteins in mouse platelets included platelet preparations from TRPC1^{-/-} and TRPC6^{-/-} as proof of the validity of the antibodies Varga-Szabo and collaborators (2008b).

A protocol allowing analysis of platelet aggregation in vitro. As a functional assay we decided to use the turbidimetric *in vitro* assay. In this case I also established the protocol that resulted to be a reliable method as previously reported (Jarvis, 2004). Most of the experiments were done using washed platelets. This kind of preparation allows testing platelet aggregation independent of coagulation factors present in the plasma. In addition, a higher number of experiments can be performed with a smaller number of mice compared to experiments using platelet rich plasma. Because the method was used for the first time in our group I compared initially the aggregation responses of platelets from wild type mice of a mixed 129SvJ/C57Bl6 genetic background. These wild type mice with the mixed genetic background were used as control mice to compare the aggregation of platelets from most of the TRPC-deficient mouse lines. The platelet aggregation experiments were focused on analyzing the effect of the four main platelets agonists ADP, Thromboxane A₂, thrombin and collagen ADP which have signaling pathways linked to PLC activity that can activate TRPC channels in many cell types (Minke, 2006; Ambudkar and Ong, 2007). The aggregation results obtained with wild type platelets with these four agonists were consistent and reproducible between different experimental series. Only small but significant differences in the *in vitro* aggregation between platelets from female and from male mice were observed, especially at some ADP concentrations. This observation was not surprising since it has been reported that platelets from female mice are intrinsically more sensitive than those from male mice, and washed platelets from

female mice aggregate more than those from male mice after ADP stimulation (Leng et al., 2004). For both genders concentration-response curves of platelet aggregation parameters were obtained. However, it was not possible to obtain intermediate aggregation responses in terms of maximal aggregation and aggregation area for thrombin and the TxA₂ analogue U46619, despite that different concentrations were tested. The very steep dose-response curve obtained with these agonists indicates that in this test the response after thrombin or U46619 stimulation was basically an all or nothing response. In contrast, the platelet shape change presented dose dependent responses for all agonists. In case of ADP and collagen the maximal aggregation and area showed continuously increasing responses over a large range of agonist concentrations for platelets of both genders. The differences among agonists could be explained by differences of their action during the thrombus formation. Beyond differences in platelet aggregation between genders we observed that platelet counts in female mice were significantly lower compared to male mice with a mixed 129SvJ/C57Bl6 genetic background. In addition, platelet counts from C57Bl6N male mice were higher than those from 129SvJ male mice. These differences pointed out one more time the importance of characterizing the wild type mouse lines that are going to be used to compare the responses from TRPC-deficient mice, since wild type mice of different genetic background vary substantially in terms of platelet counts. A survey including platelet counts of both genders from 27 mouse inbred strains showed that in 56% of the strains platelet count were higher in male mice, in 18% of the strains the platelet count were higher in female mice and in the 26% the counts were similar between both genders (Peters et al., 2006); obviously, the observed differences in platelet counts were not determined by the gender but by the genetic background of the mice.

TRPC6^{-/-}, TRPC5^{-/-} and TRPC1^{-/-} mice have unaltered platelet aggregation in vitro.

A screening of platelet aggregation using 13 mouse lines including single and compound TRPC deficient mouse lines was carried out. I used platelets from both genders in most cases and the four main platelet activating agents ADP, TxA₂ analogue, thrombin and collagen. The deletion of TRPC1, TRPC3, TRPC4 or TRPC6 proteins did not produced differences in platelet counts. The platelet aggregation screening was initially focused on TRPC6 deficient platelets because of the strong TRPC6 protein expression that we detected in mouse platelets. Surprisingly, no differences were identified in the *in vitro* aggregation in any concentration of the four agonists tested in platelets obtained from both genders. Furthermore, these results were conducted using TRPC6-deficient mice on both a C57Bl6/N and a mixed C57/Svj genetic background, which makes a possible masking effect due to the genetic background of the mice unlikely. TRPC1 expression

was also detected in mouse platelets but no obvious differences in aggregation were observed in TRPC1^{-/-} platelets. Expression of TRPC5 that was reported by other groups (see Table i4) could not be confirmed by our RT-PCR analysis. Also, using our anti-TRPC5 antibodies we did not detect TRPC5 in mouse platelets. In this line, I did not find altered aggregation in platelets from TRPC5^{-/-} mice after stimulation with most relevant concentrations of ADP, thrombin, collagen or U46619. It is possible that the lack of one of these TRPC proteins is compensated by changes in expression of other TRPC protein or by redundant function of other TRPC proteins. For these reasons I used platelets from TRPC1/TRPC6 (^{-/-})², and platelets from TRPC3/TRPC6 (^{-/-})² mice because specifically in TRPC6^{-/-} mice it was found increased TRPC3 expression (Dietrich et al., 2005). Additional evidence to this came from others who reported that TRPC1^{-/-} platelets had no impairment in SOCE or agonist induced calcium entry, and in platelet activation (Varga-Szabo et al., 2008b). It has been proposed that TRPC6 proteins are an important component of calcium entry in platelets and consequently for platelet activation (Hassock et al., 2002; Jardín et al., 2008b), but from our results the single deletion of these proteins produced no obvious aggregation defect.

TRPC1, TRPC3 and TRPC6 proteins are crucial regulators for platelet aggregation induced by ADP, TxA₂ and thrombin. Platelets from TRPC1/TRPC6 (^{-/-})² and TRPC3/TRPC6 (^{-/-})² mice presented a consistent reduction in the ADP-induced aggregation. Additionally, impaired responses to the TxA₂ analogue U46619 and to thrombin were observed in these platelets, but no reduction was detected after collagen stimulation. The common characteristic among ADP, TxA₂ and thrombin is that these agonists activate signaling pathways downstream of receptors coupled to G_q proteins (Offermanns, 2006). The signaling downstream of G_q activation includes activation of cation channels which could be formed by TRPC proteins. Therefore, there could be a shared signaling between ADP, TxA₂ and thrombin that activates the same pool of channels. Also, when platelets are stimulated by thromboxane or thrombin they secrete granules that contain ADP and thereby amplify platelet responses in a paracrine and autocrine manner (Savi and Herbert, 1996).

The reduction in ADP-induced aggregation is probably the main difference observed in TRPC1/TRPC6 and TRPC3/TRPC6 deficient platelets so far. When I compared the ADP-induced aggregation from both groups the reduction was more prominent in platelets from TRPC3/TRPC6 (^{-/-})² mice, and specially in female mice. If single deletion of TRPC1 and TRPC6 produced no obvious aggregation defect and TRPC1/TRPC6 and TRPC3/TRPC6 deficient platelets did not aggregate normally, I speculated that the deletion of all three

TRPC proteins produced an aggravated phenotype, especially after ADP stimulation. Very recently TRPC1/TRPC3/TRPC6 deficient mice were obtained and were viable and fertile. Platelets from these mice showed impaired responses to ADP, thrombin and U46619, but not the reduction in a similar range compared to the one registered for TRPC3/TRPC6 deficient platelets. Obviously, the remaining part of the aggregation is mediated by channels independent of TRPC1, TRPC3 and TRPC6. If TRPC4 proteins may contribute as suggested by Brownlow and Sage (2005) or Wakabayashi et al. (2006), this could be tested in TRPC1/TRPC3/TRPC4/TRPC6 deficient mice, although this possibility seems unlikely based on the unchanged aggregation in TRPC4/TRPC6 (-/-)² mice that were observed after stimulation with these agonists.

Since platelets can secrete ADP after stimulation with agonists like thromboxane or thrombin (Li et al., 2004b) and our most prominent difference in aggregation were obtained after ADP stimulation, we hypothesized that U46619- and thrombin-impaired responses in TRPC1/TRPC6 and TRPC3/TRPC6 deficient platelets could be at least in part secondary due to impaired ADP signaling. One supporting argument came from our results with TRPC3/TRPC6 deficient platelets where we observed that the substantial reduction in U46619-induced aggregation observed, became much smaller when the experiments were done in a ten-fold increased Apyrase concentration. Apyrase hydrolyses ADP and therefore can reduce the secreted ADP; therefore, the above experiments suggest a significant contribution of ADP signaling in the TRPC3/TRPC6 mediated aggregation induced by U46619.

TRPC1, TRPC3 and TRPC6 mediate ADP-induced platelet aggregation through P2Y₁ receptors. Since we hypothesized that the TRPC function is linked to ADP signaling we focused on the signaling pathway activated by this agonist. Stimulation of platelets with ADP leads to activation of both P2Y₁ and P2Y₁₂ receptors. P2Y₁ receptor is coupled to G_q proteins and it is responsible for the ADP-induced calcium transients (Fabre et al., 1999; León et al., 1999). The P2Y₁₂ receptor is coupled to G_i proteins and is linked to cAMP regulation after ADP stimulation, but it does not regulate calcium transients (Foster et al., 2001; André et al., 2003). To dissect between these signaling pathways I performed experiments with platelets from mice that received Clopidogrel to block P2Y₁₂ receptors at a dose that proved to be effective in rats (Savi et al., 1992). First, to test the effects of this dose in mice experiments using wild type mice were done. From those results we could conclude, first, that Clopidogrel was effective to block effectively the ADP-induced platelets aggregation *in vitro*, and second, we showed that effects of the vehicle used to solve Clopidogrel can be neglected allowing us to skip the use of vehicle treated mice and

reduced the number of mice in these experiments. In TRPC1/TRPC6 (-/-)² and TRPC3/TRPC6 (-/-)² mice pre-treated with Clopidogrel ADP-induced platelet aggregation was markedly reduced at all investigated concentrations of ADP. This reduction after in ADP-induced aggregation was much more pronounced than under conditions without blocking of P2Y₁₂ receptors indicating that ADP induces activation of TRPC1/TRPC6 and TRPC3/TRPC6 channel complexes via P2Y₁ receptors. This finding is in good agreement with the observation that the deletion or pharmacological blocking of P2Y₁ and not P2Y₁₂ abolished the ADP-induced changes in intracellular calcium transients (Offermanns, 2006; Gachet, 2008) which could be mediated by channels composed of combinations of TRPC1, TRPC3 and TRPC6 proteins (Birnbaumer, 2009). Comparison of intracellular Ca²⁺ concentration in platelets from wild type, TRPC1/TRPC6, TRPC3/TRPC6 and TRPC1/TRPC3/TRPC6 deficient mice after ADP stimulation could help to prove this.

TRPC1, TRPC3 and TRPC6 channels are expressed in mammalian megakaryocytes (Table i5), the precursor cells of platelets. Evidence supporting a link between TRPC activation through ADP receptors comes from the study of murine megakaryocytes. In murine megakaryocytes ADP activates a non-selective cation channel with a current-voltage relationship similar to currents displayed by cells overexpressing TRPC6 proteins, suggesting a role for TRPC6 in the cation influx after P2Y receptor activation (Carter et al., 2006). It was suggested that physiological agonists will evoke Ca²⁺ influx through a combination of TRPC6 and Orai1 channels in platelets and megakaryocytes (Tolhurst et al., 2008). It was proposed that in murine platelets Orai1 and STIM1 are the main components of the SOCE (Varga-Szabo et al., 2008a; Braun et al., 2009). However, the presented evidence was restricted to the signaling pathway downstream the GPVI, leaving open a role for TRPC channels in other signaling pathways. The calcium entry in STIM1 and Orai1 deficient platelets was not completely reduced after ADP, U46619 or thrombin stimulation. Moreover, the *in vitro* aggregation responses to these agonists were not affected in Orai1 and STIM1 deficient platelets. Therefore, it was proposed that a Ca²⁺ entry pathway in platelets different from Orai1 channels may be involved after stimulation with these agonists (Gilio et al., 2010b). From a study of PKC α -/- platelets it was suggested by Harper and coworkers (2010) that the mouse platelet SOCE pathway conducts Na⁺ because they observed a TG-induced Na⁺ entry in mouse platelets. If Na⁺ is also conducted within the SOCE in platelets and Orai1 is highly selective for Ca²⁺ there should be other cation channels contributing to the Store operated entry in mouse platelets. This also points to a possible role of TRPC proteins in mouse platelet since these proteins are able to form channels that conduct cations including Na⁺ (Venkatachalam and Montell, 2007).

7. Conclusions

From the evidence presented in this thesis using TRPC-deficient mice it can be concluded that distinct TRPC proteins were identified as crucial regulators for cardiac hypertrophy development and platelet aggregation.

TRPC1 and TRPC4 proteins regulate the development of neurohumoral-induced cardiac hypertrophy. In conclusion, a reliable set of protocols to evaluate *in vivo* and *in vitro* the causative role of TRPC proteins in the development of neurohumoral-induced cardiac hypertrophy was established and characterized. This was complemented by expression analysis of TRPC channels in the mouse heart, cardiomyocytes and fibroblasts. We detected TRPC6 proteins in mouse heart using preparations from TRPC6 deficient mice as control of antibody specificity. We found a differential expression pattern between cardiomyocytes and fibroblasts with restricted expression of TRPC1 to cardiomyocytes, and expression of TRPC1, TRPC3, TRPC4 and TRPC6 in non myocyte cells consisting of 95% cardiac fibroblasts.

From experiments with TRPC3/TRPC6 deficient mice we conclude that deletion of both proteins in mice did not reduce the hypertrophy responses induced by isoproterenol and ATII. In contrast, TRPC1/TRPC4 deficient mice have a significant reduced neurohumoral-induced hypertrophy produced by Iso and ATII, respectively. Deletion of either TRPC1 or TRPC4 proteins can be compensated. We could rule out that the reduced hypertrophy response of TRPC1/TRPC4 deficient mice after isoproterenol treatment was due to individual deletion of TRPC1 or TRPC4 proteins. Differences in renal renin secretion, in basal plasma angiotensinogen levels or in blood pressure regulation during isoproterenol infusion could be ruled out. I showed that ATII signaling, possible through regulation of heart rate or Ca^{2+} signaling in cardiac fibroblast are altered in TRPC1/TRPC4 (-/-)² mice. These changes may contribute to the reduced hypertrophy development induced by isoproterenol and ATII in TRPC1/TRPC4 (-/-)² mice.

The neurohumoral-induced cardiac hypertrophy by isoproterenol is a complex process mediated by different organs and cell types. This work presented evidence that both TRPC1 and TRPC4 proteins are positive regulators of the neurohumoral-induced cardiac hypertrophy development, but the cellular mechanisms still remain elusive (Figure 42).

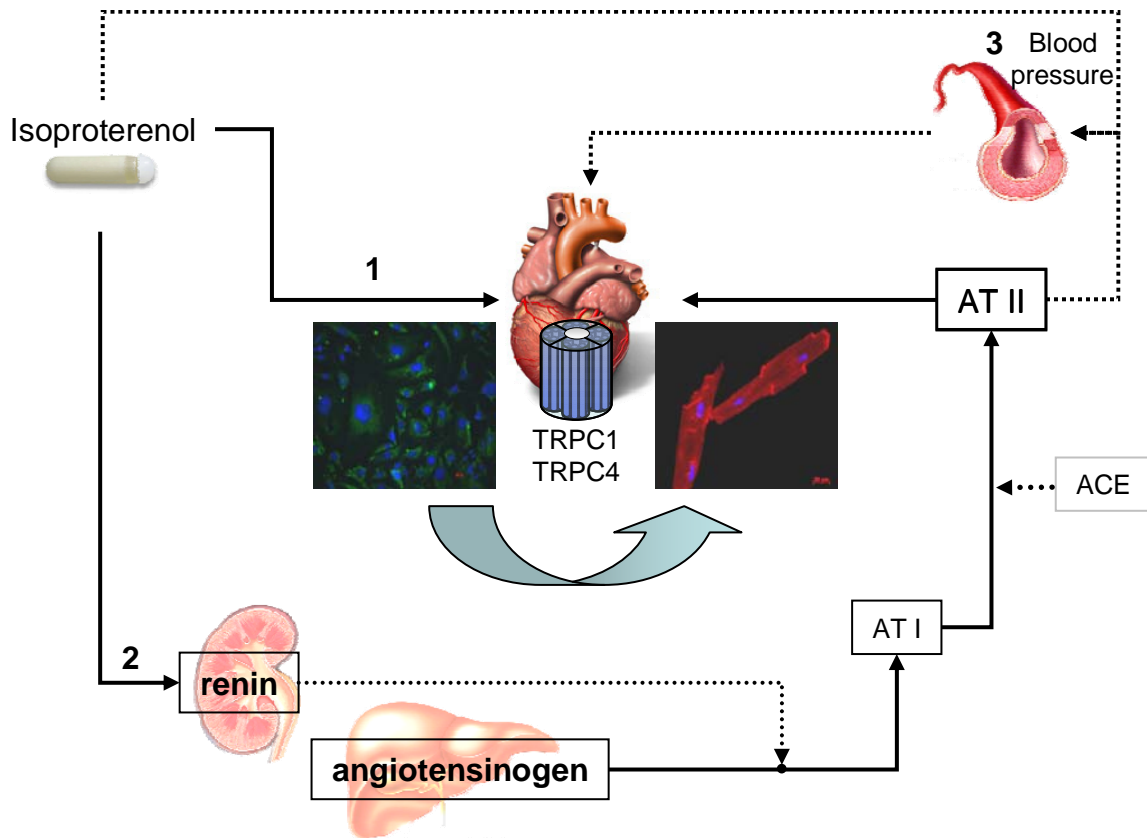


Figure 42. The isoproterenol-induced cardiac hypertrophy requires TRPC1 and TRPC4 proteins. Among the systemic effects of isoproterenol are: **1)** Direct stimulation of the heart and its different cell types which produce positive chronotropic and ionotropic responses, stimulation of the local RAAS and secretion of growth factors involved in cardiac hypertrophy development, between other responses. **2)** Stimulation of renin secretion from kidneys resulting in an increase on circulating levels of angiotensin II that can act on the heart. **3)** Changes on blood pressure by direct stimulation of blood vessels and by increasing circulating angiotensin II. From the results of this thesis using TRPC-deficient mice it is suggested that TRPC1 and TRPC4 positively regulate the Iso-induced cardiac hypertrophy. Possibly, TRPC proteins play a role in cells like fibroblasts mediating signaling that end up in the stimulation of cardiomyocytes and the hypertrophy development. My experiments showed that pathways **1** and **3** seem unlikely to contribute for TRPC1/TRPC4 mediated induction of cardiac hypertrophy by isoproterenol. ATI: Angiotensin I; ATII: Angiotensin II; ACE: Angiotensin Converting Enzyme.

TRPC1, TRPC3 and TRPC6 proteins are crucial regulators ADP-induced platelet aggregation through P2Y₁ signaling. To study platelets from TRPC-deficient mice protocols for platelet isolation and turbidimetric aggregometry were established in our group. *In vitro* platelet aggregation triggered by ADP, TxA₂ analogue U46619, thrombin and collagen was first characterized with platelets from wild type mice and then used for the analysis of platelets from several TRPC single and compound mouse lines. Using highly pure washed platelet preparation we analyzed the expression of several TRPC in mouse platelets and we were able to detect TRPC6 proteins in platelet from wild type but not from TRPC6^{-/-} mice. Transcripts from TRPC1 and TRPC6 were amplified. The deletion of TRPC1, TRPC3, TRPC4 or TRPC6 did not affect platelet counts in mice. Unexpectedly, the deletion of either TRPC1 or TRPC6 proteins did not affect platelet

aggregation. From experiments with mouse lines that lack TRPC4/TRPC6 or TRPC5 proteins a relevance of TRPC4 and TRPC5 proteins for ADP-, TxA₂-, thrombin- or collagen-induced aggregation of murine platelet seems dubious at this point.

In TRPC3/TRPC6 (-/-)² as well as in TRPC1/TRPC6 (-/-)² mice the aggregation induced by ADP and the TxA₂ analogue U46619 was significantly reduced. In addition, the thrombin-induced aggregation was defective in TRPC3/TRPC6 deficient mice. No differences in collagen-induced aggregation were observed in platelets both genotypes. The defects observed in platelet aggregation after stimulation with the TxA₂ analogue or thrombin in these two mouse lines included an impaired ADP-mediated aggregation induced by the secreted ADP, since both agonists stimulates ADP secretion in platelets and the differences were ameliorated in experiments with higher concentrations of the ADP hydrolyzing enzyme Apyrase. The reduction in the ADP-induced platelet aggregation in platelets from TRPC3/TRPC6 and TRPC1/TRPC6 deficient mice markedly increased when the mice were pre-treated with Clopidogrel. Therefore, TRPC1, TRPC3 and TRPC6 proteins could be identified as regulators in platelet aggregation mediated by ADP and P2Y₁ receptors (Figure 43) and could thereby complement the GPVI-mediated pathway triggered by collagen that depends on Orai1/Stim1 proteins.

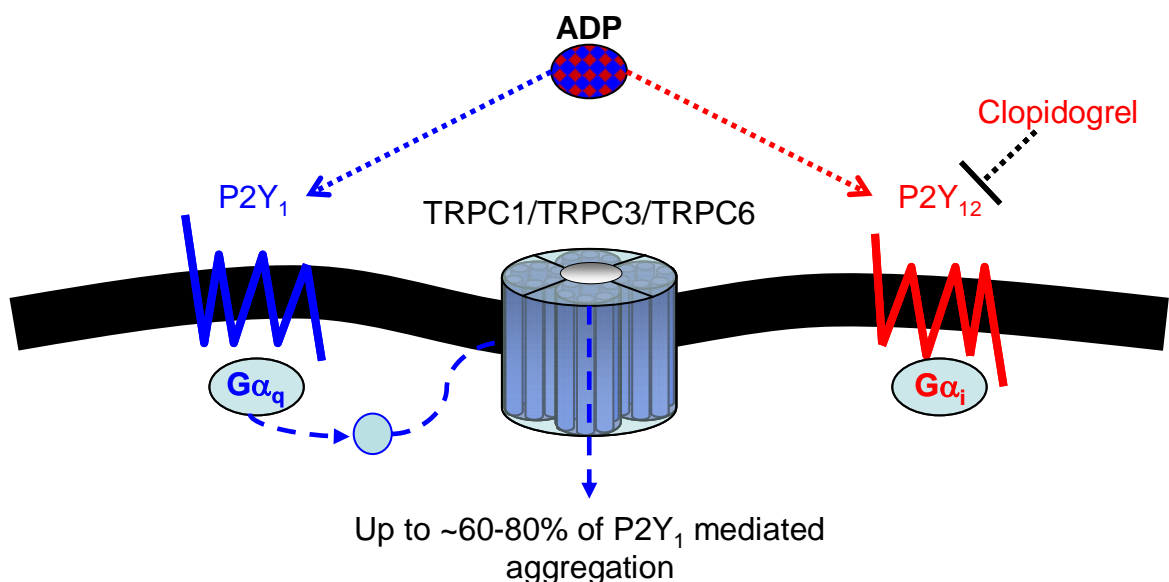


Figure 43. Model of ADP mediated platelet aggregation and the possible role of TRPC channels. In mouse platelets ADP stimulates P2Y₁ receptors that are coupled to G_q proteins and are responsible for the ADP-induced Ca²⁺ transients. ADP also stimulates P2Y₁₂ receptors that coupled to G_i proteins and are target of a metabolite of the antithrombotic drug Clopidogrel. In platelets from TRPC1/C6 (-/-)² and TRPC3/C6 (-/-)² mice pre-treated with Clopidogrel there was a ~60-80% reduction in the aggregation response measured by the area under the aggregation curve (see Figures 40 and 41). Therefore, TRPC1, TRPC3 and TRPC6 proteins are required for the ADP-induced platelet activation. Possibly, these TRPC proteins are involved in the full platelet activation after ADP stimulation mediating intracellular signaling by cation influx into the platelets.

8. References

- Abrams CS. 2005. Intracellular signaling in platelets. *Current Opinion in Hematology*. 12: 401-405.
- Abramowitz J and Birnbaumer. 2009. Physiology and pathophysiology of canonical transient receptor potential channels. *The FASEB Journal*. 23: 297-328.
- Alexander SPH, Mathie A and Peters JA. 2007. Guide to Receptors and Channels (GRAC), 2nd edition. *Br. J. Pharmacol.* 150 (Suppl. 1) S116-S121.
- Allard MF, DeVenny MF, Doss LK, Grizzle WE and Bishop SP. 1990. Alterations in Dietary Sodium Affect Isoproterenol-induced Cardiac Hypertrophy. *J Mol Cell Cardiol*. 22: 1135-1145.
- Alvarez J, Coulombe A, Cazorla O, Ugur M, Rauzier J-M, Magyar J, Mathieu E-L, Souto R, Bideaux P, Salazar G, Rassendren F, Lacampagne A, Fauconnier J and Vassort G. 2008. ATP/UTP activate cation-permeable channels with TRPC3/7 properties in rat cardiomyocytes. *Am J Physiol Heart Circ Physiol*. 295: H21-H28.
- Akhter SA, Luttrell LM, Rockman HA, Iaccarino G, Lefkowitz RJ and Koch WJ. 1998. Targeting the Receptor-G_q Interface to Inhibit in Vivo Pressure Overload Myocardial Hypertrophy. *Science*. 280:574-577.
- Ambudkar IS, Bandyopadhyay BC, Liu X, Lockwich TP, Paria B and Ong HL. 2006. Functional organization of TRPC-Ca²⁺ channels and regulation of calcium microdomains *Cell Calcium*. 40: 495-504.
- Ambudkar IS and Ong HL. 2007. Organization and function of TRPC channelosomes. *Pflügers Arch - Eur J Physiol*. 455:187-200.
- André P, Delaney SM, LaRocca T, Vincent D, DeGuzman F, Jurek M, Koller B, Phillips DR and Conley PB. 2003. P2Y₁₂ regulates platelet adhesion/activation, thrombus growth, and thrombus stability in injured arteries. *J. Clin. Invest*. 112: 398-406.
- Authi KS, Hassock S, Zhu MX, Flockerzi V and Trost C. 2002. TRPC channels and Ca²⁺ entry in human platelets. *Blood*. 100: 4246-4247.
- Authi KS. 2007. TRP Channels in Platelet Function. *Handb Exp Pharmacol*. 179: 425-443.
- Authi KS. 2009. Orai1: a channel to safer antithrombotic therapy. *Blood*. 113: 1872-1873.
- Bair A, Thippagowda PB, Freichel M, Cheng N, Ye RD, Vogel SM, Yu Y, Flockerzi V, Malik AB and Tiruppathi C. 2009. Ca²⁺ Entry via TRPC Channels Is Necessary for Thrombin-induced NF-κB Activation in Endothelial Cells through AMP-activated Protein Kinase and Protein Kinase Cδ. *JBC*. 284: 563-574.
- Barki-Harrington L, Luttrell LM and Rockman HA. 2003. Dual Inhibition of β-Adrenergic and Angiotensin II Receptors by a Single Antagonist. A Functional Role for Receptor-Receptor Interaction *In Vivo*. *Circulation*. 108: 1611-1618.
- Baudino TA, Carver W, Giles W and Borg TK. 2006. Cardiac fibroblasts: friend or foe? *Am J Physiol Heart Circ Physiol*. 291: H1015-H1026.

- Beis D, Schwarting RK and Dietrich A. 2011. Evidence for a supportive role of classical transient receptor potential 6 (TRPC6) in the exploration behavior of mice. *Physiol Behav.* 102: 245–250.
- Bendall JK, Cave AC, Heymes C, Gall N and Shah AM. 2002. Pivotal Role of a gp91^{phox}-Containing NADPH Oxidase in Angiotensin II-Induced Cardiac Hypertrophy in Mice. *Circulation.* 105: 293-296.
- Berg L-P, Shamsheer MK, El-Daher SS, Kakkar VV and Authi KS. 1997. Expression of human TRPC genes in the megakaryocytic cell lines MEG01, DAMI and HEL. *FEBS Letters.* 403: 83-86.
- Bergmeier W, Oh-hora M, McCarl C-A, Roden RC, Bray PF and Feske S. 2009. R93W mutation in Orai1 causes impaired calcium influx in platelets. *Blood.* 113: 675-679.
- Bers DM. 2002. Cardiac excitation–contraction coupling. *Nature.* 415: 198-205.
- Birnbaumer L. 2009. The TRPC Class of Ion Channels: A critical Review of Their Roles in Slow, Sustained Increases in Intracellular Ca²⁺ Concentrations. *Annu. Rev. Pharmacol. Toxicol.* 49: 395-426.
- Brancaccio M, Fratta L, Notte A, Hirsch E, Poulet R, Guazzone S, De Acetis M, Vecchione C, Marino G, Altruda, F, Silengo L, Tarone G and Lembo G. 2003. Melusin, a muscle-specific integrin β 1–interacting protein, is required to prevent cardiac failure in response to chronic pressure overload. *Nature Medicine.* 9: 68-75.
- Braun A, Varga-Szabo D, Kleinschnitz C, Pleines I, Bender M, Austinat M, Bosl M, Stoll G and Nieswandt B. 2009. Orai1 (CRACM1) is the platelet SOC channel and essential for pathological thrombus formation. *Blood.* 113: 2056-2063.
- Braz JC, Bueno OF, Liang Q, Wilkins BJ, Dai Y-S, Parson S, Braunwart J, Glascock BJ, Klevitsky R, Kimball TF, Hewett TE and Molkentin JD. 2003. Targeted inhibition of p38 MAPK promotes hypertrophic cardiomyopathy through upregulation of calcineurin-NFAT signaling. *J. Clin. Invest.* 111: 1475-1486.
- Brenner J and Dolmetsch RE. 2007. TrpC3 Regulates Hypertrophy-Associated Gene Expression without Affecting Myocyte Beating or Cell Size. *PLoS ONE.* 2(8): e802.
- Brink M, Wellen J and Delafontaine P. 1996. Angiotensin II Causes Weight Loss and Decreases Circulating Insulin-like Growth Factor I in Rats through a Pressor-independent Mechanism. *J. Clin. Invest.* 97: 2509-2516.
- Brown RD, Ambler SK, Mitchell D and Long CS. 2005. THE CARDIAC FIBROBLAST: Therapeutic Target in Myocardial Remodeling and Failure. *Annu. Rev. Pharmacol. Toxicol.* 45: 657-687.
- Brownlow SL and Sage OS. 2005. Transient receptor potential protein subunit assembly and membrane distribution in human platelets. *Thromb Haemost.* 94: 839-845.
- Bueno OF, Wilkins BJ, Tymitz KM, Glascock BJ, Kimball TF, Lorenz JN and Molkentin JD. 2002. Impaired cardiac hypertrophic response in Calcineurin A β -deficient mice. *PNAS.* 99: 4586-4591.
- Bush EW, Hood DB, Papst PJ, Chapo JA, Minobe W, Bristow MR, Olson EN and McKinsey TA. 2006. Canonical Transient Receptor Potential Channels Promote

- Cardiomyocyte Hypertrophy through Activation of Calcineurin Signaling. *JBC*. 281: 33487-33496.
- Cahalan MD, Zhang SL, Yeromin AV, Ohlsen K, Roos J and Stauderman KA. 2007. Molecular basis of the CRAC channel. *Cell Calcium*. 42: 133-144.
- Carter RN, Tolhurst G, Walmsey G, Vizquete-Forster M, Miller N and Mahaut-Smith MP. 2006. Molecular and electrophysiological characterization of transient receptor potential ion channels in the primary murine megakaryocyte. *J. Physiol*. 576: 151-162.
- Cazenave J-P, Ohlmann P, Cassel D, Eckly A, Hechler B and Gachet C. 2004. Preparation of Washed Platelet Suspensions from Human and Rodent Blood. In: *Methods in Molecular Biology, Vol. 272: Platelets and Megakaryocytes, Vol 1: Functional Assays*. (Eds.) Gibbins JM and Mahaut-Smith MP. Humana Press Inc. NJ, USA. P 13-28.
- Chen J-B, Tao R, Sun H-Y, Tse H-F, Lau C-P and Li G-R. 2010. Multiple Ca^{2+} Signaling Pathways Regulate Intracellular Ca^{2+} Activity in Human Cardiac Fibroblasts. *Journal of Cellular Physiology*. 223: 68-75.
- Cheng Y, Austin SC, Rocca B, Koller BH, Coffman TM, Grosser T, Lawson JA and FitzGerald GA. 2002. Role of Prostacyclin in the Cardiovascular Response to Thromboxane A_2 . *Science*. 296: 539-542.
- Chiang C-S, Huang C-H, Chieng H, Chang Y-T, Chang D, Chen J-Jr, Chen Y-C, Chen Y-H, Shin H-S, Campbell KP and Chen C-C. 2009. The $Ca_v3.2$ T-Type Ca^{2+} Channel Is Required for Pressure Overload-Induced Cardiac Hypertrophy in Mice. *Circ Res*. 104: 522-530.
- Cingolani E, Ramirez Correa GA, Kizana E, Murata M, Cho HC and Marbán E. 2007. Gene Therapy to Inhibit the Calcium Channel β Subunit Physiological Consequences and Pathophysiological Effects in Models of Cardiac Hypertrophy. *Circ Res*. 101: 166-175.
- Clapham DE. 2003. TRP channels as cellular sensors. *Nature*. 426: 517-524.
- Clapham DE. 2007. Mammalian TRP Channels. *Cell*. 29: 220-221.
- Colella M, Grisa F, Robert V, Turner JD, Thomas AP and Pozzan T. 2008. Ca^{2+} oscillation frequency decoding in cardiac cell hypertrophy: Role of calcineurin/NFAT as Ca^{2+} signal integrators. *PNAS*. 105: 2859-2864.
- Colman RW. 2006. Are hemostasis and thrombosis two sides of the same coin? *JEM*. 203: 493-495.
- Colston JT, Chandrasekar B and Freeman GL. 2002. A Novel Peroxide-induced Calcium Transient Regulates Interleukin-6 Expression in Cardiac-derived Fibroblasts. *JBC*. 277: 23477-23483.
- Cosens DJ and Manning A. 1969. Abnormal Electroretinogram from a *Drosophila* mutant. *Nature*. 224: 285-287.
- Crittenden JR, Bergmeier W, Zhang Y, Piffath CL, Liang Y, Wagner DD, Housman DE and Graybiel AM. 2004. CalDAG-GEFI integrates signaling for platelet aggregation and thrombus formation. *Nature Medicine*. 10: 982-986.

- Crowley SD, Gurley SB, Herrera MJ, Ruiz P, Griffiths R, Kumar AP, Kim H-S, Smithies O, Le TH and Coffman TM. 2006. Angiotensin II causes hypertension and cardiac hypertrophy through its receptors in the kidney. *PNAS*. 103: 17985-17990.
- D'Angelo, DD, Sakata Y, Lorenz JN, Boivin GP, Walsh RA, Liggett SB and Dorn II GW. 1997. Transgenic $G\alpha_q$ overexpression induces cardiac contractile failure in mice. *PNAS*. 94: 8121-8126.
- Den Dekker E, Molin DGM, Breikers G, van Oerle R, Akkerman J-W N, van Eys JJM and Heemskerk JWM. 2001. Expression of transient receptor potential mRNA isoforms and Ca^{2+} influx in differentiating human stem cells and platelets. *Biochimica et Biophysica Acta*. 1539: 243-255.
- De Smet HR, Menadue MF, Oliver JR and Phillips PA. 2003. Endothelin ET_A receptor antagonism does not attenuate Angiotensin II-induced cardiac hypertension in vivo in rats. *Clinical and Experimental Pharmacology and Physiology*. 30: 278-283.
- De Windt LJ, Lim HW, Bueno OF, Liang Q, Delling U, Braz JC, Glascock BJ, Kimball TF, del Monte F, Hajjar RJ and Molkentin JD. 2001. Targeted inhibition of calcineurin attenuates cardiac hypertrophy *in vivo*. *PNAS*. 98: 3322-3327.
- Dietrich A, Mederos y Schnitzler M, Gollasch M, Gross V, Storch, Dubrovskaja G, Obst M, Yildirim E, Salanova B, Kalwa H, Essin K, Pinkenburg O, Luft FC, Gudermann T and Birnbaumer L. 2005. Increased Vascular Smooth Muscle Contractility in TRPC6 $-/-$ Mice. *Molecular and Cellular Biology*. 25: 6980-6989.
- Dietrich A, Kalwa H, Fuchs B, Grimminger F, Weissmann N and Gudermann T. 2007a. In vivo TRPC functions in the cardiopulmonary vasculature. *Cell Calcium*. 42: 233-244.
- Dietrich A, Kalwa H, Storch U, Mederos y Schnitzler M, Salanova B, Pinkenburg O, Dubrovskaja G, Essin K, Gollasch M, Birnbaumer L and Gudermann T. 2007b. Pressure-induced and store-operated cation influx in vascular smooth muscle cells is independent of TRPC1. *Pflügers Arch - Eur J Physiol*. 455: 465-477.
- Dietrich A, Kalwa H and Gudermann T. 2010. TRPC channels in vascular cell function. *Thromb Haemost*. 103: 262-270.
- Du J, Xie J, Zhang Z, Tsujikawa H, Fusco D, Silverman D, Liang B and Yue L. 2010. TRPM7-Mediated Ca^{2+} Signals Confer Fibrogenesis in Human Atrial Fibrillation. *Circ Res*. 106: 992-1003.
- Eghbali M, Czaja M, Zeydel M, Weiner FR, Zern MA, Seifert S and Blumenfeld OO. 1988. Collagen chain mRNAs in isolated heart cells from young and adult rats. *J Mol Cell Cardiol*. 20: 267-276.
- Emmert-Buck MR, Bonner RF, Smith PD, Chuaqui RF, Zhuang Z, Goldstein SR, Weiss RA and Liotta LA. 1996. Laser Capture Microdissection. *Science*. 274: 998-1001.
- Fabre J-E, Nguyen MT, Latour A, Keifer JA, Audoly LP, Coffman TM and Koller BH. 1999. Decreased platelet aggregation, increased bleeding time and resistance to thromboembolism in $P2Y_1$ -deficient mice. *Nature Medicine*. 5: 1199-1202.
- Foster CJ, Prosser DM, Agans JM, Zhai Y, Smith MD, Lachowicz JE, Zhang FL, Gustafson E, Monsma Jr FJ, Wiekowski MT, Abbondanzo SJ, Cook DN, Bayne ML, Lira SA and Chintala MS. 2001. Molecular identification and characterization of the platelet

- ADP receptor targeted by thienopyridine antithrombotic drugs. *J. Clin. Invest.* 107: 1591-1598.
- Francois H, Athirakul K, Mao L, Rockman H and Coffman T. 2004. Role for Thromboxane Receptors in Angiotensin-II–Induced Hypertension. *Hypertension.* 43: 364-369.
- Frank D, Kuhn C, van Eickels M, Gehring D, Hanselmann C, Lippl S, Will R, Katus HA and Frey N. 2007. Calsarcin-1 Protects Against Angiotensin-II Induced Cardiac Hypertrophy. *Circulation.* 116: 2587-2596.
- Fredj S, Bescond J, Louault C and Potreau D. 2005. Interactions Between Cardiac Cells Enhance Cardiomyocyte Hypertrophy and Increase Fibroblast Proliferation. *Journal of Cellular Physiology.* 202: 891-899.
- Freichel M, Schweig U, Stauffenberger S, Freise D, Schorb W and Flockerzi V. 1999. Store-Operated Cation Channels in the Heart and Cells of the Cardiovascular System. *Cell Physiol Biochem.* 9: 270-283.
- Freichel M, Suh SH, Pfeifer A, Schweig U, Trost C, Weißgerber P, Biel M, Philipp S, Freise D, Droogmans G, Hofmann F, Flockerzi V and Nilius B. 2001. Lack of an endothelial store-operated Ca^{2+} current impairs agonist-dependent vasorelaxation in TRP4-/- mice. *Nature Cell Biology.* 3: 121-127.
- Freichel, M, Philipp, S, Cavalié, A and Flockerzi, V. 2004. TRPC4 and TRPC4-Deficient Mice. In: *Mammalian TRP Channels as Molecular Targets: Novartis Foundation Symposium, Vol 258.* (Eds) Chadwick DJ and J. Goode, John Wiley & Sons, Ltd, Chichester, UK. 189-99.
- Freichel M, Vennekens R, Olausson J, Slotz S, Philipp SE, Wießgerber P and Flockerzi V. 2005. Functional role of TRPC proteins in native systems: Implications from knockout and knock-down studies. *J Physiol.* 567.1: 59-66.
- Freichel M and Flockerzi V. 2007. Biological functions of TRPs unravelled by spontaneous mutations and transgenic animals. *Biochemical Society Transactions.* 35: 120-123.
- Frey N, McKinsey TA and Olson EN. 2000. Decoding calcium signals involved in cardiac growth and function. *Nature Medicine.* 6: 1221-1227.
- Frey N, Katus HA, Olson EN and Hill JA. 2004. Hypertrophy of the heart: A new therapeutic target? *Circulation.* 109: 1580-1589.
- Friddle CJ, Koga, T, Rubin EM and Bristow J. 2000. Expression profiling reveals distinct sets of genes altered during induction and regression of cardiac hypertrophy. *PNAS.* 97: 6745-6750.
- Gachet C. 2008. P2 receptors, platelet function and pharmacological implications. *Thromb Haemost.* 99: 466-472.
- Galán C, Zbidi H, Bartegi A, Salido GM and Rosado JA. 2009. STIM1, Orai1 and hTRPC1 are important for thrombin- and ADP-induced aggregation in human platelets. *Archives of Biochemistry and Biophysics.* 490: 137-144
- Garcia RL and Schilling WP. 1997. Differential Expression of Mammalian TRP Homologues across Tissues and Cell Lines. *BBRC.* 239: 279-283.

- Gavazzi G, Banfi B, Deffert C, Fiete L, Schappi M, Herrmann F and Krause K-H. 2006. Decreased blood pressure in NOX1-deficient mice. *FEBS Letters*. 580: 497-504.
- Gilio K, Harper MT, Cosemans JMEM, Konopatskaya O, Munnix ICA, Prinzen L, Leitges M, Liu Q, Molkentin JD, Heemskerk JWM and Poole AW. 2010a. Functional divergence of platelet PKC isoforms in thrombus formation on collagen. *JBC*. 285: 23410-23419.
- Gilio K, van Kruchten R, Braun A, Berna-Erro A, Feijge MAH, Stegner D, van der Meijden PEJ, Kuijpers MJE, Varga-Szabo D, Heemskerk JWM and Nieswandt B. 2010b. Roles of platelet STIM1 and Orai1 in Glycoprotein VI- and Thrombin-dependent procoagulant activity and thrombus formation. *JBC*. 285: 23629-23638.
- Glantz AS. 2005. Primer of biostatistics. 6th edition. McGraw-Hill. USA. 520p.
- Goel M, Sinkins WG and Schilling WP. 2002. Selective Association of TRPC Channel Subunits in Rat Brain Synaptosomes. *JBC*. 277: 48303-48310.
- Golde WT, Gollobin P and Rodriguez LL. 2005. A rapid, simple, and humane method for submandibular bleeding of mice using a lancet. *Lab Animal*. 34: 39-43.
- Goshima K. 1969. Synchronized beating of and electronic transmission between myocardial cells mediated by heterotypic strain cells in monolayer culture. *Experimental Cell Research*. 58: 420-426.
- Goshima K. 1974. Initiation of beating in quiescent myocardial cells by norepinephrine, by contact with beating cells and by electrical stimulation of adjacent FL cells. *Experimental Cell Research*. 84: 223-234.
- Grieve DJ, Cave AC and Shah AM. 2006. Cardiac hypertrophy. In: *A handbook of Mouse Models of Cardiovascular Disease*. (Ed.) Xu Q. John Wiley & Sons. West Sussex, England. P 221-233.
- Gronich N, Kumar A, Zhang Y, Efimov IR and Soldatov NM. 2010. Molecular remodeling of ion channels, exchangers and pumps in atrial and ventricular myocytes in ischemic cardiomyopathy. *Channels*. 4: 1-7.
- Grosse J, Braun A, Varga-Szabo D, Beyersdorf N, Schneider B, Zeitlmann L, Hanke P, Schropp P, Mühlstedt S, Zorn C, Huber M, Schmittwolf C, Jagla W, Yu P, Kerkau T, Schulze H, Nehls M and Nieswandt B. 2007. An EF hand mutation in Stim1 causes premature platelet activation and bleeding in mice. *J. Clin. Invest*. 117: 3540-3550.
- Guinamard R and Bois P. 2007. Involvement of transient receptor potential proteins in cardiac hypertrophy. *Biochimica et Biophysica Acta*. 1772: 885-894.
- Gupta S, Das B and Sen S. 2007. Cardiac Hypertrophy: Mechanisms and Therapeutic Opportunities. *Antioxidants and Redox Signaling*. 9: 623-652.
- Gutkind JS and Offermanns S. 2009. A New G_q-Initiated MAPK Signaling Pathway in the Heart. *Developmental Cell*. 16: 163-164.
- Hagedorn I, Vögtle T and Nieswandt B. 2010. Arterial thrombus formation. Novel mechanisms and targets. *Hämostasologie*. 30: 127-135.
- Hagedorn I, Vögtle T and Nieswandt B. 2010. Arterial thrombus formation. Novel mechanisms and targets. *Hämostasologie*. 30: 127-135.

- Hannan RD, Jenkins A, Jenkins AK and Branderburger Y. 2003. Cardiac hypertrophy: A matter of translation. *Clinical and Experimental Pharmacology and Physiology*. 30: 517-527.
- Harada K, Komuro I, Shiojima I, Hayashi D, Kudoh S, Mizuno T, Kijima K, Matsubara H, Sugaya T, Murakami K AND Yazaki Y. 1998. Pressure Overload Induces Cardiac Hypertrophy in Angiotensin II Type 1A Receptor Knockout Mice. *Circulation*. 97: 1952-1959.
- Harper AGS and Sage SO. 2007. A key role for reverse $\text{Na}^+/\text{Ca}^{2+}$ exchange influenced by the actin cytoskeleton in store-operated Ca^{2+} entry in human platelets: Evidence against the de novo conformational coupling hypothesis. *Cell Calcium*. 42: 606-617.
- Harper M and Poole AW. 2010. Protein Kinase C θ Negatively Regulates Store-independent Ca^{2+} Entry and Phosphatidylserine Exposure Downstream of Glycoprotein VI in Platelets. *JBC*. 285: 19865-19873.
- Harper MT, Molkenin JD and Poole AW. 2010 Protein kinase C alpha enhances sodium-calcium exchange during store-operated calcium entry in mouse platelets. *Cell Calcium*. 48: 333-340.
- Harrison P, Briggs C and Machim SJ. 2004. Platelet counting. In: *Methods in Molecular Biology, Vol. 272: Platelets and Megakaryocytes, Vol 1: Functional Assays*. (Eds.) Gibbins JM and Mahaut-Smith MP. Humana Press Inc. NJ, USA. P 29-46.
- Hartmann J, Dragicevic E, Adelsberger H, Henning HA, Sumser M, Abramowitz J, Blum R, Dietrich A, Freichel M, Flockerzi V, Birnbaumer L and Konnerth A. 2008. TRPC3 Channels Are Required for Synaptic Transmission and Motor Coordination. *Neuron*. 59: 392-398.
- Hassock SR, Zhu MX, Trost C, Flockerzi V and Authi KS. 2002. Expression and role of TRPC proteins in human platelets: evidence that TRPC6 forms the store-independent calcium entry channel. *Blood*. 100: 2801-2811.
- Haudek SB, Xia Y, Huebener P, Lee JM, Carlson S, Crawford JR, Pilling D, Gomer RH, Trail J, Frangogiannis NG and Entman ML. 2006. Bone marrow-derived fibroblast precursors mediate ischemic cardiomyopathy in mice. *PNAS*. 48: 18284-18289.
- Hayes JS, Pollock GD and Fuller RW. 1984. *In Vivo* Cardiovascular Responses to Isoproterenol, Dopamine and Tyramine After Prolonged Infusion of Isoproterenol. *The Journal of Pharmacology and Experimental Therapeutics*. 231: 633-639.
- Hechler B, Eckly A, Ohlmann P, Cazenave J-P and Gachet C. 1998. The P2Y₁ receptor, necessary but not sufficient to support full ADP-induced platelet aggregation, is not the target of the drug clopidogrel. *British Journal of Haematology*. 103: 858-866.
- Heineke J and Molkenin JD. 2006. Regulation of cardiac hypertrophy by intracellular signalling pathways. *Nature Reviews*. 7: 589-600.
- Hilal-Dandan R, Kanter JR and Brunton LL. 2000. Characterization of G-protein Signaling in Ventricular Myocytes From the Adult Mouse Heart: Differences From the Rat. *J Mol Cell Cardiol*. 32: 1211-1221.
- Hofmann T, Obukhof AG, Schaefer M, Harteneck C, Gudermann T and Schultz G. 1999. Direct activation of human TRPC6 and TRPC3 channels by diacylglycerol. *Nature*. 397: 259-263.

- Hofmann T, Schaefer M, Schultz G and Gudermann T. 2002. Subunit composition of mammalian transient receptor potential channels in living cells. *PNAS*. 99: 7461-7466.
- Houser SR and Molkentin. 2008. Does Contractile Ca^{2+} control Calcineurin-NFAT signaling and pathological hypertrophy in cardiac myocytes? *Sci Signal*. 1(25) pe 31.
- Houser SR. 2009. Ca^{2+} Signaling Domains Responsible For Cardiac Hypertrophy and Arrhythmias *Circ. Res*. 104: 413-415.
- Huang GN, Zeng W, Kim JY, Yuan JP, Han L, Muallem S and Worley PF. 2006. STIM1 carboxyl-terminus activates native SOC, I(crac) and TRPC1 channels. *Nature Cell Biology*. 8: 1003-1010.
- Huang W-Y, Aramburu J, Douglas PS and Izumo S. 2000. Transgenic expression of green fluorescence protein can cause dilated cardiomyopathy. *Nature Medicine*. 6: 482-483.
- Huentelman MJ, Grobe JL, Vazquez J, Stewart JM, Mecca AP, Katovich MJ, Ferrario CM and Raizada MK. 2005. Protection from angiotensin II-induced cardiac hypertrophy and fibrosis by systemic lentiviral delivery of ACE2 in rats. *Exp Physiol*. 90.5:783-790.
- Hunton DL, Lucchesi PA, Pang Y, Cheng X, Dell'Italia LJ and Marchase RB. 2002. Capacitative Calcium Entry Contributes to Nuclear Factor of Activated T-cells Nuclear Translocation and Hypertrophy in Cardiomyocytes. *JBC*. 277: 14266-14273.
- Hunton DL, Zou LY, Pang Y and Marchase RB. 2004. Adult rat cardiomyocytes exhibit capacitative calcium entry. *Am J Physiol Heart Circ Physiol*. 286: H1124-H1132.
- Iaccarino G, Dolber PC, Lefkowitz RJ and Koch WJ. 1999. β -Adrenergic Receptor Kinase-1 Levels in Catecholamine-Induced Myocardial Hypertrophy Regulation by β - but not α_1 -Adrenergic Stimulation. *Hypertension*. 33: 396-401.
- Ichihara S, Senbonmatsu T, Price E, Ichiki T, Gaffney A and Inagami T. 2001. Angiotensin II Type 2 Receptor Is Essential for Left Ventricular Hypertrophy and Cardiac Fibrosis in Chronic Angiotensin II-Induced Hypertension. *Circulation*. 104: 346-351.
- Inoue R, Jensen LJ, Shi J, Morita H, Nishida M, Honda A and Ito Y. 2006. Transient Receptor Potential Channels in Cardiovascular Function and Disease. *Circ. Res*. 99: 119-131.
- Iwata Y, Katanosaka Y, Arai Y, Komamura K, Miyatake K and Shigekawa M. 2003. A novel mechanism of myocyte degeneration involving the Ca^{2+} -permeable growth factor-regulated channel. *Journal of Cell Biology*. 161: 957-967.
- Jackson SP and Schoenwaelder SM. 2003. Antiplatelet therapy: in search of the "magic bullet". *Nature Reviews Drug Discovery*. 2: 1-15.
- Jackson SP. 2007. The growing complexity of platelet aggregation. *Blood*. 109: 5087-5095.
- Jaffré F, Callebert J, Sarre A, Etienne N, Nebigil CG, Launay J-M, Maroteaux L and Monassier L. 2004. Involvement of the Serotonin 5-HT_{2B} Receptor in Cardiac Hypertrophy Linked to Sympathetic Stimulation. Control of Interleukin-6, Interleukin-1 β , and Tumor Necrosis Factor- α Cytokine Production by Ventricular Fibroblasts. *Circulation*. 110: 969-974.

- Jaffré F, Bonnin P, Callebert J, Debbabi H, Setola V, Doly S, Monassier L, Mettauer B, Blaxall BC, Launay J-M and Maroteaux L. 2009. Serotonin and Angiotensin Receptors in Cardiac Fibroblasts Coregulate Adrenergic-Dependent Cardiac Hypertrophy. *Circ. Res.* 104: 113-123.
- Janssen BJA, De Celle T, Debets JJM, Brouns AE, Callahan MF and Smith TL. 2004. Effects of anesthetics on systemic hemodynamics in mice. *Am J Physiol Heart Circ Physiol.* 287: H1618-H1624.
- Jardín I, Lopez JJ, Salido GM and Rosado JA. 2008a. Orai1 Mediates the Interaction between STIM1 and hTRPC1 and Regulates the Mode of Activation of hTRPC1-forming Ca^{2+} Channels. *JBC.* 283: 25296-25304.
- Jardín I, Redondo PC, Salido GM and Rosado JA. 2008b. Phosphatidylinositol 4,5-Bisphosphate enhances store-operated calcium entry through hTRPC6 channel in human platelets. *Biochimica et Biophysica Acta.* 1783: 84-97.
- Jardín I, Gómez LJ, Salido GM and Rosado JA. 2009. Dynamic interaction of hTRPC6 with the Orai1-STIM1 complex or hTRPC3 mediates its role in capacitative or non-capacitative Ca^{2+} entry pathways. *Biochem J.* 420: 267-276.
- Jarvis GE. 2004. Platelet Aggregation. In: *Methods in Molecular Biology, Vol. 272: Platelets and Megakaryocytes, Vol 1: Functional Assays.* (Eds.) Gibbins JM and Mahaut-Smith MP. Humana Press Inc. NJ, USA. P 65-76.
- Ju H, Scammell- La Fleur T and Dixon IMC. 1996. Altered mRNA Abundance of Calcium Transport Genes in Cardiac Myocytes Induced by Angiotensin II. *J Mol Cell Cardiol.* 28: 1119-1128.
- Ju Y-K, Chu Y, Chaulet H, Lai D, Gervasio OL, Graham RM, Cannell MB and Allen DG. 2007. Store-Operated Ca^{2+} Influx and Expression of TRPC Genes in Mouse Sinoatrial Node. *Circ Res.* 100: 1605-1614.
- Kahn ML, Zheng Y-W, Huang W, Bigornia V, Zeng D, Moff S, Farese Jr RV, Tam C and Coughlin SR. 1998. A dual thrombin receptor system for platelet activation. *Nature.* 394: 690-695.
- Kahn ML, Nakanishi-Matsui M, Shapiro MJ, Ishihara H and Coughlin SR. 1999. Protease-activated receptors 1 and 4 mediate activation of human platelets by thrombin. *J. Clin. Invest.* 103: 879-887.
- Kakkar R and Lee RT. 2010. Intramyocardial Fibroblast Myocyte Communication. *Circ Res.* 106: 47-57.
- Kamouchi M, Philipp S, Flockerzi V, Wissenbach U, Mamin A, Raeymaekers L, Eggermont J, Droogmans G, and Nilius B. 1999. Properties of heterologously expressed hTRP3 channels in bovine pulmonary artery endothelial cells. *Journal of Physiology.* 518:345-358.
- Kato K, Kanaji T, Russell S, Kunicki TJ, Furihata K, Kanaji S, Marchese P, Reininger A, Ruggeri ZM and Ware J. 2003. The contribution of glycoprotein VI to stable platelet adhesion and thrombus formation illustrated by targeted gene deletion. *Blood.* 102:1701-1707.
- Kedzierski R, Grayburn PA, Kisanuki YY, Williams CS, Hammer RE, Richardson JA, Schneider MD and Yanagisawa M. 2003. Cardiomyocyte-Specific Endothelin A Receptor

Knockout Mice Have Normal Cardiac Function and an Unaltered Hypertrophic Response to Angiotensin II and Isoproterenol. *Molecular and Cellular Biology*. 23: 8226-8232.

Keys JR, Greene EA, Koch WJ and Eckhart AD. 2002. G_q-Coupled Receptor Agonists Mediate Cardiac Hypertrophy Via the Vasculature. *Hypertension*. 40: 660-666.

Kilić A, Bubikat A, Gaßner B, Baba HA, Kuhn M. 2007. Local actions of atrial natriuretic peptide counteract Angiotensin II stimulated cardiac remodeling. *Endocrinology*. 148: 4162-4169.

Kim MS, Hong JH, Li Q, Shin DM, Abramowitz J, Birnbaumer L and Muallem S. 2009. Deletion of TRPC3 in mice reduces Store-Operated Ca²⁺ influx and the severity of acute pancreatitis. *Gastroenterology*. 137: 1509-1517.

Kimchi T, Xu J and Dulac C. 2007. A functional circuit underlying male sexual behaviour in the female mouse brain. *Nature*. 448: 1009-1015.

Kinoshita H, Kuwahara K, Nishida M, Jiang Z, Rong X, Kiyonaka S, Kuwabara Y, Kurose H, Inoue R, Mori Y, Li Y, Nakagawa Y, Usami S, Fujiwara M, Yamada Y, Minami T, Ueshima K and Nakao K. 2010. Inhibition of TRPC6 Channel Activity Contributes to the Antihypertrophic Effects of Natriuretic Peptides-Guanylyl Cyclase-A Signaling in the Heart. *Circ Res*. 106: 1849-1860.

Kitagawa Y, Yamashita D, Ito H and Takaki M. 2004. Reversible effects of isoproterenol-induced hypertrophy on in situ left ventricular function in rat hearts. *Am J Physiol Heart Circ Physiol*. 287: H277-H285.

Kiyonaka S, Kato K, Nishida M, Mio K, Numaga T, Sawaguchi Y, Yoshida T, Wakamori M, Mori E, Numata T, Ishii M, Takemoto H, Ojida A, Watanabe K, Uemura A, Kurose H, Morii T, Kobayashi T, Sato Y, Sato C, Hamachi I and Mori Y. 2009. Selective and direct inhibition of TRPC3 channels underlies biological activities of a pyrazole compound. *PNAS*. 106: 5400-5405.

Klaiber M, Kruse M, Völker K, Schröter J, Feil R, Freichel M, Gerling A, Feil S, Dietrich A, **Camacho Londoño JE**, Baba HA, Abramowitz J, Birnbaumer L, Penninger JM, Pongs O and Kuhn M. 2010. Novel insights into the mechanisms mediating the local antihypertrophic effects of cardiac atrial natriuretic peptide: role of cGMP-dependent protein kinase and RGS2. *Basic Res Cardiol*. 105:583–595.

Kobori H, Katsurada A, Miyata K, Ohashi N, Satou R, Saito T, Hagiwara Y, Miyashita K and Navar LG. 2008. Determination of plasma and urinary angiotensinogen levels in rodents by newly developed ELISA. *Am J Physiol Renal Physiol*. 294: F1257-F1263.

Koitabashi N, Aiba T, Hesketh GG, Rowell J, Zhang M, Takimoto E, Tomaselli GF and Kass DA. 2010. Cyclic GMP/PKG-Dependent Inhibition of TRPC6 Channel Activity and Expression Negatively Regulates Cardiomyocyte NFAT Activation. *J Mol Cell Cardiol*. 48: 713-724.

Kudej RK, Mitsunori I, Uechi M, Vatner DE, Oka N, Ishikawa Y, Shannon RP, Bishop SP and Vatner SF. 1997. Effects of Chronic β -Adrenergic Receptor Stimulation in Mice. *J Mol Cell Cardiol*. 29: 2735-2746.

Kunert-Keil C, Bisping F, Kruger J and Brinkmeier H. 2006. Tissue-specific expression of TRP channel genes in the mouse and its variation in three different mouse strains. *BMC Genomics*. 7:159.

- Kuwahara K, Wang Y, McAnally, Richardson JA, Bassel-Duby R, Hill JA and Olson EN. 2006. TRPC6 fulfills a Calcineurin signaling circuit during pathologic cardiac remodeling. *J. Clin. Invest.* 116: 3114-26.
- Kuriso S, Ozono R, Oshima T, Kambe M, Ishida T, Sugino H, Kazuaki C, Teranishi Y, Iba O, Amano K and Matsubara H. 2003. Cardiac Angiotensin II Type 2 Receptor Activates the Kinin/NO System and Inhibits Fibrosis. *Hypertension.* 41: 99-107.
- Landeem LK, Aroonsakool N, Haga JH, Hu BS and Giles WR. 2007. Sphingosine-1-phosphate receptor expression in cardiac fibroblasts is modulated by in vitro culture conditions. *Am J Physiol Heart Circ Physiol.* 292: H2698-H2711.
- Larkin JE, Frank BC, Gaspard RM, Duka I, Gavras H and Quackenbush J. 2004. Cardiac transcriptional response to acute and chronic angiotensin II treatments. *Physiol Genomics.* 18: 152-166.
- Leenen FHH, White R and Yuan B. 2001. Isoproterenol-induced cardiac hypertrophy: role of circulatory versus cardiac renin-angiotensin system. *Am J Physiol Heart Circ Physiol.* 281: H2410-H2416.
- Leng X-H, Hong SY, Larrucea S, Zhang W, Li T-T, López JA and Bray PF. 2004. Platelets of Female Mice Are Intrinsically More Sensitive to Agonists Than Are Platelets of Males. *Arterioscler Thromb Vasc Biol.* 24: 376-381.
- León C, Hechler B, Freund M, Eckly A, Vial C, Ohlmann P, Dierich A, LeMeur M, Cazenave J-P and Gachet C. 1999. Defective platelet aggregation and increased resistance to thrombosis in purinergic P2Y₁ receptor-null mice. *J. Clin. Invest.* 104: 1731-1737.
- León C, Freund M, Ravanat C, Baurand, A, Cazenave J-P and Gachet C. 2001. Key Role of the P2Y₁ Receptor in Tissue Factor-Induced Thrombin-Dependent Acute Thromboembolism Studies in P2Y₁-Knockout Mice and Mice Treated With a P2Y₁ Antagonist. *Circulation.* 103: 718-723.
- Li J, McLerie M and Lopatin AN. 2004a. Transgenic upregulation of I_{K1} in the mouse heart leads to multiple abnormalities of cardiac excitability. *Am J Physiol Heart Circ Physiol.* 287: H2790-H2802.
- Li Z, Zhang G, Marjanovic JA, Ruan C and Du X. 2004b. A Platelet Secretion Pathway Mediated by cGMP-dependent Protein Kinase. *JBC.* 279: 42469-42475.
- Liu D, Maier A, Scholze A, Rauch U, Boltzen U, Zhao Z, Zhu Z and Tepel M. 2008. High Glucose Enhances Transient Receptor Potential Channel Canonical Type 6 (TRPC6)-Dependent Calcium Influx in Human Platelets via Phosphatidylinositol 3-Kinase-Dependent Pathway. *Arterioscler Thromb Vasc Biol.* 28: 746-751.
- Liu F-f, Ma Z-y, Li D-l, Feng J-b, Zhang K, Wang R, Zhang W, Li L and Zhang Y. 2009. Differential expression of TRPC channels in the left ventricle of spontaneously hypertensive rats. *Mol Biol Rep.* 37:2645-2651.
- Liu X, Cheng KT, Bandyopadhyay BC, Pani B, Dietrich A, Paria BC, Swaim WD, Beech D, Yildirim E, Singh BB, Birnbaumer L and Ambudkar IS. 2007. Attenuation of store-operated Ca²⁺ current impairs salivary gland fluid secretion in TRPC1(-/-) mice. *PNAS.* 104: 17542-17547.

- Lockyer S, Okuyama K, Begum S, Le S, Sun B, Watanabe T, Matsumoto Y, Yoshitake M, Kambayashi J and Tandon NN. 2006. GPVI-deficient mice lack collagen responses and are protected against experimentally induced pulmonary thromboembolism. *Thrombosis Research*. 118: 371-380.
- López JJ, Salido GM, Pariente JA and Rosado JA. 2006. Interaction of STIM1 with Endogenously Expressed Human Canonical TRP1 upon Depletion of Intracellular Ca²⁺ Stores. *JBC*. 281: 28254-28264.
- Lucas P, Ukhanov K, Leinders-Zufall T and Zufall F. 2003. A diacylglycerol-gated cation channel in vomeronasal neuron dendrites is impaired in TRPC2 mutant mice: mechanism of pheromone transduction. *Neuron*. 40:551–561
- Maass AH, Ikeda K, Oberdorf-Maass S, Maier SKG and Lainwand LA. 2004. Hypertrophy, Fibrosis, and Sudden Cardiac Death in Response to Pathological Stimuli in Mice With Mutations in Cardiac Troponin T. *Circulation*. 110: 2102-2109.
- Mackman N. 2008. Triggers, targets and treatments for thrombosis. *Nature*. 451: 915-919.
- Maly J, Karasová L, Simová M, Vítko S and El-Dahr SS. 2001. Angiotensin II–Induced Hypertension in Bradykinin B2 Receptor Knockout mice. *Hypertension*. 37: 967-973.
- Masur SK, Dewal HS, Dinh TT, Erenburg I and Petridou S. 1996. Myofibroblasts differentiate from fibroblasts when plated at low density. *PNAS*. 93: 4219-4223.
- Mathar I. 2010. TRPM4- und TRPC1/TRPC4-vermittelte Mechanismen der Blutdruckregulation in Mäusen. Dissertation zur Erlangung des Grades eines Doktors der Naturwissenschaften der Medizinischen Fakultät. Universität des Saarlandes. Pp 99-101.
- Mathar I, Vennekens R, Meissner M, Kees F, Van der Mieren G, **Camacho Londoño JE**, Uhl S, Voets T, Hummel B, Van den Bergh A, Herijgers P, Nilius B, Flockerzi V, Schweda F and Freichel M. 2010. Increased catecholamine secretion contributes to hypertension in TRPM4-deficient mice. *J. Clin. Invest*. 120:3267–3279.
- McRedmond JP, Park SD, Reilly DF, Coppingert JA, Maguire PB, Shields DC and Fitzgerald DJ. 2004. Integration of Proteomics and Genomics in Platelets. *Molecular and Cellular Proteomics*. 3: 133-144.
- Meissner M, Weißgerber P, **Camacho Londoño JE**, Prenen J, Link S, Molkentin JD, Nilius B, Marc Freichel M, Flockerzi V. 2011. Moderate calcium channel dysfunction in adult mice with inducible cardiomyocyte-specific excision of the CACNB2 gene. *JBC*. In press.
- Minke B. 2006. TRP channels and Ca²⁺ signaling. *Cell Calcium*. 40:261-75.
- Mitchell GF, Jeron A and Koren G. 1998. Measurements of heart rate and Q-T interval in the conscious mouse. *Am J Physiol Heart Circ Physio*. 274: H747-H751.
- Molkentin JD, Lu, J-R, Antos CL, Markham B, Richardson J, Robbins J, Grant SR and Olson EN. 1998. A Calcineurin-Dependent Transcriptional Pathway for Cardiac Hypertrophy. *Cell*. 93: 215-228.
- Molkentin JD and Dorn II GW. 2001. Cytoplasmic Signaling Pathways that regulate cardiac hypertrophy. *Annu. Rev. Physiol*. 63: 391-426.

- Molkentin JD. 2006. Dichotomy of Ca^{2+} in the heart: contraction versus intracellular signaling. *J. Clin. Invest.* 116: 623-626.
- Monassier L, Laplante M-A, Jaffré F, Bousquet P, Maroteaux L and de Champlain J. 2008. Serotonin 5-HT_{2B} Receptor Blockade Prevents Reactive Oxygen Species-Induced Cardiac Hypertrophy in Mice. *Hypertension.* 52: 1-7.
- Montell C and Rubin GM. 1989. Molecular Characterization of the *Drosophila* trp locus: A Putative Integral Membrane Protein Required for Phototransduction. *Neuron.* 2: 1313-1323.
- Montell C. 2005. The TRP Superfamily of Cation Channels. *Sci. STKE.* 272: Re3.
- Moser L, Faulhaber J, Wiesner R and Ehmke H. 2002. Predominant activation of endothelin-dependent cardiac hypertrophy by norepinephrine in rat left ventricle. *Am J Physiol Regulatory Integrative Comp Physiol.* 282: R1389-1394.
- Müller JG, Nemoto S, Laser M, Carabello BA and Menick DR. 1998. Calcineurin Inhibition and Cardiac Hypertrophy. *Science.* 282: 107a
- Munsch T, Freichel M, Flockerzi V and Pape H-C. 2003. Contribution of transient receptor potential channels to the control of GABA release from dendrites. *PNAS.* 100: 16065-16070.
- Muth JN, Yamaguchi H, Mikala G, Grupp IL, Lewis W, Cheng H, Song L-S, Lakatta EG, Varadi G and Schwartz A. 1999. Cardiac-specific Overexpression of the α_1 Subunit of the L-type Voltage-dependent Ca^{2+} Channel in Transgenic Mice. *JBC.* 274: 21503-21506.
- Muth JN, Bodi I, Lewis W, Varadi G and Schwartz A. 2001. A Ca^{2+} -Dependent Transgenic Model of Cardiac Hypertrophy. A Role for Protein Kinase C α . *Circulation.* 103: 140-147.
- Nagano M, Higaki J, Nakamura F, Higashimori K, Nagano N, Mikami H and Ogihara T. 1992. Role of cardiac angiotensin II in isoproterenol-induced left ventricular hypertrophy. *Hypertension.* 19: 708-712.
- Nakanishi-Matsui M, Zheng Y-W, Sulciner DJ, Weiss EJ, Ludeman MJ and Coughlin SR. 2000. PAR3 is a cofactor for PAR4 activation by thrombin. *Nature.* 404: 609-613.
- Nakayama H, Wilkin BJ, Bodi I and Molkentin JD. 2006. Calcineurin-dependent cardiomyopathy is activated by TRPC in the adult mouse heart. *The FASEB Journal.* 20: 1660-1670.
- Nakayama H, Chen X, Baines CP, Klevitsky R, Zhang X, Zhang H, Jaleel N, Chua BHL, Hewett TE, Robbins J, Houser SR and Molkentin JD. 2007. Ca^{2+} - and mitochondrial-dependent cardiomyocyte necrosis as a primary mediator of heart failure. *J. Clin. Invest.* 117: 2431-2444.
- Nesbitt WS, Giuliano S, Kalkarni S, Dopheide SM, Harper IS and Jackson SP. 2003. Intercellular calcium communication regulates platelet aggregation and thrombus growth. *Journal of Cellular Biology.* 160: 1151-1161.
- Nieswandt B, Schulte V, Zywertz A, Gratacap M-P and Offermanns S. 2002. Costimulation of G_I- and G₁₂/G₁₃-mediated Signaling Pathways Induces Integrin $\alpha_{1b}\beta_3$ Activation in Platelets. *JBC.* 277: 39493-39498.

- Nieswandt B, Aktas B, Moers A and Sachs UJH. 2005. Platelets in atherothrombosis: lessons from mouse models. *Journal of Thrombosis and Haemostasis*. 3: 1725-1736.
- Niizeki T, Takeishi Y, Kitahara T, Arimoto T, Ishino M, Bilim O, Suzuki S, Sasaki T, Nakajima O, Walsh RA, Goto K and Kubota I. 2008. Diacylglycerol kinase- ϵ restores cardiac dysfunction under chronic pressure overload: A new specific regulator of $G\alpha_q$ signaling cascade. *Am J Physiol Heart Circ Physiol*. 295: H245-H255.
- Nilius B and Owsianik G. 2010. Transient receptor potential channelopathies. *Pflügers Arch - Eur J Physiol*. 460: 437-450.
- Nishida M, Onohara N, Sato Y, Suda R, Ogushi M, Tanabe, S, Inoue R, Mori Y and Kurose H. 2007. $G\alpha_{12/13}$ -Mediated upregulation of TRPC6 negatively regulates endothelin-1-induced cardiac myofibroblast formation and collagen synthesis through NFAT activation. *JBC*. 282: 23117-23128.
- Nishida M and Kurose H. 2008. Roles of TRP channels in the development of cardiac hypertrophy. *Naunyn-Schmiedeberg's Arch Pharmacol*. 378: 395-406.
- Nishida M, Watanabe K, Sato Y, Nakaya M, Kitajima N, Ide T, Inoue R and Kurose H. 2010. Phosphorylation of TRPC6 channels at Thr⁶⁹ is required for anti-hypertrophic effects of phosphodiesterase 5 inhibition. *JBC*. 285: 13244-13253.
- O'Connell TD, Ni YG, Lin K-M, Han H and Yan Z. 2003. Isolation and Culture of Adult Mouse Cardiac Myocytes for Signaling Studies. *AfCS Research Reports*. Vol. 1No. 5 CM.
- Offermanns S, Toombs CF, hu Y-H and Simon M. 1997. Defective platelet activation in $G\alpha_q$ -deficient mice. *Nature*. 389: 183-186.
- Offermanns S. 2006. Activation of Platelet Function Through G Protein-Coupled Receptors. *Circ Res*. 99: 1293-1304.
- Ohba T, Watanabe H, Takahashi Y, Suzuki T, Miyoshi I, Nakayama S, Satoh E, Iino K, Sasano, H, Mori Y, Kuromitsu Y, Imagawa K, Saito Y, Iijima T, Ito H and Murukami M. 2006. Regulatory role of neuron-restrictive silencing factor in expression of TRPC1. *BBCR*. 351: 764-770.
- Ohba T, Watanabe H, Murukami M, Takahashi Y, Iino K, Kuromitsu S, Mori Y, Ono K, Iijima T and Ito H. 2007. Upregulation of TRPC1 in the development of cardiac hypertrophy. *J Mol Cell Cardiol*. 42: 498-507.
- Okada T, Shimizu S, Wakamori M, Maeda A, Kurosaki T, Takada N, Imoto K and Mori Y. 1998. Molecular cloning and functional characterization of a novel receptor-activated TRP Ca^{2+} channel from mouse brain. *JBC*. 273:10279-10287.
- Okada T, Inoue R, Yamazaki K, Maeda A, Kurosaki T, Yamakuni T, Tanak I, Shimizu S, Ikenaka K, Imoto K and Mori Y. 1999. Molecular and Functional Characterization of a Novel Mouse Transient Receptor Potential Protein Homologue TRP7. Ca^{2+} -permeable cation channel that is constitutively activated and enhanced by stimulation of G protein-coupled receptor. *JBC*. 274: 27359-27370.
- Olivetti G, Cigola E, Maestri R, Lagrasta C, Corradi D and Quaini F. 2000. Recent advances in cardiac hypertrophy. *Cardiovascular Research*. 45: 68-75.

- Olson ER, Shamhart PE, Naugle JE and Meszaros JG. 2008. Angiotensin II–Induced Extracellular Signal–Regulated Kinase 1/2 Activation Is Mediated by Protein Kinase C δ and Intracellular Calcium in Adult Rat Cardiac Fibroblasts. *Hypertension*. 51: 704-711.
- Onohara N, Nishida M, Inoue R, Kobayashi H, Sumimoto H, Sato Y, Mori Y, Nagao T and Kurose H. 2006. TRPC3 and TRPC6 are essential for angiotensin II-induced cardiac hypertrophy. *The EMBO JOURNAL*. 25: 5305-5316.
- Ostrom RS, Naigles JE, Hase M, Gregorian C, Swaney JS, Insel PA, Brunton LL and Meszaros JG. 2003. Angiotensin II Enhances Adenylyl Cyclase Signaling via Ca²⁺/Calmodulin. G_i-G_s CROSS-TALK REGULATES COLLAGEN PRODUCTION IN CARDIAC FIBROBLASTS. *JBC*. 278: 24461-24468.
- Parekh AB and Putney Jr JW. 2005. Store-Operated Calcium Channels. *Physiol Rev*. 85: 757-810.
- Parekh AB. 2010. Store-operated CRAC channels: function in health and disease. *Nature Reviews*. 9: 399-410.
- Park H-S and Hourani SMO 1999. Differential effects of adenine nucleotide analogues on shape change and aggregation induced by adenosine 5'-diphosphate (ADP) in human platelets. *British Journal of Pharmacology*. 127: 1359-1366.
- Patterson AJ, Zhu W, Chow A, Agrawal R, Kosek J, Xiao RP and Kobilka B. 2004. Protecting the myocardium: A role for the β 2 adrenergic receptor in the heart. *Crit Care Med*. 32: 1041-1048.
- Patterson AJ, Zhu W, Chow A, Agrawal R, Kosek J, Xiao RP and Kobilka B. 2004. Protecting the myocardium: A role for the β 2 adrenergic receptor in the heart. *Crit Care Med*. 32: 1041-1048.
- Pedersen SF, Owsianik G and Nilus B. 2005. TRP channels: An overview. *Cell Calcium*. 38: 233-252.
- Peters LL, Cheever EM, Ellis HR, Magnani PA, Stevenson KL, Von Smith R and Bogue MA. 2006. Large-scale, high-throughput screening for coagulation and hematologic phenotypes in mice. *Physiol Genomics*. 11: 185-193.
- Philipp S, Cavalié A, Freichel M, Wissenbach U, Zimmer S, Trost C, Marguart A, Murakami M and Flockerzi V. 1996. A mammalian capacitative calcium entry channel homologous to Drosophila TRP and TRPL. *The EMBO JOURNAL*. 15:6166–6171.
- Phillips DR, Conley PB, Sinha U and Andre P. 2005. Therapeutic approaches in arterial thrombosis. *Journal of Thrombosis and Haemostasis*. 3: 1577-1589.
- Phillips PA. 1999. Interaction between Endothelin and Angiotensin II. *Clinical and Experimental Pharmacology and Physiology*. 26: 517-518.
- Pillai JB, Gupta M, Rajamohan SB, Lang R, Raman J and Gupta MP. 2006. Poly(ADP-ribose) polymerase-1-deficient mice are protected from angiotensin II-induced cardiac hypertrophy. *Am J Physiol Heart Circ Physiol*. 291: H1545-H1553.
- Reid AC, Silver R and Levi R. 2007. Renin: at the heart of the mast cell. *Immunological Reviews*. 217: 123–140.

- Riccio A, Li Y, Moon J, Kim K-S, Smith KS, Rudolph U, Gapon S, Yao GL, Tsvetkov S, Rodig SJ, Van't Veer A, Meloni EG, Carlezon Jr. WA, Bolshakov VY and Clapham DE. 2009. Essential Role for TRPC5 in Amygdala Function and Fear-Related Behavior. *Cell*. 137: 761-772.
- Rink TJ and Sage SO. 1990. Calcium Signaling in Human Platelets. *Annu. Rev. Physiol.* 52: 431-439.
- Ritchie R and Delbridge LMD. 2006. Cardiac Hypertrophy, substrate utilization and metabolic remodelling: Cause or effect? *Clinical and Experimental Pharmacology and Physiology*. 33: 159-166.
- Roberts DE, McNicol A and Bose R. 2004. Mechanism of Collagen Activation in Human Platelets. *JBC*. 279: 19421-19430.
- Roderick HL, Higazi DR, Smyrnias I, Fearnley C, Harzheim D and Bootman MD. 2007. Calcium in the heart: when it's good, it's very very good, but when it's bad, it's horrid. *Biochemical Society Transactions*. 35: 957-961.
- Rosado JA and Sage SO. 2000a. Protein kinase C activates non-capacitative calcium entry in human platelets. *J. Physiol.* 529: 159-169.
- Rosado JA and Sage SO. 2000b. Coupling between inositol 1,4,5-trisphosphate receptors and human transient receptor potential channel 1 when intracellular Ca^{2+} stores are depleted. *Biochem. J.* 350: 631-635.
- Rosado JA and Sage SO. 2001. Activation of store-mediated calcium entry by secretion-like coupling between the inositol 1,4,5-trisphosphate receptor type II and human transient receptor potential (hTrp1) channels in human platelets. *Biochem. J.* 356: 191-198.
- Rosado JA and Sage SO. 2002. The ERK Cascade, a New Pathway Involved in the Activation of Store-Mediated Calcium Entry in Human Platelets. *Trends in Cardiovasc Med.* 12: 229-234.
- Rosado JA, Brownlow SL and Sage SO. 2002. Endogenously Expressed Trp1 Is Involved in Store-mediated Ca^{2+} Entry by Conformational Coupling in Human Platelets. *JBC*. 277: 42157-42163.
- Rosado JA, López JJ, Harper AG, Harper MT, Redondo PC, Pariente JA, Sage SO and Salido GM. 2004. Two Pathways for Store-mediated Calcium Entry Differentially Dependent on the Actin Cytoskeleton in Human Platelets. *JBC*. 279: 29231-29235.
- Rose RA, Hatano N, Ohya S and Giles WR. 2007. C-type natriuretic peptide activates a non-selective cation current in acutely isolated rat cardiac fibroblasts via natriuretic peptide C receptor-mediated signalling. *J. Physiol.* 580.1: 255-274.
- Rothermel BA, McKinsey TA, Vega RB, Nicol RL, Mammen P, Jang J, Antos CL, Shelton JM, Bassel-Duby R, Olson EN and Williams RS. 2000. Myocyte-enriched calcineurin-interacting protein, MCIP1, inhibits cardiac hypertrophy *in vivo*. *PNAS*. 98: 3328-3333.
- Saadane N, Alpert L and Chalifour LE. 2000. Altered molecular response to adrenoreceptor-induced cardiac hypertrophy in Egr-1-deficient mice. *Am. J. Physiol. Heart Circ. Physiol.* 278: H796-H805.
- Sage SO. 1997. Calcium entry mechanisms in human platelets. *Experimental Physiology*. 82: 807-823.

- Sage SO, Brownlow SL and Rosado JA. 2002. TRP channels and calcium entry in human platelets. *Blood*. 100: 4245-4247
- Samaha FF and Kahn ML. 2006. Novel Platelet and Vascular Roles for Immunoreceptor Signaling. *Arterioscler Thromb Vasc Biol*. 26: 2588-2593.
- Sambrano GR, Weiss EJ, Zheng Y-W, Huang W and Coughlin SR. 2001. Role of thrombin signalling in platelets in haemostasis and thrombosis. *Nature*. 413: 74-78.
- Satoh S, Tanaka H, Ueda Y, Oyama J-i, Sugano M, Sumimoto H, Mori Y, Makino N. 2007. Transient receptor potential (TRP) protein 7 acts as a G protein-activated Ca^{2+} channel mediating angiotensin II-induced myocardial apoptosis. *Molecular and Cellular Biochemistry*. 294: 205-215.
- Savi P, Herbert JM, Pflieger AM, Dol F, Delebasse D, Combalert J, Defreyn G and Maffrand JP. 1992. Importance of hepatic metabolism in the antiaggregating activity of the thienopyridine clopidogrel. *Biochemical Pharmacology*. 44: 527-532.
- Savi P and Herbert J-M. 1996. ADP Receptors on Platelets and ADP-Selective Antiaggregating Agents. *Medicinal Research Reviews*. 16: 159-179.
- Schaefer M, Plant TD, Obukhov AG, Hofmann T, Gudermann T and Schultz G. 2000. Receptor mediated regulation of the nonselective cation channels TRPC4 and TRPC5. *JBC*. 275:17517-17526.
- Schmidt K, Dubrovskaja G, Nielsen G, Fesüs G, Uhrenholt TR, Hansen PB, Gudermann T, Dietrich A, Gollasch M, de Wit C and Köhler R. 2010. Amplification of EDHF-type vasodilatations in TRPC1-deficient mice. *British Journal of Pharmacology*. 161: 1722-1733.
- Schulze-Bahr E and Breithardt G. 2005. Short QT Interval and Short QT Syndromes. *J Cardiovasc Electrophysiol*. 16: 397-398.
- Schütze K and Lahr G. 1998. Identification of expressed genes by laser-mediated manipulation of single cells. *Nature Biotechnology*. 16: 737-742.
- Sel S, Rost BR, Yildirim AÖ, Sel B, Kalwa H, Fehrenbach H, Renz H, Gudermann T and Dietrich A. 2008. Loss of classical transient receptor potential 6 channel reduces allergic airway response. *Clinical and Experimental Allergy*. 38: 1548-1558.
- Seth M, Sumbilla C, Mullen SP, Lewis D, Klein MG, Hussain A, Soboloff J, Gill DL and Inesi G. 2004. Sarco(endo)plasmic reticulum Ca^{2+} ATPase (SERCA) gene silencing and remodeling of the Ca^{2+} signaling mechanism in cardiac myocytes. *PNAS*. 101: 16683-16688.
- Seth M, Zhang Z-S, Mao L, Graham V, Burch J, Stiber J, Tsiokas L, Winn M, Abramowitz J, Rockman HA, Birnbaumer L and Rosenberg. 2009. TRPC1 Channels Are Critical for Hypertrophic Signaling in the Heart. *Circ. Res*. 105:1020-1030.
- Shan D, Marchase RB and Chatham JC. 2008. Overexpression of TRPC3 increases apoptosis but not necrosis in response to ischemia/reperfusion in adult mouse cardiomyocytes. *Am J Physiol Cell Physiol*. 294: 833-841.
- Shen W-H, Chen Z, Shi S, Chen H, Zhu W, Penner A, Nu G, Li W, Boyle DW, Rubart M, Field LJ, Abraham R, Liechty EA and Shou W. 2008. Cardiac Restricted Overexpression

of Kinase-dead Mammalian Target of Rapamycin (mTOR) Mutant Impairs the mTOR-mediated Signaling and Cardiac Function. *JBC*. 283: 13842-13849.

Shizukuda Y, Buttrick PM, Geenen DL, Borczuk AC, Kitsis RN and Sonnenblick EH. 1998. β -Adrenergic stimulation causes cardiocyte apoptosis: influence of tachycardia and hypertrophy. *Heart Circ. Physiol*. 44: H961-H968

Shumilina E, Lampert A, Lupescu A, Myssina S, Strutz-Seebohm N, Henke G, Grahmmer F, Wulff P, Kuhl D and Lang F. 2005. Deranged Kv Channel Regulation in Fibroblasts From Mice Lacking the Serum and Glucocorticoid Inducible Kinase SGK1. *Journal of Cellular Physiology*. 204: 87-98.

Singh A, Hildebrand, Garcia E and Snutch TP. 2010. The transient receptor potential channel antagonist SKF96365 is a potent blocker of low-voltage-activated T-type calcium channels. *British Journal of Pharmacology*. 160: 1464-1475.

Smyth SS, Woulfe DS, Weitz JI, Gachet C, Conley PB, Goodman SG, Roe MT, Kuliopulos A, Moliterno DJ, French PA, Steinhubl SR and Becker RC. 2009. G-Protein-Coupled Receptors as Signaling Targets for Antiplatelet Therapy. *Arterioscler Thromb Vasc Biol*. 29:449-457.

Snider P, Satndley KN, Wang J, Azhar M, Doetschman T and Conway SJ. 2009. Origin of Cardiac Fibroblasts and the Role of Periostin. *Circ Res*. 105: 934-947.

Song K, Backs J, McAnally J, Qi X, Gerard RD, Richardson JA, Hill JA, Bassel-Duby R and Olson EN. 2006. The Transcriptional Coactivator CAMTA2 Stimulates Cardiac Growth by Opposing Class II Histone Deacetylases. *Cell*. 125: 453-466.

Sours-Brothers S, Ding M, Graham S and Ma R. 2009. Interaction between TRPC1/TRPC4 assembly and STIM1 contributes to Store-operated Ca^{2+} entry in mesangial cells. *Experimental Biology and Medicine*. 234:673-682.

Souders CA, Bowers SLK and Baudino TA. 2009. Cardiac Fibroblast. The Renaissance Cell. *Circ. Res*. 105: 1164-1176.

Stagg MA, Malik AH, MacLeod KT and Terracciano CMN. 2004. The effects of overexpression of the $\text{Na}^+/\text{Ca}^{2+}$ exchanger on calcium regulation in hypertrophied mouse cardiac myocytes. *Cell Calcium*. 36: 111-118.

Stowers L, Holy TE, Meister M, Dulac C and Koentges G. 2002. Loss of sex discrimination and male-male aggression in mice deficient for TRP2. *Science*. 295: 1493-1500.

Strübing C, Krapivinsky G, Krapivinsky L and Clapham DE. 2001. TRPC1 and TRPC5 Form a Novel Cation Channel in Mammalian Brain. *Neuron*. 29: 645-655.

Sucharov CC and Bristow MR. 2005. TRPC Channels and β 1-Adrenergic-Mediated Activation of Fetal Gene Program. (2nd Annual Symposium of the American Heart Association Council on Basic Cardiovascular Sciences). *Circ. Res*. 97: e9-e50 (abstract).

Suh SH, Vennekens R, Manolopoulos VG, Freichel M, Schweig U, Prenen J, Flockerzi V, Droogmans G and Nilius B. 1999. Characterisation of explanted endothelial cells from mouse aorta: electrophysiology and Ca^{2+} signalling. *Pflügers Arch - Eur J Physiol*. 438: 612-620.

Sugden PH and Clerk A. 1998. Cellular mechanisms of cardiac hypertrophy. *J Mol Med*. 76: 725-746.

- Sussman MA, Lim HW, Gude N, Taigen T, Olson EN, Robbins J, Colbert MC, Gualberto A, Wieczorek DF and Molkentin JD. 1998. Prevention of Cardiac Hypertrophy in Mice by Calcineurin Inhibition. *Science*. 281:1690-1693.
- Tandan S, Wang Y, Wang TT, Jiang N, Hall DD, Hell JW, Luo X, Rothermel BA and Hill JA. 2009. Physical and Functional Interaction Between Calcineurin and the Cardiac L-Type Ca^{2+} Channel. *Circ. Res.* 105: 51-60.
- Tang C-M and Insel PA. 2004. GPCR expression in the heart. *TCM*. 14: 94-99.
- Tavi P, Pikkarainen S, Ronkainen J, Niemelä P, Ilves M, Weckström M, Vuolteenaho O, Bruton J, Westerblad H and Ruskoaho H. 2004. Pacing-induced calcineurin activation controls cardiac Ca^{2+} signalling and gene expression: *J Physiol*. 554.2: 309-320.
- Thomas DW, Mannon RB, Mannon PJ, Latour A, Oliver JA, Hoffmann M, Smithies O, Koller BH and Coffman TM. 1998. Coagulation Defects and Altered Hemodynamic Responses in Mice Lacking Receptors for Thromboxane A_2 . *J. Clin. Invest.* 102: 1994-2001.
- Thum T, Gross C, Fiedler J, Fischer T, Kissler S, Bussen M, Galuppo P, Just S, Rottbauer W, Frantz S, Castoldi M, Soutschek J, Koteliensky V, Rosanwald A, Basson MA, Licht JD, Pena JTR, Rouhanifard SH, Muckenthaler MU, Tuschl T, Martin GR, Bauersachs J and Engelhardt S. 2008. MicroRNA-21 contributes to myocardial disease by stimulating MAP kinase signalling in fibroblasts. *Nature*. 456: 980-986.
- Tiruppathi C, Freichel M, Vogel SM, Paria BC, Mehta D, Flockerzi V and Malik AB. 2002. Impairment of Store-Operated Ca^{2+} Entry in TRPC4-/- Mice Interferes With Increase in Lung Microvascular Permeability. *Circ Res*. 91: 70-76.
- Tolhurst G, Vial C, Léon C, Gachet C, Evans RJ and Mahaut-Smith MP. 2005. Interplay between $P2Y_1$, $P2Y_{12}$, and $P2X_1$ receptors in the activation of megakaryocyte cation influx currents by ADP: evidence that the primary megakaryocyte represents a fully functional model of platelet P2 receptor signaling. *Blood*. 106: 1644-1651.
- Tolhurst G, Carter RN, Amisten S, Holdich JP, Erlinge D and Mahaut-Smith MP. 2008. Expression profiling and electrophysiological studies suggest a major role for Orai1 in the store-operated Ca^{2+} influx pathway of platelets and megakaryocytes. *Platelets*. 19: 308-313.
- Toko H, Shiojima I and Komuro I. 2007. Promotion of cardiac hypertrophy by TRPC-mediated calcium entry. *J Mol Cell Cardiol*. 42: 481-483.
- Tokudome T, Kishimoto I, Horio T, Arai Y, Schwenke DO, Hino J, Okano I, Kawano Y, Kohno M, Miyazato M, Nakao K and Kangawa K. 2008. Regulator of G-Protein Signaling Subtype 4 Mediates Antihypertrophic Effect of Locally Secreted Natriuretic Peptides in the Heart. *Circulation*. 117: 2329-2339.
- Tozakidou M, Goltz D, Hagenström T, Budack MK, Vitzthum H, Szlachta K, Bähring R and Ehmke H. 2010. Molecular and functional remodeling of Ito by angiotensin II in the mouse left ventricle. *J Mol Cell Cardiol*. 48: 140-151.
- Trebak M, Lemonnier L, Smyth JT, Vazquez G and Putney Jr. JW. 2007. Phospholipase C-Coupled Receptors and Activation of TRPC Channels. *Handb Exp Pharmacol*. 179: 593-614.

- Tsvilovskyy VV, Zholos AV, Aberle T, Philipp SE, Dietrich A, Zhu MX, Birnbaumer L, Freichel M and Flockerzi V. 2009. Deletion of TRPC4 and TRPC6 in Mice Impairs Smooth Muscle Contraction and Intestinal Motility In Vivo. *Gastroenterology*. 137: 1415-1424.
- Van Berlo JH, Elrod JW, van den Hoogenhof MMG, York AJ, Aronow BJ, Duncan SA and Molkenin JD. 2010. The Transcription Factor GATA-6 Regulates Pathological Cardiac Hypertrophy. *Circ. Res.* 107: 1032-1040.
- Vandecasteele G, Eschenhagen T, Scholz H, Stein B, Verde I and Fischmeister R. 1999. Muscarinic and β -adrenergic regulation of heart rate, force of contraction and calcium current is preserved in mice lacking endothelial nitric oxide synthase. *Nature Medicine*. 5: 331-334.
- Van Rooij E, Doevendans PA, de Theije CC, Babiker FA, Molkenin JD and De Windt LJ. 2002. Requirement of Nuclear Factor of Activated T-cells in Calcineurin-mediated Cardiomyocyte Hypertrophy. *JBC*. 277: 48617-48626.
- Varga-Szabo Braun A, Kleinschnitz C, Bender M, Pleines I, Pham M, Renné T, Stoll G and Nieswandt B. 2008a. The calcium sensor STIM1 is an essential mediator of arterial thrombosis and ischemic brain infarction. *J. Exp. Med.* 205: 1583-1591.
- Varga-Szabo D, Authi KS, Braun A, Bender M, Ambily A, Hassock SR, Gudermann T, Dietrich A and Nieswandt B. 2008b. Store-operated Ca^{2+} entry in platelets occurs independently of transient receptor potential (TRP) C1. *Pflügers Arch - Eur J Physiol*. 457: 377-87.
- Vega RB, Rothermel BA, Weinheimer CJ, Kovacs A, Naseem RH, Bassel-Duby, Williams RS and Olson EN. 2003. Dual roles of modulatory calcineurin-interacting protein 1 in cardiac hypertrophy. *PNAS*. 100: 669-674.
- Venkatachalam K and Montell C. 2007. TRP channels. *Annu. Rev. Biochem.* 76: 387-417.
- Viero C, Kraushaar U, Ruppenthal S, Kaestner L and Lipp P. 2008. A primary culture system for sustained expression of a calcium sensor in preserved adult rat ventricular myocytes. *Cell Calcium*. 43:59-71.
- Vindis C, D'Angelo R, Mucher E, Nègre-Salvayre A, Parini A, Mialet-Perez J. 2010. Essential role of TRPC1 channels in cardiomyoblasts hypertrophy mediated by 5-HT_{2A} serotonin receptors. *BBRC*. 391: 979-983.
- Wakabayashi I, Marumo M, Graziani A, Poteser M and Groschner K. 2006. TRPC4 expression determines sensitivity of the platelet-type capacitance Ca^{2+} entry channel to intracellular alkalosis. *Platelets*. 17: 454-461.
- Walther DJ, Peter J-U, Winter S, Höltje M, Paulmann N, Grohmann M, Vowinkel J, Alamo-Bethencourt V, Wilhelm CS, Ahnert G and Bader M. 2003. Serotonylation of Small GTPases Is a Signal Transduction Pathway that Triggers Platelet α -Granule Release. *Cell*. 115: 851-862.
- Wang H, Oestreich EA, Maekawa N, Bullard TA, Vikstrom KL, Dirksen RT, Kelley GG, Blaxall BC and Smrcka AV. 2005. Phospholipase C ϵ Modulates β -Adrenergic Receptor-Dependent Cardiac Contraction and Inhibits Cardiac Hypertrophy. *Circ Res*. 97: 1305-1313.

- Wang J, Chen H, Seth A and McCulloch CA. 2003. Mechanical force regulation of myofibroblast differentiation in cardiac fibroblasts. *Am J Physiol Heart Circ Physiol.* 285: H1871-1881.
- Watanabe H, Murakami M, Ohba T, Ono K and Ito H. 2009. The Pathological Role of Transient Receptor Potential Channels in Heart Disease. *Circ J.* 73: 419-427.
- Watson SP, Asazuma N, Atkinson B, Berlanga O, Best D, Bobe R, Jarvis G, Marshall S, Snell D, Stafford M, Tulasne D, Wilde J, Wonerow P and Frampton J. 2001. The Role of ITAM- and ITIM-coupled Receptors in Platelet Activation by Collagen. *Thromb Haemost.* 86: 276-288.
- Weber A-A, Reimann S and Schör K. 1999. Specific inhibition of ADP-induced platelet aggregation by clopidogrel in vitro. *British Journal of Pharmacology.* 126: 415-420.
- Weiss EJ, Hamilton JR, Lease KE, Coughlin SR. 2002. Protection against thrombosis in mice lacking PAR3. *Blood.* 100: 3240-3244.
- Weissgerber P, Held B, Bloch W, Kaestner L, Chien KR, Fleischmann BK, Lipp P, Flockerzi V and Freichel M. 2006. Reduced Cardiac L-Type Ca^{2+} Current in $Ca_v\beta 2^{-/-}$ Embryos Impairs Cardiac Development and Contraction With Secondary Defects in Vascular Maturation. *Circ. Res.* 99: 749-757.
- Weissmann N, Dietrich A, Fuchs B, Kalwa H, Ay M, Dumitrascu R, Olschewski A, Storch U, Mederos y Schnitzler M, Ghofrani HA, Schermuly RT, Pinkenburg O, Seeger W, Grimminger F and Gudermann T. 2006. Classical transient receptor potential channel 6 (TRPC6) is essential for hypoxic pulmonary vasoconstriction and alveolar gas exchange. *PNAS.* 103: 19093-19098.
- Wettschureck N, Rütten H, Zywietz A, Gehring D, Wilkie TM, Chen J, Chien KR and Offermanns S. 2001. Absence of pressure overload induced myocardial hypertrophy after conditional inactivation of $G\alpha_q/G\alpha_{11}$ in cardiomyocytes. *Nature Medicine.* 7: 1236-1240.
- Wettschureck N and Offermanns S. 2005. Mammalian G proteins and Their Cell Type Specific Functions. *Physiol Rev.* 85: 1159-1204.
- Wilkins BJ and Molkentin JD. 2002. Calcineurin and cardiac hypertrophy: Where have we been? Where are we going? *Journal of Physiology.* 541.1: 1-8.
- Wilkins BJ, De Windt LJ, Bueno OF, Braz JC, Glascock BJ, Kimball TF and Molkentin JD. 2002. Targeted Disruption of *NFATc3*, but Not *NFATc4*, Reveals an Intrinsic Defect in Calcineurin-Mediated Cardiac Hypertrophic Growth. *Molecular and Cellular Biology.* 22: 7603-7613.
- Wilkins BJ and Molkentin JD. 2004. Calcium–calcineurin signaling in the regulation of cardiac hypertrophy. *BBRC.* 322: 1178-1191.
- Wilkins BJ, Dai Y-S, Bueno OF, Parsons SA, Xu J, Plank DM, Jones F, Kimball TR and Molkentin JD. 2004. Calcineurin/NFAT Coupling Participates in Pathological, but not Physiological, Cardiac Hypertrophy. *Circ Res.* 94: 110-118.
- Wittköpper K, Fabritz L, Neef S, Ort KR, Grefe C, Unsöld B, Kirchhof P, Maier LS, Hasenfuss G, Dobrev D, Eschenhagen T and El-Armouche A. 2010. Constitutively active phosphatase inhibitor-1 improves cardiac contractility in young mice but is deleterious after catecholaminergic stress and with aging. *J. Clin. Invest.* 120: 617-626.

- Woulfe D, Yang J, Prevost N, O'Brien P, Fortna R, Tognolini M, Jiang H, Wu J and Brass LF. 2004. Signaling Receptors on Platelets and Megakaryocytes. In: *Methods in Molecular Biology, Vol. 273: Platelets and Megakaryocytes, Vol 2: Perspectives and Techniques*. (Eds.) Gibbins JM and Mahaut-Smith MP. Humana Press Inc. NJ, USA. P 3-31.
- Wu L-J, Sweet T-B and Clapham DE. 2010a. International Union of Basic and Clinical Pharmacology. LXXVI. Current Progress in the Mammalian TRP Ion Channel Family. *Pharmacological Reviews*. 62: 381-404.
- Wu X, Zhang T, Bossuyt J, Li X, McKinsey TA, Dedman JR, Olson EN, Chen J, Brown JH and Bers DM. 2006. Local InsP₃-dependent perinuclear Ca²⁺ signaling in cardiac myocyte excitation-transcription coupling. *J. Clin. Invest.* 116: 675-682.
- Wu X, Chang B, Blair NS, Sargent M, York AJ, Robbins J, Shull GE and Molkentin JD. 2009. Plasma membrane Ca²⁺-ATPase isoform 4 antagonizes cardiac hypertrophy in association with calcineurin inhibition in rodents. *J. Clin. Invest.* 119: 976-985.
- Wu X, Eder P, Chang B and Molkentin JD. 2010b. TRPC channels are necessary mediators of pathologic cardiac hypertrophy. *PNAS*. 107: 7000-7005.
- Xue B, Gole H, Pamidimukkala J and Hay M. 2003. Role of the area postrema in angiotensin II modulation of baroreflex control of heart rate in conscious mice. *Am J Physiol Heart Circ Physiol*. 284: H1003-H1007.
- Xue B, Pamidimukkala J and Hay M. 2005. Sex differences in the development of angiotensin II-induced hypertension in conscious mice. *Am J Physiol Heart Circ Physiol*. 288: H2177-2184.
- Yue L, Xie J and Nattel S. 2011. Molecular determinants of cardiac fibroblast electrical function and therapeutic implications for atrial fibrillation. *Cardiovascular Research*. 89: 744-753.
- Zeisberg EM and Kalluri R. 2010. Origins of Cardiac Fibroblasts. *Circ. Res.* 107: 1304-1312.
- Zeng W, Yuan JP, Kim MS, Choi YJ, Huang GN, Worley PF and Muallem S. 2008. STIM1 Gates TRPC Channels, but Not Orai1, by Electrostatic Interaction. *Molecular Cell*. 32: 439-448.
- Zhang J. 2002. Myocardial energetics in cardiac Hypertrophy. *Clinical and Experimental Pharmacology and Physiology*. 29: 351-359.
- Zhang G-X, Ohmori K, Nagai Y, Fujisawa Y, Nishiyama A, Abe Y and Kimura S. 2007. Role of AT1 receptor in isoproterenol-induced cardiac hypertrophy and oxidative stress in mice. *J Mol Cell Cardiol*. 42: 804-811.
- Zobel C, Rana OR, Saygili E, Bölck B, Saygili E, Diedrichs H, Reuter H, Frank K, Müller-Ehmsen J, Pfitzer G and Schwinger RHG. 2007. Mechanisms of Ca²⁺-Dependent Calcineurin Activation in Mechanical Stretch-Induced Hypertrophy. *Cardiology*. 107: 281-290.

9. Acknowledgments

I would like to thank specially to my PhD supervisor Prof. Dr. Marc Freichel who directed and corrected this thesis. I thank him for his constant support; for challenging me to learn everyday; for believing on me and my ideas which was essential to finish this work.

I would like to thank to Prof. Dr. Veit Flockerzi for his help, constructive critics and support. For teaching with his example the rigor required to generate and find answers.

I am very grateful to my college and friend Ilka Mathar for the daily time enriched by discussions about life around Science. Special thanks to Sebastian Uhl for his friendship and collaboration on the organ bath. Thank you to my colleagues Ulrich Kriebs, Stefanie Mannebach, and Dominic Vogte for the nice time in the group. I thank Stefanie Buchholz, Christin Matka, Sabine Schmidt, Tanja Volz, Sven Wagner, Kerstin Fischer and Christine Wesely for expert technical assistance. I would like to thank all the people from the animal house that have been taking care of all our mice. Thanks to Christa Seelinger, Claudia Ecker Claudia and Inge Vehar for their excellent support in daily stuffs. As well, especial thanks to Martin Simon-Thomas for his technical assistance and determination to make things possible around the laboratory. I would like to thank PD Dr. Stephan Philipp for the good cooperation and scientific advices. I thank all the members from the Pharmacology and Toxicology Department that somehow contribute to my Ph.D work.

I would like to thank to Prof. Dr. Peter Lipp, his team and his technical assistant Mrs. Anne Vecerdea for the fruitful cooperation. I thank to Prof. Dr. Ulrich Laufs, his group and Dr. Jan Reil from the Cardiology Department for the cooperation in the hypertrophy project. Also I thank to Prof. Dr. Dieter Bruns, Judith Wolf and Marina Wirth from the GK1326.

I have a deep grateful to my parents Rosita and Eduardo, my sister Ana María and my brother Gabriel who despite the distance gave me their unconditional support and love through this phase of my life. Orión. Also, I thank specially to Raquel for helping and being with me; for her lovely and patient support during all this time, thank you.

Finally, this thesis was supported by the Deutsche Forschungsgemeinschaft (DFG) and the Saarland University through the GK1326 "Calcium Signaling and Cellular Nanodomains", the SFB530 "Räumlich-zeitliche Interaktionen zellulärer Signalmoleküle" and the Klinische Forschergruppe 196 "Signaltransduktion bei adaptativen und maladaptativen kardialen Remodeling-Prozessen".

Appendices

Appendix A. Materials and reagents

Reagent	Catalog number	Company/Supplier
Acetic acid	222140025	Acrös
Acetylcholine chloride	A6625	Sigma
ADP (Sodium salt)	A2754	Sigma
Ammonium oxalate monophosphate	221716	Sigma
Angiotensin II, human	05-23-0101	Calbiochem
Angiotensin II, human	A9525	Sigma
anti- α IIb β 3 (FITC labelled)	M025-1	emfret analytics
anti- α -actinin (mouse monoclonal)	A7811	Sigma
anti- α -smooth muscle actin	ab15734	abcam
anti-CD31 (mouse monoclonal)	ab24590	abcam
anti-mouse (goat IgG)-AlexaFluor®594	A11005	Invitrogen/Molecular Probes
anti-P4HB	11245-1-AP	Acris
anti-rabbit (goat IgG)-AlexaFluor®488	A11008	Invitrogen/Molecular Probes
Apyrase from potato grade VII	A6535	Sigma
Avertin (2,2,2-tribromoethanol)	90710	Fluka
BDM (2,3-Butanedione monoxime)	B0753	Sigma
Bradykinin	B3259	Sigma
Bromophenol Blue	A3640,0005	AppliChem
BSA (albumin fraction V pH 7.0)	A1391,0250	AppliChem
CaCl ₂ -2H ₂ O	5239.1	Carl Roth
Citric acid	A2344,1000	AppliChem
Clopidogel hydrogensulfate	BN0680	BIOTREND (Switzerland)
Collagen (Kollagenreagens Horm®)	1130630	Nycomed (Austria)
DAPI, dilactate	D3571	Invitrogen/Molecular Probes
DePex	18243	Serva
DNase (Deoxiribonuclease I)	D4527	Sigma
DTT	D9163	Sigma
EDTA disodium salt 2H ₂ O	A1104,1000	AppliChem
EGTA	E4378	Sigma
Ethanol 99%	702543	Universität des Saarlandes
Ethanol absolute	32205	Sigma
Ethidium Bromide	2218.2	Carl Roth
Eosin Y-solution 0.5% aqueous	X883.1	Carl Roth
Eukitt	3989	Fluka
Fetal Calf Serum (FCS)	10270-106	Gibco
Fibrinogen from human plasma	F3879	Sigma
FURA-2-AM	F1221	Invitrogen/Molecular Probes
Glucose (D+) monohydrate	6780.1	Carl Roth
Glucose (D+) anhydrous	X997.2	Carl Roth
Glycine	3908.3	Carl Roth
Glycerin (Glycerol)	A2957	AppliChem
HCl 37%	20252.420	AnalaR Normapur - VWR
Hepes	9105.4	Carl Roth
Isoflurane	HDG9623	Baxter

Reagent	Catalog number	Company/Supplier
(±)-Isoproterenol hydrochloride	I5627	Sigma
Kanamycin Sulphate	K 1377	Sigma
KCl	701080 or A1164	Grüssing / AppliChem
KH ₂ PO ₄	26.936.320	VWR
Liberase TM (Research grade)	05 401 127 001	Roche
Liberase Blendzyme 4	Discontinued	Roche
M199 Earle's salts and L-Glutamine	31153-026	Gibco
Mayer Hemalaum solution	T865.2	Carl Roth
Methanol	20.847.320	AnalaR Normapur - VWR
MgCl ₂ ·6H ₂ O	2189.2	Carl Roth
MgSO ₄ ·7H ₂ O	1.058.861.000	Merck
Mygliol (Neutralöl 812)	1304M-01998	mLiter (Apotheke UKS)
NaCl 0.9% (sterile)	2350748	Braun
NaCl	27.810.295	VWR
NaHCO ₃	12143	Grüssing
Na-Heparin (5000 I.E/ml)		B.Braun Melsungen AG
Na-Heparin (25000 I.E/ml)	pzn-7833909	Rathipharm
Na ₂ HPO ₄ (2H ₂ O)	1.065.801.000	Merck
NaOH	12.155	Grüssing / AppliChem
Na-pyruvat	8793.2	Carl Roth
Paraplast® (tissue embedding medium)	A6330	Sigma
Paraformaldehyde (PFA)	P6148	Sigma
PBS Ca ²⁺ /Mg ²⁺ free (Dulbecco's-PBS)	14190-094	Gibco
Penicillin/Streptomycin	15140-122	Gibco
Penicillin/Streptomycin	P4333	Sigma
(L)-Phenylephrine hydrochloride	P6126	Sigma
Picric acid solution	80.456	Fluka
Prostacyclin (PGI ₂) sodium salt	P6188	Sigma
Proteinase K	A3830	AppliChem
Serotonin hydrochloride	H9523	Sigma
Sirius Red (Direct Red 80)	365548	Sigma
Tamoxifen	T5648	Sigma
TaqPolymerase	—	Home Made
Terg-A-Zyme	1304	Alconox Inc.
Tertiary amylalcohol	1.009.991.000	Merck
Thapsigargin	T-9033	Sigma
Thrombin from bovine plasma	T 4648	Sigma
Tris	4855.2	Carl Roth
Tris pH8.3	A4281	AppliChem
Tri-Sodium Citrate Dihydrated	3580.1	Carl Roth
Trypsin 10X/EDTA	154000-054	Gibco
Tween 20	A7564.0500	AppliChem
U46619 (9,11-Dideoxy-11α,9α-epoxymethanoprostaglandin F ₂ α)	D8174	Sigma
Urea	A1360,1000	AppliChem
Vectashield mountig media	H-1400	Linaris
Xylene	4436.1	Carl Roth
Xylene-Cyanol	A1408,0010	AppliChem

Appendix B. Solutions

- 10X PCR buffer (store RT):

Tris pH 8.3	100mM
MgCl ₂	15mM
KCl	500mM

- Tail-Lysis buffer (in ddH₂O):

10X PCR buffer	10% (v/v)
Proteinase K (10mg/ml)	2% (v/v)

- 10X Loading buffer for DNA electrophoresis

20g Urea
5ml EDTA 0.5M pH 8.0
0.5ml Tris 1M pH 7.0
0.25% Bromophenol blue
0.25% Xylene-Cyanol
Complete 50ml with d-diH ₂ O (warm ~60°C during stirring)

- Avertin (2,2,2-tribromoethanol) stock solution (Store RT, dark):

1g 2,2,2-tribromoethanol 99%
0.63ml tertiary amylalcohol

Incubate at 65° in order to get tribromoethanol into solution

Ready to use solution:

- 60µl stock solution + 5ml NaCl 0.9% (Incubate 65°C)

Dose: 0.5mg/g body weight or 25µl/g body weight (From 2010 this solution is prepared 2X concentrated to reduce the i.p injected volume into the mice).

- PBS 1X (pH 7.4, autoclaved)

NaCl	137mM
KCl	2.7mM
Na ₂ HPO ₄	8.1mM
KH ₂ PO ₄	1.8mM

Adjust pH with HCl

- PBST: 1ml Tween-20 in 1 litter PBS (pH 7.4).

- PFA 4% (pH 7.4) in PBS always prepared one day before its use and solved during constant stirring at ~60°C for several hours. Store at 4°C.

- Picrosirius red solution

Sirius Red 0.1% in Picric Acid (0.5g Sirius Red in 500ml, stirring o/n in a dark bottle and controlling that the final pH is 2.0, use NaOH 10N for this)

Solutions for cardiac myocytes/fibroblasts isolation:

- Solution A:

NaCl	134mM
Glucose	11mM
KCl	4mM
MgSO ₄ -7H ₂ O	1.2mM
Na ₂ HPO ₄ -2H ₂ O	1.2mM
Hepes	10mM

Prepared with autoclaved d-diH₂O, filtrated with Vacuum filter (Filtropur V50 0.45µm-500ml No. 83.1823, Sarstedt) and pH adjusted to 7.36 with NaCl 10N. A 10X filtered and sterile solution without glucose can be stored for months at 4°C.

- Solution A+: Solution A with 200µM EGTA, filtered and saturated with Carbogen (5% CO₂/ 95% O₂) for at least 15min at RT. For isolation of cardiomyocytes that were not going to be used for functional analysis was included 10mM of BDM (2,3-Butanedione monoxime), a reversible myosin AT-Pase inhibitor

- Solution A++extra: 4-5% BSA (alternatively 5% FCS) in Solution A supplemented with DNAase solution (100µl DNAse per 100ml final volume) of and 12.5µM CaCl₂ from a 100mM solution. The solution is sterile filtered (Filtropur V25 0.2 -250ml, Sarstedt) before adding the DNAse solution. It is gassed before use with Carbogen and kept at 37°C during its use.

- DNase solution in Tris-buffer

Deoxyribonuclease I	4KU/ml
NaCl	50mM
MgCl ₂	10mM
DTT	1mM

The DNase, NaCl, MgCl₂ and DTT are solved in a final volume of 5ml Tris-buffer (10mM) and 5ml of Glycerin are added to complete 10ml. The solution is kept in 200µl aliquots at -20°C.

- Liberase stock solution prepared with autoclaved d-diH₂O at a final concentration of 10mg/ml and 200µl aliquots kept at -20°C.

- Macrophage's solution:

DPBS (Ca ²⁺ /Mg ²⁺ free)	100ml
EDTA	2 mM
BSA	0.5%

The solution is sterile filtered (Filtropur V25 0.2 -250ml, No83.1822.001, Sarstedt) and is maintained at 4°C during its use. Frozen aliquots can be stored at -20°C.

- Medium 199-complete

Penicillin/Streptomycin	1:200
Kanamycin	1:1000
FCS	10%

The FCS is sterile filtrated (Filtropur V25 0.2µm -250ml, Sarstedt) to remove debris and 50ml aliquots are maintain at -20°C. Kanamycin is solved (50mg/ml) in d-diH₂O, sterile filtrated with a syringe filter (0.22µm Fisherbrand, Fisher Scientific Cat.No. 09-719A) and aliquots are stored at -20°C.

- Trypsin 1X (Trypsin/EDTA 10X Gibco 15400-054) obtained solving the 10X 1:10 in PBS Ca²⁺/Mg²⁺ free with EDTA 0.2mM. Thaw just before its use, preferably use fresh aliquots always.

- Krebs-Henseleit solution (for organ bath):

NaCl	118mM
NaHCO ₃	24.88mM
KCl	4.7mM
Glucose	5.56mM
Na-pyruvat	1mM
MgSO ₄ -7H ₂ O	1.64mM
KH ₂ PO ₄	1.18mM
CaCl ₂	1.8mM

The pH is adjusted with HCl to 7.2 and the solution is gassed constantly during its use.

- Tyrode's modified (FB's calcium imaging):

Hepes	5mM
NaCl	137mM
KCl	2mM
NaHCO ₃	12mM
Na ₂ HPO ₄ -2H ₂ O	0.3mM
MgCl ₂ -6H ₂ O	1mM
Glucose	5mM
CaCl ₂	1.8mM

Filtrate the solution, afterwards check the pH and adjust to 7.4 with NaOH 10N.

- ACD (Acid-Citrate-Dextrose):

Tri-Sodium Citrate-2H ₂ O	2.5% (85.01mM)
Citric acid	1.4% (72.87mM)
Glucose	2% (100.92mM)

The solution is prepared with autoclaved d-diH₂O and then can be maintained at 4°C.

- Platelet's solution:

Hepes	5mM
NaCl	137mM
KCl	2mM
NaHCO ₃	12mM
Na ₂ HPO ₄ -2H ₂ O	0.3mM
MgCl ₂ -6H ₂ O	1mM
Glucose	4.54mM
CaCl ₂	2mM
BSA	0.35% (w/v)

Always prepared fresh in small volume (30ml) and gassed with carbogen, the pH is then 7.4. Keep warm at 37°C during its use.

Appendix C. ECG analysis from TRPC1/TRPC4 (-/-)² mice

During cardiac hypertrophy experiments with TRPC-deficient mice ECGs before and at the end of the hypertrophy induction were recorded. Differences in heart rate from wild type and TRPC1/TRPC4 (-/-)² mice treated with isoproterenol were observed (Figure 10). In addition, from the analysis of ECG traces performed in these mice a reduced QT interval in TRPC1/TRPC4 (-/-)² mice was observed (Figure 1Ap, Ba). However, due to differences in heart rate between wild type and TRPC1/TRPC4 (-/-)² mice a corrected QT interval was calculated revealing a difference in the QT interval only between the saline treated groups (Figure 1Ap, A and Bb-c). It is difficult to interpret this observation since only little about the electric physiology of the mouse heart and more over about short QT syndromes in mice have been described. In humans short QT syndromes have been only related with mutations in few potassium channels (Schulze-Bahr and Breithardt, 2005). Regarding the role of TRPC proteins in the regulation of the cardiac electrophysiology not now much is known. It has been described that the murine Sino-Atrial Node (SAN) displays store-operated Ca²⁺ activity. This was correlated with the expression of several TRPC transcripts including TRPC1 and TRPC4 in the SAN, in addition to expression assessed by immunocytochemistry of pacemaker cells (Ju et al., 2007). Although, the specificity of the antibodies used has not been fully proved. To define if the reduced QT interval observed in TRPC1/TRPC4 deficient mice is a reproducible observation, in the future it will be required to analyze ECG recordings of these mice using different ECG leads as recommended by Dr. Hans-Ruprecht Neuberger from the Cardiology Department. With dose measurements further experiments could be planned to determine if these TRPC proteins are involved in the electrophysiology of the heart.

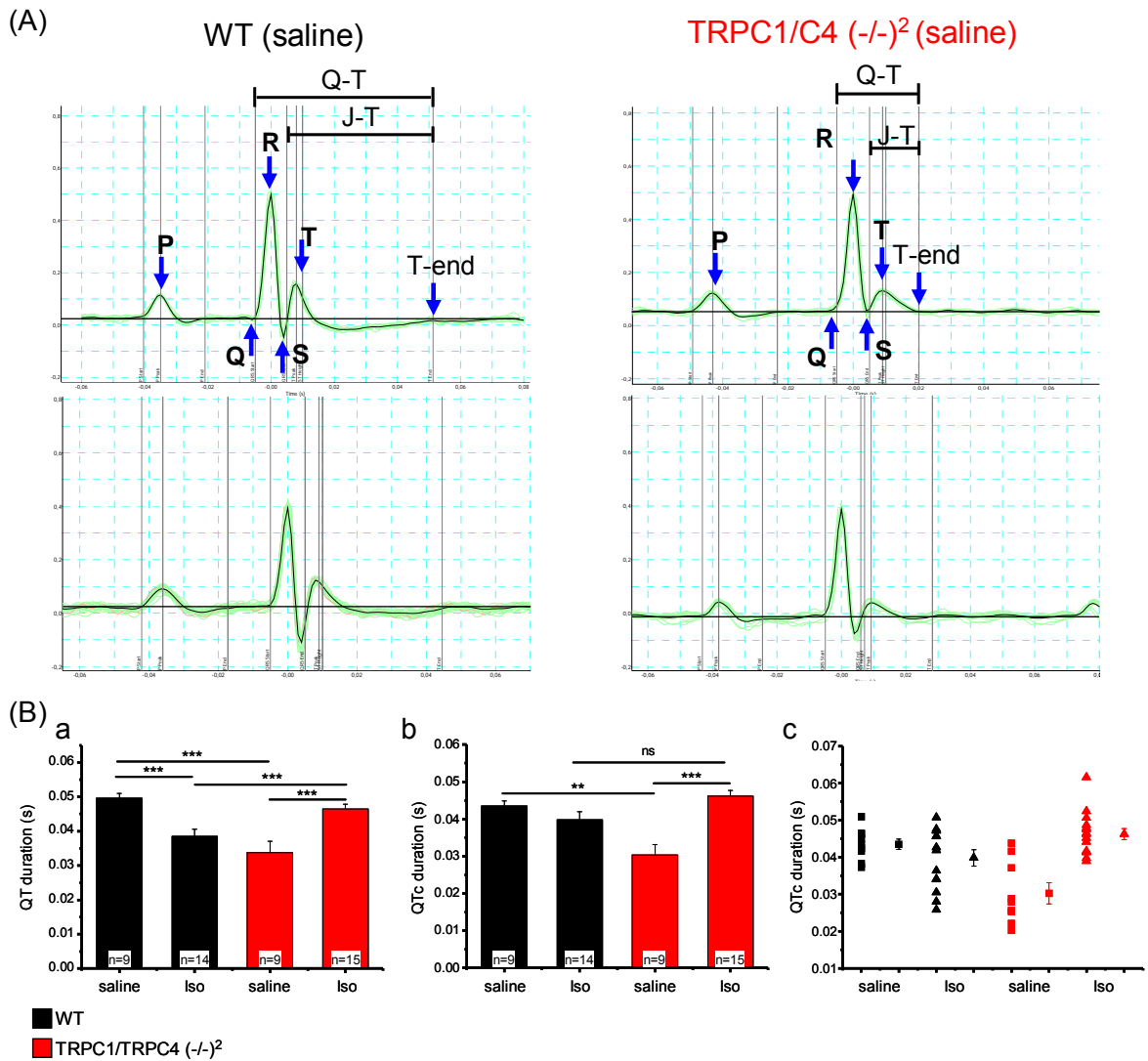


Figure 1Ap. ECG analysis from TRPC1/TRPC4 (-/-)² mice during cardiac hypertrophy induction by isoproterenol. ECG recordings from wild-type and from TRPC1/TRPC4 (-/-)² mice were obtained at the 6th day of Iso-30 treatment under anesthesia. **(A)** Representative original ECG traces of mean cardiac cycles from 10 beats recorded in wild type and in TRPC1/TRPC4 (-/-)² mice. The different ECG waves P, Q, R, S and T and limits of the wave's intervals used for the analysis are depicted. In these kind of recordings a shorter duration of the QT interval from TRPC1/TRPC4 (-/-)² saline treated mice was observed. **(B)** Statistical analysis of the QT interval duration. In **Ba** the QT interval, in **Bb** the QT corrected (QTc) interval using the formula $QTc = QT / \sqrt{RR} \times 10$ from Mitchell et al. (1998) and in **Bc** dot plot from the QTc interval where each dot represents data from one mouse. n=: number of mice. **p<0.01, ***p<0.001 and ns (not significant) according to the one-way ANOVA.